28

0-315-13274-4

National Library of Canada | Bibliothèque nationale du Canada

CANADIAN THESES ON MICROFICHE | *THÈSES CANADIENNES SUR MICROFICHE*

61184

NAME OF AUTHOR/*NOM DE L'AUTEUR* Ishmael Hassan

TITLE OF THESIS/*TITRE DE LA THÈSE* "The Crystal Structure and Crystal Chemistry of the Cancrinite and Sodalite Groups of Minerals"

UNIVERSITY/*UNIVERSITÉ* McMaster

DEGREE FOR WHICH THESIS WAS PRESENTED/*GRADE POUR LEQUEL CETTE THÈSE FUT PRÉSENTÉE* Ph.D.

YEAR THIS DEGREE CONFERRED/*ANNÉE D'OBTENTION DE CE DEGRÉ* 1983

NAME OF SUPERVISOR/*NOM DU DIRECTEUR DE THÈSE* Dr. H.D. Grundy

Permission is hereby granted to the NATIONAL LIBRARY OF CANADA to microfilm this thesis and to lend or sell copies of the film.

The author reserves other publication rights, and neither the thesis nor extensive extracts from it may be printed or otherwise reproduced without the author's written permission.

L'autorisation est, par la présente, accordée à la BIBLIOTHÈQUE NATIONALE DU CANADA de microfilmer cette thèse et de prêter ou de vendre des exemplaires du film.

L'auteur se réserve les autres droits de publication; ni la thèse ni de longs extraits de celle-ci ne doivent être imprimés ou autrement reproduits sans l'autorisation écrite de l'auteur.

DATED/*DATÉ* February 17, 1983. SIGNED/*SIGNÉ* I Hassan

PERMANENT ADDRESS/*RÉSIDENCE FIXÉ*

NL-91 (11-73)

THE CRYSTAL STRUCTURE AND CRYSTAL CHEMISTRY OF SODALITE AND CANCRINITE GROUPS OF MINERALS

By

© ISHMAEL HASSAN, B.Sc., M.Sc.

A Thesis

Submitted to the Faculty of Graduate Studies

in Partial Fulfilment of the Requirements

for the Degree

Doctor of Philosophy

McMaster University

July 1982

The Crystal Chemistry of Sodalites and Cancrinites

To My Wife

DOCTOR OF PHILOSOPHY (1982)
(Geochemistry)

McMASTER UNIVERSITY
Hamilton, Ontario

TITLE: The Crystal Structure and Crystal Chemistry of Sodalite and Cancrinite Groups of Minerals

AUTHOR: Ishmael Hassan, B.Sc. (McMaster University)
M.Sc. (McMaster University)

SUPERVISOR: Dr. H. D. Grundy

NUMBER OF PAGES: xiv, 236

ABSTRACT

The crystal structures of three cancrinites, four sodalites, six helvites and tugtupite have been refined using x-ray diffraction data. The nature of the crystal structure and crystal chemistry of the cancrinites and sodalites have been elucidated, with emphasis on 1) the significance of the superstructures, 2) the space group problem, 3) the order-disorder, 4) the structural variation, and 5) the stoichiometry.

Also, a geometrical structural model for sodalite has been developed and it has the following uses:

a) Allows the accurate prediction of the structures of all members of the sodalite group of minerals.

b) The prediction of the chemical limits of structural stability of all materials based on the sodalite structural type.

c) Permits the published thermal expansion data for sodalites to be rationalized in terms of rotation of the $Al/Si-O_4$ tetrahedra.

ACKNOWLEDGEMENTS

I would like to express my sincere thanks to my supervisor, Dr. H. D. Grundy, for his valuable suggestions, continuous support and encouragement. Dr. B. J. Burley and Dr. I. D. Brown have also been generous with time and advice throughout the project. Mr. R. Faggiani gave invaluable assistance with his diffractometer and Mr. J. Whorwood was kind in preparing the photographs.

My sincere thanks to my wife Jackie who contributed in many ways to the success of this project, and also for her patience and understanding and typing of this manuscript. Also thanks to Azar and newcomer Sabrina, -- they helped me keep my wits throughout it all.

CONTENTS

LIST OF TABLES

LIST OF FIGURES

CHAPTER 1

INTRODUCTION

Cancrinite and sodalite groups of minerals generally occur in alkali-rich silica-deficient rocks. Natural cancrinite and sodalite compositions lie primarily in the system Na_2O-Al_2O_3-SiO_2-H_2O-Cl^--$SO_4^=$-$CO_3^=$, together with CaO, K_2O, and sulphur; these are all important components in one or more of the mineral types. The essential conditions of their formation are known only in outline. Although cancrinites and sodalites are not as common as felspars, they are, nevertheless, important rock-forming minerals occurring in a wide variety of geological settings, However, their geological significance have not been fully assessed.

Considerable amount of work has been done on cancrinites (see Deer, Howie & Zussman, 1963) and sodalites (see Deer et al., 1963; or Dempsey & Taylor, 1980) in the past century. Despite the large amount of available information, major uncertainties exist concerning their detailed structure and chemistry, and an overall view of the problems has not been presented for the closely-related sodalites and cancrinites.

Indeed the minerals in the sodalite and cancrinite groups have not received intensive modern mineralogical studies as other important groups of rock-forming minerals. The structure refinements of sodalite (Lons and Schulz, 1967), hauyne (Lohn and Schulz, 1968) and nosean (Schulz, 1970) have been based on film data that is relatively inaccurate

by current standards. The only modern structural analysis of a sodalite-type mineral--helvite was reported by Holloway et al. (1972). The structure of only one cancrinite has been fully refined (Hassan, 1980). Furthermore, the structure of lazurite has not been precisely determined nor the new cancrinite-like minerals (liottite, afghanite, franzinite, giuseppettite, sacrofanite).

The purpose of the present studies, in general, is the characterization of the minerals in the cancrinite and sodalite groups. To examine structure controls as a function of chemical composition, thereby mapping possible chemical domains. To examine the polytypic relationships between the two groups of minerals and their relative stability. Finally, to examine the superstructures of these minerals and to provide answers to such pertinent questions as the following:

(1) What are the end-member compositions for cancrinites?

(2) What is the relationship between crystal structure and non-stoichiometry of cancrinites and sodalites? Does any variation of structural property correspondingly reflect the characteristics of their non-stoichiometry?

(3) What are the space groups of nosean, hauyne and lazurite? Does a Si/Al ratio of 1:1 always conform to the so-called Al-avoidance rule?

(4) Is complete miscibility possible between the three end-members of the helvite group, (Mn, Fe^{2+}, Zn) $(Be_6Si_6O_{24})S_2$?

(5) Are the framework compositions of tugtupite ($Be_2Al_2Si_8O_{24}$) and helvite ($Be_6Si_6O_{24}$) unique?

(6) What are the characteristics and significance of the superstructures in the two groups of minerals? Do they signify stacking faults? Do they signify domains? Do they signify substitutional/positional

ordering? Are they related to non-stoichiometry?

(7) What is the nature of the order-disorder polytypic transformation involved in hexagonal cancrinite to cubic sodalite? Does it involve continuous change of atomic arrangement within a single phase or does it involve unmixing? What is the relative stability of cancrinite, sodalite and possible unmixed phases?

(8) Are the newly discovered cancrinite-like minerals possible mixed phases? Do they show superstructures?

The author attempts to answer these questions through X-ray diffraction study of selected composition of cancrinites and sodalites. The cancrinites are CO_3-rich (Hassan, 1980), Cl-rich (davyne), SO_4-rich (vishnevite) and OH/H_2O-rich (hydroxycancrinite) and the sodalites are Cl-rich (sodalite proper), SO_4-rich (nosean, hauyne and lazurite) and OH/H_2O-rich (hydroxysodalite). Materials of other cancrinite-like phases are not available for experimental work but published data is re-examined on the basis of results obtained in this study.

To complete the study on the sodalite type minerals, the helvite-genthelvite compositional series and tugtupite are also characterized by X-ray diffraction.

Finally, published thermal expansion data for sodalites are re-examined on the basis of present structural analyses and the feasibility of applying present results to determine the complex structures of zeolites is discussed.

CHAPTER 2

HISTORICAL REVIEW

2.1 Chemical Composition

The chemistry of the sodalite group of minerals has been discussed by Taylor (1967) and Deer et al. (1963). The latter show that sodalite closely approaches the ideal formula $Na_8(Al_6Si_6O_{24})Cl_2$. However, many of the sodalite analyses show appreciable amounts of water, all of which cannot be accepted in the structure, as pointed out by Deer et al., (1963).

Nosean and hauyne are generally treated as a solid solution series, principally because they both have sulphate as the interframework anion. Published analyses of these minerals, many of which are pre-1900 in date, show significant variation in the amounts of sodium, potassium, calcium and the sulphate anion and a range of water contents up to 2.15wt.%. According to Barth (1932) the generalized structural formula of the sodalite group should be $A_8(B_{12}O_{24})M_2$, where B represents the framework ions Si and Al, and A and M represent the interframework cations and anions respectively. Barth (1932) proposed the ideal formula $Na_8(Al_6Si_6O_{24})SO_4$ for nosean, where there is one interframework anion vacancy in the unit cell. For hauyne he proposed the general formula $(Na,Ca)_{4-8}(Al_6Si_6O_{24})(SO_4)_{1-2}$ with solid solution between hauyne and nosean. Based on chemical analyses, Taylor (1967) proposed the general formula $(Na_{5-7}Ca_{0-2}K_{0-3})(Al_6Si_6O_{24})(SO_4)_{1-2}$ for hauyne.

The hydrothermal studies of Peteghem and Burley (1963) have shown that at 600°C and 1000 bars P_{H_2O} there is complete solid solution between nosean, $Na_8(Al_6Si_6O_{24})SO_4$ and hauyne $Na_6Ca_2(Al_6Si_6O_{24})(SO_4)_2$.

The chemistry of lazurite has recently been studied by Hogarth and Griffin (1976). They proposed the general formula $(Na,Ca)_{7.5-8}(Al,Si)_{12}(O,S)_{24}(SO_4,H_2O,Cl)_2 \cdot nH_2O$ and noted that Si exceeds Al by 0.1 to 0.6 atoms per unit cell.

Dunn (1976) has shown with the aid of seventy-five new analyses of the helvite group of minerals, $(Mn, Fe^{2+},Zn)_8(Be_6Si_6O_{24})S_2$, and seventy-five analyses from the literature that there is an indication of complete miscibility between the Mn and Fe members (helvite and danalite), and between the Fe and Zn members (danalite and genthelvite) but not between the Mn and Zn members (helvite and genthelvite). Tugtupite (Danø, 1966; Sørensen, Danø and Peterson, 1971) has the ideal composition $Na_8(Al_2Be_2Si_8O_{24})Cl_2$.

The compositional variation in the cancrinite group may be represented by the general formula (Deer et al. 1963):

$$(Na,Ca,K)_{6-8}(Al_6Si_6O_{24})(CO_3,SO_4,Cl)_{1-2} \cdot 1\text{-}5H_2O.$$

Many new cancrinite-like minerals have recently been discovered and it is therefore necessary to review the naming of minerals in this group. Deer et al. (1963) proposed to restrict the name cancrinite to minerals containing between 100 and 80% of the cancrinite end-member, sulphatic cancrinite to between 80 and 50%; carbonate vishnevite to between 50 and 20% and vishnevite to between 20 and 0% of the cancrinite end-members. This is an acceptable scheme providing end-member can be

defined for cancrinite and a solid solution series exist between the CO_3-SO_4 members. The names microsommite and davyne have been used to describe cancrinites rich in K and Cl, but Deer et al. (1963) retain the term microsommite to describe this variety. However, the term davyne should be used since microsommite is now used to describe a cancrinite whose a-dimension is 'twice' that of cancrinite (Bariand et al., 1968). The new cancrinite-like minerals, based on integral multiple of cancrinite c-parameter are given various names (Table 2.1).

2.2 Structure

The general features of the crystal structure of both cancrinite and sodalite are well known (Pauling, 1930). However, the detailed structure and the origin of the observed superstructures are not clear.

Structure refinements of cancrinite in the space group $P6_3$ were done by Nitholion (1955), Jarchow (1965) and Barrer et al. (1970, 1971). Microsommite positional parameters only were given by Klaska and Jarchow (1977). The new cancrinite-like minerals are currently being refined by Italian researchers using various space groups (Table 2.1).

The structure of a cancrinite has been imaged by High Resolution Electron Microscopy and subsequently the structure has been fully refined to R = 0.028 (Hassan, 1980; Grundy and Hassan, 1982).

There has been some controversy over the space groups of the sodalite minerals which Saalfeld (1959, 1961) has discussed. Table 2.2 gives the minerals of the sodalite group and the space groups which have been assigned to them or used by various workers. Although Barth (1932) considers that the structure of all the sodalite minerals can be

Table 2.1: Cancrinite-like minerals

Minerals	a(Å)	c(Å)	n*	c/n	Z**	Space Group	Stacking Sequence
1 Cancrinite	12 590(3)	5.117(1)	1	---	1	$P6_3$	AB
2 Hydroxy-cancrinite	12.664(2)	5.159(1)	1	---	1	$P6_3$	AB
3 Vishnevite	12.685(6)	5.179(1)	1	---	1	$P6_3$	AB
4 Davyne	12.881(6)	5.368(1)	1	---	1	$P6_3$	AB
5 Micro-sommite (syn)	22.138	5.248	--	$a_o = \frac{a}{\sqrt{3}}$ = 12.781	3	$P6_3$	AB
6 Losod (syn)	12.906(3)	10.541(3)	2	5.271	2	$P6_3/mmc$	ABAC
7 Liottite	12.842(3)	16.091(5)	3	5.364	3	$P\bar{6}m2$	ABABAC
8 Afghanite	12.77 (3)	21.35 (4)	4	5.34	4	$P6_3mc$	ABABACAC
9 Franzinite	12.884(9)	26.58 (2)	5	5.32	5	$P\bar{3}m1$	ABCABCBACB
10 Giuseppettite	12.850(1)	42.22 (3)	8	5.28	8	$P\bar{6}2c$	--
11 Sacrofanite	12.865(4)	72.24 (1)	14	5.30	14	$P6_3mc$, $P\bar{6}2c$ or $P6_3/mmc$	--

* n = integral multiple of cancrinite c-parameter

** The general formula on which Z is based:

$$(Na,Ca,K)_{6-8}(Al_6Si_6O_{24})(CO_3,SO_4,Cl,OH)_{1-2}\cdot 1\text{-}5H_2O.$$

The number of layers of six-membered rings in the stacking sequence is 2Z.

Selected Reference

1-4 Present work; 5 - Klaska & Jarchow (1977); 6 - Sieber & Meier (1974); 7 - Merlino & Orlandi (1977a); 8 - Merlino & Mellini (1976); 9 - Merlino & Orlandi (1977b); 10 - Mazzi & Tadini (1981); 11 - Burragato et al. (1980).

Table 2.2: Space Group assigned to the sodalite group of minerals

	Sodalite	Hydroxysodalite	Nosean	Hauyne	Lazurite	Helvite	Danalite	Genthelvite
Pauling (1930)	$P\bar{4}3n$	----	----	----	----	$P\bar{4}3n$	----	----
Barth (1932)	$P\bar{4}3m$	----	$P\bar{4}3m$	$P\bar{4}3m$	----	----	----	----
Machatschki (1933, 1934)	$P\bar{4}3n$	----	$P\bar{4}3n$	$P\bar{4}3n$	----	----	----	----
Saalfeld (1959, 1961)	----	----	$P\bar{4}3m$	$P\bar{4}3n$	----	----	----	----
Lons and Schulz (1967)	$P\bar{4}3n$	----	----	----	----	----	----	----
Lohn and Schulz (1968)	----	----	----	$P\bar{4}3n$				
Schulz (1970)	----	----	$P\bar{4}3m$	----	----	----	----	----
Taylor (1967)	$P\bar{4}3n$	----	$P\bar{4}3m$	$P\bar{4}3n$	----	----	----	----
Glass et al. (1944)	----	----	----	----	----	$P\bar{4}3m$	$P\bar{4}3m$	$P\bar{4}3m$
Strunz (1957)	----	----	----	----	$P\bar{4}3m$	----	----	----
Schulz and Saalfeld (1965)	----	----	$P\bar{4}3m$	----	----	----	----	----
Holloway et al. (1972)	----	----	----	----	----	----	$P\bar{4}3n$	----
This study	$P\bar{4}3n$	$P\bar{4}3n$	$P\bar{4}3n$	$P\bar{4}3n$	$P\bar{4}3n$	$P\bar{4}3n$	$P\bar{4}3n$	$P\bar{4}3n$

expressed in terms of $P\bar{4}3m$, he agrees that the true space group for sodalite is $P\bar{4}3n$. The difference between the two possible space groups $P\bar{4}3m$ and $P\bar{4}3n$ should be evident from extinctions. Space group $P\bar{4}3m$ has no condition limiting possible reflections, whereas the presence of the diagonal glide plane in the space group $P\bar{4}3n$ limits the possible reflections from hhl planes to those where l=2n.

The structure of sodalite was refined by Lons and Schulz (1967) in the space group $P\bar{4}3n$ and that of nosean was refined by Schulz (1970) in the space group $P\bar{4}3m$. Lohn and Schulz (1968) examined the structure of hauyne $(Na_5K_1Ca_2)(Al_6Si_6O_{24})(SO_4)_{1.5}$ in the space group $P\bar{4}3n$. The volcanic specimen shows faint diffuse streaks and superstructure reflections. The SO_4 occupies two positions with some displacement of oxygens from the triad axes. The cations occupy two positions. The structure of helvite was determined by Pauling (1930) and refined by Holloway et al. (1972) in the space group $P\bar{4}3n$. The structure of tugtupite was determined and refined by Danø (1966) in the space group $I\bar{4}$.

Recently, many sodalites have been synthesized (Henderson and Taylor, 1978) and a computer model of the sodalite structure was developed by Taylor and Henderson (1978). This model was later replaced by the Distance Least Squares (DLS) Model by Dempsey and Taylor (1980). These models were used by the authors to calculate structural parameters and in the interpretation of sodalite thermal expansion behaviour.

2.3 Cancrinite and Sodalite Structures

Minerals of the cancrinite and the sodalite groups are characterized by an ordered framework of Al/Si-O tetrahedra. Many

members of the sodalite group of minerals are polymorphic with cancrinites. The hexagonal symmetry of cancrinite is the result of the close packing of inter-connected and parallel 6-fold rings of alternating Al-Si tetrahedra in an ABAB... type stack, while the cubic symmetry of sodalite is due to an ABCABC... stacking sequence. The difference in stacking gives important structural dissimilarities between the two mineral groups.

Cancrinite has a large continuous framework channel which is parallel to the 6-fold screw axis (c-axis) in which are located interframework cations and anions, in sodalite this channel is offset (or closed) by the C-type layer to give a network of large cages (Fig. 2.1). In addition cancrinite has 'chains' of small cages parallel to the c-axis consisting of framework cavities between successive A type or B type layers (Fig. 2.2) which also contain cations and anions. The difference in structure between these two groups suggests that the cancrinite minerals are more likely to be the low temperature polymorphs as the continuous channel facilitates diffusion and thereby decomposition at elevated temperatures. In the case of the hydroxy varieties this has been experimentally verified (Van Peteghem and Burley, 1962).

The polymorphism between sodalite and cancrinite should be viewed in the more restricted sense of polytypism since the polymorphs differ only in the manner of stacking identical layers and therefore simple relationships between the cell edges of the polytypes should exist. For example, the unit cell edge of hydroxysodalite is 8.8899Å; one-third of the body diagonal [111] is 5.133Å and the c-dimension of hydroxycancrinite (5.159Å) is nearly obtained. Moreover, the cube face diagonal $[1\bar{1}0]$ is 12.572Å compared with 12.664Å, the a-axis of hydroxycancrinite.

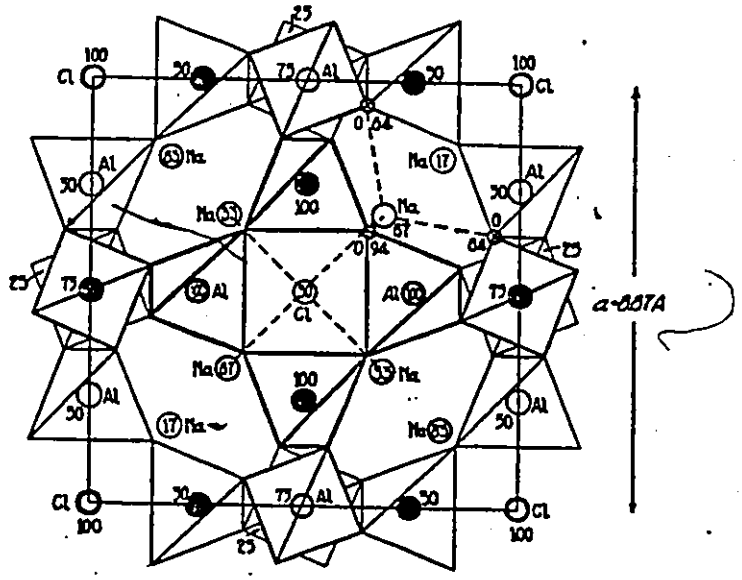

The framework of tetrahedral groups in sodalite, $Na_4Al_3Si_3O_{12}Cl$. The scheme may be grasped by realizing that the cubic unit cell has a ring of four tetrahedra on each face and a ring of six tetrahedra around each corner.

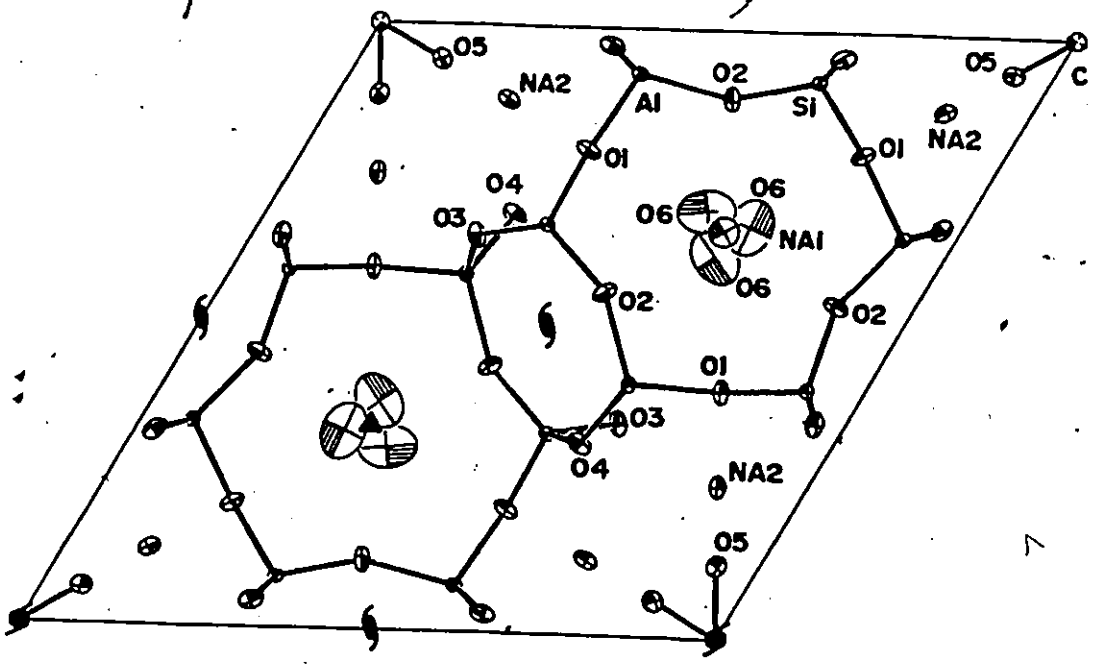

Diagramatic projection of the trial structure down [001], showing the site nomenclature and also the symmetry elements for space group $P6_3$.

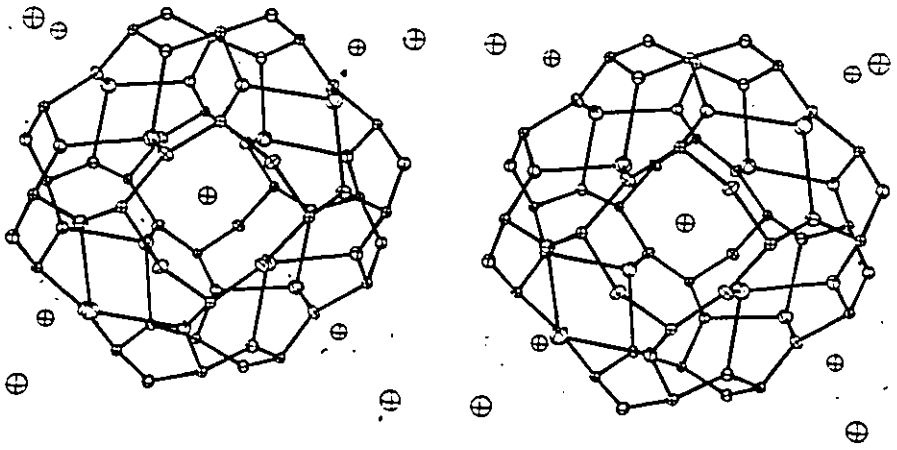

Fig. 2.1: Stereographic schematic of sodalite showing a complete cage viewed down the a_3-axis.

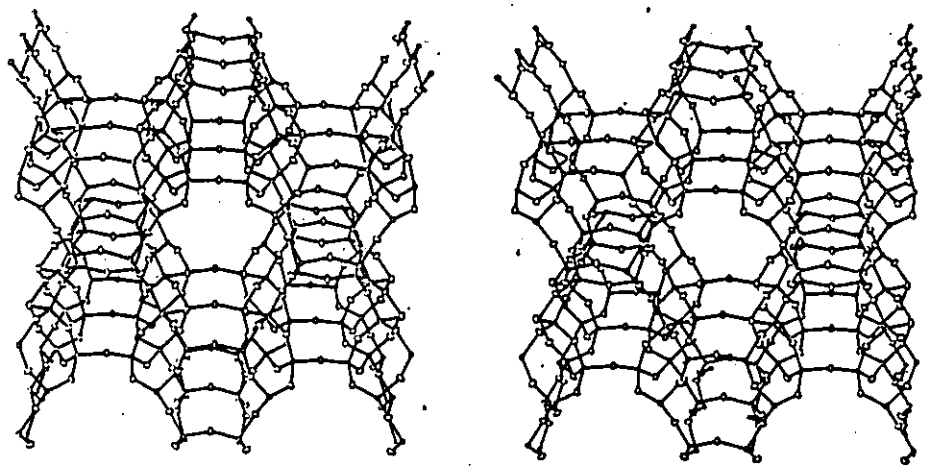

Fig. 2.2: Stereographic schematic of the framework of cancrinite viewed down the c-axis. The large channel is defined by the 'chains' of interconnected small cages parallel to the c-axis.

Gossner and Mussgang (1930) noted this similarity between the two minerals before the structure of either mineral had been worked out.

The sodalite-cancrinite polytypism is not restricted to the stacking sequence ABAB... and ABCABC... since stacks of six-membered rings can be obtained from a combination of AB, BA, AC, CA, BC or CB, thereby giving, at least theoretically, infinitely many different framework structures. AB is converted to BC by simple translation and to AC by rotation in the plane. Some of the naturally occurring cancrinite-like phases have been reported to have complicated stacking sequences (Table 2.1). These cancrinite-like minerals show different c-periods, which are integral multiples of cancrinite c-parameter.

All of the polytypes are characterized by a 1:1 ratio of Al:Si; this is a strong indication of an ordered distribution of these cations as was found in the structural studies of cancrinite (Jarchow, 1965; Hassan, 1980) and sodalite (Lons and Schulz, 1967). Current crystal structure analyses of liottite, afghanite and franzinite (Merlino and Mellini, 1976) indicate that these minerals do not present any long-range order in the distribution of the tetrahedral cations but these minerals appear to be characterized by short-range ordering of the tetrahedra cations with development of antiphase domains.

Although the frameworks of these groups of minerals are well-defined, essentially a 1:1 ratio of Al:Si-O tetrahedra, the inter-framework ions are chemically diverse and are typical of zeolitic materials. The large channels in cancrinite are found to contain Na^+, K^+, Ca^{++}, OH^-, $CO_3^=$, $SO_4^=$, H_2O and the small cages Na^+, Ca^{++}, OH^-, H_2O, Cl^- whereas the sodalite group cavity can contain Na^+, K^+, Ca^{++},

OH^-, $SO_4^=$, Cl^-, H_2O. The disorder that results from substitution of these ionic species for each other gives $P6_3$ symmetry for the cancrinite group and $P\bar{4}3n$ symmetry for the sodalite group.

CHAPTER 3

EXPERIMENTAL METHODS

3.1 Sample Description

In order to define chemical boundaries, possible end-member compositions were selected for structure refinements. For the cancrinite group of minerals, a synthetic hydroxycancrinite, a vishnevite and a davyne were selected. Synthetic hydroxysodalite, sodalite, a nosean, a hauyne and a lazurite were selected for the sodalite group. Also, six members of the helvite-genthelvite series and tugtupite were selected.

The synthetic samples were supplied by Dr. B. J. Burley while the natural cancrinites were obtained from the British Museum and the other natural specimens as well as additional cancrinites were obtained from the Royal Ontario Museum. The electron microprobe was the method chosen for chemical analyses since samples were available in limited amounts. Analyses of these samples are very difficult since they contain large amounts of sodium, volatiles as well as OH/H_2O; the OH/H_2O cannot be determined by the electron microprobe.

A further check on the chemistry of these materials was obtained from the estimation of electron density in the x-ray structure analysis. This method is not always suitable, for example, it usually cannot distinguish the proportions of two or more cations if they are sitting on the same site and are of similar atomic number. However, the two methods should complement each other and provide good crystallochemical formulae.

Cell contents were calculated on the basis of twelve framework cations. Chemical analyses and unit cell contents for the specimens which have been used in the x-ray refinements, together with other pertinent information are given in the appropriate sections on structure refinement.

A general discussion of the mineral chemistry, using new analyses and analyses from the literature, will be given in Chapter 8, where also, the chemistry will be rationalized in terms of the crystal structures.

3.2 Unit Cell Dimensions and Space Groups

Fresh, homogenous grains with suitable size and more or less block form were selected. These selected grains were further checked under a polarizing microscope to detect any inhomogeneity or fracture. Some grains were shaped into either spheres or cylinders. These optically confirmed single crystals were studied by the precession method and those crystals that showed single spots without 'tails' or streaks connecting them were chosen for intensity measurements.

The single crystals were mounted on an automatic four-circle diffractometer and were automatically aligned. The cell parameters were determined by least-squares from at least fifteen substructure reflections.

Long-exposed precession photographs were taken generally for all crystals used for the collection of intensities. These photographs reveal any superstructure that may be present and also serve as a check on the symmetry. All the cancrinites examined show symmetry which is

consistent with the accepted space group $P6_3$ (Jarchow, 1965) and many cancrinites also show a well-developed superstructure, all observed diffraction maxima are sharp.

Except for nosean and lazurite, all the other sodalites and helvites show symmetry which is consistent with the space group $P\bar{4}3n$. Nosean, lazurite and some hauynes show superstructure reflections and these may violate the space group $P\bar{4}3n$. Consequently, the structure of nosean, lazurite and also hauyne were refined in both the space groups $P\bar{4}3n$ and $P\bar{4}3m$ and it was found that the space group $P\bar{4}3n$ consistently gave better structural models for all these minerals. Nosean and lazurite, but not the hauyne used, show well-developed superstructures. Tugtupite shows symmetry which is consistent with the accepted space group $I\bar{4}$ (Danø, 1966).

3.3 X-Ray Intensity Collection and Data Reduction

The single crystals were mounted on either a Syntex $P\bar{1}$ or Nicolet P3 automatic four-circle diffractometer and were automatically aligned. The intensities were collected with graphite-monochromated Mo radiation and a scintillation counter. A θ-2θ scan method was used in a variable-scan-rate mode with a minimum range of 2°/min and a maximum range of 24°/min, depending on the peak count through an angle of 2° and the α_1-α_2 separation. Two standard reflections were monitored every fifty reflections to check for constancy of crystal alignment. Intensities were collected over more than one asymmetric unit up to a 2θ value of 65°.

Data were not corrected for absorption. However, steps were taken in the selection of the crystals to reduce this effect. Small

equidimensional crystals (~0.2mm) were chosen and few crystals were shaped into either spheres or cylinders. Furthermore, the linear absorption coefficient is quite small for cancrinites and sodalites. All data were corrected for background, Lorentz and polarization effects. Equivalent reflections were averaged to produce an asymmetric set and were converted to structure factors. The resulting structure factors are classified as observed if the magnitude is greater than that of three standard deviations based on counting statistics. Only observed reflections were used in the refinement. Extinct reflections served as a check on the space group. All crystallographic calculations were made using the XRAY76 Crystallographic System (Stewart, 1976), adapted by H. D. Grundy for the CYBER730.

3.4 X-Ray Structure Refinement

Initial parameters for least-squares refinement were the final parameters of the structure taken from either this study or the literature. Scattering curves for neutral atoms were taken from Cromer and Mann (1968). All R-factors are of the form

$$R = \Sigma (|F_o| - |F_c|) / \Sigma |F_o|$$

and all R_w-factors are of the form

$$R_w = \left\{ \frac{\Sigma w (|F_o| - |F_c|)^2}{\Sigma w |F_o|^2} \right\}^{\frac{1}{2}}$$

with w = 1 (unit weights).

Isotropic temperature factor, U, is obtained from the expression

$$\exp -B\left(\frac{\sin\theta}{\lambda}\right)^2$$

where $B = 8\pi^2\bar{u}^2$, where $\bar{u}^2$ is the mean-square amplitude of vibration and

$U = \frac{1}{8\pi^2}B$; and the anistropic temperature-factor expression is the following:

$$\exp -2\pi^2(U_{11}h^2a^{*2} + U_{22}k^2b^{*2} + U_{33}l^2c^{*2} + 2U_{12}hka^*b^*\cos\gamma^* + 2U_{13}hla^*c^*\cos\beta^* + 2U_{23}klb^*c^*\cos\alpha^*)$$

where the U_{ij} are the thermal parameters expressed in terms of mean-square amplitudes of vibration in angstroms.

The full-matrix least-squares refinement procedure was fairly similar in all cases. Refinement was carried out in the general sequence of refining scale factors and coordinates, isotropic temperature factors and population parameters, anisotropic temperature factors and final cycles with simultaneous refinement of all variables until convergence. During the final stages of the refinement, large-scale Fourier maps of electron density were prepared using the observed structure factors and phase information from the refinement at that stage, in order to detect details such as splitting of atoms, which could lead to better models for the structures.

Interatomic distances and angles were computed and their associated standard deviations were obtained from errors both in atomic positions and cell parameters.

Refinement of crystal structures involves expensive computing time and since many structures were refined in this project the cost was kept to a minimum by not using the unobserved reflections and by weighting the observed reflections equally.

CHAPTER 4

CRYSTAL STRUCTURES OF MINERALS IN THE SODALITE GROUP

4.1 Sodalite

4.1.1 Introduction:

Sodalite is the type structure for all the minerals in the sodalite group, the helvite group and tugtupite. Furthermore, it is the type structure of many synthetic sodalite-like phases and is also related to complicated structures such as α-Mn, Sb_2Tl_7, etc. (Nyman and Hyde, 1981) in that, by tilting the framework tetrahedra through various angles equivalent frameworks are obtained. Complete structures are obtained by filling the large interstices in these frameworks with various atoms and/or atom groups. Moreover, detailed structural effects which arise from the structure as a whole, can provide parameters necessary to calculate other sodalite-type structures. Sodalite is cubic, with the space group $P\bar{4}3n$ and is of the ideal formula $Na_8(Al_6Si_6O_{24})Cl_2$. The structure is a typical alumino-silicate consisting of equal numbers of linked Si and Al-O tetrahedra in which all the oxygens are shared. The linkage of the $(Al,Si)O_4$ tetrahedra results in cage-like cubo-octahedral units bounded by eight rings of six-tetrahedra parallel to {111} and six rings of four-tetrahedra parallel to {100}. Each of the four- and six-membered rings are shared by two cages. There are two cages per unit cell. The six-membered rings form a set of

channels parallel to the cube body diagonals which intersect at the corners and centres of the unit cells to form large cavities, at the centre of which chlorine is located. The chlorine ions are tetrahedrally coordinated by sodium ions which are situated on the cube body diagonals. Figure 4.1.1 shows the complete sodalite structure and Figure 4.1.2 shows the four-fold coordination of a sodium ion.

The structure of sodalite was described by Barth (1926, 1927, 1932), by Pauling (1930) and it was refined to an isotropic R-factor of 8.2% by Lons and Schulz (1967) using three-dimensional film data.

4.1.2 Experimental:

The sodalite used in this investigation is from Bancroft, Ontario. The chemical analysis (Table 4.1.1) shows that its composition is close to ideal. Cell parameters were determined by least squares refinement of fifteen reflections that were aligned on an automatic 4-circle diffractometer. These parameters are presented in Table 4.1.1, together with other information pertinent to X-ray data collection and refinement.

A regular cleavage fragment mounted on a Nicolet P3 diffractometer was used to collect the intensity data. A total of 1558 intensities were measured to give an asymmetric set of 309 unique reflections of which 157 were classified as observed. The extinct reflections (Structure Factor Table, Appendix 1) and precession photographs confirm the space group $P\bar{4}3n$.

4.1.3 Refinement:

The initial positional and isotropic temperature factors were those of Lons and Schulz (1967) and atomic scattering factors for

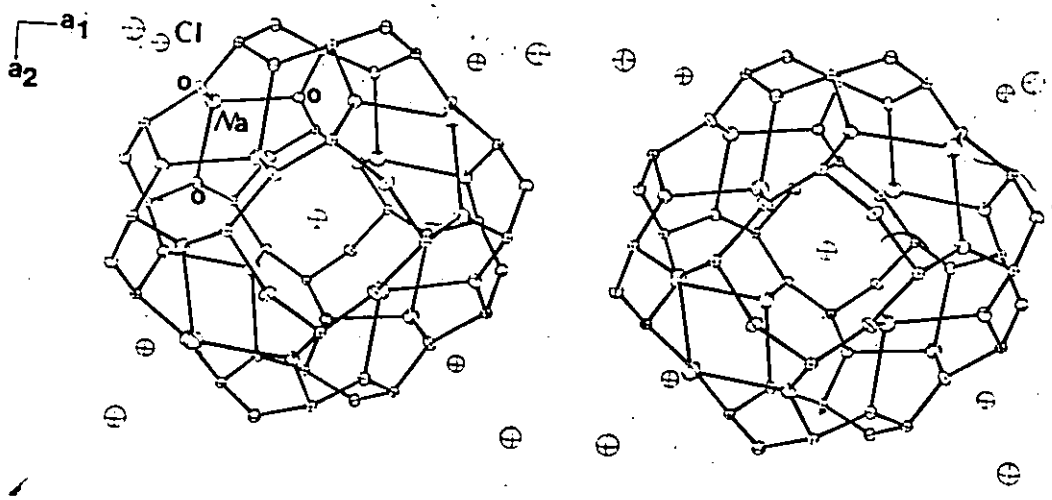

Fig. 4.1.1: Stereographic projection of the sodalite structure viewed down the a_3-axis. Chlorine is at the centres and corners of the cell and sodium is attached to the oxygens of the six-membered rings and chlorine (Na-Cl bond is not shown).

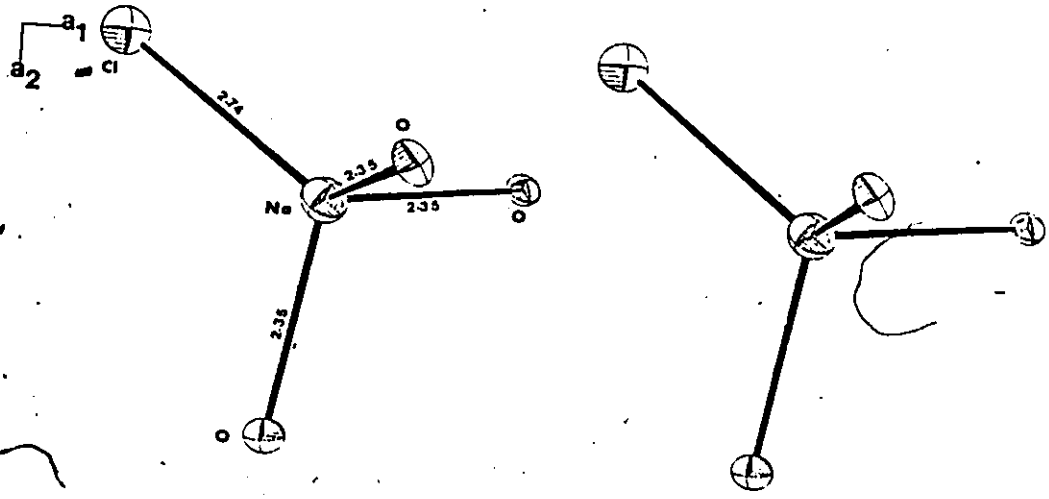

Fig. 4.1.2: Stereographic drawing in the vicinity of the Na site showing its four-fold coordination in sodalite.

Table 4.1.1: Crystal data and data collection information for sodalite from Bancroft+

Chemical Analysis++		Cell Contents**		Miscellaneous	
Si_2O_3	36.55	Si	5.928	a (Å)	8.8823(7)
Al_2O_3	31.78	Al	6.072	v ($Å^3$)	700.8
Na_2O	25.30	Na	7.952	Space group	$P\bar{4}3n$
CaO	0.25	Ca	0.043	Z	1
Fe_2O_3	0.19	Fe	0.023	Density calc. (gcm^{-3})	2.30
K_2O	0.10	K	0.021	Crystal size (mm)	0.20 x 0.23 x 0.23
MnO	0.01	Mn	0.001	Linear absorption coefficient, μ (cm^{-1})	9.5
MgO	0.19	Mg	0.046	Radiation/Monochromator	Mo/C
Cl	5.94	Cl	1.632	Total no. of I	1558
S	0.02	S	0.006	No. of non-equivalent	309
	100.33			No. of non-equivalent $\lvert F_{obs}\rvert > 3\sigma$	157
O=Cl,S	0.86				
wt. %	99.47				

Isotropic refinement

$R_{(obs)} = 2.2\%$

$R_{w(obs)} = 2.4\%$

Anisotropic refinement

Final $R_{(obs)} = 1.7\%$

Final $R_{w(obs)} = 2.1\%$

Chemical formula used in refinement

$Na_8(Al_6Si_6O_{24})Cl_2$

\+ McMaster Collection

++ X-ray Fluorescence, O. Mudrock, McMaster University

** Calculated from chemical analysis based on Si + Al = 12

neutral atoms were taken from Cromer and Mann (1968).

A full-matrix least-squares refinement was made by varying the atomic positions, the isotropic temperature factors and the scale factor. The refinement was constrained to the idealized formula and the structure converged at an R-factor of 2.2%. The temperature factors were then converted to the anisotropic form and further cycles of refinement varying all the refinable parameters resulted in a final R-factor of 1.7%. The refined values of the population parameters agree well with the ideal formula and except for Cl, with the chemical analysis which shows 1.6 instead of 2 chlorine per cell (Table 4.1.1).

The final atomic positions and isotropic temperature factors are given in Table 4.1.2 and final anisotropic temperature factors are listed in Table 4.1.3. Interatomic distances and angles are presented in Table 4.1.4 and included in these tables, for comparison with the present result, are the data of Lons and Schulz (1967). Structure factors are presented in Appendix 1.

4.1.4 Discussion:

The general features of the structure have been described in the Section 4.1.1 and the important distances and angles are shown in Table 4.1.4.

Recently, sodalite models (Taylor and Henderson, 1978; Henderson and Taylor, 1978; Dempsey and Taylor, 1980) have been developed based on the results of Lons and Schulz (1967). To evaluate the confidence that can be placed on these models, we must evaluate the accuracy of Lons and Schulz (1967) data.

The cell edge reported by Lons and Schulz (1967) is markedly

Table 4.1.2: Atomic parameters and isotropic temperature factor ($\times 10^4$) for sodalite

Atom	Site		Present Work	Lons and Schulz (1967)	Total Change
Na	8(e)	x	0.1778(2)	0.1777	+0.0001
		y	0.1778	0.1777	
		z	0.1778	0.1777	
		U	196(5)	189	+7
Cl	2(a)	x	0	0	
		y	0	0	
		z	0	0	
		U	247(5)	241	+6
Si	6(c)	x	$\frac{1}{4}$	$\frac{1}{4}$	
		y	$\frac{1}{2}$	$\frac{1}{2}$	
		z	0	0	
		U	75(5)	44	+31
Al	6(d)	x	$\frac{1}{4}$	$\frac{1}{4}$	
		y	0	0	
		z	$\frac{1}{2}$	$\frac{1}{2}$	
		U	83(5)	101	-18
O	24(i)	x	0.1390(3)	0.1401	-0.0011
		y	0.1494(3)	0.1487	+0.0007
		z	0.4383(2)	0.4385	-0.0002
		U	120(4)	113	+7
a(Å)			8.8823(7)	8.870(4)	+0.0123

Table 4.1.3: Anisotropic temperature factors (x 10^4) for sodalite.

Atom	U_{11}	U_{22}	U_{33}	U_{12}	U_{13}	U_{23}
Na	198(5)	198	198	11(5)	11	11
Cl	249(5)	249	249	0	0	0
Si	77(10)	80(5)	80	0	0	0
Al	74(11)	85(6)	85	0	0	0
O	137(16)	113(16)	115(8)	43(7)	2(13)	-6(14)

different from that obtained from the present study and also from that of Taylor and Henderson (1978). The difference cannot be due to composition since this does not vary significantly. Furthermore, there are significant differences in the oxygen fractional coordinates (Table 4.1.2). Therefore, there are differences in the bond-lengths that occur in the second decimal place (Table 4.1.4). As a result of these discrepancies, models based on Lons and Schulz (1967) data can only be regarded as approximate.

Moreover, Lons and Schulz (1967) reported isotropic temperature factors differing by almost 50% for Al and Si. This symptom is usually indicative of Al being incorrectly assigned to a site occupied by Si. It should be noted that Schulz (1970) transformed the coordinates of Lons and Schulz (1967) incorrectly. Either the Al and Si position or the oxygen x and y parameter should have been interchanged.

The Al-O and Si-O distances of 1.742 and 1.620Å respectively indicate complete Al-Si order. Each sodalite cage contains one Cl at the center tetrahedrally coordinated at 2.736Å to four Na displaced

Table 4.1.4: Interatomic distances and angles in sodalite

	Present Study	Lons and Schulz (1967)	Total Change
	Silicon tetrahedra:		
Si-O	4 x 1.620(2)Å	1.628(4)	-0.008
O-O	4 x 2.616(3)	2.629(8)	-0.013
	2 x 2.701(3)	2.714(8)	-0.013
Mean	2.644	2.657	-0.013
O-Si-O	4 x 107.7(1)°	107.7	0
	2 x 113.0(1)	113.0	0
Mean	109.5	109.5	0
	Aluminum tetrahedra:		
Al-O	4 x 1.742(2)Å	1.728(4)	+0.014
O-O	4 x 2.831(3)	2.806(8)	+0.025
	2 x 2.871(3)	2.855(8)	+0.016
Mean	2.844	2.822	+0.022
O-Al-O	4 x 108.7(1)°	108.5	+0.2
	2 x 111.0(1)	111.3	-0.3
	109.5	109.5	0
Si-O-Al	138.2(1)°	138.3	-0.1
Si-Al	3.140(1)Å	3.136	+0.004
Al/Si-O	1.681	1.678	+0.003
ϕ_{Si}	23.9°	23.7	+0.2
ϕ_{Al}	22.4	22.5	-0.1
	Sodium tetrahedra		
Na-Cl	2.736(1)Å	2.730(4)	+0.006
Na-O	3 x 2.353(2); 3x3.078(2)	2.351(8)	+0.002
Cl-O	3 x 4.294(1)		
O-O	3 x 3.696(3)		
Cl-Na-O	3 x 114.9(1)°		
O-Na-O	3 x 103.5(1)		

inwards from four of the eight six-membered rings (Fig. 4.1.1). Each Na atom is bonded tetrahedrally to one Cl atom at 2.736Å and to three framework oxygen atoms at 2.353Å. Therefore each Na-anion tetrahedron is appreciably distorted into a trigonal pyramid (Fig. 4.1.2). Each six-membered ring has only one neighbouring Na atom and the ring is strongly distorted so that three framework oxygen atoms are at 2.353Å and three at 3.678Å from a Na atom. This distortion results from the Cl atom which pulls the Na atom about 1.11Å from the mean plane of the six-membered ring into the sodalite cage.

4.2 Helvite Group

4.2.1 Introduction:

Minerals of the helvite group have a general formula $(Mn,Fe^{2+},Zn)_8(Be_6Si_6O_{24})S_2$. The Mn end-member is helvite, Fe is danalite and Zn is genthelvite. These minerals are cubic with space group $P\bar{4}3n$. Their structure is isotypic with sodalite. The Al atoms of the sodalite structure may be considered to be replaced by Be, the Na by Mn, Fe^{2+} or Zn, and the Cl by S (Pauling, 1930).

Helvite was reported to have space group $P\bar{4}3n$, by Barth (1926) and Gottfried (1927). Both of these authors noted that helvite appeared to be isotypic with sodalite. Pauling (1930) determined the structure of helvite from Schwarzenberg, Saxony. A sample of helvite from the same locality was refined by Holloway et al. (1972) to an anisotropic R-factor of 4.0%.

The helvite group of minerals are a source of beryllium. They occur in iron-rich skarns, greisens, and related metasomatic rocks (Glass et al., 1944; Beus, 1966; Dunn, 1976). Glass et al. (1944) described the general mineralogy of the helvite group and recently, Dunn (1976) also studied its mineralogy and in particular, its chemistry. He plotted seventy-five new analyses of members of the helvite group and fifty-seven analyses from the literature and concluded that there is complete miscibility between the Fe and Zn members and between the Fe and Mn members but not between Mn and Zn members. The latter could not be explained. Although he examined samples from various localities around the world, he did not find pure danalite. The closest approach to 'danalite' in analyzed natural specimens is 87 mole percent of the Fe

end member (Dunn, 1976). In a laboratory study (Mel'nikov et al., 1968), danalite was the only end member of the helvite group that could not be synthesized.

The above data might suggest that end-member danalite is unstable. This uncertainty cannot be determined without further experimental work. However, structural work may provide an explanation for the absence of miscibility between the Mn and Zn members and may be able to predict the existence of pure danalite.

4.2.2 Experimental:

Minerals of the helvite group used in this investigation are from various localities (Table 4.2.1). The six samples selected for structural

Table 4.2.1: Localities of minerals

No.	Mineral Name	Locality	ROM+ Collection No.
1	Helvite	Lexington Mine, Butte, Montana	M30349
2	Helvite	Sunnyside, San Juan Co., Colorado	M36390
3	Danalite	Mt. Francisco Pegmatite, Ribawa Area, Western Australia	M37261
4	Danalite	Government, Connway, New Hampshire	M34769
5	Genthelvite	Diamond Hill, Rhode Island	M37267
6	Genthelvite	Mt. St. Hilaire, Rouville Co., Quebec	M32727

+ Specimens courtesy of the Royal Ontario Museum.

study cover a range of composition and cell edges. The chemical analyses (Table 4.2.2) of the minerals were taken from Dunn (1976) since they correspond to samples from the same localities. However, Dunn's (1976) analyses were re-calculated on the basis of 12 (Be + Al + Si), the unit cell contents. On this basis, the sums of the interframework cations are consistently higher than 8.0; the Be is also higher than six while the Si is lesser than six consistently. If the analyses were recalculated on the basis of 26(O + S) the same trends would exist. Thus these analyses are not quite accurate.

Cell parameters were determined by least-squares refinement of at least 15 reflections that were aligned on an automatic 4-circle diffractometer. These parameters are presented in Table 4.2.3, together with other information pertinent to X-ray data collection and refinement.

Regular cleavage fragments of maximum dimension less than 0.25mm were used to collect the intensity data. The crystals were mounted either on a Nicolet P3 or Syntex $P2_1$ diffractometer. Reflections were collected from an octant of reciprocal space up to a maximum 2θ of 65°. Table 4.2.3 lists the total number of measured intensities, the number of unique and the number of observed reflections for each crystal.

4.2.3 Refinement:

For helvite (M30438), the initial parameters were those of Holloway et al. (1972) and thereafter, the results of the mineral closest in composition was used. Atomic scattering factors for neutral atoms were taken from Cromer and Mann (1968).

The full matrix least squares refinement was similar in all cases. The first stage involved the refinement of the atomic positions,

Table 4.2.2: Chemical Analyses+ of the Helvite Group Samples

	1. Helvite (M30349)	3. Danalite (M37261)	4. Danalite (M34769)	5. Genthelvite (M37267)	6. Genthelvite (M32727)
ZnO	0.38	4.12	9.68	41.44	54.43
FeO	0.21	24.00	32.07	10.79	0.00
MnO	52.50	24.97	10.65	1.93	0.95
CaO	0.17	0.05	0.04	0.10	0.08
Na_2O	--	--	--	--	--
BeO	13.51	13.40	13.29	12.79	12.58
SiO_2	31.29	30.56	30.71	29.97	29.66
Al_2O_3	0.33	0.10	0.02	--	--
S	5.65	5.73	5.54	5.64	5.61
Cl	--	--	--	--	--
Total*	101.22	100.08	99.23	99.84	100.51
	Number of ions on the basis of 12(Al + Be + Si)				
Zn	0.05	0.58	1.37	6.05	8.05
Fe	0.03	3.83	5.14	1.78	0.00
Mn	8.32 8.43	4.04 8.46	1.73 8.25	0.32 8.17	0.16 8.23
Ca	0.03	0.01	0.01	0.02	0.02
Na	--	--	--	--	--
Be	6.07	6.14	6.11	6.07	6.06
Si	5.85 11.99	5.83 11.99	5.88 11.99	5.93 12.00	5.94 12.00
Al	0.07	0.02	0.00	--	--
S	1.98	2.05	1.99	2.09	2.11
Cl	--	--	--	--	--

+ Analyses for the helvite group are from Dunn (1976)
* All totals less O=S,Cl
Note: No chemical analysis available for sample #2.

Present #	Dunn's #	Location
1	46	Lexington Mine, Butte, Montana
3	74	Mt. Francisco, Australia
4	33	Government Pits, North Conway, N.H.
5	16	Cumberland, Rhode Island
6	2	Mt. St. Hilaire, Quebec, Canada

Table 4.2.3: Crystal data and data collection information for minerals in the helvite group.

Miscellaneous	1. Helvite (M30348)	2. Helvite (M36390)	3. Danalite (M37261)	4. Danalite (M34769)	5. Genthelvite (M37267)	6. Genthelvite (M32727)
a(Å)	8.2913(6)	8.2365(4)	8.2317(9)	8.2183(2)	8.1493(5)	8.1091(4)
V(Å^3)	570.0	558.8	557.9	555.1	541.2	533.2
Space group	←	←	$P\bar{4}3n$	→	→	→
Z	←	←	1	→	→	→
Density$_{calc}$ (gcm^{-3})	3.23	---	---	---	---	3.72
Crystal size (mm)	0.1 x 0.13 x 0.15	0.15 x 0.2 x 0.2	0.15 x 0.15 x 0.2	0.12 x 0.15 x 0.20	0.2 x 0.2 x 0.2	0.12 x 0.16 x 0.18
μ(cm^{-1})	49.7	---	---	---	---	96.7
Radiation /Monochromator	←	←	Mo/C	→	→	→
Total no. of I	1283	1273	1271	1271	1224	1214
No. of non-equivalent	256	254	254	254	245	243
No. of non-equivalent $\|F_{obs}\| > 3\sigma$	156	163	166	162	164	153
Isotropic Refinement R(%)	2.5	3.7	2.6	2.7	2.6	2.9
Isotropic Refinement Rw(%)	3.2	4.3	2.9	3.2	3.2	3.3
Anisotropic Refinement R(%)	2.4	2.9	2.4	2.5	2.5	2.8
Anisotropic Refinement Rw(%)	3.1	3.7	2.7	3.1	3.1	3.4

the isotropic temperature factors and the scale factor, using unit weighting; then the isotropic temperature factors were converted to the anisotropic form and the refinement continued until convergence. The R-factors at convergence in both stages are given in Table 4.2.3. Finally, as a check on the chemical analyses, the population parameters of Si, S and the dominant interframework cation were introduced as variables and refined together with their temperature factors.

The population parameter obtained for Si in each case is 1.00(1). The values of the population for the total amount of interframework cation, C, in terms of the dominant element, is very close to 1.0 (Table 4.2.5). This site is thus completely filled. In refining the population of S, it was observed that the isotropic temperature factor decreased and thus a value of less than 1.0 was obtained. However, there was no value less than 0.92 for any structure; in fact, much higher values were obtained for most structures. Therefore, this site is also completely filled.

It was not worthwhile to calculate the relative amounts of Mn and Fe from the refinement since they have a difference of only one electron and also Zn may be present. Moreover, none of the danalites used in this study had appreciable Zn while the genthelvites contained essentially Zn. Hence the relative amounts of Fe and Zn were not determined from the refinement. Furthermore, it was not possible to obtain a good refined value for the population of Be.

Danalite (M37261) was classified as helvite by Dunn (1976). However, the refinement gave population and R-values of 1.06(1) and 2.4% respectively in terms of Fe; and 1.12(1) and 2.5% respectively in terms of Mn; thus indicating that this sample is danalite-rich.

The final atomic parameters and isotropic temperature factors are given in Table 4.2.4 and the final anisotropic temperature factors are listed in Table 4.2.5. Interatomic distances and angles are presented in Table 4.2.6. Included in these Tables, for comparison with the present results, are data from a refinement of the crystal structure of helvite (Holloway et al., 1972). Structure Factor Tables are presented in Appendix 1.

4.2.4 Discussion:

The general features of the structures of minerals in the helvite group are similar to those of sodalite. The silicon tetrahedra have dimensions that are slightly larger than those in sodalite while the beryllium tetrahedra are only slightly larger. The helvite group of minerals show temperature factors that range from similar magnitude as in sodalite (compare helvite (M30349)) to decreasing values in genthelvite (Table 4.2.4). This trend parallels the increase in linear absorption (Table 4.2.3).

The six members which were investigated in the helvite group cover the entire range of cell dimensions-- from pure helvite (8.2913Å) to pure genthelvite (8.1091Å). Although the range in cell edges is quite small (0.1822Å) compared to sodalites (0.0884Å), (Henderson & Taylor, 19 the framework tetrahedra dimensions are statistically constant throughout the isomorphous series. In particular, the two equal O-O distances in the respective framework tetrahedra, the Si-O and Be-O distances are all constant within the experimental errors (Table 4.2.7). It will be shown in Chapter 5 that these four distances are sufficient and necessary to calculate the framework geometry in the helvite group, providing the cell edge is known.

Table 4.2.4: Atomic parameters, site populations and isotropic temperature factors ($\times 10^4$) for the helvite group of minerals

		Helvite*	Helvite (M30349)	Helvite (M36390)	Danalite (M37261)	Danalite (M34769)	Genthelvite (M37267)	Genthelvite (M32727)
a(Å)		8.294(7)	8.2913(6)	8.2365(4)	8.2317(9)	8.2183(2)	8.1493(5)	8.1091(4)
Cavity cation Coordinate	x	0.1693(1)	0.1709(1)	0.1687(1)	0.1693(1)	0.1687(1)	0.1674(1)	0.1668(1)
Oxygen Coordinates	x	0.1404(3)	0.1407(6)	0.1393(6)	0.1395(4)	0.1394(5)	0.1382(6)	0.1377(7)
	y	0.1418(3)	0.1411(6)	0.1400(6)	0.1401(5)	0.1400(5)	0.1385(6)	0.1381(7)
	z	0.4171(4)	0.4168(4)	0.4134(4)	0.4126(3)	0.4114(4)	0.4029(4)	0.4060(5)
Population Parameters in terms of the dominant cavity cation C			$0.97(1)_{Mn}$	$1.03(1)_{Mn}$	$1.06(1)_{Fe}$ $1.12(1)_{Mn}$	$1.05(1)_{Fe}$	$1.00(1)_{Zn}$	$1.00(2)_{Zn}$
Isotropic temperature factors ($U \times 10^4$)	C	127	79(1)	82(3)	69(2)	68(2)	60(2)	59(3)
	S	150	112(5)	140(9)	103(7)	96(5)	68(7)	62(14)
	Si	72	72(6)	46(6)	32(5)	31(4)	25(4)	36(8)
	Be	109	85(26)	77(29)	65(21)	69(17)	57(19)	59(24)
	O	82	100(7)	79(8)	66(7)	63(6)	49(7)	61(12)

* Data from Holloway et al. (1972).

C = cavity cation (Mn, Fe, Zn)

Table 4.2.5: Anisotropic temperature factors (x 10^4) for the helvite group of minerals.

		Helvite*	Helvite (M30349)	Helvite (M36390)	Danalite (M37261)	Danalite (M34269)	Genthelvite (M37267)	Genthelvite (M32727)
	U_{11}	127(3)	79(3)	82(3)	69(2)	68(3)	60(2)	59(3)
	U_{22}	127	79	82	69	68	60	59
	U_{33}	127	79	82	69	68	60	59
C	U_{12}	17(3)	2(3)	18(3)	3(2)	4(3)	5(2)	3(3)
	U_{13}	17	2	18	3	4	5	3
	U_{23}	17	2	18	3	4	5	3
	U_{11}	150(7)	112(8)	140(9)	103(7)	96(8)	68(7)	65(9)
	U_{22}	150	112	140	103	96	68	65
	U_{33}	150	112	140	103	96	68	65
S	U_{12}	0	0	0	0	0	0	0
	U_{13}	0	0	0	0	0	0	0
	U_{23}	0	0	0	0	0	0	0
	U_{11}	63(17)	62(14)	50(15)	37(12)	34(14)	30(15)	33(18)
	U_{22}	77(10)	77(9)	44(8)	29(7)	30(8)	23(8)	40(10)
	U_{33}	77	77	44	29	30	23	40
Si	U_{12}	0	0	0	0	0	0	0
	U_{13}	0	0	0	0	0	0	0
	U_{23}	0	0	0	0	0	0	0
	U_{11}	104(70)	69(63)	85(75)	78(58)	97(69)	66(72)	24(82)
	U_{22}	57(40)	93(35)	74(38)	59(30)	55(34)	53(37)	79(46)
	U_{33}	57	93	74	59	55	53	79
Be	U_{12}	0	0	0	0	0	0	0
	U_{13}	0	0	0	0	0	0	0
	U_{23}	0	0	0	0	0	0	0
	U_{11}	70(13)	109(23)	77(24)	70(19)	71(22)	50(24)	67(32)
	U_{22}	73(13)	114(23)	83(25)	68(19)	70(22)	57(24)	77(33)
	U_{33}	104(13)	77(13)	78(14)	58(11)	47(13)	40(14)	38(16)
O	U_{12}	40(13)	24(13)	31(13)	23(10)	26(11)	22(12)	27(14)
	U_{13}	10(10)	4(17)	12(18)	12(14)	8(15)	22(16)	-15(21)
	U_{23}	-10(10)	-24(17)	4(18)	12(14)	9(15)	14(16)	-24(21)

* Holloway et al. (1972).

Table 4.2.6: Interatomic distances and angles in the helvite group of minerals

		Helvite*	Helvite (M30349)	Helvite (M36390)	Danalite (M37261)	Danalite (M34769)	Genthelvite (M37267)	Genthelvite (M32727)	Selected averages
a(Å)		8.294(7)	8.2913(6)	8.2365(4)	8.2317(9)	8.2183(2)	8.1493(5)	8.1091(6)	
SiO_4 tetrahedra									
Si-O	4 x	1.623(3)Å	1.629(4)	1.627(5)	1.629(4)	1.631(4)	1.630(4)	1.628(5)	1.629
O-O	4 x	2.622(4)	2.634(6)	2.634(6)	2.635(5)	2.637(6)	2.640(6)	2.636(8)	2.636
	2 x	2.704(6)	2.711(6)	2.703(6)	2.710(5)	2.714(6)	2.706(6)	2.703(7)	2.708
O-Si-O	4 x	107.8(1)°	107.9(2)	108.1(2)	107.9(2)	107.9(2)	108.1(2)	108.1(2)	2.660 Mean
	2 x	112.9(2)	112.7(2)	112.3(2)	112.6(2)	112.7(2)	112.2(2)	112.2(3)	
BeO_4 tetrahedra									
Be-O	4 x	1.638(3)Å	1.633(4)	1.634(5)	1.636(4)	1.637(4)	1.633(4)	1.632(5)	1.634
O-O	4 x	2.649(4)	2.641(6)	2.646(6)	2.647(5)	2.649(6)	2.645(6)	2.643(7)	2.645
	2 x	2.725(6)	2.717(6)	2.712(6)	2.719(5)	2.723(6)	2.710(6)	2.708(7)	2.715
O-Be-O	4 x	107.9(1)°	107.9(2)	108.1(2)	108.0(2)	108.0(2)	108.1(2)	108.2(2)	2.668 Mean
	2 x	112.6(2)	112.6(2)	112.2(2)	112.4(2)	112.5(2)	112.2(2)	112.1(3)	
Si-O-Be		128.2(2)°	128.0(2)	126.5(2)	126.1(2)	125.5(2)	124.0(2)	123.1(2)	
Si-Be		2.932 Å	2.9314(1)	2.9121(1)	2.9104(2)	2.9056(1)	2.8812(1)	2.8670(1)	
Si/Be-O		1.631	1.631	1.631	1.633	1.634	1.632	1.630	1.632
ϕ_{Si}		30.6°	30.6	31.9	32.1	32.4	33.7	34.3	
ϕ_{Be}		30.3	30.5	31.7	31.9	32.3	33.6	34.3	
Cavity cation tetrahedra									E_{all}=2.664
C-S		2.432(2)Å	2.4541(5)	2.4067(5)	2.4132(4)	2.4016(4)	2.3624(4)	2.3423(4)	
C-O	3 x	2.082(4)	2.069(3)	2.043(4)	2.033(3)	2.023(3)	1.989(3)	1.968(4)	
S-O	3 x	3.835(5)	3.830(4)	3.774(4)	3.767(3)	3.751(3)	3.687(4)	3.652(4)	
O-O	3 x	3.238(7)	3.235(6)	3.188(6)	3.176(5)	3.159(5)	3.107(6)	3.095(7)	
S-C-O	3 x	116.1(1)°	115.5(1)	115.7(1)°	115.6(1)	115.7(1)	115.6(1)	115.6(2)	
O-C-O	3 x	102.1(1)	102.8(1)	102.6(2)	102.8(1)	102.6(2)	102.7(2)	102.7(2)	

* Holloway et al. (1972)

Table 4.2.7: Deviations of a few bond distances from their mean+ for the helvite group. The standard deviations in parentheses are taken from Table 5.2.6.

	Silicon tetrahedra		Beryllium tetrahedra	
	Si-O	O-O	Be-O	O-O
Mean (Å)	1.629	2.708	1.634	2.715
Sample	Deviations from mean (Å)			
Helvite*	0.006(3)	0.004(6)	-0.004(3)	-0.010(6)
Helvite (M30349)	0.000(4)	-0.003(6)	0.001(4)	-0.002(6)
Helvite (M36390)	0.002(5)	0.005(6)	0.000(5)	0.003(6)
Danalite (M37261)	0.000(4)	-0.002(5)	-0.002(4)	-0.004(5)
Danalite (M34769)	-0.002(4)	-0.006(6)	-0.003(4)	-0.008(6)
Genthelvite (M37267)	-0.001(4)	0.002(6)	0.001(4)	0.005(6)
Genthelvite (M32727)	0.001(5)	0.005(7)	0.002(5)	0.007(7)

+ The mean values do not include data of Holloway et al. (1972) which is indicated by * (see Table 5.2.6).

The rotation angle, ϕ, is the angle through which the framework tetrahedra are rotated relative to their position in the ideal, fully-expanded structure (see Chapter 5). These angles for the helvite group of minerals are listed in Table 4.2.6. The cell edge, the rotation angle of the tetrahedra and the Be-O-Si angle for the helvite group of minerals are directly related to the interframework cations since these are the only variables in the isomorphous series.

The effective ionic radii for four-fold coordination for the interframework cations, C, vary as follows: Mn^{2+} H.S. 0.66 > Fe^{2+} H.S. 0.63 > Zn^{2+} 0.60 (Shannon, 1976). The Mn and Fe are in high-spin state due to their tetrahedral crystal field. Going from the Mn-member through the Fe-member to the Zn-member, the cation radius decreases and hence the effective charge increases. As a result, the following parallel trends are observed:

(1) The framework tetrahedra rotation angle increases, that is, the framework collapse increases.

(2) The cell edge decreases.

(3) The Be-O-Si angle decreases.

(4) The cation-sulphur bond length decreases.

(5) The cation-oxygen bond length decreases.

(6) All the dimensions of the SC_4 tetrahedra decrease.

The same trends hold for intermediate members in the helvite group. For these members, weighted average cation radii may be used and parameters for pure danalite should be mid-way between the pure Mn- and Zn-members since Fe^{2+} radius is the mean of Mn^{2+} and Zn^{2+}. As a result, the difference in rotation angle between the Mn- and Fe-members and

between the Fe-Zn members is about 2^{o} and that between the Mn- and Zn-members is about 4^{o}. The small differences in rotation angles compared with those of the NaCl end-member and KCl end-member sodalites (Chapter 5) suggest that pure danalite should exist and also there should be complete miscibility among the three isomorphous members of the helvite group.

In nature, the Mn member is more common than the Fe^{2+} member while the Zn member is, by far, the rarest (Dunn, 1976). This may be related to the chalcophile-lithophile tendencies of the elements (Burt, 1974). The chalcophile tendencies of the helvite group elements can be expressed as the inequality Zn$\gg$Fe$>$Mn (Marakushev and Bezmen, 1969). This concept explains the tendency for genthelvite to occur in distinctly alkaline, sulphur-poor igneous environments (Burt, 1977), and it also explains the otherwise puzzling gap between the Zn and Mn ends of the helvite series noted by Dunn (1976).

4.3 Hydroxysodalite

4.3.1 Introduction:

Hydroxysodalite is cubic with the space group $P\bar{4}3n$ and has one formula unit, $Na_8\ Al_6Si_6O_{24}\ (OH)_2.2H_2O$ per unit cell. The structure is isotypic with sodalite, $Na_8\ Al_6Si_6O_{24}\ Cl_2$. Many sodalite group minerals are polymorphic with cancrinites and in particular, hydroxy-cancrinite has exactly the same composition as that of hydroxysodalite, the latter being the higher temperature polymorph (Van Peteghen and Burley, 1962 and Anderson and Burley, 1981). This can be rationalized solely on the different frameworks.

Bukin and Makarov (1967) reported a neutron diffraction structure of a synthetic hydroxysodalite (a = 8.887Å) having an unusual chemical composition:

$$Na_{7.1}\ Al_6\ Si_{5.5}(H_4)_{0.5}\ O_{24}\ Cl_{0.4}(OH)_{0.7}.0.7H_2O.$$

They concluded that 1/12 of the SiO_4 tetrahedra was substituted statistically by tetrahedral H_4O_4 groups with definite hydrogen bonds and that the OH and Cl anions occupy different sites. They could not find the $0.7H_2O$ reported by the chemical analysis and the OH group was placed on the three-fold axes in the Na vacancies.

Galitskii et al. (1973a) used the proton magnetic resonance to study the composition and localization of OH and H_2O in a synthetic hydroxysodalite. They found no H_4O_4 group and suggested an idealized formula: $Na_8\ Al_6Si_6O_{24}\ (OH)_2.6H_2O$.

They also indicate that the OH and H_2O occupied the 8(e) position, x = 0.80. This position was reconfirmed by Galitskii et al. (1973b) using

the NMR spectra of ^{23}Na. They also concluded that the symmetry was trigonal polar at -120°C and that circular diffusion and reorientation of hydrogen bonds occurred. Moreover, at 275°C the Na was diffusing with an estimated energy barrier of 75 kJ/mole.

4.3.2 Experimental:

The synthetic hydroxysodalite used in this investigation was prepared at 15,000 p.s.i. total pressure and at 450°C (see Anderson and Burley, 1981).

Precession photographs show that all the observed diffraction maxima are sharp. No superstructure reflections were observed. These photographs also show symmetry which is consistent with the space group $P\bar{4}3n$. Cell parameter determined by least-squares refinement of at least 15 reflections aligned on a 4-circle automatic diffractometer is presented in Table 4.3.1, together with other information pertinent to x-ray data collection and refinement.

A regular cleavage fragment of dimensions 0.17 x 0.20 x 0.23 mm was used to collect the intensity data. The crystal was mounted on a Nicolet P3 4-circle x-ray diffractometer. A total of 1570 intensities were measured to give an asymmetric set of 310 unique reflections of which 152 were classed as observed. The extinct reflections also confirm the space group as $P\bar{4}3n$ (see Structure Factor Table 5 in Appendix I).

4.3.3 Refinement:

Initial positional parameters and isotropic temperature factors were those of sodalite and atomic scattering factors for neutral atoms were taken from Cromer & Mann (1968).

Table 4.3.1: Crystal data and data collection information for synthetic hydroxysodalite

Chemical Analysis+		Cell Contents++		Miscellaneous	
SiO_2	37.38	Si	5.97	a (Å)	8.8899(1)
				V (Å^3)	702.6
Al_2O_3	32.09	Al	6.03	Space group	$P\bar{4}3n$
				Z	1
Na_2O	25.35	Na	7.84	Density calc. (gcm^{-3})	2.29
H_2O	5.50	H_2O	1.95	Crystal size (mm)	0.17 x 0.20 x 0.20
wt. %	100.32	OH^-	1.95	Linear absorption coefficient, μ (cm^{-1})	7.75
				Radiation/Monochromator	Mo/C
				Total no. of I	1570
				No. of non-equivalent	310
				No. of non-equivalent $\lvert F_{obs}\rvert > 3\sigma$	152

Isotropic refinement

$R_{(obs)} = 2.8\%$

$R_{w(obs)} = 3.2\%$

Anisotropic refinement

Final $R_{(obs)} = 2.0\%$

Final $R_{w(obs)} = 2.4\%$

Chemical formula used in refinement

$Na_8Al_6Si_6O_{24}(OH^-)_2.2H_2O$

+ J. Muysson, McMaster University

++ Calculated from chemical analysis based on Si + Al = 12

A full matrix least squares refinement was made on the framework atoms and sodium by varying the atomic positions, the isotropic temperature factors and the scale factor, using unit weighting. This refinement of the partial structure converged to an R-factor of 4.8% and it shows a geometry which is satisfactorily comparable to that found in sodalite (section 4.1). The temperature factors of these atoms showed nothing unusual. The Na-O distance and the sodium temperature factor were slightly larger than those found in sodalite.

A trial structure was attempted with four oxygens of the OH group and H_2O placed on an O1 site. The O1 site on the 8(e) position with O1: x = 0.9 is a good starting position in terms of both the chemistry and Na-O1 distance. This position was refined to x = 0.9191 and the isotropic temperature factor, U, was 1104 x 10^{-4} $Å^2$. The populations of sites O1 and Na were then refined and were found to be consistent with the chemical analysis (Table 4.3.1). The isotropic model was then converted to the anisotropic form and the refinement continued. On the final cycle after varying all refinable parameters the structure converged with an R-factor of 2.6%. Fourier maps were then examined but nothing was found elsewhere--not even in the 2(a) position (the Cl position in sodalite).

The coordination of sodium is shown in Figure 4.3.1A. The sodium is six-fold coordinated by three framework oxygens and statistically by three O1 oxygens. The O1 oxygens have unusually large temperature factors and their thermal ellipsoids, although approximately spherical, tend to be moving in the direction of the Na-O1 bond rather than at right angles.

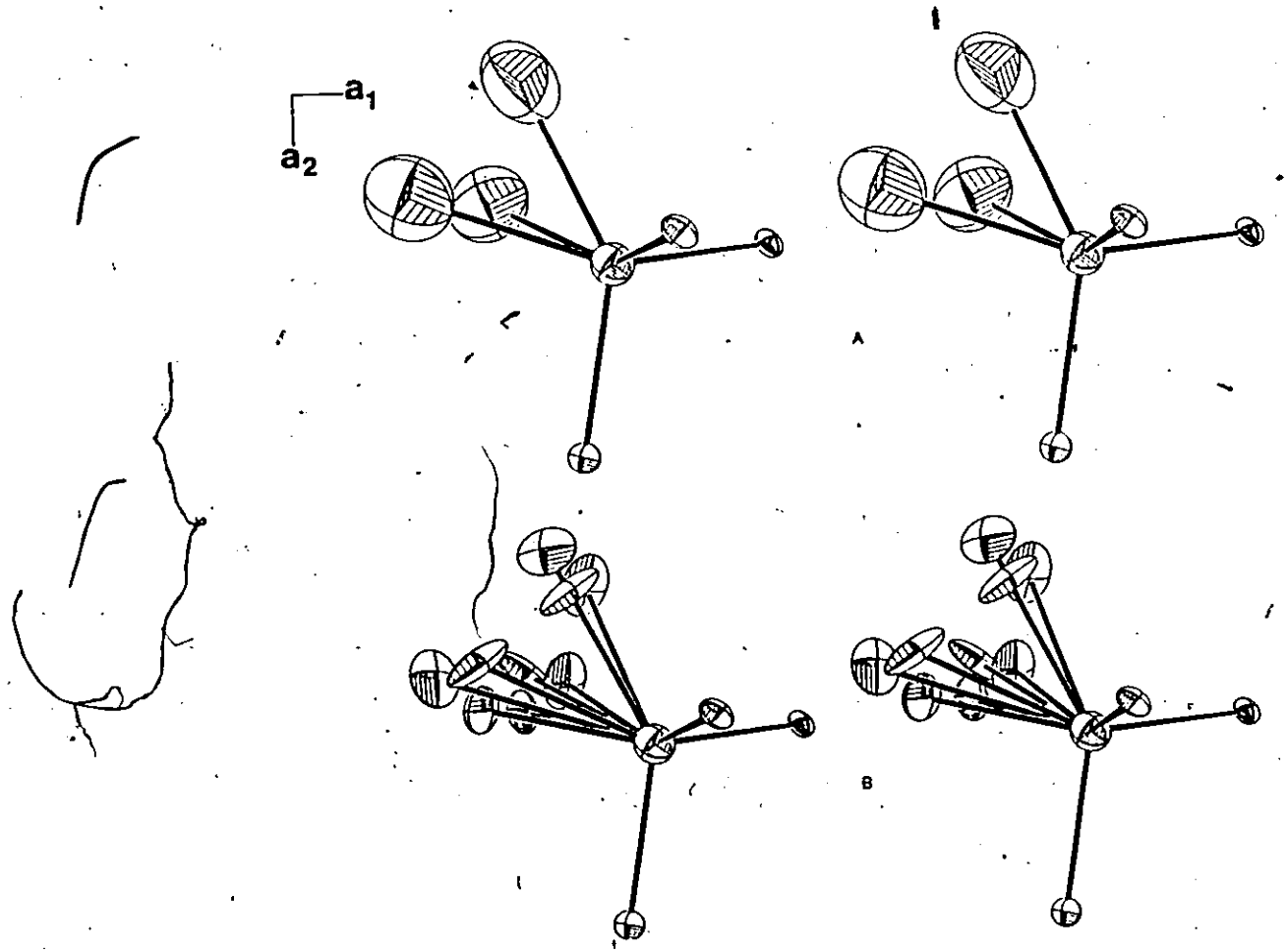

Fig. 4.3.1A: Stereoscopic pair showing the coordination of the Na atom by framework oxygens (small ellipsoids) and O(1) oxygens of the OH and H_2O anions (O(1) on the 8(e) position). The rotation about a_2 is 20°.

Fig. 4.3.1B: Same as Fig. (A) but with the O(1) oxygen disordered on the 24(i) position. Each O(1) in (A) is by symmetry represented by 3 positions in (B).

Interatomic distances and bond strength calculation (Brown and Shannon, 1973) of this trial structure are given in Table 4.3.2. The Al and Si cations are charge-balanced and accordingly these sites have full occupancy. The framework oxygen have a valence of 1.95 v.u. instead of 2.0 v.u. and the sodium cation have a valence of 0.77 v.u. instead of 1.0 v.u. Moreover, on considering oxygen-oxygen contact distance we find that the O1-O1 distance is too short to be justifiable. Furthermore, this model would not explain why there are just two water molecules instead of the theoretical maximum of six.

The bond strength calculation show that the framework oxygens are slightly underbonded and the O1-O distance is quite large (Table 4.3.2) suggesting very weak hydrogen bonding between the O1 oxygens and that of the framework (Brown, 1976). Since each cavity contains one OH group and one H_2O, such hydrogen bonding interactions cannot be locally symmetrical. As a result, the O1 oxygens should move off the 3-fold axes. A similar situation was found in cancrinite (Hassan, 1980; Grundy and Hassan, 1982). Consequently, the O1 site was disordered about the 3-fold axes and the refinement was recommenced and on the final cycle after varying all the refinable parameters, the structure converged with a final R-factor of 2.0%. The decrease in R-factor from 2.6 to 2.0 for the two models is significant at the 0.005 (0.5%) level of significance according to the Hamilton's test.

The observed and calculated structure factors together with their phase angles are given in Appendix 1; final atomic parameters and isotropic temperature factors are given in Table 4.3.3 and the final anisotropic temperature factors are presented in Table 4.3.4.

Table 4.3.2: Bond distances and bond strengths for trial structure

Bond	Distance(Å)	Bond strength (v.u.)
Si-O	4 x 1.616(3)	4 x 1.019(10)
		Total* 4.075(21)
		Expected** 4.0
Al-O	4 x 1.743(3)	4 x 0.734(7)
		Total 2.938(14)
		Expected 3.0
Na-O	3 x 2.382(2)	3 x 0.194(1)
	3 x 3.079(3)	+ 3 x 0.046(1)
Na-O1	3 x 2.571(30)	+ 3 x 0.5 x 0.126(8)
		Total 0.909(14)
		Expected 1.0
O1-O1	3 x 2.035(47)	
O1-O	3 x 3.451(25)	

Bond strength about O = 1.019 + 0.734 + 0.194 + .046 = 1.993

Expected = 2.0

Bond strength about O1 = 3 x 0.126(8) = 0.378(14)

Expected = 0.50

* universal curves
** Expected from site population

Table 4.3.3: Atomic parameters and isotropic temperature factor ($\times 10^4$) for hydroxysodalite

Atom	Site	x	y	z	U, $Å^2$ (iso)
Na	8(e)	0.1755(2)	0.1755	0.1755	281(8)
O(1)	24(i)	0.0704(64)	0.1178(35)	-0.0526(50)	491(77)
Si	6(c)	$\frac{1}{4}$	$\frac{1}{2}$	0	81(7)
Al	6(d)	$\frac{1}{4}$	0	$\frac{1}{2}$	83(8)
O	24(i)	0.1397(4)	0.1506(4)	0.4399(3)	134(5)

Table 4.3.4: Anisotropic temperature factors ($\times 10^4$) for hydroxysodalite

Atom	U_{11}	U_{22}	U_{33}	U_{12}	U_{13}	U_{23}
Na	285(7)	285	285	13(8)	13	13
O(1)	637(295)	410(136)	385(149)	13(178)	-385(142)	-44(95)
Si	14(27)	121(20)	121	0	0	0
Al	162(39)	49(20)	49	0	0	0
O	125(28)	143(29)	143(10)	55(10)	-9(19)	14(19)

Table 4.3.5: Selected interatomic distances, angles and bond-strength calculation in hydroxysodalite

Silicon tetrahedra:		**Bond-strength (v.u.)**	
Si-O	4 x 1.616(4)Å		4 x 1.019(10)
O-O	4 x 2.604(5)	Total	4.075(21)
	2 x 2.705(5)		
Mean	2.638	Expected	4.0
O-Si-O	4 x 107.4(2)°		
	2 x 113.7(2)		
Mean	109.5		
Aluminum tetrahedra			
Al-O	4 x 1.743(4)Å		4 x 0.734(7)
O-O	4 x 2.829(5)	Total	2.938(14)
	2 x 2.883(6)		
Mean	2.847	Expected	3.0
O-Al-O	4 x 108.4(1)°		
	2 x 111.6(2)		
Mean	109.5		
		Oxygen coordination	
Si-O-Al	138.7(2)		
ϕ_{Si}	23.3	O	= 1.019(10)+0.734(7)+0.194(1)+0.046(1)
ϕ_{Al}	21.8		= 1.993(12)v.u.
Al/Si-O	1.680(Å)	O1	= 0.241(29)+0.148(19)+0.056(3)
Si-Al	3.143		= 0.445(35)v.u.
Sodium-coordination			
Na-O	3 x 2.382(3)Å; 3 x 3.079Å		3 x 0.194(1) + 3 x 0.046(1)
Na-O1	3 x 2.291(46)		0.17 x 3 x 0.241(29)
-O1	3 x 2.496(54)		0.17 x 3 x 0.148(19)
-O1	3 x 2.977(36)		0.17 x 3 x 0.056(3)
O1-O1	2.440(56)	Total	0.947(35)
O1-O	3.287(48)		
-O	3.410(37)	Expected	1.0
-O	3.425(41)		

Table 4.3.6: Deviations of a few bond distances from their mean for sodalite and hydroxysodalite. The standard deviations in parentheses are from hydroxysodalite.

	Silicon tetrahedra		Aluminum tetrahedra	
	Si-O	O-O	Al-O	O-O
Mean Å	1.618	2.703	1.743	2.887
Deviation from mean	±0.002(4)	±0.002(5)	±0.001(4)	±0.006(6)

4.3.4 Discussion:

The framework features of hydroxysodalite are identical to that of sodalite (Table 4.3.6). This aspect of the structure has been described earlier (section 5.1) and only additional details will be presented here. Selected interatomic distances and angles are presented in Table 4.3.5 together with bond-strength calculations (Brown and Shannon, 1973). As pointed out earlier, the tetrahedral bond lengths and bond valence analyses indicate full occupancy and complete ordering of the Al and Si.

According to the chemical analysis, each cavity is occupied by 4 Na, 1(OH) and 1 H_2O. This is consistent with the refined O(1) occupancy of 0.17 atoms per site and full occupancy of the sodium site. Twelve of the possible twenty-four positions for the O(1) oxygen are within a single cavity. For each O(1) position there are eleven associated O(1)-O(1) distances which are 2.44Å, 2.29Å, 2.26Å, 2.26Å, 2.08Å, 2.08Å, 1.91Å, 1.91Å, 1.56Å, 0.73Å and 0.73Å. The location of the

three hydrogen atoms within a cavity could not be determined experimentally. The space group symmetry requires a completely disordered O(1)-O(1) configuration within the cavity and this is consistent with the lack of superstructure.

The co-ordination of sodium for O(1) on the 24(i) position is shown in Figure 4.3.1B and the bond lengths are given in Table 4.3.5. This figure should be compared with the initial model (Fig. 4.3.1A) where the O(1) oxygen is on the body diagonal. The temperature factor of the sodium atom in hydroxysodalite is larger than that in sodalite and this would suggest slight positional disorder.

We can also analyse the cavity contents using bond valence. Each non-framework oxygen is coordinated to three Na atoms at distances of 2.29Å, 2.50Å and 2.98Å. Using the universal curves of Brown and Shannon (1973), three sodium atoms contribute 0.445v.u. to an O(1) oxygen (Table 4.3.5). The total bond-valence requirement of the Na atoms from the non-framework oxygen is approximately 1v.u., which corresponds to two oxygens. The ideal chemical formula of hydroxysodalite is therefore

$$Na_8Al_6Si_6O_{24}(OH)_2.2H_2O.$$

It is likely at high temperatures, that expansion will allow three oxygens into the cavity. However, it is highly improbable that this expansion would be great enough to accommodate more than three oxygens prior to melting. Therefore, depending on the rate of diffusion of H_2O from the structure on cooling we can expect a range of composition from

$$Na_8Al_6Si_6O_{24}(OH)_22H_2O$$

to

$$Na_8Al_6Si_6O_{24}(OH)_2{}^4H_2O.$$

An increase in the size of the cell parameter should reflect the presence of water in excess of 2 molecules.

4.4 Tugtupite

4.4.1 Introduction:

The mineral tugtupite is tetragonal and is of the idealized formula $Na_8(Al_2Be_2Si_8O_{24})Cl_2$ (Danø, 1966; Sørensen, Danø and Patterson, 1971). It is isotypic with the sodalite structure as are the minerals of the helvite group. The framework of tugtupite may be regarded as intermediate in composition between the frameworks of sodalite $(Al_6Si_6O_{24})^{6-}$ and helvite $(Be_6Si_6O_{24})^{12-}$. The tetragonal symmetry is the result of an ordered framework of Al, Be and Si-O tetrahedra.

Danø (1966) determined the space group $I\bar{4}$ for tugtupite with a = 8.538(4); c = 8.817(4), utilizing precession and Weissenberg photographs. He also determined and refined the structure by making full use of the isotypic relationship with the sodalite structure. His refinement of atomic and isotypic temperature factors, based on film-data, resulted in a final R-factor of 8.9%.

Interest in tugtupite arises primarily from the detailed structural effects which result from the framework consisting of three different cations. The structure was re-refined to obtain better parameters for comparison with new structural data on sodalite and the helvite group of minerals.

4.4.2 Experimental:

The tugtupite used in this investigation is from Ilimanssaq, Narssaq Kommune, South Greenland. The chemical analysis given in Table 4.4.1 is taken from Danø (1966) since his sample was one from the same locality. Cell parameters determined by least squares refinement

Table 4.4.1: Crystal data and data collection information for tugtupite (M32790)*

Chemical Analysis+		Cell Contents++		Miscellaneous	
				a (Å)	8.640(1)
				c (Å)	8.873(1)
SiO_2	51.58	Si	7.98	V (Å^3)	662.4
BeO	5.40	Be	2.00	Space group	$I\bar{4}$
				Z	1
Al_2O_3	11.15	Al	2.03	Density calc. gmcm^{-3}	2.34
Na_2O	25.52	Na	7.62	Crystal size (mm)	0.16 x 0.20 x 0.26
K_2O	0.12	K	0.02	Linear absorption coefficient, μ (cm^{-1})	9.56
MgO	0.20	Mg	0.05		
Cl	7.28	Cl	1.90	Radiation/monochromator	Mo/C
S	0.33	S	0.09	Total no. of I	1413
wt. %	101.58			No. of non-equivalent	647
				No. of non-equivalent $\lvert F_{obs}\rvert > 3\sigma$	621
				Isotropic refinement	
				$R_{(obs)}$ = 3.0%	
				$R_{w(obs)}$ = 3.5%	
				Anisotropic refinement	
				Final $R_{(obs)}$ = 2.3%	
				Final $R_{w(obs)}$ = 3.0%	

Chemical formula used in refinement

$Na_8Al_2Be_2Si_8O_{24}Cl_2$

* Specimen courtesy of the Royal Ontario Museum (no. M32790)
\+ Taken from Danø (1966)
++ Calculated from the chemical analysis based on Si + Al = 12

of fifteen high-angle reflections aligned on an automatic 4-circle diffractometer are presented in Table 4.4.1, together with other information pertaining to X-ray data collection and refinement.

The intensity data was collected from a cleavage fragment mounted on a Nicolet P3. Reflections allowable in the space group $I\bar{4}$ (i.e. $h + k + l = 2n$) were collected from two octants of reciprocal space to a maximum 2θ of 65°. A total of 1413 intensities were measured to give an asymmetric set of 647 unique reflections of which 621 were classed as observed.

4.4.3 Refinement:

The initial positional parameters and isotropic temperature factors were the final parameters given by Danø (1966). Atomic scattering factors for neutral atoms were taken from Cromer and Mann (1968).

A full-matrix least-squares refinement was made by varying the atomic positions, the isotropic temperature factors and the scale factor. The refinement was constrained to the idealized formula (Table 4.4.1) and the structure converged at an R-factor of 3.0%. The temperature factors were then converted to the anisotropic form and further cycles of refinement varying all the refinable parameters resulted in convergence at a final R-factor of 2.3%. The population and thermal parameters for both Na and Cl were refined and the value of 1.00(1) was obtained for both species, which agrees well with the ideal formula and also the chemical analysis of Danø (1966). The interatomic distances and thermal parameters for the atoms showed nothing unusual and the refinement was considered complete at this point.

The final atomic positions and isotropic temperature factors are given in Table 4.4.2 and final anisotropic temperature factors are listed in Table 4.4.3. Interatomic distances and angles are presented in Table 4.4.4 and included in these tables for comparison with the present result are the data of Danø (1966). Structure factors are presented in Appendix 1.

4.4.4 Discussion:

The cell parameters obtained for the red tugtupite used in this investigation are quite different from those used by Danø (1966) whose parameters are also well outside of the ranges a: 8.634 - 8.643; c: 8.867 - 8.870 quoted by Sørensen, Danø and Peterson (1971). The refinement does not indicate that the sample used in this study has a different composition from that of Danø (1966). However, the atomic positions (Table 4.4.2) are not significantly different. Consequently, differences in bond lengths (Table 4.4.4) between the present structure and that of Danø (1966) are due to his inaccurate cell parameters.

The isotropic temperature factors obtained by Danø (1966) are quite small and are attributed to the crystal not being small enough (~0.3mm) for absorption to be negligible (μ~86cm^{-1}, Cu-Kα). The crystal used in this study is slightly smaller (Table 4.4.1) and the absorption is quite low (μ= 9.5 cm^{-1}; Mo-Kα). Therefore the isotropic thermal values are comparable to those of sodalite and minerals in the helvite group.

The general features of the structure are the same as those of sodalite. The framework is shown in stereographic projection down an

Table 4.4.2: Atomic parameters and isotropic temperature factors ($\times 10^4$) for tugtupite

Atom	Site		Present Work	Dano (1966)	Total Change
Na	8(g)	x	0.1563(2)	0.1575(5)	-0.0012
		y	0.1972(2)	0.1970(5)	+0.0072
		z	0.1818(2)	0.1850(8)	-0.0032
		U	188(3)	142(13)	+46
Cl	2(a)	x	0	0	---
		y	0	0	---
		z	0	0	---
		U	234(3)	190(14)	+44
Si	8(g)	x	0.0127(1)	0.0134(3)	-0.0007
		y	0.2533(1)	0.2535(3)	-0.0002
		z	0.4958(1)	0.4956(5)	+0.0002
		U	74(1)	28(10)	+46
Be	2(c)	x	0	0	---
		y	$\frac{1}{2}$	$\frac{1}{4}$	---
		z	$\frac{1}{4}$	$\frac{1}{4}$	---
		U	98(14)	84(52)	+14
Al	2(d)	x	0	0	---
		y	$\frac{1}{2}$	$\frac{1}{2}$	---
		z	3/4	3/4	---
		U	76(4)	33(13)	+43
O(1)	8(g)	x	0.1504(3)	0.1471(8)	+0.0033
		y	0.1343(2)	0.1332(8)	+0.0011
		z	0.4417(2)	0.4431(13)	-0.0014
		U	123(4)	80(18)	+43
O(2)	8(g)	x	0.3472(2)	0.3467(9)	+0.0005
		y	0.0385(3)	0.0362(9)	+0.0023
		z	0.6488(2)	0.6512(15)	-0.0024
		U	119(4)	109(16)	+10
O(3)	8(g)	x	0.4256(2)	0.4261(8)	-0.0005
		y	0.1486(2)	0.1506(8)	-0.0020
		z	0.1377(3)	0.1347(14)	+0.0030
		U	120(4)	100(16)	+20

Table 4.4.3: Anisotropic temperature factors (x 10^4) for tugtupite

Atom	U_{11}	U_{22}	U_{33}	U_{12}	U_{13}	U_{23}
Na	206(7)	160(6)	199(6)	7(5)	24(5)	12(5)
Cl	228(4)	228	244(7)	0	0	0
Si	71(3)	63(3)	86(3)	-2(2)	-2(3)	-3(3)
Be	86(18)	86	123(34)	0	0	0
Al	78(5)	78	74(8)	0	0	0
O(1)	126(9)	116(9)	128(9)	46(7)	10(8)	1(7)
O(2)	107(8)	119(8)	132(9)	-3(6)	-35(8)	-4(8)
O(3)	112(8)	114(8)	135(9)	-1(6)	5(7)	38(8)

a-axis in Figure 4.4.1 and is characterized by rings of four tetrahedra in each of the faces of the unit cell which are linked together forming rings of six tetrahedra about each of the cell corners. The four-membered rings in the faces normal to the a-axes have an ordered disposition of tetrahedra consisting of two Si, one Al and one Be-O tetrahedra. The four-membered rings in the faces normal to the c-axis consist only of SiO_4 tetrahedra. As a result of the linkage of the four-membered rings, the six-membered rings also have an ordered disposition of tetrahedra consisting of one Al, one Be and four Si-O tetrahedra; the Be and Al are diametrically opposite in the ring. The large sodalite-type cages contain sodium and chlorine.

The sodium ion is five-fold coordinated by four oxygens and one chlorine in tugtupite (Fig. 4.4.2), in contrast with its four-fold coordination (Fig. 4.1.2) in sodalite. However, the Na-Cl bond length

Table 4.4.4: Selected interatomic distances and angles in tugtupite

	Present work	Danø (1966)	Total Change
	Silicon tetrahedra:		
Si-O(1)	1.644(2)Å	1.646(14)Å	-0.002
-O(1)*	1.647(2)	1.611(13)	+0.036
-O(2)	1.581(2)	1.580(18)	+0.001
-O(3)	1.609(2)	1.566(17)	+0.043
Mean	1.620	1.601(8)	+0.019
O(1)-O(1)*	2.672(3)Å		
-O(2)	2.587(3)		
-O(3)	2.640(3)		
O(1)*-O(2)	2.637(3)		
-O(3)	2.601(3)		
O(2)-O(3)	2.723(3)		
Mean	2.643		
O(1)-Si-O(1)*	108.6(1)°		
-O(2)	106.7(1)		
-O(3)	108.5(1)		
O(1)*-Si-O(2)	109.5(1)		
-O(3)	106.0(1)		
O(2)-Si-O(3)	117.2(1)		
Mean	109.4		
	Beryllium tetrahedra		
Be-O(2)	4 x 1.631(2)Å	1.608(12)	+0.023
O(2)-O(2)	4 x 2.633(3)		
	2 x 2.722(3)		
Mean	2.663		
O(2)-Be-O(2)	4 x 107.7(1)°		
	2 x 113.2(1)		
Mean	109.5		

Table 4.4.4 (continued)

	Present work	Dano (1966)	Total Change
	Aluminum tetrahedra:		
Al-O(3)	4 x 1.748(2)Å	1.762(14)	-0.014
O(3)-O(3)	4 x 2.845(3)		
	2 x 2.872(3)		
Mean	2.854		
O(3)-Al-O(3)	4 x 109.0(1)		
	2 x 110.5(1)		
Mean	109.5		
	Bridging		
Si-O(1)-Si 140.8(2)°	Si-Al 3.100(1)Å		
Si-O(2)-Be 143.6(1)	Si-Be 3.051(1)		
Si-O(3)-Al 135.3(1)	Si-Al 3.105(1)		
	Sodium-coordination sphere:		
Na-Cl	2.707(1)Å		
-O(1)	2.370(3)		
-O(2)	2.303(3)	mean = 2.356	
-O(3)	2.396(3)		
-O(2)	2.603(3)		
O(1)-Na-Cl	115.2(1)°		
-O(2)	110.5(1)		
-O(3)	98.0(1)		
O(2)-Na-Cl	122.8(1)		
-O(3)	99.5(1)		
O(3)Na-Cl	106.1(1)		
a	8.640(1)Å	8.538(4)	+0.102
c	8.873(4)	8.817	+0.056

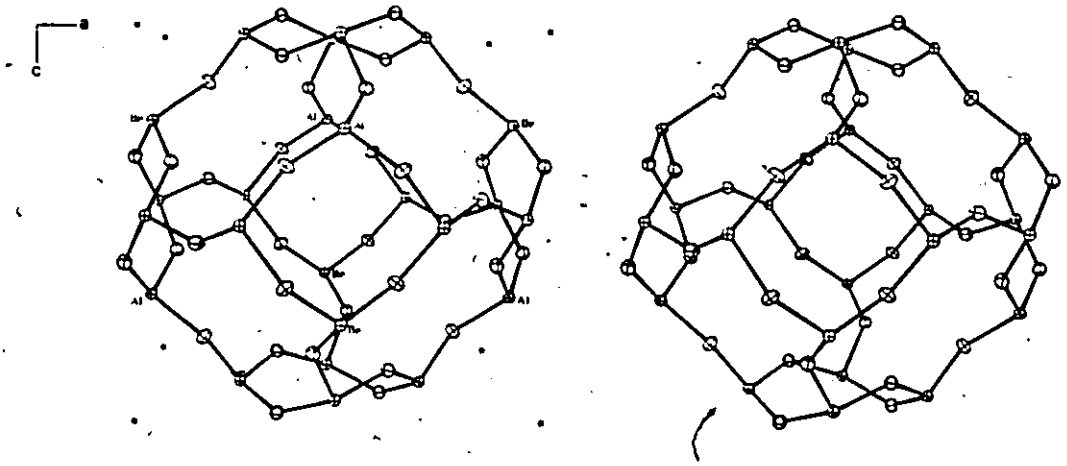

Fig. 4.4.1: Stereographic projection of the framework of tugtupite viewed down an a-axis. The silicon and oxygen atoms are unlabelled.

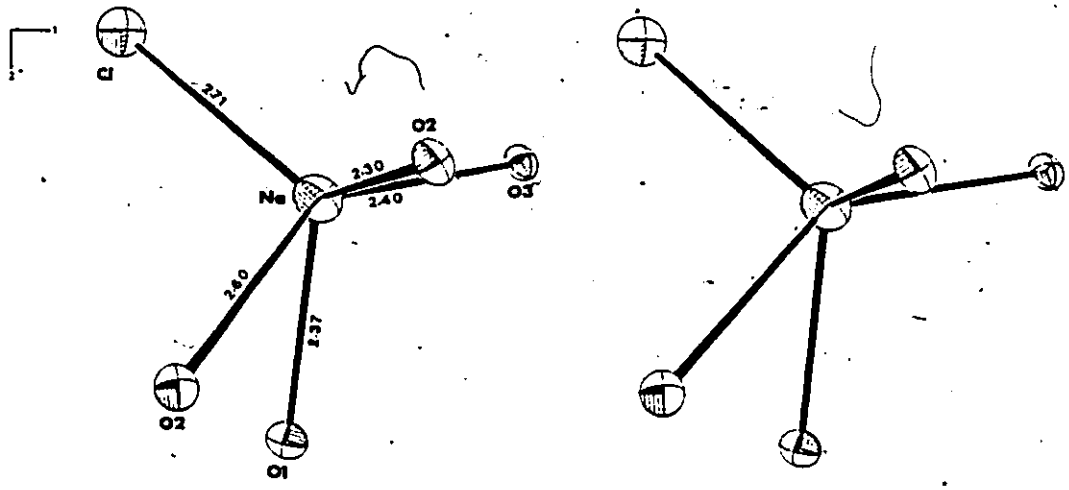

Fig. 4.4.2: Stereographic drawing in the vicinity of the Na site showing its five-fold coordination in tugtupite.

(2.707Å) in tugtupite is smaller than in sodalite (2.736Å). Of the four oxygens bonded to sodium, three have a mean bond distance (2.356Å) which is identical to that in sodalite (2.353Å). The fourth oxygen is further away (2.603Å) but is within bonding distance because in sodalite the other oxygens are much further away (3.087Å).

The Be and Al-O tetrahedra are close to being regular tetrahedra with the Be-O and Al-O distances being 1.631 and 1.748Å respectively. The Si-O tetrahedra are quite distorted. In the pure Si-O-Si linkage, the Si-O distances are 1.644 and 1.647Å; this distance is 1.581Å when the linkage contains a Be and it is 1.609Å when it contains an Al. The mean Si-O distance is 1.620Å. These distances are discussed further, below.

4.4.5 Comparison of Framework Geometry

Tugtupite, the helvite group of minerals, sodalite and hydroxysodalite provide an excellent opportunity to compare the effects on the framework tetrahedra having dissimilar cations on the T sites (Si^{4}, Al^{3+}, Be^{2+}); and of very different interframework cations (Na^{+}, Mn^{2+}, Zn^{2+}, Fe^{2+}) and anions (Cl^{-}, S^{2-}, OH^{-}, H_2O).

The mean Be-O and Si-O distances for minerals in the helvite group are 1.634 and 1.629Å respectively. Individual members in this group shows no statistical variation from these values (Table 4.2.7). The mean Si-O distance for the helvite group is slightly larger than the Si-O distance in sodalite (1.620Å), and hydroxysodalite (1.616Å) and the mean Si-O distance in tugtupite (1.620Å) with the last three being statistically identical. This result is seemingly inconsistent with the bond model of Brown et al. (1969) which requires the Si-O bond

length to be affected by the T-atom. The Al-O bond length in sodalite (1.742Å) is also identical to that in tugtupite (1.748Å) while the Be-O distance in tugtupite (1.631Å) is identical to the mean in the helvite group (1.634Å).

The principal difference is in the T-O-T angle. The Si-O-Si angle is 140.8° in tugtupite; the Si-O-Al angles are 138.2° and 135.3° in sodalite and tugtupite respectively; and the Si-O-Be angles are about 125° in the helvite group and 143.6° in tugtupite. The value of the T-O-T angle has been proposed to be a qualitative measure of the degree of d-p π bonding in the silicate framework (Cruickshank, 1961; Brown et al., 1969; Gibbs et al., 1972) so that a bond angle of 180° corresponds to the maximum d-p π interactions. Both Al and Si have 3d orbitals available for such interactions. However, in helvite, Be has no available orbitals of the correct symmetry to produce interactions of this type with the oxygens coordinating it (Holloway et al., 1972). Therefore, a small Si-O-Be angle in helvite may be expected as a result of the lesser contribution to the bonding of the framework while a large angle in tugtupite would be surprising, but there is no simple explanation.

In conclusion, the T-O-T angle in sodalite type materials is controlled mainly by the interframework ions. The greater the effective charge of the interframework cation, the smaller is the T-O-T angle (sec. 4.2.4). The larger the ionic radius of the interframework anions, the larger is the T-O-T angle.

CHAPTER 5

MODEL OF THE SODALITE STRUCTURE

5.1 Introduction

"In sodalite the framework collapses, the tetrahedra rotating about the two-fold axes until the oxygen ions come into contact with the sodium ions, which themselves are in contact with the chlorine ions. This partial collapse of the framework reduces the edge of the unit from its maximum value, about 9.4Å to 8.87Å" (Pauling, 1930). Pauling's idea has been developed by Taylor (1972) and has since been used extensively in the study of the sodalite group of minerals (Taylor, 1975; Henderson and Taylor, 1977, 1978, 1979); moreover Taylor and Henderson (1978) have devised a computer model for the sodalite structure but now Dempsey and Taylor (1980) prefer the distance least squares (DLS) model. Furthermore, several different cubic structures such as α-Mn, Sb_2Tl_7, tetrahedrite, etc. can be described and related to that of sodalite (Nyman and Hyde, 1981).

Consider a maximally-expanded sodalite framework of perfectly regular tetrahedra and of equal size, sharing corners (Fig. 5.1). This array of tetrahedra can be collapsed, without changing its topology, by rotating tetrahedra about their 4-axes. If the edge length of the regular tetrahedron is E and the rotation angle is ϕ, the unit-cell is given by

$$a = E(2\cos\phi + \sqrt{2}) \qquad (1)$$

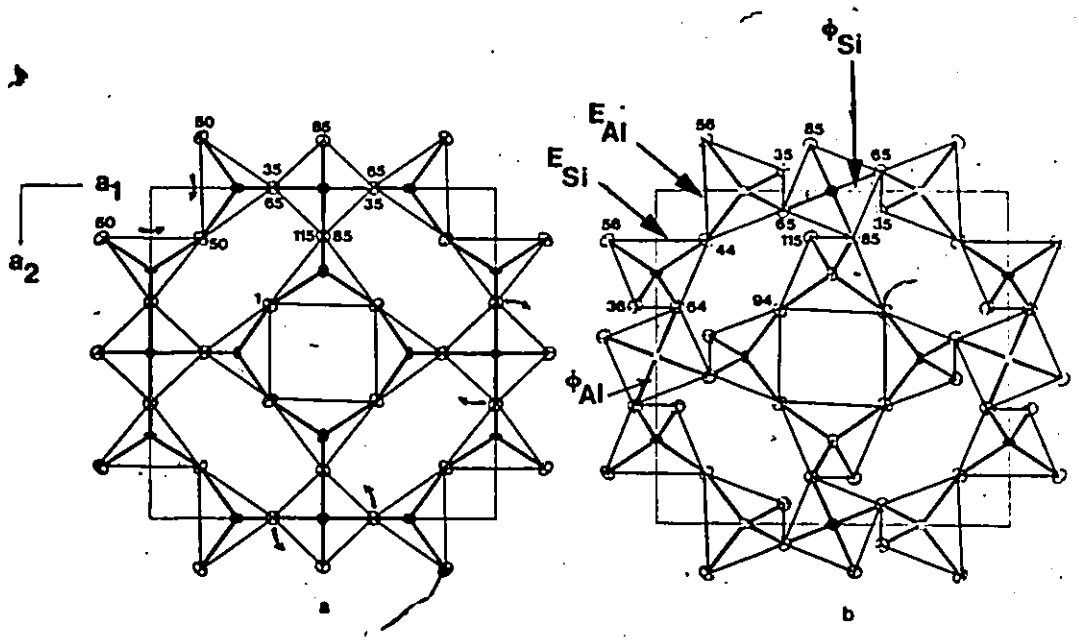

Fig. 5.1: Upper half of unit cell (a) The fully expanded framework of regular tetrahedra of equal sizes (space group $Im\bar{3}m$). Arrows indicate the rotation of some tetrahedra (about axes parallel to the cell edges) which collapse the structure. Along each row of tetrahedra with $\bar{4}$ axes parallel to a cell edge, alternate tetrahedra are rotated clockwise and anti-clockwise. (b) Rotation angles and tetrahedra edges are shown in the partially collapsed structure of sodalite (proper). The Si atoms are shown as filled and the Al atoms as opened (space group $P\bar{4}3n$). Numbers indicate atom heights in units of one-hundredth of the projection axis, a_3.

and the parameters of the corners (x, x, z) (that is, oxygen coordinates) are

$$x = \frac{\cos\phi}{2(2\cos\phi+\sqrt{2})}, \quad z = \frac{\sin\phi}{2(2\cos\phi+\sqrt{2})}, \tag{2}$$

and

$$\phi = \tan^{-1}(z/x). \tag{3}$$

When the tetrahedra are rotated, the framework symmetry remains cubic, but the space group is changed from $Im\bar{3}m$ (fully open array of tetrahedra) to $I\bar{4}3m$. As the rotation angle increases, the cavities shrink and become more and more distorted, at $\phi = 45^{\circ}$ they become truncated tetrahedra (Nyman & Hyde, 1981). In sodalite the symmetry is lowered to $P\bar{4}3n$ due to ordering of Al and Si. Of course, the Al and Si tetrahedra are not regular and are not of equal size, they are slightly compressed along the rotation axes. Consequently, there are two rotation angles, ϕ_{Si} and ϕ_{Al}, corresponding to the rotations of the Si and Al tetrahedra respectively.

5.2 The Sodalite Model

A comparison of the framework dimensions for the six-members of the helvite group (Table 4.2.7) shows that both the Be- and Si-O tetrahedra edges are constant although the cell edges are different. Similar results were observed in the comparison of sodalite and hydroxysodalite (Table 4.3.7). The model that is developed below is based on the above observations and on the assumption that changes in the framework bonds with composition will be negligible at 293K and only slight at high temperatures (Young, 1962; Peacor, 1968; Winter et al., 1979). Slight changes at high temperatures, attributed to the anisotropic thermal motion of the framework oxygen (Megaw, 1973) will not be corrected in this study since the general variation of the sodalite structure with temperature will be investigated.

In any one of the framework tetrahedra, symmetry requires two O-O edges to be equal. Let these edges be represented by E_{Si}, E_{Al} and E_{Be} for the three respective cation tetrahedra. Also, let ϕ_{Si}, ϕ_{Al} and ϕ_{Be} be the rotation angles through which the respective tetrahedra are rotated relative to their positions in the 'ideal' fully-expanded structure (Fig. 5.1).

Where needed, the following average parameters obtained from the helvite group of minerals (Table 4.2.6) will be used for this mineral group:

$$\text{Be-O} = 1.634\text{Å}$$

$$\text{Si-O} = 1.629$$

$$E_{Be} = 2.715$$

$$E_{Si} = 2.708$$

The following parameters from sodalite (Table 4.1.4) will be used

for the sodalite group of minerals since these parameters are from a better refined structure than hydroxysodalite and since sodalite is of similar composition to the alkali-halide sodalites being investigated.

$$\text{Al-O} = 1.7417\text{Å}$$

$$\text{Si-O} = 1.6195$$

$$E_{Al} = 2.8710$$

$$E_{Si} = 2.7010$$

We now derive some simple geometrical relationships for the sodalite structure based on the atomic positions given in Table 4.1.2. Consider the Al($\frac{1}{4}$, 0, $\frac{1}{2}$)-O(x, y, z)-Si(0, $\frac{1}{4}$, $\frac{1}{2}$) triangle. The distance between Al and Si is related to the cell edge by

$$\text{Al-Si} = \frac{a}{2\sqrt{2}} \qquad (4)$$

and for the oxygen fractional coordinates (x, y, z) we get

$$(y-x) = \frac{2}{a}[(\text{Al-O})^2-(\text{Si-O})^2]. \qquad (5)$$

Since Al-O is greater than Si-O, it follows that y is greater than x. Therefore, if Al and Si are interchanged then x and y must be interchanged. Although the difference between x and y is small, structure refinements cannot make this adjustment. However, inconsistencies should be obvious from the Al-O and Si-O bond lengths and in the temperature factors of Al and Si. The latter differ by about 50%. Such a difference was reported by Lons and Schulz (1967) although their atomic positions and bond distances were consistent. However, Schulz (1970) transformed the coordinates of Lons and Schulz (1967) incorrectly. Either the Al and Si positions or the oxygen x and y parameters should have been interchanged.

However, to make the Al- and Si-O bonds consistent in hauyne, Lohn and Schulz (1968) consider the framework oxygen to be statistically twinned on the (110) mirror plane, thereby having two oxygen positions.

The relationship obtained between the Al-O-Si angle and cell edge from the above triangle is

$$\cos(\text{Al-O-Si}) = \frac{\text{Si-O}}{2(\text{Al-O})} + \frac{\text{Al-O}}{2(\text{Si-O})} - \frac{a^2}{16(\text{Si-O})(\text{Al-O})}. \qquad (6)$$

In Figure 5.1b, the length of the cell edge, a_1, can be obtained from the geometry of two types of tetrahedra. One of these types of tetrahedron shows a square face on projection, and E (the two O-O edges mentioned above) are its body diagonals. The angle of rotation, ϕ, of a tetrahedron is also shown. The axis of rotation is parallel to the a_3-axis. The other type of tetrahedron has E normal to the a_1-axis (e.g. O_{56}-O_{44} and O_{35}-O_{65}). The axis of rotation for this tetrahedron is parallel to the a_1-axis. The geometry of these tetrahedra give

$$a = 2E_{Si}\cos\phi_{Si} + 4\left\{(\text{Al-O})^2 - (E_{Al}/2)^2\right\}^{\frac{1}{2}} \qquad (7)$$

and by transforming we get

$$\cos\phi_{Si} = \frac{1}{2E_{Si}}\left\{a - 4\left\{(\text{Al-O})^2 - (E_{Al}/2)^2\right\}^{\frac{1}{2}}\right\}. \qquad (8)$$

Equations 7 and 8 are symmetrical with respect to Al and Si and they give the variations of ϕ_{Si} and ϕ_{Al} with cell edge since the other terms are constants. Substituting values for the constant terms, we get:

(a) sodalite: $a = 5.742 \cos\Phi_{Al} + 3.5717$
$= 5.402 \cos\Phi_{Si} + 3.9475$ (7)'

and (b) helvite group: $a = 5.430 \cos\Phi_{Be} + 3.6229$
$= 5.416 \cos\Phi_{Si} + 3.6397$ (7)'

The maximum cell edges are obtained when $\Phi_{Al} = 0$ for sodalite and $\Phi_{Be} = 0$ for helvite. We have therefore:

a) sodalite:

$$a_{max} = 9.3137\text{Å}$$
$$\phi_{Al} = 0^{\circ}$$
$$\phi_{Si} = 6.596^{\circ}$$

and b) helvite group:

$$a_{max} = 9.0529\text{Å}$$
$$\phi_{Be} = 0^{\circ}$$
$$\phi_{Si} = 1.107^{\circ}$$

The Be-O tetrahedra in helvite is slightly larger than the Si-O tetrahedra compared to the larger difference between the Al- and Si-O tetrahedra in sodalite. Therefore at a_{max}, ϕ_{Si} is closer to zero for helvite than for sodalite and furthermore, for a given change in ϕ, there is a larger change in the cell edge for the helvite group than the sodalite. As a result, we can expect a larger value for a_{max} if the framework were to disorder (space group $P\bar{4}3m$) since the two framework tetrahedra would have about equal dimensions. In this case a maximum cell edge of about 9.365Å is expected. Minimum cell edge for sodalite is obtained by considering the smallest ions that enter the structure, that is, the LiF-sodalite for which $a_{min.}$ is 8.141Å.

The variation of Φ with cell edge (eqn. 8) reduces to:

a) sodalite:

$$\cos \Phi_{Si} = a/5.402 - 0.7303$$
$$\cos \Phi_{Al} = a/5.742 - 0.6227 \qquad (8)$$

and b) helvite:

$$\cos \Phi_{Si} = a/5.416 - 0.6717$$
$$\cos \Phi_{Be} = a/5.430 - 0.6672 \qquad (8)'$$

In sodalite, the atomic coordinates of the oxygen at the top left of Figure 5.1, are obtained from the two tetrahedra which it shares. The coordinates are:

$$x = \frac{1}{a}(E_{Si}/2)\cos \Phi_{Si}$$
$$y = \frac{1}{a}(E_{Al}/2)\cos \Phi_{Al}$$
$$z_{Al} = \tfrac{1}{2} - \frac{1}{a}(E_{Al}/2)\sin \Phi_{Al} \qquad (9)$$
$$z_{Si} = \tfrac{1}{2} - \frac{1}{a}(E_{Si}/2)\sin \Phi_{Si}$$
$$z = \tfrac{1}{2}(z_{Al} + z_{Si})$$

The z parameter (z_{Al} and z_{Si}) is obtained from either the AlO_4 or SiO_4 tetrahedra. The values obtained should be equal. However, to avoid any bias in the calculation, the mean is used. On substitution of values in equation (9), the oxygen fractional coordinates for sodalite reduce to the following:

$$x = \tfrac{1}{4} - 0.9863/a$$
$$y = \tfrac{1}{4} - 0.8938/a$$
$$z_{Si} = \tfrac{1}{2} - 1.3505(\sin \Phi_{Si}/a) \qquad (9)'$$
$$z_{Al} = \tfrac{1}{2} - 1.4355(\sin \Phi_{Al}/a)$$

From equation (6), we also obtain:

$$\Phi_{Si} = \tan^{-1}\{(\tfrac{1}{2}-z)/x\}$$
$$\Phi_{Al} = \tan^{-1}\{(\tfrac{1}{2}-z)/y\}$$

We can now calculate the oxygen coordinates for sodalite for any

given cell edge using equations (9)' and (8)' and therefore the complete framework geometry can be calculated. The above derivations are specifically for the space group $P\bar{4}3n$, however, with minor adjustments they are applicable to the disorder framework of the space group $P\bar{4}3m$ or $I\bar{4}3m$ where the equations have simpler forms (Eqns. 1-3). Furthermore, the model may be applied to all sodalite framework, regardless of the framework cation, providing they have the above space groups.

The complete sodalite structure is calculated by fixing the bond length of either the interframework cation-oxygen (C-O) or the intraframework cation-anion(C-A) bond. The former distance can be predicted with greater accuracy than the latter and is therefore used in the calculation of sodalite structures if the cell edge is known.

It is evident from the above that the cell edge for the sodalite must be measured and thus the particular sodalite must exist. However, the model can predict cell edges and possible existence of sodalite of any composition. This is done by fixing both the C-O and C-A distances since the fractional coordinate X, of the interframework cation, C, must satisfy both distances. The cation, C, has coordinates (X, X, X), the anion, A, has coordinates (o, o, o) and the framework oxygen, O, has coordinates (x, y, z). Using the distance between two points, we obtain

$$X_C^2 - \{\tfrac{2}{3}(x + y + z)\}X_C + \left\{\tfrac{1}{3}\{x^2 + y^2 + z^2 - (\tfrac{C-O}{a})^2\}\right\} = 0 \qquad (10)$$

and

$$X_C = \frac{C-A}{\sqrt{3}\,a} \qquad (11)$$

from which X_C and a are obtained graphically.

5.3 Calculated Structures for Alumino-silicate Sodalites

The C-O and C-A distances are derived from the effective ionic radii of Shannon (1976). However, for sodalite the Na-O and Na-Cl distances are 2.353Å and 2.736Å respectively. The radius of Na is 0.99Å, therefore, $r_{O=}$ is 1.36Å and r_{Cl^-} is 1.746Å. These radii and others were used to obtain the following bond lengths: K-O = 2.730Å; Rb-O = 2.883Å; Cs-O = 3.033Å and Li-O = 1.953Å. Using this Li-O distance, the Li-Cl distance calculated for the LiCl- sodalite is much larger than the Li-Cl distance, 2.565Å, in lithium chloride, whereas the reverse is the case for the other sodalites and the corresponding alkali halides. To correct this anomaly and to make calculated Li-halide distances at least equal to that obtained from the sum of the ionic radii, Li-O distance of 2.102Å is used in the calculation. The less predictible C-A distance obtained from the effective radii sum is used only where a cell edge is not known.

Structures were computed for several alkali-halide alumino-silicate sodalites. Hereafter, the composition of the various sodalites are abbreviated as follows: NaCl for the end-member $Na_8(Al_6Si_6O_{24})Cl_2$ etc. and for the solid solution $Na_4K_4(Al_6Si_6O_{24})Cl_2$ we use $Na_4K_4Cl_2$ etc. The method of calculating the structures has been outlined previously and the results are presented in Tables 5.1 and 5.2 (a-g).

Table 5.1 consists of the end-member sodalites that have been predicted to exist. The cell edges were obtained from predicted C-O and C-A distances (Eqns. (10) and (11)). Therefore, the results obtained must be regarded as an approximation. The structure of $Na_{0.5}K_{7.5}Br_2$ sodalite (Taylor and Henderson, 1978) is also given in Table 5.1. Included in

Table 5.1: Calculated structural data for aluminosilicate-sodalites

Sodalite		LiF	LiBr	LiI	NaF	KF	$Na_{0.5}K_{7.5}Br_2$	RbF	Fully expanded framework
	a(Å)*	8.141	8.520	8.633	8.659	9.154	9.281	9.295	9.317
	x	.1288	.1342	.1358	.1361	.1423	.1437	.1439	.1441
O:	y	.1402	.1451	.1465	.1468	.1524	.1537	.1538	.1541
	z	.3943	.4150	.4218	.4234	.4619	.4800	.4831	.4921
C:	x	.1362	.1730	.1874	.1522	.1648	.1964	.1753	$\frac{1}{4}$
	ϕ_{Si}(°)	34.9	32.3	30.0	29.4	15.0	7.9	6.7	3.1
	ϕ_{Al}(°)	37.0	30.4	28.1	27.6	24.0	7.4	6.3	2.9
Si-O-Al(°)		117.7	127.3	130.5	131.2	148.7	155.1	155.9	157.6
C-A(Å)		1.921	2.552	2.802	2.282	2.612	3.157	2.822	8 x 4.035**
C-O(Å)	3x	2.102	2.102	2.102	2.353	2.730	2.706	2.883	2.619 3 x 2.747**

* The cell edge for $Na_{0.5}K_{7.5}Br_2$-sodalite is measured and the others are calculated

** When $X_C=\frac{1}{4}$, the anion, A, is 8-fold coordinated by cations, C, and the cation, C, is 8-fold coordinated by six-oxygens and two anions

Table 5.2: Calculated structural data for synthetic aluminosilicate-sodalites at various temperatures*. (a) No. 1: $Li_{7.97}Na_{0.03}(Al_6Si_6O_{24})Cl_2$

T(°C)		20	200	300	400	500	600	695	800
	a(Å)	8.4466	8.4698	8.4837	8.4999	8.5173	8.5379	8.5533	8.5757
	x	.13323	.13355	.13374	.13396	.13420	.13448	.13468	.13498
O:	y	.14418	.14447	.14464	.14484	.14506	.14531	.14550	.14577
	z	.41081	.41213	.41293	.41386	.41487	.41607	.41697	.41830
C:	x	.16483	.16733	.16886	.17067	.17266	.17507	.17692	.17971
Si-O-Al(°)		125.3	125.9	126.3	126.8	127.2	127.8	128.1	128.8
ϕ_{Si}(°)		33.8	33.3	33.1	32.7	32.4	32.0	31.7	31.2
ϕ_{Al}(°)		31.7	31.3	31.0	30.7	30.4	30.0	29.7	29.3
C-A(Å)		2.411	2.455	2.481	2.513	2.547	2.589	2.621	2.669
C-O(Å) 3x		←			2.102				→

* The cell edges are experimental parameters

Table 5.2: (b) No. 2: $Li_{4.4}Na_{3.6}(Al_6Si_6O_{24})Cl_2$

T(°C)		20	200	300	400	500	600	695	800
	a(Å)	8.6575	8.6803	8.6960	8.7107	8.7285	8.7477	8.7655	8.7869
	x	.13607	.13637	.13658	.13677	.13700	.13725	.13748	.13775
O:	y	.14676	.14703	.14721	.14739	.14760	.14782	.14803	.14828
	z	.42328	.42470	.42569	.42663	.42777	.42902	.43020	.43163
C:	x	.17099	.17368	.17558	.17742	.17969	.18222	.18467	.18722
Si-O-Al (°)		131.2	131.8	132.3	132.7	133.2	133.9	134.4	135.1
ϕ_{Si} (°)		29.4	28.9	28.5	28.2	27.8	27.3	26.9	26.4
ϕ_{Al} (°)		27.6	27.1	26.8	26.5	26.1	25.6	25.2	24.8
C-A(Å)		2.564	2.611	2.645	2.677	2.717	2.761	2.804	2.857
C-O(Å) 3x		←			2.215				→

Table 5.2: (c) No. 3: $Na_8(Al_6Si_6O_{24})Cl_2$

T(°C)		20	195	300	400	500	610	705	805	920
	a(Å)	8.8810	8.8975	8.9116	8.9257	8.9405	8.9593	8.9765	8.9997	9.019
	x	.13894	.13914	.13932	.13949	.13968	.13991	.14012	.14040	.14064
O:	y	.14935	.14954	.14970	.14986	.15002	.15023	.15043	.15069	.15089
	z	.43819	.43940	.44045	.44151	.44264	.44410	.44547	.44736	.44898
C:	x	.17764	.17989	.18188	.18393	.18614	.18907	.19190	.19593	.19955
Si-O-Al(°)		138.2	138.7	139.2	139.7	140.2	140.9	141.5	142.4	143.1
ϕ_{Si}(°)		24.0	23.5	23.1	22.7	22.3	21.8	21.3	20.6	19.9
ϕ_{Al}(°)		22.5	22.1	21.7	21.3	20.9	20.4	19.9	19.3	18.7
C-A(Å)		2.732	2.772	2.807	2.843	2.883	2.934	2.984	3.054	3.117
C-O(Å) 3x		←				2.353				→

Table 5.2: (d) No. 4: $Na_8(Al_6Si_6O_{24})Br_2$

T(°C)		20	195	300	400	500	600	700	810	900	950	1000	1060
	a(Å)	8.9338	8.9541	8.9667	8.9794	8.9961	9.0173	9.0379	9.0610	9.0941	9.1179	9.1523	9.1568
	x	.13960	.13985	.14000	.14016	.14036	.14062	.14087	.14114	.14154	.14182	.14223	.14228
O:	y	.14995	.15018	.15032	.15046	.15064	.15088	.15110	.15135	.15171	.15197	.15234	.15239
	z	.44213	.44370	.44469	.44571	.44706	.44883	.45060	.45266	.45574	.45808	.46169	.46218
C:	x	.18513	.18826	.19028	.19240	.19528	.19921	.20334	.20847	.21720	.22495	.24539	$\frac{1}{4}$
Si-O-Al(°)		140.0	140.7	141.2	141.6	142.2	143.0	143.9	144.8	146.1	147.1	148.6	148.8
ϕ_{Si}(°)		22.5	21.9	21.6	21.2	20.7	20.0	19.3	18.5	17.4	16.5	15.1	14.9
ϕ_{Al}(°)		21.1	20.6	20.2	19.8	19.4	18.7	18.1	17.4	16.3	15.4	14.1	13.9
C-A(Å)		2.865	2.920	2.955	2.992	3.043	3.111	3.183	3.271	3.420	3.553	3.890	8 x 3.965
C-O(Å)	3x	2.353	←									2.353	3 x 2.355 3 x 2.953

Table 5.2: (e) No. 5: $Na_8(Al_6Si_6O_{24})I_2$

T(°C)		20	205	305	415	505	610	710	820	870	915	960
	a(Å)	9.0076	9.0283	9.0442	9.0641	9.0823	9.1061	9.1413	9.1685	9.1732	9.1760	9.1784
	x	.14050	.14075	.14094	.14118	.14140	.14168	.14210	.14242	.14248	.14251	.14254
O:	y	.15077	.15100	.15117	.15139	.15159	.15184	.15222	.15251	.15256	.15259	.15262
	z	.44802	.44977	.45116	.45294	.45462	.45691	.46050	.46350	.46404	.46439	.46465
C:	x	.19746	.20137	.20469	.20920	.21379	.22083	.23591	¼	¼	¼	¼
Si-O-Al(°)		142.7	143.5	144.1	144.9	145.6	146.6	148.1	149.3	149.6	149.7	149.8
ϕ_{Si}(°)		20.3	19.6	19.1	18.4	17.8	16.9	15.5	14.4	14.2	14.0	13.9
ϕ_{Al}(°)		19.0	18.4	17.9	17.3	16.7	15.8	14.5	13.5	13.3	13.1	13.0
C-A(Å)		3.081	3.149	3.207	3.284	3.363	3.483	3.735	8 x 3.970	8 x 3.972	8 x 3.973	8 x 3.974
C-O(Å)	3x	2.353	←					2.353	3 x 2.367 3 x 2.945	3 x 2.372	3 x 2.375	3 x 2.378 3 x 2.938

Table 5.2: (f) No. 6: $Na_4K_4(Al_6Si_6O_{24})Cl_2$

T(°C)		20	200	300	405	505	605	705	805	905	1000
	a(Å)	9.0527	9.0730	9.0865	9.1035	9.1153	9.1345	9.1507	9.1651	9.1762	9.1847
	x	.14105	.14129	.14145	.14165	.14179	.14202	.14221	.14238	.14251	.14261
O:	y	.15126	.15148	.15163	.15181	.15194	.15215	.15232	.15247	.15259	.15268
	z	.45191	.45375	.45502	.45665	.45782	.45978	.46151	.46311	.46439	.46540
C:	x	.17411	.17719	.17934	.18215	.18420	.18769	.19085	.19384	.19269	.19826
Si-O-Al(°)		144.4	145.2	145.8	146.5	147.0	147.8	148.5	149.2	149.7	150.1
ϕ_{Si}(°)		18.8	18.1	17.6	17.0	16.6	15.8	15.1	14.5	14.0	13.6
ϕ_{Al}(°)		17.6	17.0	16.5	15.9	15.5	14.8	14.2	13.6	13.1	12.8
C-A(Å)		2.730	2.785	2.823	2.872	2.908	2.970	3.025	3.077	3.120	3.154
C-O(Å) 3x		2.541	←								→ 2.541

Table 5.2: (g) No. 7: $Na_{0.4}K_{7.6}(Al_6Si_6O_{24})Cl_2$

T(°C)		20	200	295	395	500	605	705	800
	a(Å)	9.2531	9.2604	9.2662	9.2725	9.2779	9.2848	9.2890	9.2968
	x	.14340	.14349	.14356	.14363	.14369	.14377	.14382	.14391
O:	y	.15340	.15348	.15354	.15360	.15366	.15373	.15378	.15386
	z	.47486	.47608	.47710	.47827	.47932	.48075	.48168	.48357
C:	x	.18713	.18911	.19078	.19272	.19448	.19691	.19851	.20183
Si-O-Al(°)		153.5	153.9	154.2	154.5	155.0	155.3	155.6	156.0
ϕ_{Si}(°)		9.9	9.5	9.1	8.6	8.2	7.6	7.3	6.5
ϕ_{Al}(°)		9.3	8.9	8.5	8.1	7.7	7.1	6.8	6.1
C-A(Å)		2.999	3.033	3.062,	3.095	3.125	3.167	3.194	3.250
C-O(Å)	3x	2.711	←						→ 2.711

Table 5.1 has a calculation for a hypothetical fully-expanded sodalite framework with the cation C at $\frac{1}{4}$. The Table also shows the range of possible Al-O-Si angles (117.7 to 157.6°).

Table 5.2(a-g) consists of calculated structures for sodalites that have been synthesized by Henderson and Taylor (1978) whose cell parameters, temperature and composition have been used. The structures are from room- to the highest temperature studied. The room temperature structure parameters are different from those calculated by Taylor and Henderson (1978) and Dempsey and Taylor (1980). The differences exist mainly in the assumptions made in their models and in their calibration of their models to that of Lons and Schulz (1967). The distance least squares (DLS) model used by Dempsey and Taylor (1980) is only as good as the accuracy to which bond distances can be predicted. In the case of sodalite, they had to use eight inequivalent prescribed distances: Si-O, Al-O, 4 x O-O; C-O and C-A in order to obtain atomic coordinates, interatomic distances and angles.

5.4 Thermal Expansion of Sodalites

With increasing temperature (Taylor, 1968, 1972; Henderson and Taylor, 1978) it is thought that the observed expansion of sodalites is due almost entirely to the untwisting of the partially-collapsed framework by gradual removal of the tilting. The Cl- and Br-bearing aluminosilicate-sodalites show increasing rates of expansion up to the highest temperatures studied, whereas the SO_4- and I-bearing sodalites show a change from a relatively high and increasing rate of expansion to a relatively low and constant rate. This change in the expansion rate is referred to as a discontinuity.

An interpretation of the thermal expansion behaviour of the sodalite structure (Henderson and Taylor, 1978), based on a computer model of the sodalite structure (Taylor and Henderson, 1978), indicates that the discontinuity in the expansion curve could occur when the ideal fully-expanded state was achieved (case 1) or when the coordinate of the cavity cation became $\frac{1}{4}$ (case 2). Case 2 was favoured by Henderson and Taylor (1978) on the evidence of the thermal expansion of a wide range of synthetic aluminosilicate sodalites and natural noseans and hauynes. According to Henderson and Taylor (1978), the mechanism of expansion of the sodalite structure involves the C-A bond being increased by thermal expansion forcing the cavity cation between the framework oxygens and untwisting the partially collapsed structure (suggested to them by Dr. H. D. Megaw). If the coordinate of the cation reaches $\frac{1}{4}$, due to these processes, further migration and further expansion due to the cavity cation forcing apart the framework oxygens would be prevented since at $\frac{1}{4}$ the cation is in the plane of the 6-member ring of the framework. The result would be a change in the rate of expansion of the sodalite structure.

Dempsey and Taylor (1980) now believe that the C-A and C-O bonds are unduly stressed by the untwisting of the framework and that the driving force for the untwisting lies in the framework itself. However, the discontinuity still occurs when $X = \frac{1}{4}$ for the cation (NaI sodalite).

The thermal expansion raw-data for sodalites presented by Henderson and Taylor (1978) will be used in this study. At high temperatures, three types of structural changes need to be considered. The first involves changes in the dimensions of the framework tetrahedra,

the second is in the C-A distance and the third type of change is in the C-O distance. Changes in the framework tetrahedra dimensions will be slight and to a first approximation may be neglected since no sodalite structure data is available for high temperature. In the mechanism of sodalite proposed by Dr. Megaw to Henderson and Taylor (1978), it is implied that the C-O bond is constant to the point where the cation is at $\frac{1}{4}$ and thereafter it expands as the temperature is raised further. The expansion of the C-O bond can be calculated after the cation has reached $\frac{1}{4}$ as then there is no need to make any assumption about C-O and C-A distances. After such C-O calculations are made, the curve for temperatures when the cation is less than $\frac{1}{4}$ is then extrapolated.

This method is used for $Na_8(Al_6Si_6O_{24})I_2$. The results are presented in Figure 5.2b, where it is seen that the expansion of the Na-O bond is quite small when the cation is less than $\frac{1}{4}$. This result can now be generalized: the expansion of the C-O bond is negligible when the cation is less than $\frac{1}{4}$; therefore the C-O values at room temperature may be used to calculate high-temperature sodalite structures. Table 5.2 gives calculated structures for sodalites at various temperatures up to the highest temperature determined and their structural variations are shown in Figure 5.2.

In Figure 5.2a, the thermal expansion curves for seven synthetic aluminosilicate-sodalites are shown using the raw-data of Henderson and Taylor (1978). For additional intermediate sodalites, the reader is referred to the original paper.

Henderson and Taylor (1978) has recognized the discontinuity for NaI sodalite at 810°C and a cell edge of 9.168Å. However, based on the

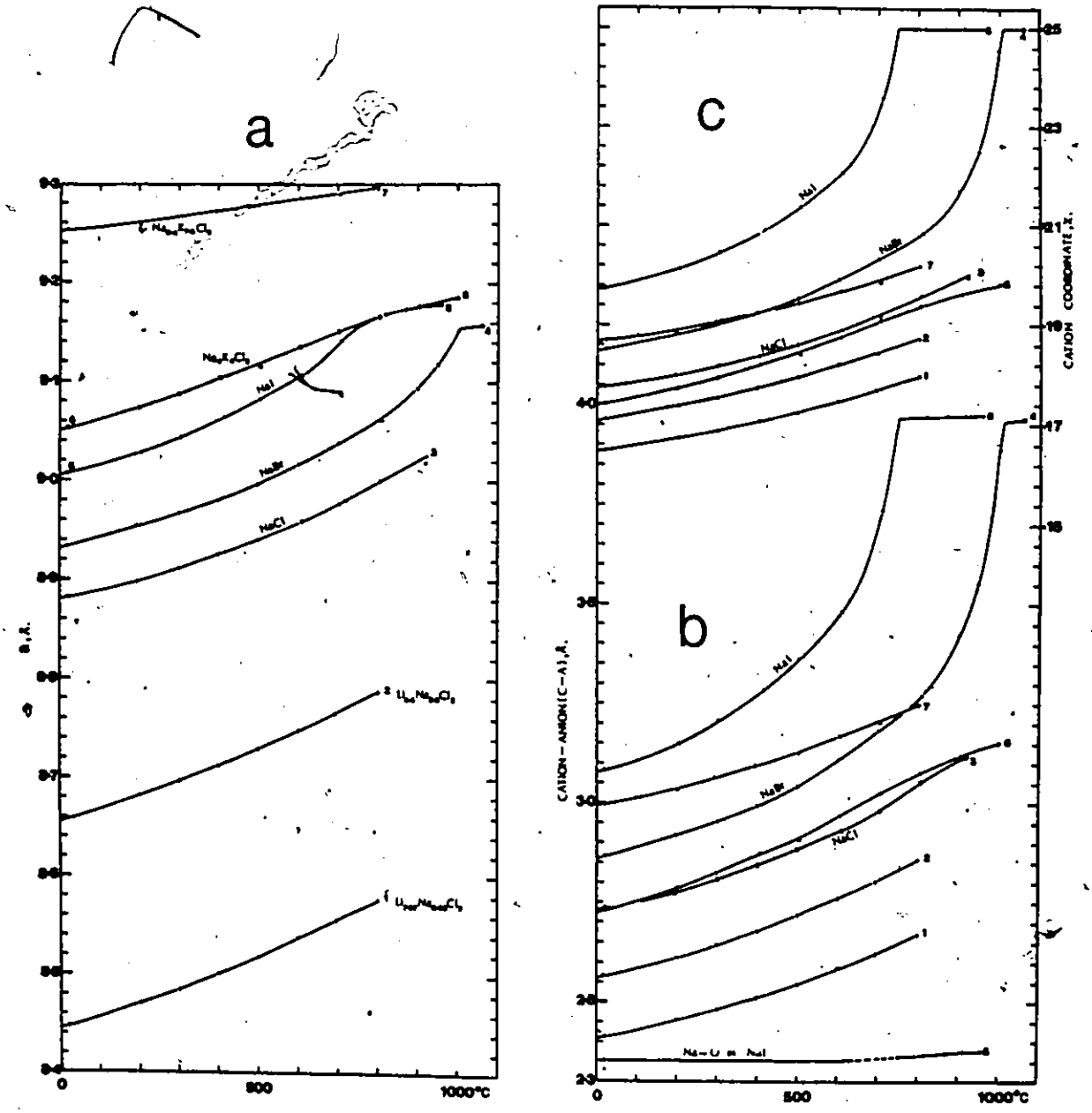

Fig. 5.2: (a) Thermal expansion curves for synthetic aluminosilicate-sodalites (replotted from data of Henderson and Taylor (1978). (b) Variation of the interframework cation-anion distance with temperature. (c) Variation of the interframework cation fractional coordinate, x, with temperature. The full compositions corresponding to the numbers are given in Table 5.2 and Figure 5.3.

replotted data and the structural calculation, the author considers the discontinuity to occur at 750°C and a cell edge of 9.155Å.

No discontinuity was reported for NaBr sodalite by Henderson and Taylor (1978). These authors, however, listed the cell edge at 1060°C, but did not consider this data point to be significant. Even if we ignore this data point and use the point at 1000°C, the calculation shows that the discontinuity in the thermal expansion curve is just about to be reached. In fact, the discontinuity occurs at 1010°C, indicating that the data point mentioned above is valid. Therefore, there is a discontinuity for NaBr sodalite (Fig. 5.2a) when the cell edge is 9.155Å, see later).

Fig. 5.2b,c shows the variations of the Na-O bond in NaI sodalite, C-A, and the cation x-parameter as a function of temperature. Discontinuities occur in all of these parameters for the NaI- and NaBr-sodalites. In particular, they occur when the cation is at $\frac{1}{4}$ and the cell edge is 9.155Å.

Figure 5.2 clearly shows discontinuities if they occur in the temperature range studied, and it also shows the reason for such discontinuities. However, it does not show why discontinuities do not occur for sodalites that have larger ions and cell parameters than NaI-sodalite and whether discontinuity may or may not occur at higher temperatures. To examine these aspects of the sodalite structure the results must be displayed differently. It is seen that the C-O distance is more or less constant until the cation reaches $\frac{1}{4}$. Therefore, equation (10) can be used to show the variation of the cation coordinate with the cell edge for constant C-O distances. (Note: the intersection of these curves with the curves of equation (11) gives unknown cell edges.) Curves for

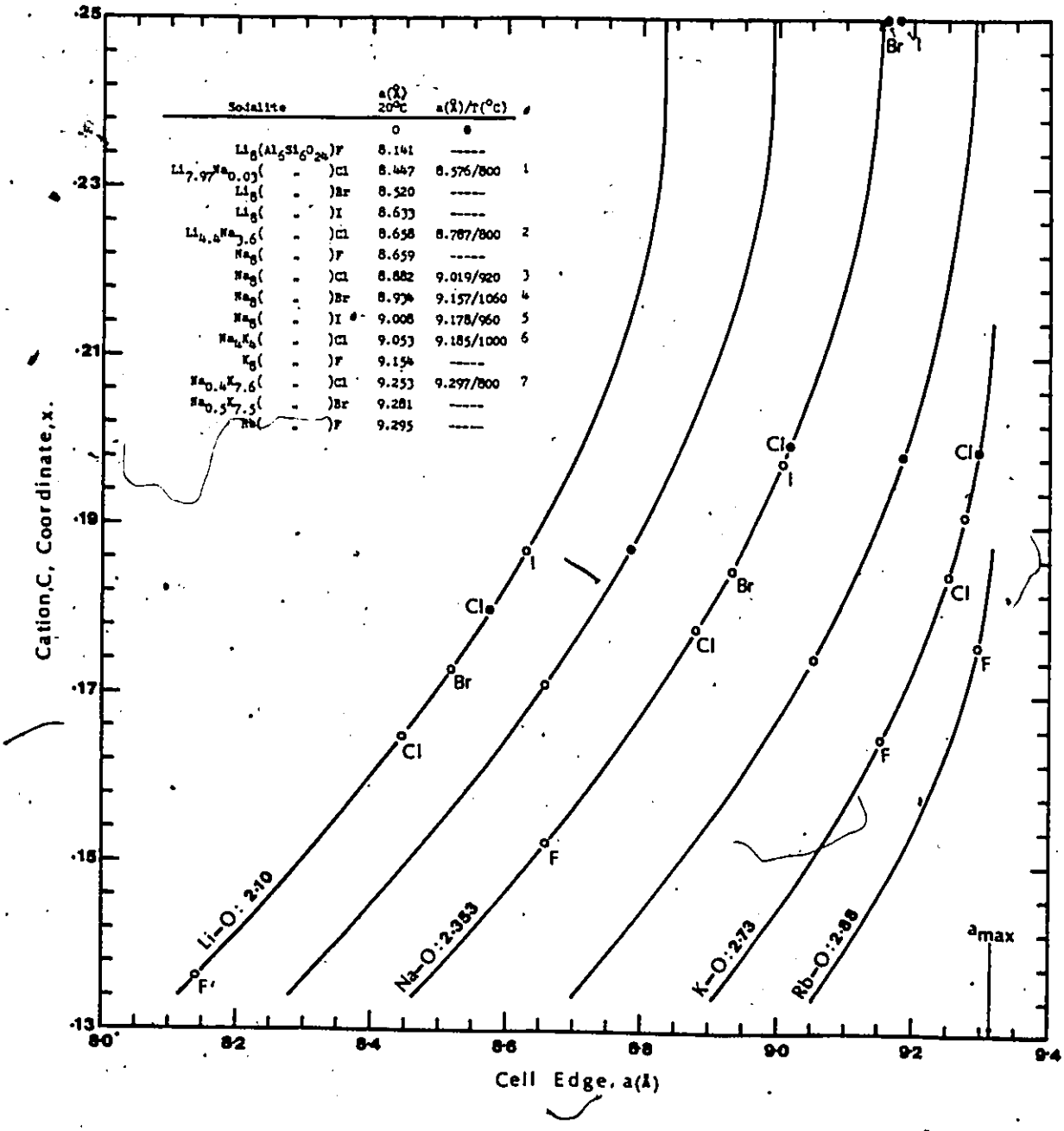

Fig. 5.3: Variation of the interframework cation fractional coordinate, x, with cell edge for constant interframework cation-framework oxygen (C-O) distances. Intersection of the interframework cation-anion (C-A) curve with the C-O curve gives the position of that particular sodalite represented by the anion (A) (see text). The filled circles correspond to high temperature and opened circles to the room temperature sodalites. The diagram shows the entire sodalite compositional field.

various C-O distances are shown in Figure 5.3. All the sodalites discussed are shown on this diagram for both room-temperature (open circle) and the highest-temperature (full circle) studied.

Figure 5.3 clearly shows that all sodalites having C-O distances slightly greater than 2.54Å should show discontinuities. That is, a C-O curve slightly greater than the $Na_4K_4Cl_2$ curve. The Na-halide sodalite end-members expansion should follow the Na-O curve to a cell edge of 9.155Å where the Na is at $\frac{1}{4}$ and a discontinuity would occur. Similarly, for the Li-halide sodalite end-members, the discontinuity would occur at a cell edge of 8.835Å and when the Li is at $\frac{1}{4}$. Whether a discontinuity occurs or not in practice depends on the thermal stability of the sodalite in question. Present results indicate that the NaF, NaCl, and the Li-halide sodalites would decompose before the temperature is raised to the discontinuity point.

The pure end-member K-halide and Rb-F sodalites have a different thermal expansion behaviour than the Li- and Na-halide sodalites. They would first expand in a similar manner but instead of the cation reaching $\frac{1}{4}$, the maximum cell edge is reached. At this point, one may expect a discontinuity. However, the changes involved at this point are very subtle and cannot be detected from thermal expansion curves. As the maximum cell edge is reached, further expansion is achieved only through slight readjustments of the framework tetrahedra itself in addition to the normal C-A and C-O bonds and thus changes in the thermal expansion curve would be undetectable. The Al/Si-O tetrahedra would distort in such a way as to make the tetrahedra more regular and equal in dimensions. Unfortunately, none of the sodalites under consideration has reached the

maximum cell edge at the highest temperature studied and thus it was not possible to practically analyze the above situation.

Sodalite $Na_{0.3}K_{2.9}Rb_{4.8}(Al_6Si_6O_{24})Cl_2$ cell edge at room temperature is 9.3164Å which is at the maximum cell edge (9.317Å). On heating to 700°C, the cell edge is 9.3355Å which is greater than the maximum cell edge allowable in the space group $P\bar{4}3n$. It is possible that this sodalite has considerable Al-Si disorder, in which case the model for the space group $P\bar{4}3m$ is appropriate where the maximum cell edge of about 9.365Å is allowed.

In summary, the mechanism of the thermal expansion proposed by Dr. H. D. Megaw is preferred over that of Dempsey and Taylor (1980). If the cation is small enough to get into the plane of the 6-member ring, that is at $\frac{1}{4}$, and still forms reasonable bond-distance to the framework oxygen, then a discontinuity in the thermal expansion curve occurs. Only the small Li^+ and Na^+ cations are capable of doing this. When these cations are at a $\frac{1}{4}$, the C-A distance is larger than that at room temperature. At this point, however, the anion is eight-fold coordinated while at room temperature it is tetrahedrally-coordinated.

The large K^+ and Rb^+ cations are too large to reach $\frac{1}{4}$ and form reasonable bonds to the framework oxygens. As a result, on expanding, the maximum cell edge is reached. Calculation of the structure at this stage having hypothetical cations at $\frac{1}{4}$ is given in Table 5.1. When the maximum cell edge is reached, no change in the thermal expansion curve is observable since it involves minor adjustments of the framework tetrahedra as well as the normal expansion of the C-O and C-A bonds.

5.5 Mean Expansion Coefficients for Sodalite

Henderson and Taylor (1978) show that the relationship between the mean linear expansion coefficients, 0° to 500°C, and the room temperature cell edge for the synthetic aluminosilicate-sodalites are close to two lines, one fitted to specimens with cell edges less than 8.955Å:

$$\alpha = 79.8\text{-}7.4a_o \ (\times 10^{-6}\ ^{\circ}C^{-1}),$$

and the other fitted to specimens with cell edges greater than 8.955Å:

$$\alpha = 383.8\text{-}40.8a_o \ (\times 10^{-6}\ ^{\circ}C^{-1}),$$

where α is the mean linear expansion coefficient (0-500°C). They interpreted these results as being due to the different C-A bonds having broadly similar expansion coefficients. However, they noted that several Na/K solid solutions, in particular $Na_4K_4(Al_6Si_6O_{24})Cl_2$, should have a mean expansion coefficient that lies mid-way between those of the NaCl- and KCl-end members but instead it lies close to the NaCl-end member sodalite. No explanation was offered for this behaviour.

Dempsey and Taylor (1980) interpreted the mean expansion coefficients as being due to the different C-A bonds having broadly similar force constants and to the dependence of the cell edge on the cosine of the tilt angle (Eqn. (1)). They still do not offer an explanation for the $Na_4K_4Cl_2$ sodalite anomalous behaviour.

The anomalous behaviour for $Na_4K_4Cl_2$ will now be considered with respect to the NaCl- and KCl end-members. For comparison, the normal behaviour of $Li_{4.4}Na_{3.6}Cl_2$ with respect to the LiCl- and NaCl end-members, will also be considered. The predicted structures for all six of these sodalites are given in Table 5.2. The expansion of their C-A bonds as a function of temperature is given in Figure 5.2b.

For the $Li_{4.4}Na_{3.6}Cl_2$ sodalites, the weighted mean of the C-A bond occurs between that of the Na-Cl bond and the Li-Cl bond and therefore the expansion of the intermediate member is mid-way between the end members.

For the $Na_4K_4Cl_2$ sodalite, the weighted mean of the (Na, K)-Cl bond is identical to that of the Na-Cl bond in sodalite and is not midway between the K-Cl bond and the Na-Cl bond of the respective end-members. Therefore, the thermal expansion of $Na_4K_4Cl_2$ is governed mainly by the Na-Cl bond, with the K playing only a minor role. Thus, its mean thermal expansion coefficient and C-A expansion is similar to the NaCl end member and is not midway between the NaCl and KCl end-members. As the temperature is increased and the cations move towards $\frac{1}{4}$, the K plays a major role since it cannot enter the plane of the six-member ring.

5.6 Chemical Boundaries for Sodalite

The entire sodalite field is shown in Figure 5.3 which is constructed from equations (10) and (11). The field is bounded on the left by the Li-O curve and on the right by the Rb-O curve, since Cs-halide sodalites can be seen to be non-existent. The field is also bounded to the right by the maximum cell edge (9.3173Å). The bottom of the sodalite field is bounded by lines connecting Li-, Na-, K-, and Rb-F sodalites.

At room temperature, the top of the field is limited by lines connecting Li-I, Na-I and some point on the a_{max}- boundary where the cation x coordinate is somewhat greater than 0.214. At high temperatures this boundary is where the cation is at $\frac{1}{4}$.

Solid solutions between various end-members can only be extrapolated

by using weighted average for C-A and C-O distances. Two such solid solution members are also shown in Figure 5.3.

In general, going upward in Figure 5.3, the effect of increasing size of the halide ion is seen, and going to the right the effect of increasing size of the cation, C, is seen. The figure clearly shows the existence of all the end-member halide sodalites except K-I, Rb-Cl, Br, I and Cs-halide sodalites. Solid solutions are also possible between Li and Na, Na and K and to some extent between K and Rb sodalites. Also, it is possible to have mixed halide sodalites, for example $Na_8(Al_6Si_6O_{24})$ ClBr. However, only sodalites solid solutions with respect to the C cations have been synthesized (Henderson and Taylor, 1978).

CHAPTER 6

THE CRYSTAL STRUCTURES OF SULPHATIC SODALITES (HAUYNE, NOSEAN, LAZURITE)

The sulphatic sodalites are similar in many respects. They have similar cell dimensions and they contain SO_4^{2-} group as the dominant interframework anion group. Lazurite may also contain S^{2-} anion. The ideal end-member formulae for nosean and hauyne are $Na_8(Al_6Si_6O_{24})SO_4$ and $Na_6Ca_2(Al_6Si_6O_{24})(SO_4)_2$ respectively.

Satellite reflections have been reported for both nosean and hauyne (Saalfeld, 1959, 1961; Taylor, 1967) and Taylor (1967) reported the same for lazurite from Afghanistan, but he called the material hauyne.

Lohn and Schulz (1968) gave a refinement of hauyne in the space group $P\bar{4}3n$ and Schulz (1970) gave a refinement of nosean in the space group $P\bar{4}3m$. The chemical analyses (Taylor, 1967) of these sulphatic sodalites show an Al/Si ratio of 1:1 and thus the space group $P\bar{4}3n$ is preferred over $P\bar{4}3m$ in accordance with the Al-avoidance rule. Nevertheless, attempts were made to refine these structures in both space groups. However, it was found that the space group $P\bar{4}3n$ gave better results. In particular, the unobserved reflections were calculating very high in $P\bar{4}3m$. These reflections were not taken into account in the previous refinements which were based on film data. Therefore, the choice of space group in this study is $P\bar{4}3n$.

6.1 Experimental

Several single crystals of the sulphatic sodalites were studied. Long exposed precession photographs were taken of all promising crystals and, more than one complete data set was collected from different crystals of each of the three species so as to obtain good data sets for structural analyses.

Figures 6.1, 6.2 and 6.3 are precession photographs showing the hhl net of hauyne, nosean and lazurite respectively. The hauyne is the only species that does not show any superstructure. The superstructures in nosean and lazurite are well-developed and are very similar in appearance. In all of the three species, the observed diffraction maxima are sharp and they also show symmetry which is consistent with the space group $P\bar{4}3n$. Also, no hhl ($l = 2n + 1$) reflection can be seen.

Lazurite samples from Afghanistan were studied. These materials are poorly crystallized and do not provide good single crystals. In most cases the single crystals were too small to give good intensity measurements. Optically, the crystals have various shades of blue which may reflect small-scale compositional variations. The crystal used for Figure 6.3 gave a poor quality data set that could not be refined -- not even the framework. The cell parameter was 9.083(1)Å. The cell dimensions were determined by least-squares from fifteen substructure reflections automatically aligned on a 4-circle diffractometer and are presented in Table 6.1 and Table 6.2 for hauyne and nosean respectively, together with other information pertaining to the materials chosen, X-ray data collection and refinement.

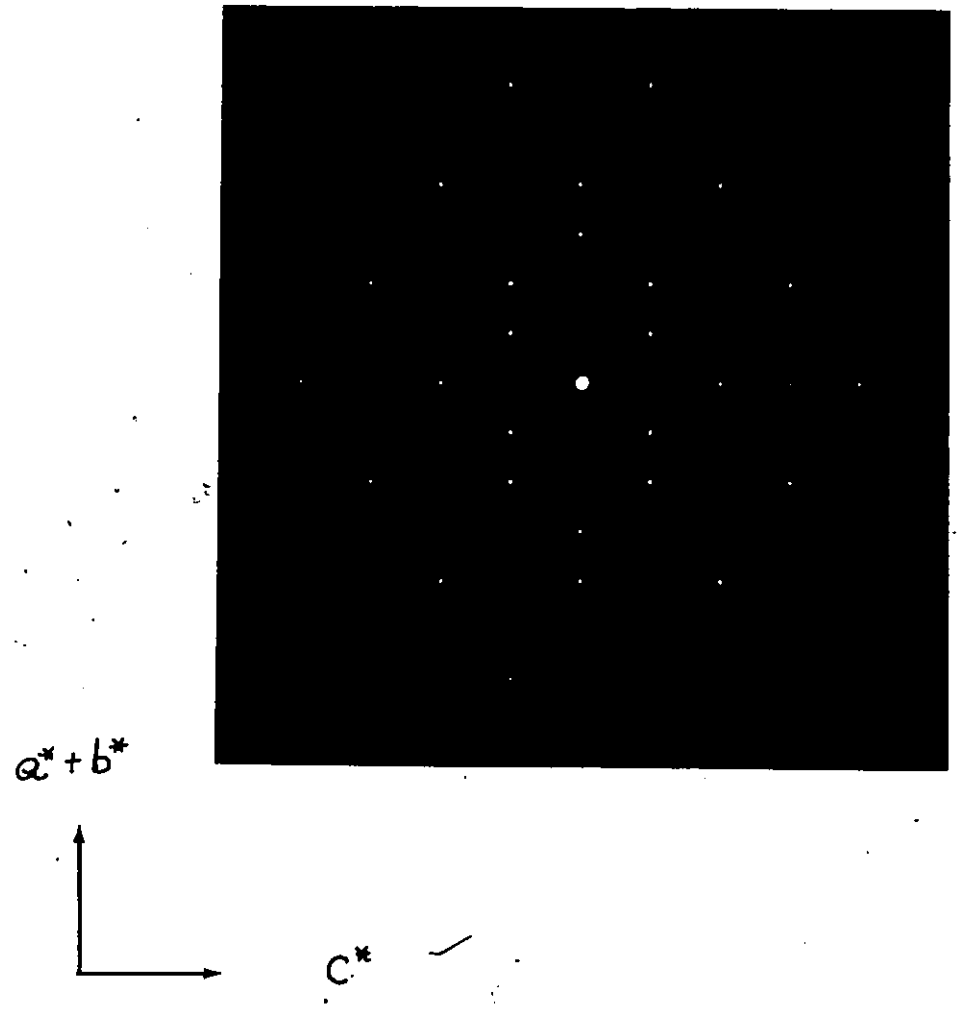

Fig. 6.1: Hauyne. Precession photograph showing the hhl net. Satellites are absent. ($\mu = 20^{o}$, MoK_{α}, Zr filter)

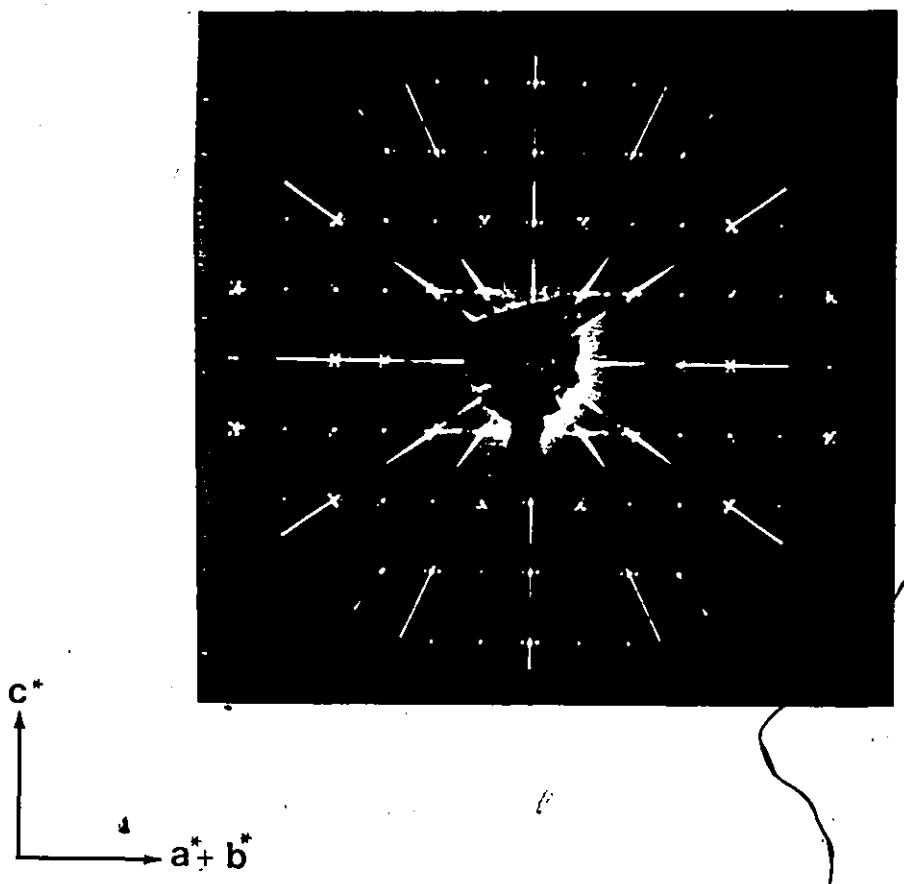

Fig. 6.2: Nosean. Precession photograph showing the hhl net. Well-developed satellite reflections are shown. ($\mu = 20^{\circ}$, MoK_{α}, Zr filter)

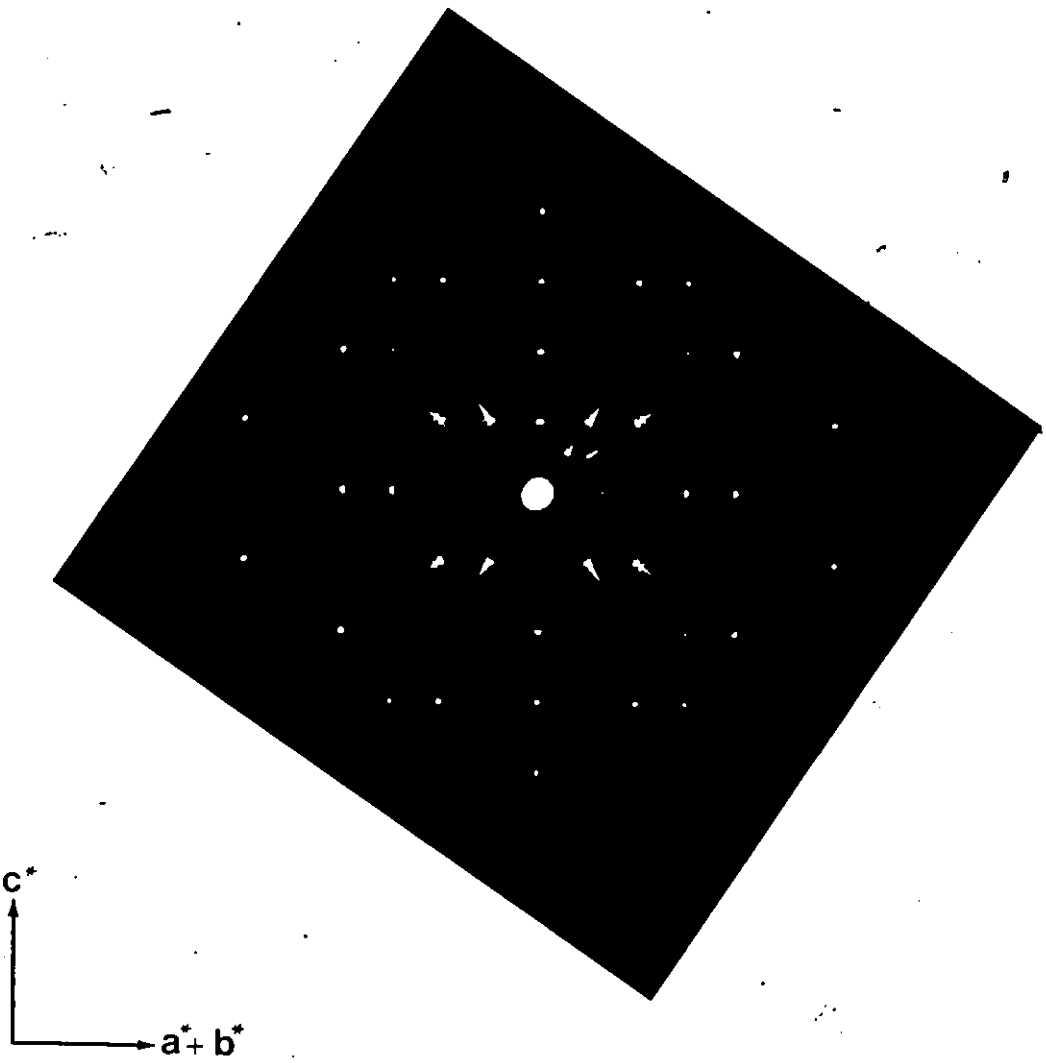

Fig. 6.3: Lazurite: Precession photograph showing the hhl net. Well-developed satellite reflections are shown. ($\mu = 20^{o}$, MoK_{α}, Zr filter)

Table 6.1: Crystal data for hauyne from Sacrafano, Rome+

	293K	153K
a(Å)	9.1164(5)	9.1097(8)
V(Å^3)	757.65	755.98
Space group	$P\bar{4}3n$	
Z	1	
μ(cm^{-1})	13.02	13.06
Density calc. (g/cm^{-3})	2.41	2.42
Crystal size(mm)	0.23 x 0.23 x 0.17	
Radiation/Monochromator	Mo/C	
Total no. of I	1649	1087
No. of non-equiv. $\|F_{obs}\| > 3\sigma$	164	133
Final $R_{(obs)}$ =	0.037	0.040
Final $R_{w(obs)}$ =	0.034	0.037

Chemical formula (Lohn & Schulz, 1968):

$$Na_{4.82}Ca_{2.22}K_{0.91}(Al_6Si_6O_{24})(SO_4)_{1.56}(?OH)_{1.05}$$

Chemical formula found by refinement:

$$Na_{4.32}Ca_{2.4}K_{1.6}(Al_6Si_6O_{24})(SO_4)_{1.52}(?OH)_{1.68}$$

+ Specimen courtesy of the Royal Ontario Museum (no. M 35731)

Table 6.2: Crystal data for nosean from Lacheer See, W. Germany+

Chemical Analysis*		Cell Contents**
SiO_2	35.96	6.090
Al_2O_3	29.63	5.910
Fe_2O_3	0.42	0.053
MgO	0.16	0.040
CaO	1.30	0.236
Na_2O	21.94	7.199
K_2O	1.06	0.229
H_2O^+	0.90	0.508
SO_3	6.82	0.866
S	0.26	0.082
Cl	0.59	0.169
	99.04	
O=Cl, S	0.19	
Total	98.85	

Miscellaneous	
a (Å)	9.084(2)
V (Å^3)	749.60
Space group	$P\bar{4}3n$
Z	1
μ(cm^{-1})	7.34
Density calc. (gcm^{-3})	2.05
Crystal size(mm)	0.20 x 0.20 x 0.33
Radiation/Monochromator	Mo/C
Total no. of I	1675
No. of non-equiv. $\|F_{obs}\| > 3\sigma$	146
Final $R_{(obs)}$ =	0.054
Final $R_{w(obs)}$ =	0.049
w = 1	

Chemical formula found by refinement:

$$Na_{8.2}(Al_6Si_6O_{24})(SO_4)_{1.08}\cdot 1H_2O(?)$$

+ specimen courtesy of the Royal Ontario Museum (no. M5279)
* wet analysis, Taylor (1967)
** Calculated from chemical analysis based on Si + Al = 12

6.2 Refinement of the Structure of Hauyne

Atomic scattering factors for neutral atoms were taken from Cromer and Mann (1968). Initial isotropic temperature factors used were those of sodalite and initial positional parameters were calculated using the sodalite model (Chapter 5). The SO_4 group was assumed to be positioned with the S in the 2(a) position and the oxygen on an 8(e) position where $x = 0.40$ or 0.60 since this gives a perfect tetrahedral geometry and a reasonable S-O distance of 1.6Å.

Refinement of the structure was attempted first by using a set of intensities measured at room temperature. Considerable disorder was observed for the interframework ions. In order to resolve the structural parameters more clearly, a second set of intensities was measured at 153K using the same crystal. The structures at both temperatures are reported here but only the refinement based on the room temperature measurements will be discussed in detail since the low temperature measurements provided little additional information.

The framework atoms were refined first isotropically then anisotropically and a framework geometry comparable to that of sodalite was found. The temperature factors for these atoms showed no unexpected values. The interframework cation position was then examined. The cation 8(e) site occupancy was constrained to the chemical formula of Lohn and Schulz (1968) (Table 6.1). However, its positional coordinate did not refine properly and its isotropic temperature factor was unusually large. Therefore this site was divided between two 8(e) positions and their positional coordinates, isotropic temperature factors and occupancy factors were refined. At this stage, the difference Fourier map still showed electron density on another 8(e) site close to the other two. A

third cation site was therefore incorporated into the structural model. The coordinates of the three cation sites (Na(1), Na(2) and Na(3)) are given in Table 6.2.1a.

The position of the sulphate group was next examined. The difference Fourier map, calculated with the S(1) site removed from the 2(a) position, showed that the S atom is not on the 2(a) site but is displaced onto the 8(e) site with x = 0.47 (see Figs. 6.2.1a, b: p. 103, p. 104). A similar Fourier map calculated with the O(1) oxygen site removed from the structural model (Fig. 6.2.2: p. 105) showed electron density only at one 8(e) site, that with x = 0.60.

At this stage, it was noticed that the calculated and observed structure factors for the reflections 110 and 200 showed large disagreement. The measured intensity for these reflections seemed reasonable but, they could have been affected by extinction. Therefore these reflections were temporarily removed from the calculation and the refinement continued.

The population parameter and the isotropic temperature factor for each of the interframework site were again refined together in separate refinements and their occupancy factors were held invariant thereafter. The O(1) site did not refine well because of the correlation between the occupancy factor and the temperature factor. The occupancy of the O(1) site was therefore set at 0.75 in accordance with the occupancy of the S(1) site and the chemical formula and the temperature factor refined on its own.

At this stage the allowable positional and temperature coordinates of all the sites were refined simultaneously and the refinement converged to an R-factor of 0.037. Using the refined set of structural parameters

and including the reflection 110 and 200 an R-factor of 0.043 was obtained.

For the purpose of illustration a series of difference Fourier maps are given (Figs. 6.2.1 to 6.2.5* p. 103-p. 107) in each of which one interframework site has been omitted from the structure factor calculation. In each case the R-factor is also noted in the figure caption to show which site has the most pronounced effect on the refinement of the structural model.

In this model the scattering curve for Na was used for the interframework cation sites. However, the chemical formula (Table 6.1) of a sample from the same general locality as the sample in this study shows that there are about 2.41 Na, 1.11 Ca, 0.46 K and 0.78 SO_4 atoms per cavity. We can consider which of the Na sites these cations occupy by examining their population parameters and their distances to the framework oxygen atoms.

SITE	POPULATION PARAMETERS			
	By ref. as Na	Calculated as K	Calculated as Ca	By ref.
Na(1)	0.33	0.19	0.18	0.20K
Na(2)	0.52	0.30	0.29	0.30Ca
Na(3)	0.54	0.31	0.30	0.54Na
Expected from chem. anal.	0.60	0.11	0.28	

The population parameter of each of the three sites is shown above in terms of the different cations. When the occupancy factors are compared with that expected from the chemical analysis, it is seen that the K atom probably occupies the Na(1) site but the Ca and Na atoms could

* Figure 6.2.5 is given on p. 233

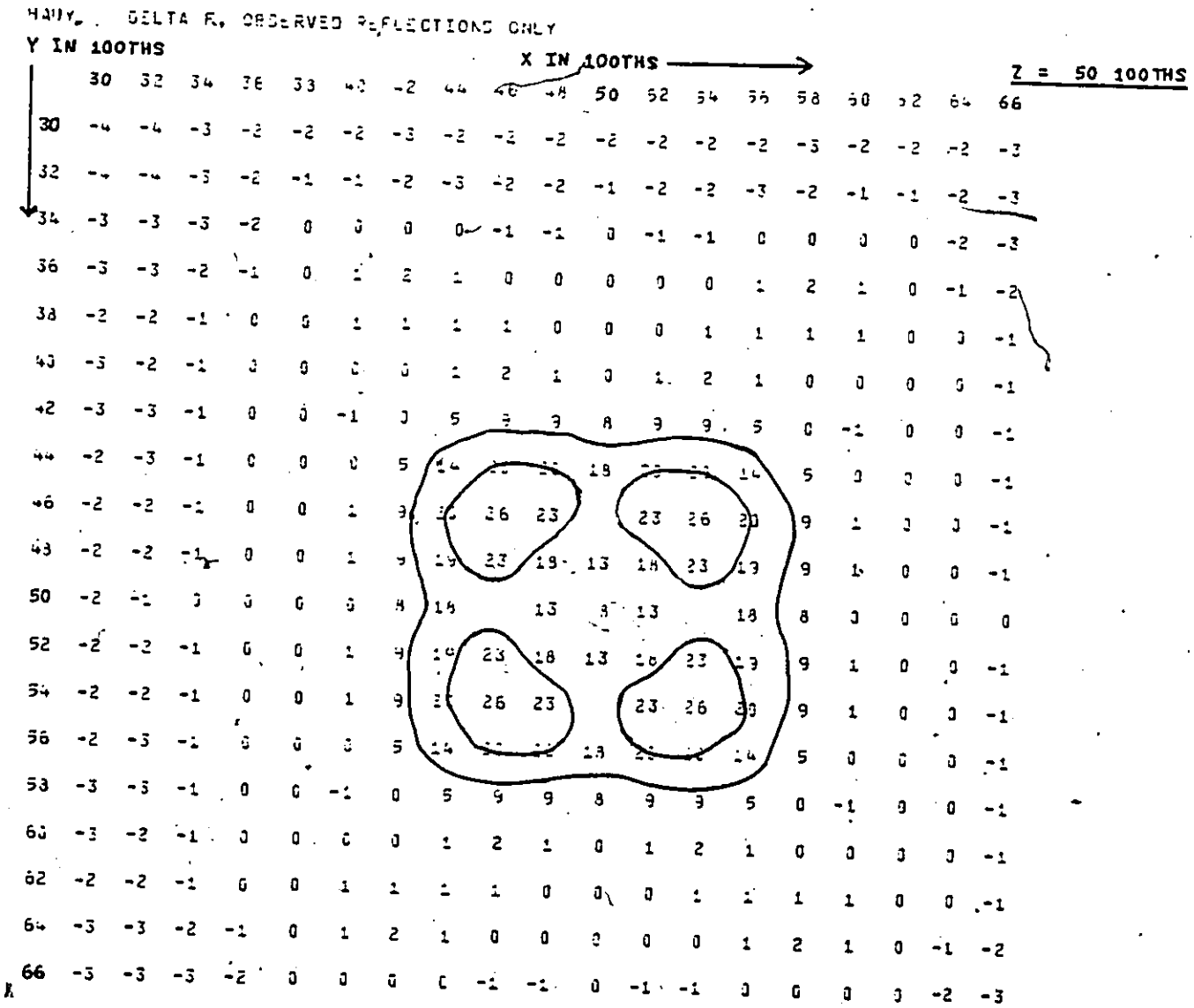

Fig. 6.2.1a: Difference Fourier synthesis through the 2(a) position calculated with the S(1) site removed from the structural model (R = 0.067). This section shows that the S^{6+} cation is displaced from the 2(a) position to the 8(e) position (see Fig. 6.2.1b).

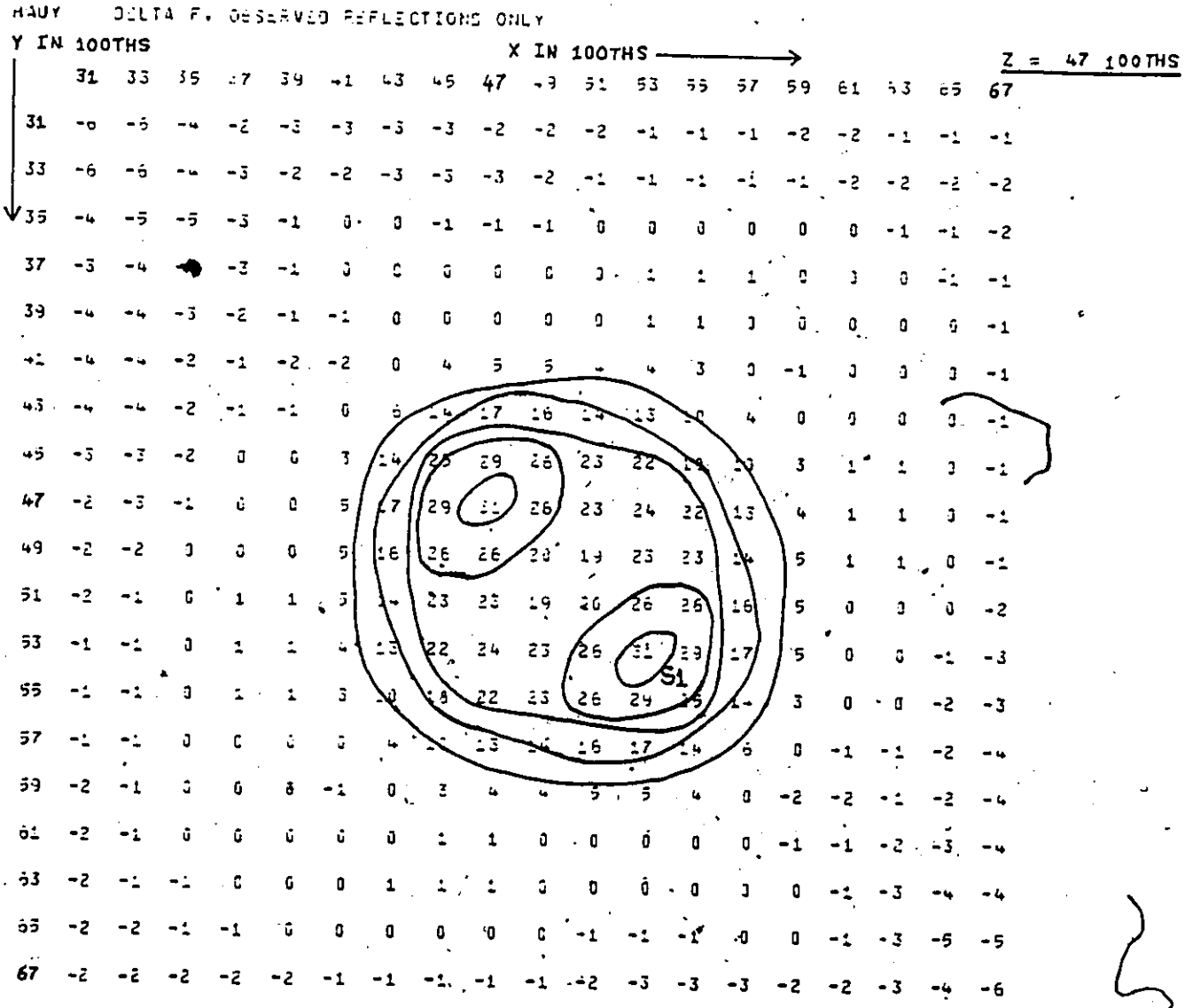

Fig. 6.2.1b: Difference Fourier synthesis calculated with the S(1) cation site removed from the structural model (R = 0.067).

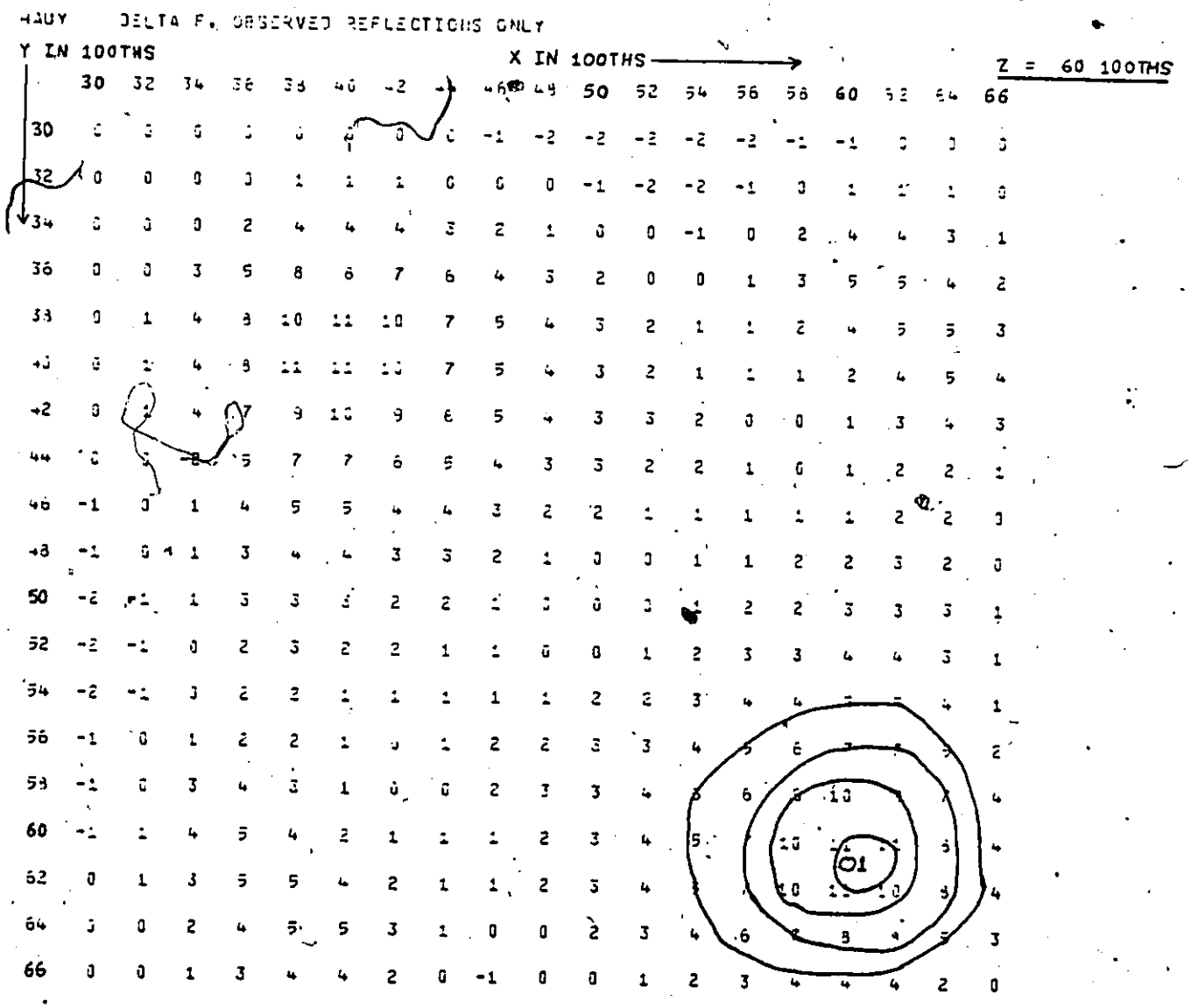

Fig. 6.2.2: Difference Fourier synthesis calculated with the O(1) site removed from the structural model (R = .051).

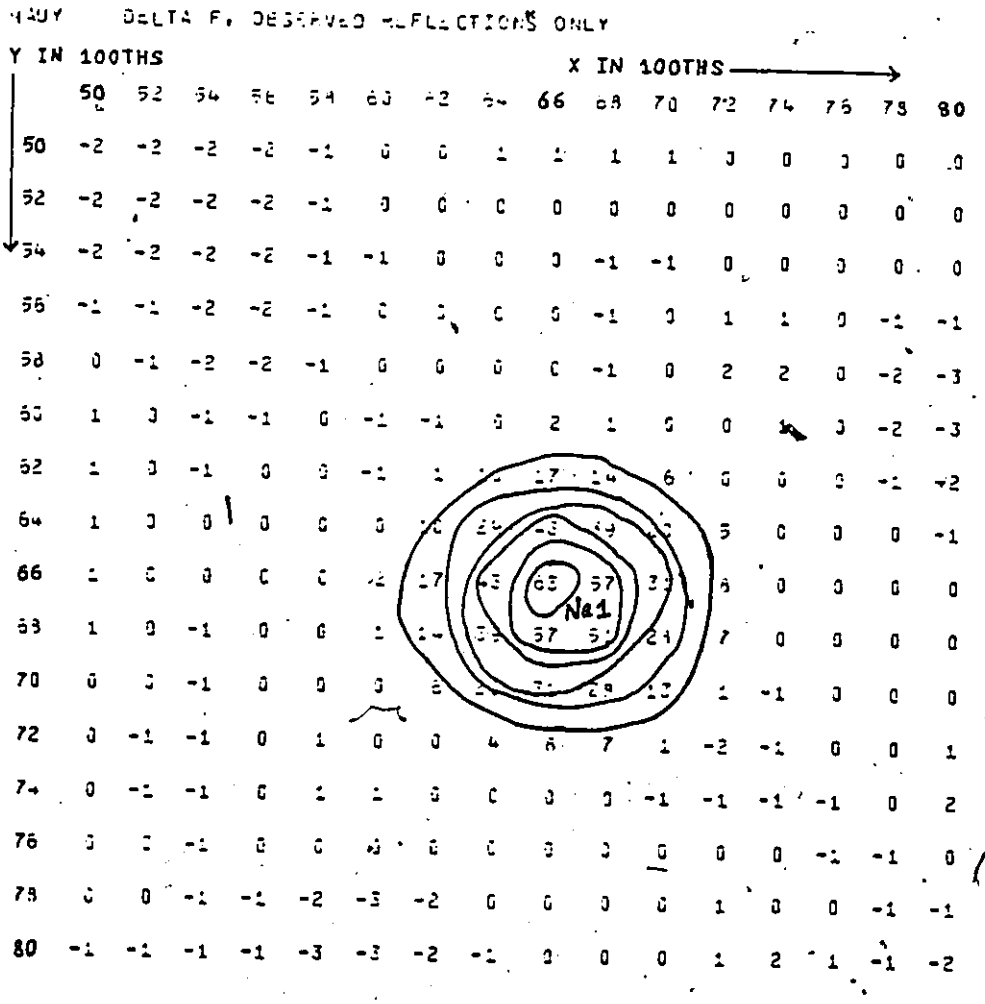

Y \ X	50	52	54	56	58	60	62	64	66	68	70	72	74	76	78	80
50	-2	-2	-2	-2	-1	0	0	1	1	1	1	0	0	0	0	0
52	-2	-2	-2	-2	-1	0	0	0	0	0	0	0	0	0	0	0
54	-2	-2	-2	-2	-1	-1	0	0	0	-1	-1	0	0	0	0	0
56	-1	-1	-2	-2	-1	0	0	0	0	-1	0	1	1	0	-1	-1
58	0	-1	-2	-2	-1	0	0	0	0	-1	0	2	2	0	-2	-3
60	1	0	-1	-1	0	-1	-1	0	2	1	0	0	1	0	-2	-3
62	1	0	-1	0	0	-1	1	3	17	14	6	0	0	0	-1	-2
64	1	0	0	0	0	0	6	24	43	49	25	5	0	0	0	-1
66	1	0	0	0	0	2	17	43	68	57	33	8	0	0	0	0
68	1	0	-1	0	0	1	14	39	57	51	24	7	0	0	0	0
70	0	0	-1	0	0	0	6	25	33	29	13	1	-1	0	0	0
72	0	-1	-1	0	1	0	0	4	8	7	1	-2	-1	0	0	1
74	0	-1	-1	0	1	1	0	0	0	0	-1	-1	-1	-1	0	2
76	0	0	-1	0	0	0	0	0	0	0	0	0	0	-1	-1	0
78	0	0	-1	-1	-2	-2	-2	0	0	0	0	1	0	0	-1	-1
80	-1	-1	-1	-1	-2	-2	-2	-1	0	0	0	1	2	1	-1	-2

Fig. 6.2.3: Difference Fourier synthesis calculated with the Na(1) cation site removed from the structural model (R = 0.106).

HAUY DELTA F, OBSERVED REFLECTIONS ONLY

Y IN 100THS

X IN 100THS →

Z = 70 100THS

	50	52	54	56	58	60	62	64	66	68	70	72	74	76	78	80
50	0	0	0	0	1	2	2	1	0	-2	-2	-1	0	0	0	0
52	0	-1	-2	-1	0	1	2	1	0	-2	-2	0	0	0	0	0
54	0	-2	-2	-1	0	1	1	0	0	-1	-1	0	0	0	0	0
56	0	-1	-1	-1	-1	0	0	0	0	0	0	1	0	-1	-2	-1
58	1	0	0	-1	-2	-2	-1	0	0	1	1	1	0	-1	-3	-2
60	3	2	1	0	-2	-3	-2	0	0	1	2	1	0	-1	-2	-2
62	3	2	1	0	-1	-2	-2	-2	0	1	2	1	0	-1	-1	-1
64	2	1	1	0	0	0	-2	-1	2	3	3	2	0	-2	-2	0
66	0	0	0	0	0	0	0	2	23	27	33	23	7	-2	-4	-2
68	-2	-1	-1	0	1	1	1	4	27	52	62	43	13	3	-6	-4
70	-2	-2	-1	0	1	2	2	1	33	62	78	61	29	2	-7	-5
72	-1	0	0	1	1	1	1	0	23	43	61	43	23	0	-7	-5
74	-1	0	0	0	0	0	0	0	7	13	29	23	7	-4	-6	-4
76	-1	0	0	-1	-1	-1	-1	-3	-3	0	2	0	-4	-7	-5	-3
78	-2	-1	-1	-2	-2	-2	-1	-2	-5	-6	-7	-6	-6	-5	-4	-3
80	-2	-2	-1	-2	-2	-2	-1	-1	-2	-4	-5	-5	-3	-2	-2	-3

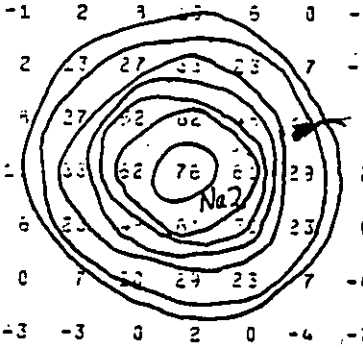

Fig. 6.2.4: Difference Fourier synthesis calculated with the Na(2) cation site removed from the structural model (R = 0.120).

be on either the Na(2) or Na(3) sites.

The distances between Na(1), Na(2) and Na(3) and the framework oxygen O(2) are 2.78Å, 2.52Å and 2.39Å respectively. The ranges of cation-oxygen distances normally found are: K-O: 2.6-2.9Å; Ca-O: 2.2-2.4Å and Na-O: 2.2-2.5Å (BIDICS, 1981). This confirms that the K atom is on the Na(1) site but again the Ca and Na atoms could occupy either the Na(2) or Na(3) site. In sodalite (proper) and hydroxysodalite the sodium atom occupies a position similar to the Na(3) site in hauyne. If Na(3) is the site occupied by Na, by elimination the Ca atom occupies the Na(2) site. The scattering curves for the respective cations were then used in the refinement to determine the occupancy factors of the site. The results summarized above are in satisfactory agreement with the chemical analysis and result in the R-factor dropping from 0.037 to 0.036. Although this decrease is not significant at the 0.05 level according to the Hamilton's test, the agreement with the chemical analysis and the satisfactory bond distances that result give confidence that the model is essentially correct.

The final structural parameters are listed in Tables 6.2.1a to 6.2.3a for the room temperature structure and the corresponding tables for the low temperature (153K) structure are given in Tables 6.2.1b to 6.2.3b. The final R-factor for the low temperature structure was 0.040 and the model with the reflections 110 and 200 included was 0.048. Except for smaller temperature factors, this structure is not significantly different from that at room temperature.

Table 6.2.1a: Atomic parameters and isotropic temperature factor ($\times 10^4$) for hauyne at room temperature

Atom	Site	PP	x	y	z	U equiv. ($Å^2$)
Na(1)	8(e)	0.33(2)	0.6636(9)	0.6636	0.6636	188(22)*
Na(2)	8(e)	0.52(2)	0.7008(8)	0.7008	0.7008	321(21)*
Na(3)	8(e)	0.54(1)	0.7374(5)	0.7374	0.7374	173(16)*
S(1)	8(e)	0.19(1)	0.4657(9)	0.4657	0.4657	501
O(1)	8(e)	0.75	0.5972(24)	0.5972	0.5972	1628(114)*
Al(1)	6(d)	1.0	$\frac{1}{4}$	0	$\frac{1}{2}$	89
Si(1)	6(c)	1.0	$\frac{1}{4}$	$\frac{1}{2}$	0	92
O(2)	24(i)	1.0	0.1443(5)	0.1559(5)	0.4681(4)	228

* isotropic refinement

Table 6.2.2a: Anisotropic temperature factors ($\times 10^4$) for hauyne at room temperature

Atom	U_{11}	U_{22}	U_{23}	U_{12}	U_{13}	U_{23}
S(1)	501(51)	501	501	-101(35)	-101	-101
Al(1)	80(31)	94(17)	94	0	0	0
Si(1)	87(28)	95(15)	95	0	0	0
O(2)	154(27)	232(27)	298(24)	118(15)	6(24)	19(26)

Table 6.2.3a: Selected interatomic distances and angles in hauyne at room temperature

Silicon tetrahedra		**Aluminum tetrahedra**	
Si(1)-O(2)	4 x 1.597(4)Å	Al(1)-O(2)	4 x 1.742(5)Å
O(2)-O(2)	4 x 2.564(6)	O(2)-O(2)	4 x 2.815(6)
	2 x 2.695(6)		2 x 2.902(7)
Mean	2.608	Mean	2.844
O(2)-Si(1)-O(2)	4 x 106.8(2)°	O(2)-Al(1)-O(2)	4 x 107.8(2)°
	2 x 115.0(2)		2 x 112.8(2)
Mean	109.5	Mean	109.5
Si(1)-O(2)-Al(1)	149.7(3)°	**SO_4 tetrahedra**	
ϕ_{Si}	12.4	S(1)-O(1)	3 x 1.447(9)Å
ϕ_{Al}	11.6		1 x 2.076(13)
Al/Si-O	1.670Å	Mean	1.604
Si(1)-Al(1)	3.223(1)		
		O(1)-S(1)-O(1)	3 x 88.8(6)°
			3 x 120.0(7)
		Mean	104.4

Sodium coordinations

Na(1)		Na(2)	
Na(1)-O(2)	3 x 2.783(4)Å	Na(2)-O(2)	3 x 2.524(4)Å
-O(2)	3 x 2.992(6)	-O(2)	3 x 2.864(5)
		-O(1)	1 x 1.636(13)
-O(1)	1 x 1.049(13)	**Na(3)**	
-S(1)	3 x 2.457(6)	Na(3)-O(2)	3 x 2.386(4)Å
		-O(2)	3 x 2.852(4)
		-O(1)	1 x 2.214(13)

Table 6.2.1b: Atomic parameters and isotropic temperature factor ($\times 10^4$) for hauyne at 153K

Atom	Site	PP	x	y	z	U equiv. ($Å^2$)
Na(1)	8(e)	0.33	0.6640(12)	0.6640	0.6640	128(29)*
Na(2)	8(e)	0.52	0.7009(9)	0.7009	0.7009	247(26)*
Na(3)	8(e)	0.54	0.7392(8)	0.7392	0.7392	177(21)
S(1)	8(e)	0.19	0.4669(11)	0.4669	0.4669	450
O(1)	8(e)	0.75	0.5995(27)	0.5995	0.5995	1448(120)
Al(1)	6(d)	1.0	$\frac{1}{4}$	0	$\frac{1}{2}$	73
Si(1)	6(c)	1.0	$\frac{1}{4}$	$\frac{1}{2}$	0	59
O(2)	24(i)	1.0	0.1443(5)	0.1558(6)	0.4669	195

* Isotropic refinement

Table 6.2.2b: Anisotropic temperature factors ($\times 10^4$) for hauyne at 153K

Atom	U_{11}	U_{22}	U_{33}	U_{12}	U_{13}	U_{23}
S(1)	450(68)	450	450	-123(40)	-123	-123
Al(1)	43(22)	87(13)	87	0	0	0
Si(1)	68(21)	54(11)	54	0	0	0
O(2)	142(27)	193(30)	250(35)	121(19)	8(25)	-14(28)

Table 6.2.3b: Selected interatomic distances and angles in hauyne at 153K

Silicon tetrahedra		Aluminum tetrahedra	
Si(1)-O(2)	4 x 1.599(5)Å	Al(1)-O(2)	4 x 1.741(5)Å
O(2)-O(2)	4 x 2.566(7)	O(2)-O(2)	4 x 2.814(7)
	2 x 2.698(7)		2 x 2.902(7)
Mean	2.610	Mean	2.843
O(2)-Si(1)-O(2)	4 x 106.8(2)°	O(2)-Al(1)-O(2)	4 x 107.8(2)°
	2 x 115.1(2)		2 x 112.9(2)
Mean	109.6	Mean	109.5
Si(1)-O(2)-Al(1)	149.3(3)		
ϕ_{Si}	12.0	SO_4 tetrahedra	
ϕ_{Al}	12.9	S(1)-O(1)	3 x 1.480(11)Å
Al/Si-O	1.670Å		1 x 2.092(15)
Si(1)-Al(1)	3.221(1)	Mean	1.633
		O(1)-S(1)-O(1)	3 x 90.0(6)°
			3 x 120.0(7)
		Mean	105.0

Sodium coordinations

Na(1)		Na(2)	
Na(1)-O(2)	3 x 2.765(4)Å	Na(2)-O(2)	3 x 2.511(5)Å
-O(2)	3 x 2.995(8)	-O(2)	3 x 2.871(6)
		-O(1)	1 x 1.600(15)
		Na(3)	
		Na(3)-O(2)	3 x 2.372(5)Å
		-O(2)	3 x 2.863(5)
		-O(1)	1 x 2.204(15)

6.2.1 Discussion of the structure of hauyne:

In their structure refinement of hauyne Lohn and Schulz (1968) found that the temperature factors for Al and Si differed by 50% and they twinned the framework oxygen atom on the (110) mirror plane in order to give reasonable Al-O and Si-O distances. Their results are in direct contrast with those found in this study which shows similar temperature factors for Al and Si and Al-O and Si-O distances that are indicative of complete ordering of Al and Si. No evidence was found for a twinned or split framework oxygen.

Lohn and Schulz (1968) also reported a disordered SO_4 group which occupied two positions which are rotated 90° against each other and has the sulphur atom on the 2(a) position. This gives a regular tetrahedral group with S-O = 1.52Å. They also mentioned that the inter-framework cations force the SO_4 group out of the above position but were unable to incorporate this feature into their refinement. Finally, they found only two cation sites which correspond to the Na(1) and Na(3) sites in this refinement.

In contrast to Lohn and Schulz (1968) the present work shows that the sulphur atom is on an 8(e) position rather than on the 2(a) position. Moreover, the oxygen atoms of the SO_4 group occupy only one set of 8(e) positions. Four of the possible eight 8(e) positions are within a single cavity. The S(1)-S(1) and O(1)-O(1) distances are 0.88Å and 2.51Å respectively. The short S-S distance allows one sulphur atom per cavity. The geometry of the resulting SO_4 group is far from typical with three O(1)-S(1)-O(1) angles of 90° and three of 120°. There are also three S(1)-O(1) distances of 1.45Å and one of 2.08Å. The latter

is longer than the S-O bond expected for the SO_4 group and the average S(1)-O(1) distance is 1.60Å. We can shorten the long S-O distance to the average value if one of the four O atoms (O(1)') in a cavity is placed on 8(e) with x = 0.5673.

Lohn and Schulz (1968) did not report a chemical analysis for hauyne in terms of wt. % oxides. They give a chemical formula which was based on microprobe analysis. This formula and that obtained from the refinement are not electrically neutral as they have an excess of +1.05v.u. and +1.68v.u. respectively. The excess charge may be balanced by OH^-. Lohn and Schulz (1968) reported 4.82 Na, 2.22 Ca and 0.91 K (sum = 7.95) and the present refinement shows 4.32 Na, 2.4 Ca and 1.6 K (sum = 8.32). The total number of cations should not be greater than eight. Both methods show about 1.5 SO_4 per cell. Therefore 75% of the cavities are occupied by SO_4 and the other 25% may contain OH^-.

We could assume that the OH^- would be on a site in close proximity to the S(1) or O(1) sites when these sites are vacant since no electron density was found elsewhere. The S(1) site would allow one OH per cavity while the O(1) site could accommodate two OH per cavity.

Consider the coordination of the Na(1) cation site for which Na(1)-O(1) and Na(1)-S(1) distances are 1.05Å and 2.46Å respectively (Table 6.2.3a). When K atom occupies the Na(1) site, the cavity cannot contain an SO_4 group because of the short distances that would result. In this case, the cavity may contain one OH^- on the S(1) site vacancy.

The Na(2) site is much too close to O(1) for a bond. If this site is occupied then the cavity may contain one OH^- which may be located between the O(1) and S(2) sites. It is also possible for a cavity to

have an SO_4 group and to occupy one of the four Na(2) positions in a cavity since one oxygen of the SO_4 group could move to the O(1)' position to make Na(2)-O(1)' = 2.11Å as was pointed out earlier. This distance is comparable to the Na(3)-O(1) distance of 2.21Å.

The four Na(3) positions in a cavity can be occupied if the cavity contains a SO_4 group in view of the Na(3)-O(1) distance. In the absence of SO_4, the cavity could contain $2OH^-$ which could be located on the O(1) site.

Consider the charge requirement of each cavity and assume that each cavity is electrically neutral. The framework oxygens have a residual charge of -3v.u. per cavity. If a cavity contains $1SO_4^{2-}$ or $2OH^-$ then a total of +5v.u. are required from the cations. Because of the close proximity of the three cation sites only one position can be occupied. Both the chemical analysis and the refinement show that there are about 4 cations per cavity. In order to satisfy the +5v.u the cavity must contain 1 divalent and 3 univalent cations. The K^+ ion is excluded due to spatial requirements since the cavity contains $1SO_4$ or $2OH^-$. Therefore, the cavity contains $3Na^+$, $1Ca^{2+}$ and either $1SO_4^{2-}$ or $2OH^-$. Cavities of the type $(Na_3CaSO_4)^{3+}$ are expected to make up 75% of the structure. This gives 4.5 Na, 1.5 Ca and 1.5 SO_4 per cell. Since this is the number of sodium atoms shown by the chemical analysis and the refinement, we have used up all the sodium atoms. Therefore, a cavity containing $3Na^+$, $1Ca^{2+}$ and $2OH^-$ is unlikely in this material. Moreover, all of the 4.5 Na and 1.5 Ca atoms in the cavity cannot be on the Na(3) site since this would be inconsistent with the occupancy factor of 0.54 Na atoms on the Na(3) site. However, the 4.5 Na atoms on the Na(3)

site would give an occupancy factor of 0.56 which is in agreement with the refinement. Therefore, the Ca atom is likely to be on the Na(2) site. Consequently, the cavity discussed above, contains 3Na on three Na(3) positions, 1Ca on a Na(2) position, a SO_4 group with three oxygens on three O(1) positions and the other oxygen on a O(1)' position. The Ca^{2+} cation would force the S^{6+} atom off the 2(a) position as indicated by the refinement.

Since we have used up all the SO_4^{2-} and Na^+ ions, the other cavities must contain one OH^-. Therefore, we need four cations having a total charge of +4v.u. to neutralize the cavity. This can be done with $4K^+$ ions. However, the chemical formula requires more Ca atoms. Since cavities containing $4Ca^{2+}$ atoms and $10OH^-$ are unlikely, the only other possibility is a cavity containing $2K^+$, $1Ca^{2+}$, $1OH^-$ and a vacant K- site. This type of cavity occurs in 25% of the structure. Therefore, the amount of these ions per cell is 1K, 0.5Ca and $0.5OH^-$. This gives an overall composition of $Na_{4.5}Ca_{2.0}K_{1.0}(Al_6Si_6O_{24})(SO_4)_{1.5}(OH)_{0.5}$ which does not disagree significantly with the chemical formula of Lohn and Schulz (1968) nor with the refinement. In this material, the ratio of $Na:SO_4$ is 3:1 and the amount of Ca is fixed at 2 atoms per cell since both types of cavities contain Ca.

If the SO_4- type of cavity occurs exclusively, the composition would be $Na_6Ca_2(Al_6Si_6O_{24})(SO_4)_2$, which is the ideal composition for hauyne. If the other type of cavity occurs exclusively, then the composition would be $K_4Ca_2(Al_6Si_6O_{24})(OH)_2$ which is an unknown end-member.

Finally, the hauyne used for this study did not show superstructures. However, superstructures have been reported for other hauynes (Taylor, 1967). The temperature factors for the framework atoms and the Al-O and

Si-O distances in hauyne are comparable to those found in sodalite. Therefore, if this material is representative of hauyne, the lack of superstructure would be due to the disorder between different types of cavities.

6.3 Refinement of the Structure of Nosean

The starting model for nosean was the same as that used for hauyne (sec. 6.2) and atomic scattering factors for neutral atoms were taken from Cromer and Mann (1968).

The framework atoms were first refined by using isotropic temperature factors, but the z coordinate of the oxygen atom did not refine. The isotropic temperature factors were then converted to the anisotropic form. The U_{33} component for the oxygen atom became quite large and did not refine. The Al and Si had large temperature factors but they were similar. Fourier map shows that the electron density for the framework oxygen atom was quite elongated. Therefore, this site was split into O(1) and O(2) positions and their occupancy factors were both set at 0.5. The positional and isotropic temperature coordinates for these O(1) and O(2) sites then refined easily and the temperature factor for both sites were identical.

The refinement procedure for the interframework ions was similar to that of hauyne and only additional details will be given here. Three cation positions (Na(1), Na(2), Na(3)) were found (Table 6.3.1). The Na(1) and Na(2) sites are in similar positions as the Na(1) and Na(3) sites respectively in hauyne, and they are on a body diagonal separated by about 1Å. The Na(3) site is on the same body diagonal but in the adjacent cavity at a distance of 1Å from the Na(2) site. The sum of the occupancy factors of the three sites is 1.03. Therefore, there are 4 sodium atoms per cavity.

Difference Fourier map (Fig. 6.3.1) shows that the sulphur atom is on the 2(a) site and the refinement shows that this site is one-half occupied. This is consistent with the chemical analysis (Table 6.2) as are the occupancy factors of the interframework cation sites.

The oxygen atoms of the SO_4 group refined on an 8(e) position to x = 0.4352. This position should be at x = 0.40 since the sulphur is on the 2(a) position. The other 8(e) position with x = 0.60 was also examined for electron density but none was evident. The isotropic temperature factor for the oxygen atom of the SO_4 group was larger than that of the sulphur atom. Therefore, the oxygen site was split into O(3) and O(4) positions which were both on 8(e) sites and are shown in Table 6.3.1. Since the O(4) site is part of the SO_4 group, its population was set equal to the S(1) site. The population of the O(3) site was set at 0.12 on the assumption that this site represents $1H_2O$ per cell.

As in hauyne, two reflections, 110 and 220, were judged unreliable and were temporarily omitted from the model. At this final stage, the allowable positional and temperature coordinates of all the sites were refined simultaneously and the refinement converged to an R-factor of 0.054. Using the refined set of structural parameters and including the reflections 110 and 220, an R-factor of 0.060 was obtained.

For the purpose of illustration, a series of difference Fourier maps is given (Figs. 6.3.1 to 6.3.6*; p. 118-p. 120) in each of which one interframework site has been omitted from the structure factor calculation. In each case the R-factor is also noted in the figure caption to show which site has the most pronounced effect on the refinement of the model. The final structural parameters are given in Tables 6.3.1 to 6.3.3.

* Figures 6.3.4–6.3.6 are given on pp. 234–236.

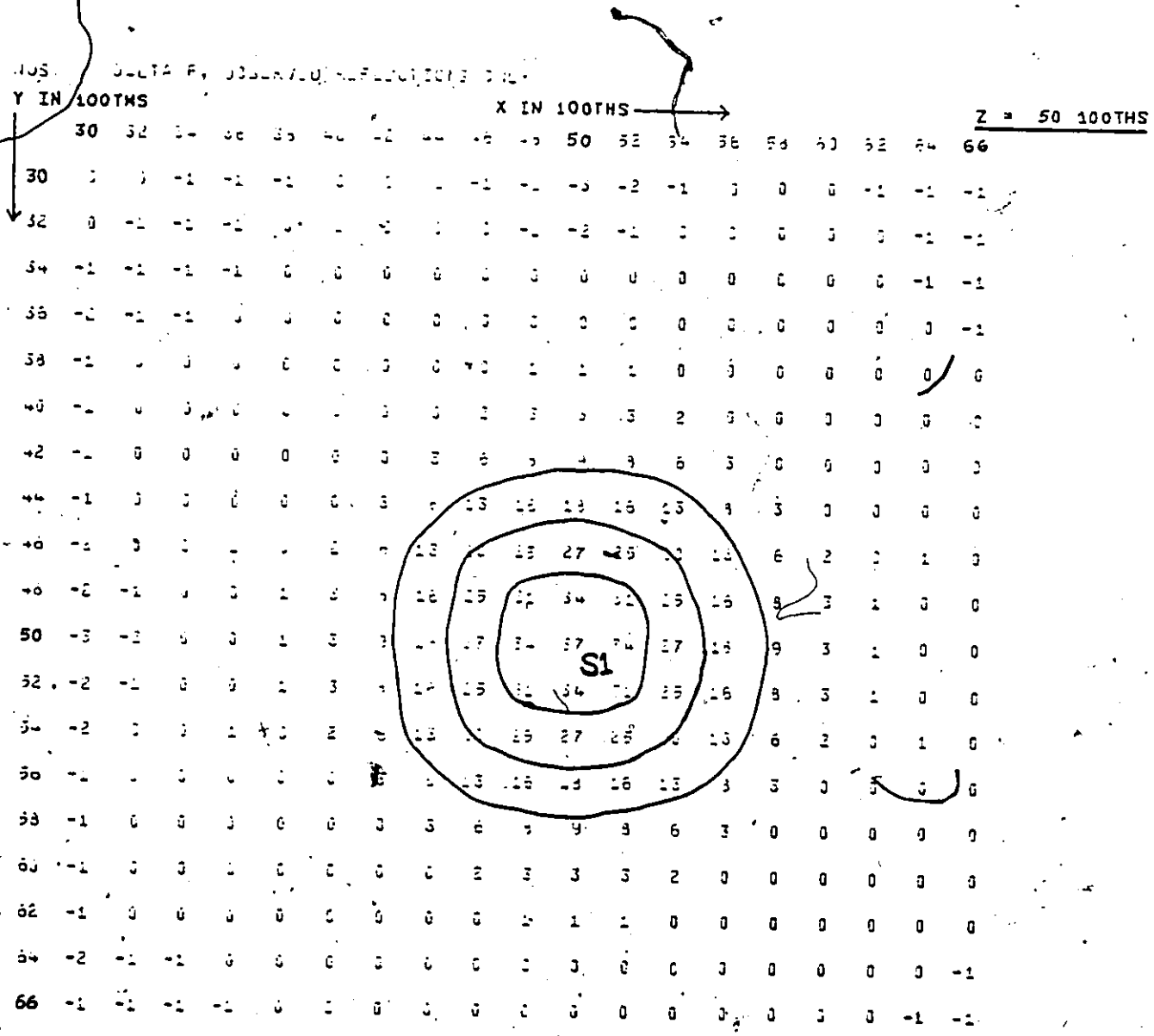

Fig. 6.3.1: Difference Fourier synthesis calculated with S(1) site removed from the structural model (R = 0.086).

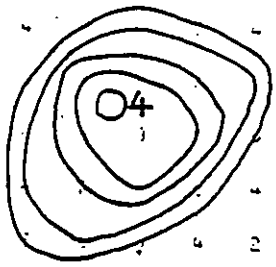

DELTA F, OBSERVED REFLECTIONS ONLY

Y IN 100THS ↓ X IN 100THS →

Z = 40 100THS

Y \ X	30	32	34	36	38	40	42	44	46	48	50	52	54	56	58	60	62	64	66
30	0	1	0	0	0	1	0	0	0	0	-1	-1	-1	0	0	1	1	0	-1
32	0	0	0	0	1	1	1	1	0	0	0	0	0	0	1	2	2	1	0
34	-1	0	1	2	3	3	3	2	2	1	1	1	1	2	3	4	3	2	0
36	-1	1	2	4	5	5	4	3	3	2	2	2	3	5	6	6	4	2	
38	0	1	3	5	6	6	5	4	3	2	2	2	4	6	8	9	6	4	
40	0	1	3	5	6	6	5	3	2	1	1	2	3	6	8	9	6	4	
42	0	1	3	5	6	6	4	2	1	0	0	1	2	4	6	6	5	3	
44	0	1	3	5	6	5	4	2	1	0	0	0	1	2	2	3	4	3	1
46	0	1	2	3	4	3	2	1	0	0	0	0	1	1	1	2	2	2	1
48	0	0	2	2	3	2	1	0	0	0	0	0	1	1	1	1	2	1	1
50	0	0	1	2	2	1	0	0	0	0	0	0	0	0	1	2	2	1	
52	0	0	1	1	2	1	1	1	1	0	0	0	0	0	1	2	3	2	2
54	-1	0	1	2	2	2	1	1	1	0	0	0	0	1	2	3	4	3	2
56	0	0	1	3	4	3	3	2	1	0	0	0	1	2	4	5	6	5	3
58	0	1	3	5	6	6	4	2	1	0	0	1	2	4	6	8	7	6	3
60	1	2	4	6	8	8	6	3	2	1	1	2	3	5	8	9	8	6	3
62	1	2	4	6	8	9	6	4	2	2	2	3	4	6	7	8	8	5	3
64	0	1	2	4	6	6	5	3	2	2	2	3	3	4	5	6	5	4	2
66	-1	0	0	2	4	4	3	2	1	1	1	1	2	2	3	3	3	2	1

Fig. 6.3.2: Difference Fourier synthesis calculated with O(4) site removed from the structural model (R = 0.070).

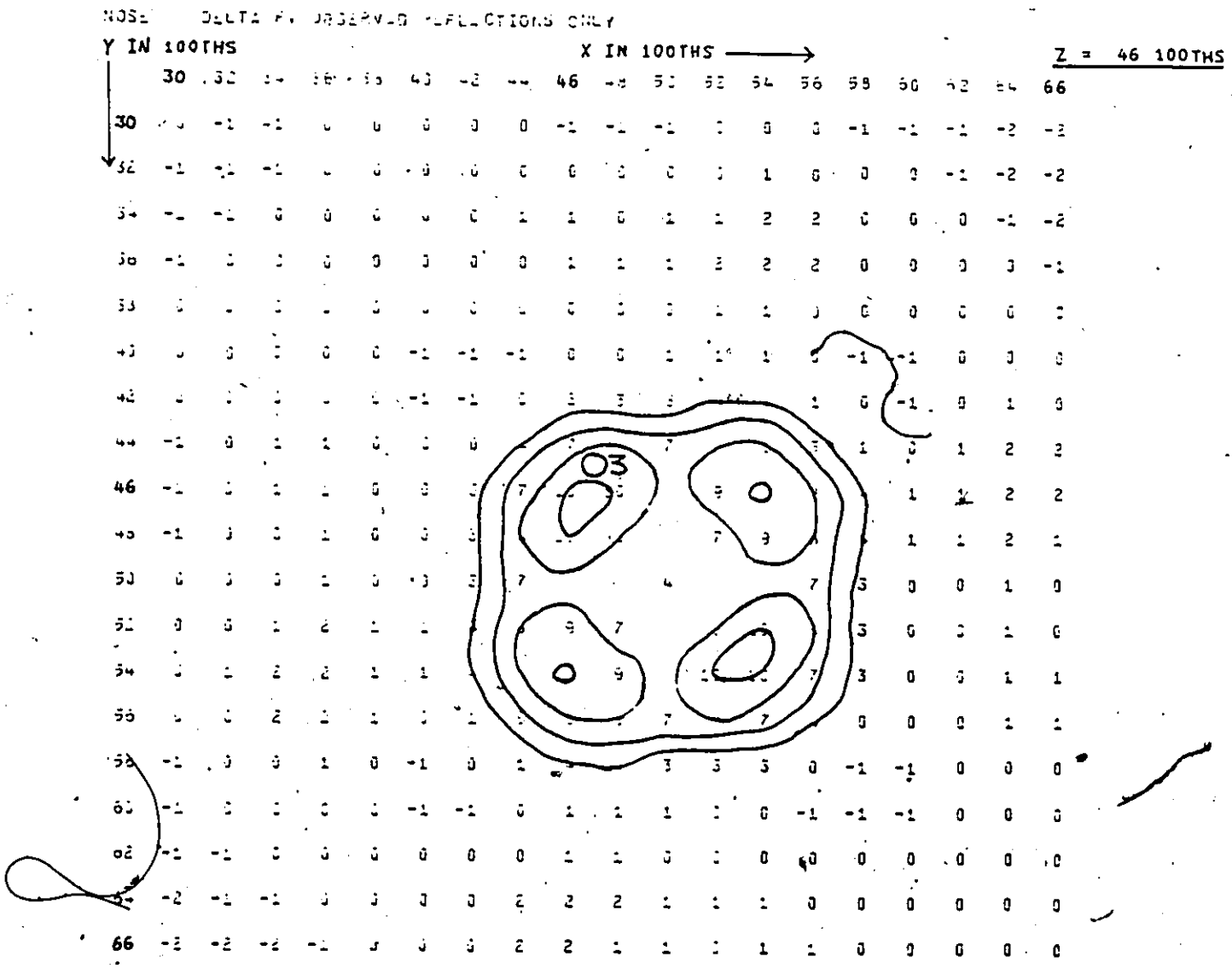

Fig. 6.3.3: Difference Fourier synthesis calculated with O(3) site removed from the structural model (R = 0.063).

Table 6.3.1: Atomic parameters and isotropic temperature factor ($x\ 10^4$) for nosean

Atom	Site	PP	x	y	z	U($Å^2$)
Al	6(d)	1.0	$\frac{1}{4}$	0	$\frac{1}{2}$	306
Si	6(c)	1.0	$\frac{1}{4}$	$\frac{1}{2}$	0	291
O(1)	24(i)	0.50	0.1371(29)	0.1465(30)	0.5460(16)	369(30)
O(2)	24(i)	0.50	0.1527(30)	0.1591(30)	0.4775(16)	369(31)
Na(1)	8(e)	0.16(3)	0.6629(22)	0.6629	0.6629	259(63)
Na(2)	8(e)	0.31(2)	0.7384(9)	0.7384	0.7384	137(25)
Na(3)	8(e)	0.56(2)	0.3020(8)	0.3020	0.3020	461(30)
O(3)	8(e)	0.12	0.4635(31)	0.4635	0.4635	290(155)
O(4)	8(e)	0.54	0.4023(27)	0.4023	0.4023	1590(184)
S(1)	2(a)	0.54(2)	$\frac{1}{2}$	$\frac{1}{2}$	$\frac{1}{2}$	1411(114)

Table 6.3.2: Anisotropic temperature factor ($x\ 10^4$) for Al and Si in nosean

Atom	U_{11}	U_{22}	U_{33}	U_{12}	U_{13}	U_{23}
Al	375(51)	272(28)	272	0	0	0
Si	210(35)	331(27)	331	0	0	0

Table 6.3.3: Selected interatomic distances and angles in nosean

Silicon tetrahedra		Aluminum tetrahedra	
Si-O(1)	4 x 1.615(26)Å	Al-O(1)	4 x 1.732(26)Å
O(1)-O(1)	4 x 2.628(36)	O(1)-O(1)	4 x 2.791(37)
	2 x 2.643(35)		2 x 2.846(35)
Mean	2.633	Mean	2.809
O(1)-Si-O(1)	4 x 109.8(9)°	O(1)-Al-O(1)	4 x 110.5(9)°
	2 x 108.9(9)		2 x 107.4(9)
Mean	109.5	Mean	109.5
Si-O(2)	4 x 1.627(27)Å	Al-O(2)	4 x 1.706(27)Å
O(2)-O(2)	4 x 2.581(34)	O(2)-O(2)	4 x 2.804(38)
	2 x 2.717(34)		2 x 2.919(38)
Mean	2.626	Mean	2.842
O(2)-Si-O(2)	4 x 104.9(8)°	O(2)-Al-O(2)	4 x 105.7(8)°
	2 x 119.0(9)		2 x 117.6(9)
Mean	109.6	Mean	109.7
Si-O(1)-Al	147.3(9)°		
Si-O(2)-Al	148.9(9)°	SO_4 tetrahedra	
Mean	148.1	S-O(4)	4 x 1.537(14)Å
		O(4)-S-O(4)	6 x 109.5(7)°

Sodium coordinations

	Na1	Na2	Na3
-O(1)	3 x 2.725(27)Å	2.329(21)	2.435(16)
-O(3)	3 x 2.432(13)	---	1 x 2.542(16)
-O(2)	3 x 2.860(15)	2.417(18)	2.463(23)
-O(2)	3 x 2.874(26)	2.732(18)	2.997(15)
-O(4)	3 x 2.511(8)	1 x 2.579(15)	1 x 1.579(15)!!
-S	1 x 2.562(12)!!	---	---

6.3.1 Discussion of the structure of nosean:

Schulz (1970) gave a refinement of nosean using the space group $P\bar{4}3m$. The 6Al and 6Si atoms of the framework were disordered on a twelve-fold position and the 24 O atoms of the framework were on two sets of twelve-fold positions. Although the two cavities in a cell are not identical in the space group $P\bar{4}3m$, SO_4 group was found in both cavities. In each cavity the SO_4-tetrahedron occupied two positions, which are rotated 90° against each other.

This work shows that the framework oxygen occupies two positions and despite this splitting, the Al-O and Si-O bonds (Table 6.3.3) are indicative of complete ordering of Al and Si. The Al and Si atoms also have identical but large temperature factors.

The SO_4 group in nosean is ordered and its geometry is a regular tetrahedron with S-O = 1.54Å. However, the temperature factors for both the S and O atoms are large but they are of similar magnitude.

Both the chemical analysis and the refinement show 8 Na atoms and 1 SO_4^{2-} per cell. Moreover, the refinement indicates 1 H_2O molecule per cell. The oxygen atom of the H_2O molecule is on the O(3) site but the difference Fourier map (Fig. 6.3.3: p. 122) shows another site close to the O(3) position for the H_2O molecule. However, due to short distances between the positions of the H_2O molecule only one position can be occupied. The chemical formula for nosean is therefore $Na_8(Al_6Si_6O_{24})(SO_4).1H_2O$ and each cavity may contain $(Na_4\ SO_4)^{2+}$ or $(Na_4.H_2O)^{4+}$. The ratio of the two types of cavities is 1:1.

The two types of cavities obviously have different charge and since the framework oxygens of each cavity require 3v.u., we can expect $(Na_4SO_4)^{2+}$- type of cavity to be surrounded by $(Na_4.H_2O)^{4+}$- type of

cavity and vice-versa so that the charge on the framework atoms will be satisfied within the smallest volume.

We can now identify the positions of the sodium atoms in the two types of cavities by considering the coordination of the cation sites. When a cavity contains a SO_4 group, it is clear that the 4Na atoms are on the Na(2) site since the Na(1) and Na(3) sites are too close to either the S atom or the oxygen atom of the SO_4 group (Table 6.3.3). Since SO_4^{2-} is in 50% of the cavities, the population of the Na(2) site should be 0.50 instead of 0.31. The difference in population parameter may suggest a high correlation between U and PP. It should be noted that the temperature factor for the Na(2) site is about 1/3 that of the Na(3) site (Table 6.3.2).

If a cavity contains a H_2O molecule on the O(3) site, the 4Na atoms could be on either the Na(1) or the Na(3) site or both. The population parameter indicates that the Na(3) site is occupied more often than the Na(1) site.

The ordering of the $(Na_4SO_4)^{2+}$ and $(Na_4H_2O)^{4+}$ cavities may be seen by considering the stereoscopic projection of the sodalite structure shown in Fig. 4.1.1(p. 21). There are eight six-membered rings with which the eight cations are associated. If the centre of the cage contains a H_2O molecule then the four nearest sodiums are either on the Na(1) or Na(3) sites. The other four sodiums (which normally would bond to the Cl at the corners of the cell) are on Na(2) sites which are still within the cavity but they are bonded to SO_4 group in the cavities at the corners of the cell. The occupancy of the Na(2) site forces the orientation of the SO_4 group.

The Al and Si atoms contribute identical valence to the O(1) and O(2) framework oxygen atoms. It is therefore difficult to model the charge distribution in detail between cavities containing $(Na_4SO_4)^{2+}$ and $(Na_4H_2O)^{4+}$. The split framework oxygen is a result of the difference in size of the SO_4^{2-} ion and the H_2O molecule, and due to the ordering of the different cavities the split framework positions are well resolved. The charge difference between the two types of cavities imposes clustering of one about the other. As a result, strong superstructure reflections are observed (Fig. 6.2).

Finally, it is impossible that $(Na_4SO_4)^{4+}$- cavities can occur exclusively in nosean because the structure would not be electrically neutral. Cavities containing only 4 Na atoms are also unlikely. Therefore the ideal composition is $Na_8(Al_6Si_6O_{24})SO_4.1H_2O$ for nosean. Although the refinement indicates $1H_2O$ per cell it is possible that the amount can vary but to no more than $2H_2O$ per cell.

CHAPTER 7

CRYSTAL STRUCTURES OF MINERALS IN THE CANCRINITE GROUP

The structure of a cancrinite (proper): $Na_6(Al_6Si_6O_{24})Ca_{1.5}1.6CO_3.2H_2O$ has been fully refined in the space group $P6_3$ to a conventional R-factor of 2.8% (Hassan, 1980 or Grundy and Hassan, 1982). The structural model obtained is the basis on which more chemically-complex species of cancrinite were refined.

Here the structure of three additional members of the cancrinite group (synthetic hydroxycancrinite, vishnevite and davyne) will be considered and compared to cancrinite. It may be necessary for readers to refer to the above reference, in particular for details of the structure, however, some of the description is given in section 2.3(p. 9).

Previous structural work has not been done on vishnevite nor davyne. However, recently Pahor et al. (1982) did a structure of a basic cancrinite using a single crystal. This material is hereafter referred to as hydroxycancrinite.

7.1 Hydroxycancrinite

7.1.1 Experimental:

Long exposure precession photographs (Figs. 7.1.1 and 7.1.2) show that all the observed diffraction maxima are sharp and they also show symmetry which is consistent with the space group $P6_3$.

The occurrence of satellite reflections in hydroxycancrinite is

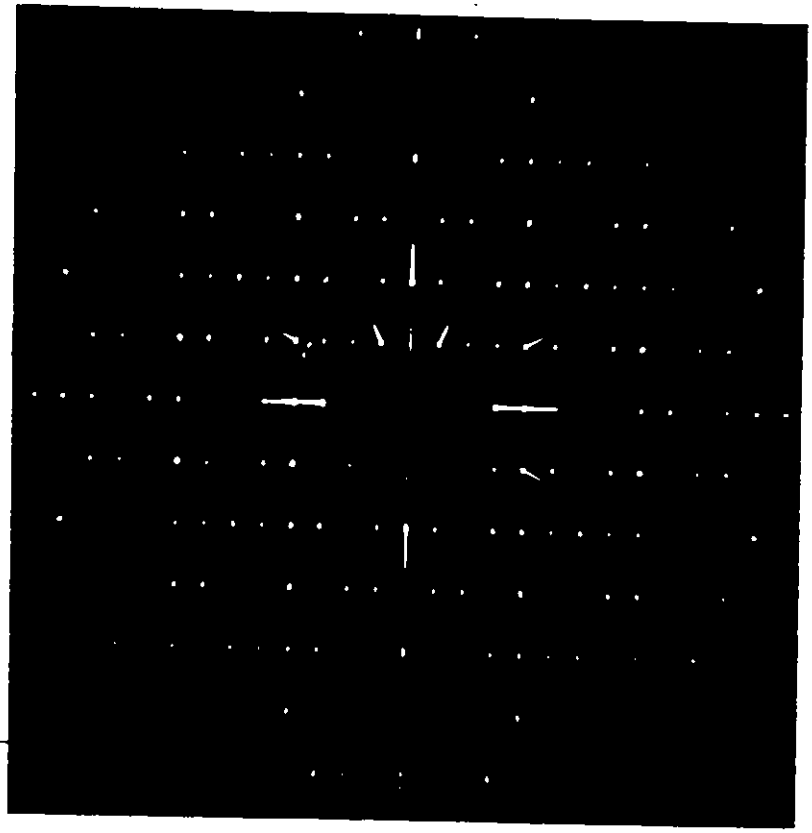

Fig. 7.1.1: X-ray diffraction photograph of the a^*c^* plane of the reciprocal lattice plane of hydroxycancrinite showing very weak satellite reflections in rows parallel to a^*. ($\mu = 25^\circ$, MoK_α, Zr filter)

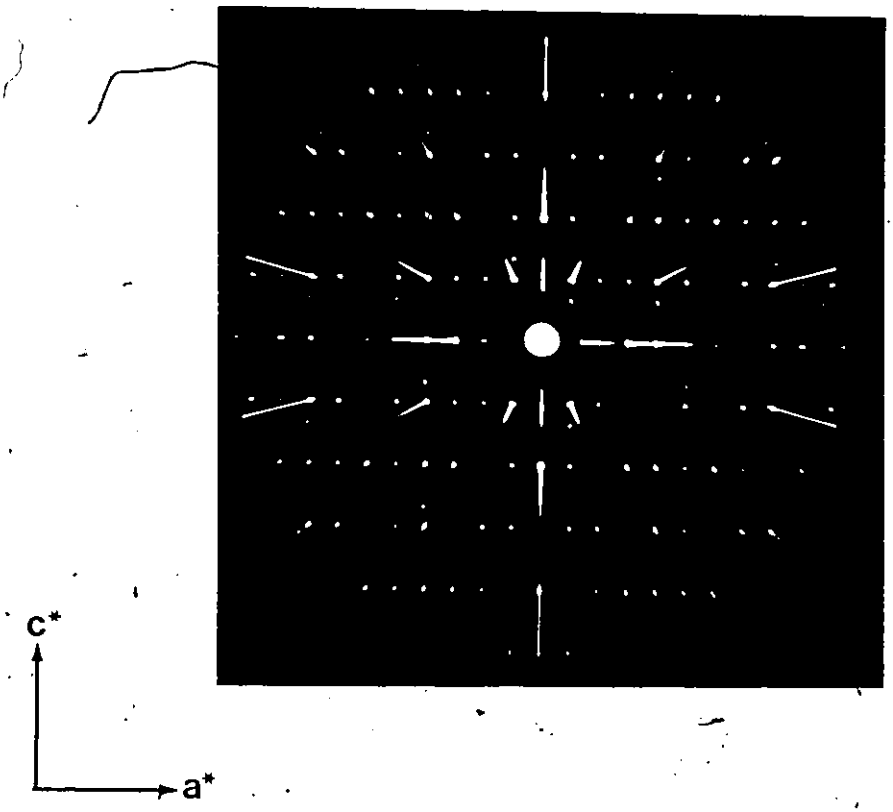

Fig. 7.1.2: X-ray diffraction photograph of the a^*c^* plane of the reciprocal lattive plane of hydroxycancrinite showing "extra" reflections due to the presence of another phase. No superstructure is present. ($\mu = 20^o$, MoK_α, Zr filter).

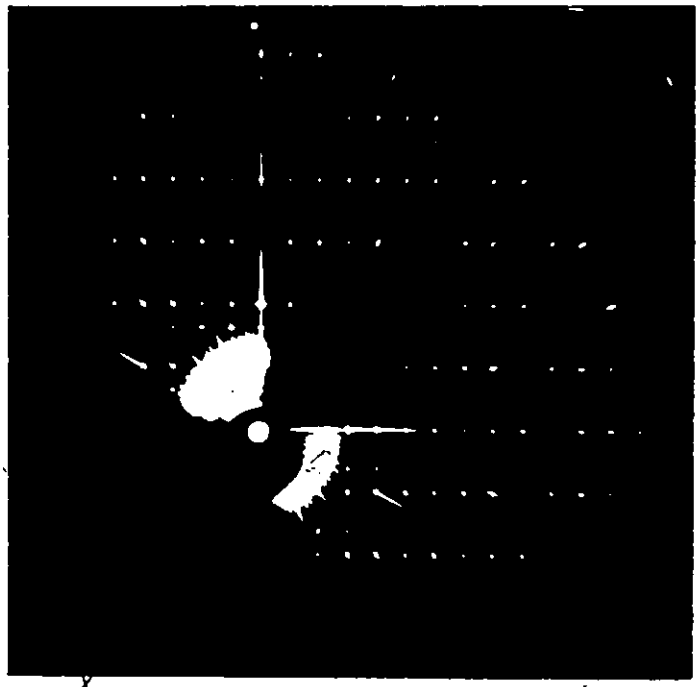

Fig. 7.1.3. Cancrinite showing well-developed superstructure reflections in rows parallel to a*. ($\mu = 25^{o}$, MoK_{α}, Zr filter).

highly variable. Figure 7.1.1 shows a very weak one-dimensional superstructure affecting the c^*-axis. These reflections also show streaking parallel to the c^*-axis (easily seen from negative but not from print). On the other hand, another crystal shows no superstructure (Fig. 7.1.2). The 'extra' reflections seen in Figure 7.1.2 are not superstructure but they reflect the presence of another phase since they are not aligned with the substructure diffraction maxima. Pahor et al. (1982) did not mention anything about satellite reflections for their specimen. The variability of the satellites in hydroxycancrinite may depend on the different conditions of synthesis and therefore composition. The samples were prepared at 15,000 p.s.i and at various temperatures from 450°C to 600°C (see Anderson and Burley, 1982).

Figure 7.1.3 of cancrinite is included here for comparison. It shows well-developed and strong satellites. Additional photographs of cancrinite can be found in Chen (1970).

Two crystal structures of hydroxycancrinite were refined. One shows satellites and the other does not have satellites. The identical results were finally obtained, only the structure obtained from the latter crystal will be presented here.

Cell dimensions determined by least-squares from 26 substructure reflections automatically aligned on a 4-circle diffractometer are presented in Table 7.1.1 together with other information pertaining to the material chosen, x-ray data collection and refinement.

7.1.2 Refinement:

The final positional parameters and temperature factors of cancrinite (Hassan, 1980) were used as the starting model. That is, in

Table 7.1.1: Crystal data and data collection information for synthetic+ hydroxycancrinite

Chemical Analysis*		Cell Contents**		Miscellaneous	
SiO_2	36.27	Si	6.19	a	12.664(2)Å
Al_2O_3	28.93	Al	5.81	c	5.159(1)Å
Na_2O	24.06	Na	7.95	V	716.54 Å^3
H_2O	6.24	H_2O	2.37	Space Group	$P6_3$
		OH	2.37	Z	1
wt %	95.50			Density Calc. (g/cm^{-3})	2.27
				Crystal size (mm)	0.20 x 0.20 x 0.23
				μ(cm^{-1})	7.63
				Radiation/Monochromator	$\hat{M}o/C$
				Total no. of I	2029
				No. of non-equiv.	959
				No. of non-equiv. $\lvert F_o \rvert > 3\sigma$	870

Chemical formula used in refinement:

$Na_8(Al_6Si_6O_{24})(OH)_2.2.68H_2O$

Final R(obs) = 4.7%
$= \sum(\lvert F_o \rvert - \lvert F_c \rvert)/\sum\lvert F_o \rvert$

Final R_w(obs) = 5.7%
$= (\sum w(\lvert F_o \rvert - \lvert F_c \rvert)^2/\sum w\lvert F_o \rvert^2)^{\frac{1}{2}}$

w = 1

+ Anderson and Burley (1981)
* wet analysis, J. Muysson, McMaster University
** Calculated from chemical analysis based on Si + Al = 12

addition to the framework atom parameters, one oxygen and one sodium were placed in each cage and the other six sodiums were placed in the channels. Scattering factors for neutral atoms were taken from Cromer and Mann (1968) and that for hydrogen was from Stewart et al. (1968).

Using the starting model and anisotropic temperature factors, the R-factor obtained was 6.1%. Large scale difference Fourier maps of electron density prepared for the channel using the observed structure factors and phase information from the refinement at this stage show electron density all along the 6_3 axis. Two significant peaks are shown in Figure 7.1.4a. Also split peaks are shown in similar positions as the oxygens of the carbonate group in cancrinite (Fig. 7.1.4b). Oxygens were placed on these sites and their population was initially adjusted to that indicated by the chemical analysis. These site populations and isotropic temperature factors were then refined. Subsequent cycles of refinement resulted in a final R-factor of 4.7%.

Difference Fourier maps of the channel at this stage showed no residual density off the 6_3 axis. However, on the 6_3 axis, small amounts of residual density (Figure 7.1.5) were seen at (0, 0, 0.97). Hydrogen atoms were placed on this site and its isotropic temperature factor was set at 20% above that of the O52 oxygen site and was held invariant. However, the positional parameter could not be refined properly. This may be due to the small amount of electron density. Therefore, this site was ignored.

The population parameters for the sodium cation sites (Na1 and Na2) were then refined and the results were consistent with that of full occupancy. Similar results were obtained for the disorder oxygen site O(6).

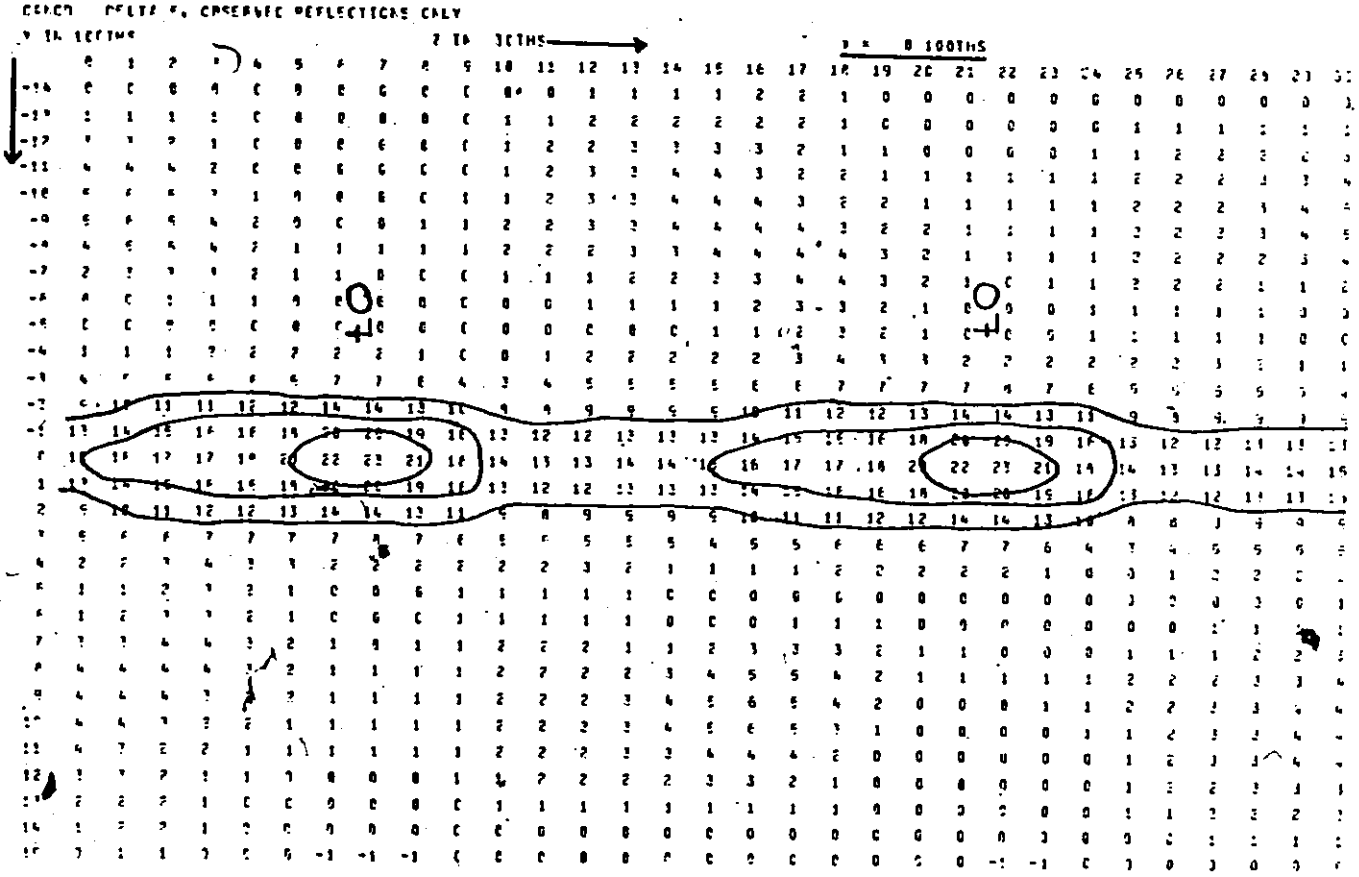

Fig. 7.1.4a: Difference Fourier section through the 6_3 axis. This section shows the O7 oxygen site position.

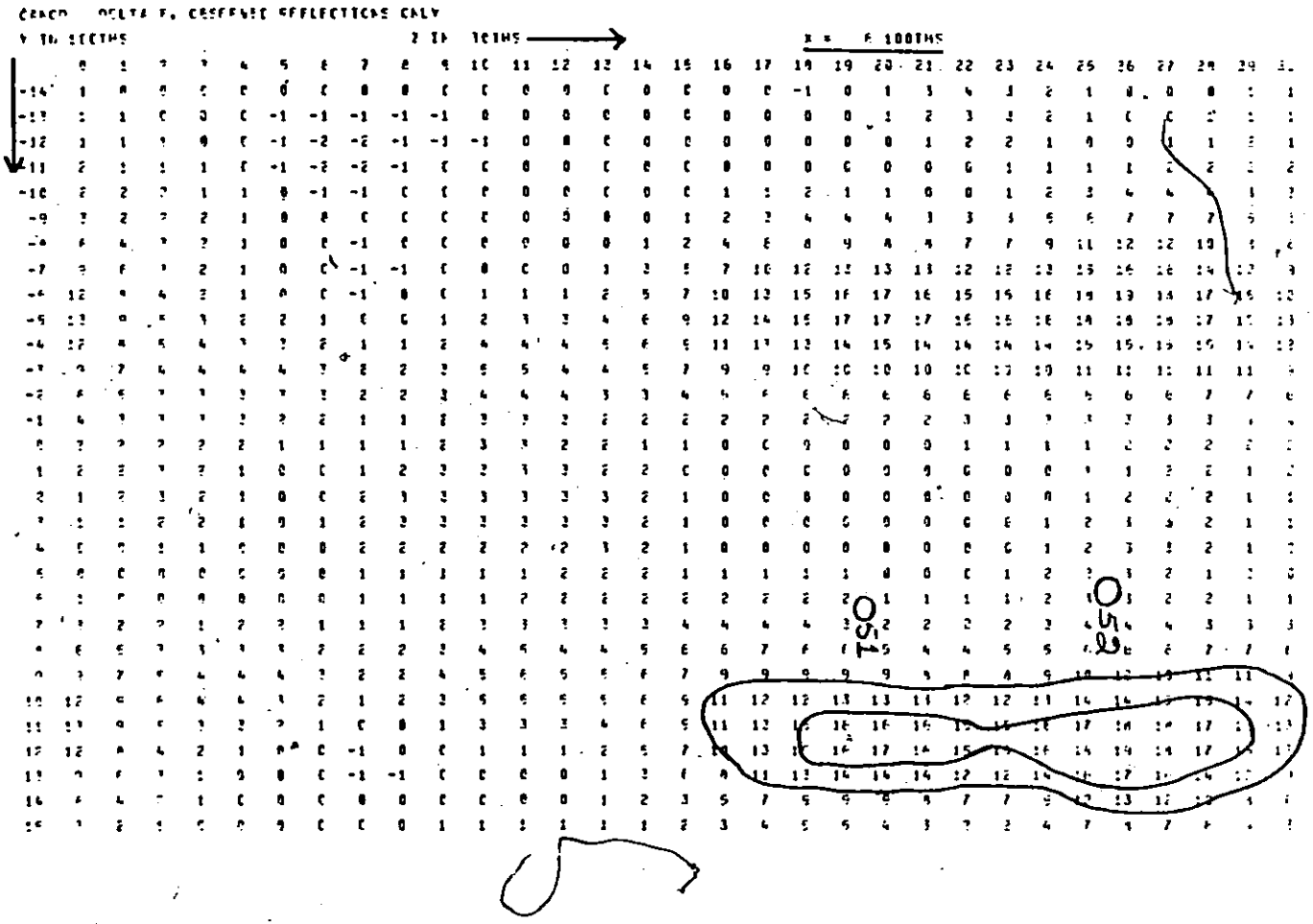

Fig. 7.1.4b: Difference Fourier section through the 051 and 052 sites, calculated with the oxygen on these sites removed from the structural model.

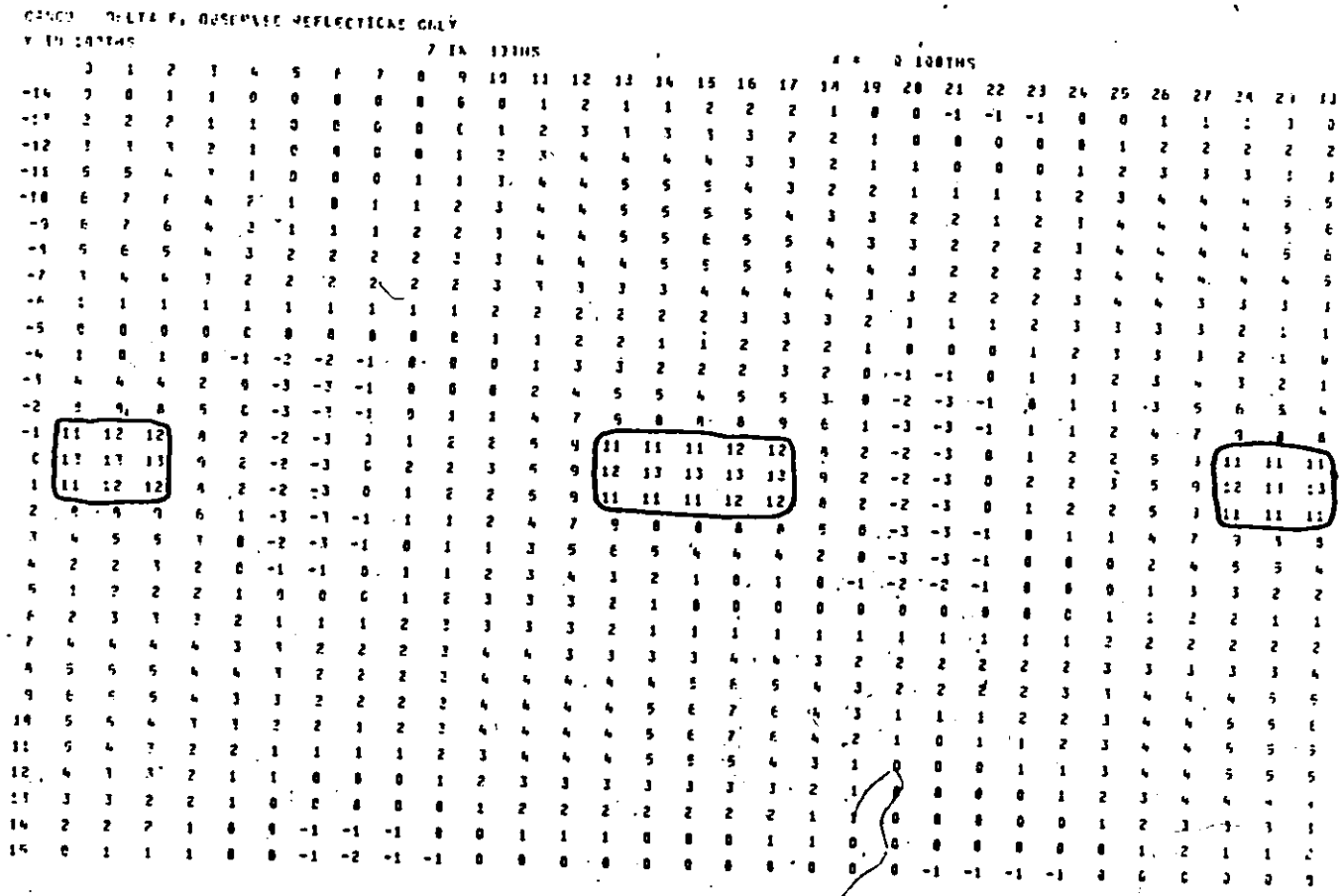

Fig. 7.1.5: Difference Fourier section through the 6_3 axis calculated with the final structural model. The small residual density still seen may be due to hydrogen which was not incorporated in the model.

Figures 7.1.6a and b show the final form of the electron density of the 07, 051 and 052 oxygen sites. These Fourier maps were prepared using only the observed reflections.

The final positional parameters are shown in Table 7.1.2 and the anisotropic temperature factors are presented in Table 7.1.3. The observed and calculated structure factors are given in Appendix 1.

7.1.3 Discussion:

The general features of the structure have been described in section 2.3 and only additional details are given here. Important interatomic distances are shown in Table 7.1.4 and interframework angles are given in Table 7.1.5.

The overall geometry of the structure is remarkably similar to that of cancrinite. The average Si-O and Al-O bond lengths are 1.621Å and 1.727Å respectively and these compare well to 1.612Å and 1.733Å respectively in cancrinite. The average Si-O bond length obtained is experimentally within 1.616Å which corresponds to full occupancy by Si (Bauer, 1978) thus by implication, the framework is fully ordered. Bond valence calculations (Brown and Shannon, 1973) given in Table 7.1.4 show that the charge on all the cations is fully satisfied and correspond to full occupancy.

Figure 7.1.7 shows a stereoscopic view of the framework of cancrinite down the c-axis and the coordination of Na1 is shown in Figure 7.1.8. The two possible coordinations of the cation site Na2 are shown in Figure 7.1.9. The coordination of the sites Na1 and Na2 are exactly the same as in cancrinite (proper).

All the framework atoms in hydroxycancrinite have larger

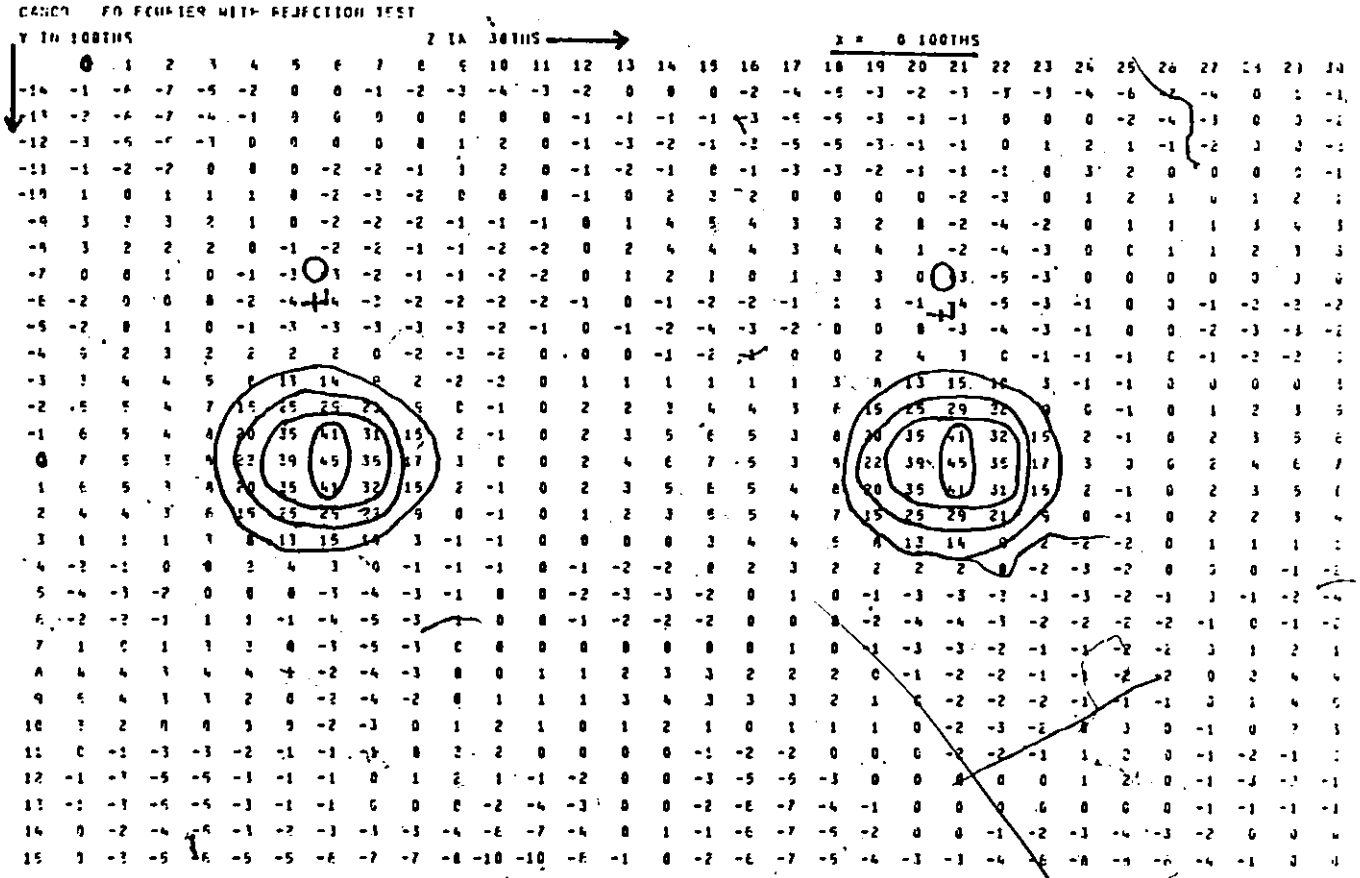

Fig. 7.1.6a: Fourier section showing the final form of the 07 site, calculated using only the observed reflections.

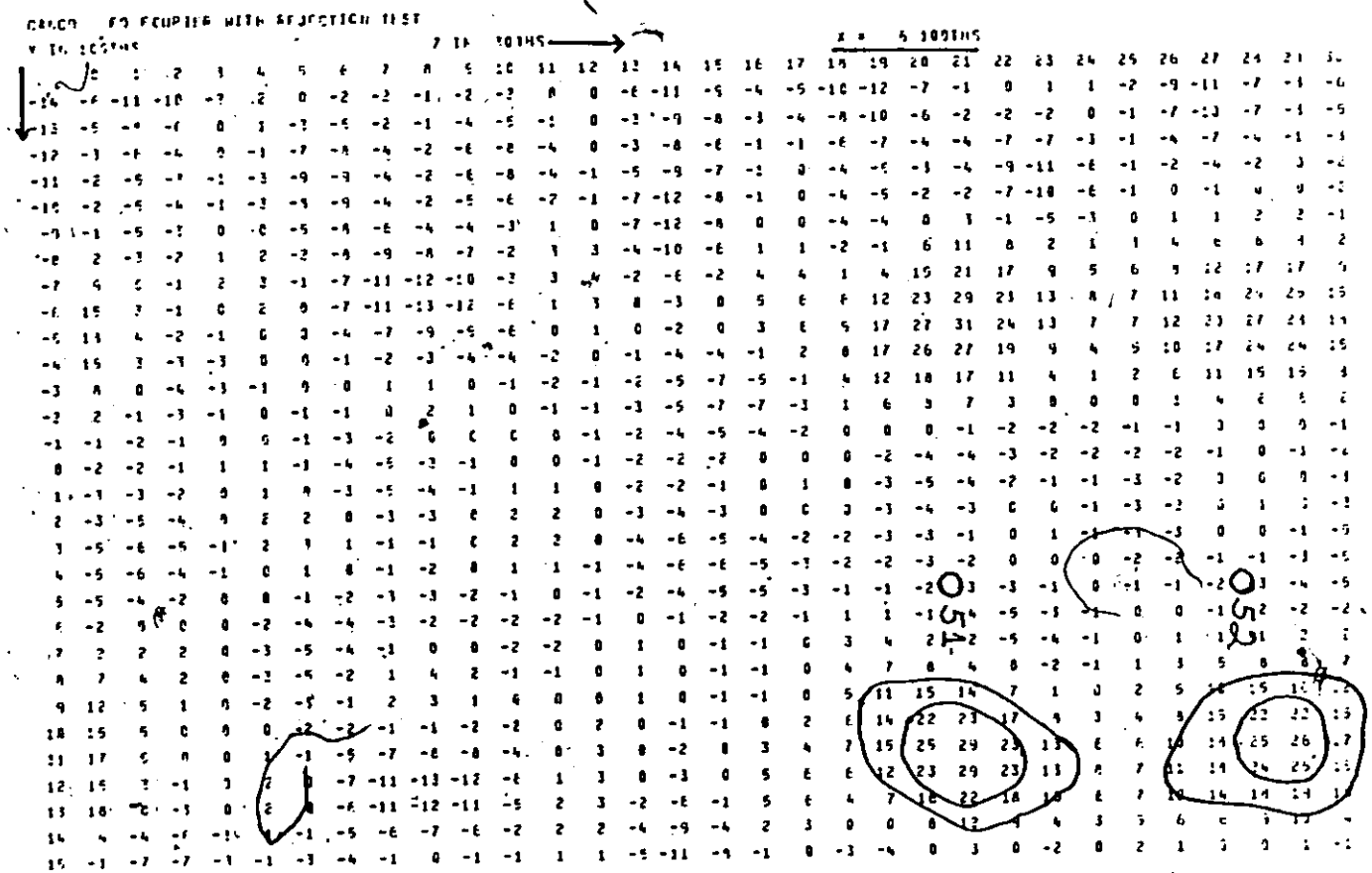

Fig. 7.1.6b: Fourier section showing the final form of the 051 and 052 sites, calculated using only the observed reflections.

Table 7.1.2: Positional parameters, population parameters and isotropic temperature factors (x 10^4) for hydroxycancrinite

Framework atoms

atom	site	site content	x	y	z	$U_{(equiv)}$ Å^2
O1	c	O	.2022(4)	.4034(4)	.6653(10)	176
O2	c	O	.1184(4)	.5647(4)	.7269(15)	235
O3	c	O	.0287(4)	.3531(4)	.0579(9)	170
O4	c	O	.3190(4)	.3611(5)	.0421(9)	207
T1	c	Si	.3298(1)	.4125(1)	.7500	88
T2	c	Al	.0764(1)	.4133(1)	.7515(6)	80

Non-framework atoms*

O51	c	0.17	O+.83 □	.0514(27)	.1087(26)	.6714(59)	214 ch
O52	c	0.17	O+.83 □	.0541(32)	.1096(30)	.9377(74)	236 ch
O7	a	0.34	O+.66 □	0	0	.6931(61)	361 ch
O6	c	0.33	O	.6152(21)	.3097(42)	.6835(50)	587 cg
Na1	b	1.0	Na	2/3	1/3	.1250(15)	334 cg
Na2	c	1.0	Na	.1320(3)	.2669(3)	.2867(9)	410 ch

* chemical symbol □ is vacancy
ch located in channel
cg located in cage

Table 7.1.3: Anisotropic temperature factors ($\times 10^4$) for hydroxycancrinite

Framework atoms						
Atom	U_{11}	U_{22}	U_{33}	U_{12}	U_{13}	U_{23}
O1	104(16)	252(20)	173(18)	116(16)	-2(15)	5(16)
O2	204(17)	141(16)	359(29)	106(14)	54(26)	40(25)
O3	172(18)	264(21)	74(20)	120(17)	37(16)	44(17)
O4	254(21)	267(21)	101(20)	197(19)	11(17)	26(18)
T1	89(5)	96(5)	79(5)	55(4)	-11(8)	3(7)
T2	71(5)	86(5)	84(6)	35(5)	-5(8)	11(9)
Non-framework atoms						
O51	214(55)					
O52	236(58)					
O7	361(59)					
O6	637(152)	653(206)	471(129)	232(220)	56(101)	90(157)
Na1	218	218	567(40)	109(7)	0	0
Na2	286(14)	563(20)	383(24)	288(14)	-32(16)	-62(19)

Table 7.1.4: Selected interatomic distances[+] and Bond Strength (valence units)[*] for hydroxycancrinite

Bond	Å	Bond strength (v.u.)	Bond	Å	Bond strength (v.u.)
T1-01	1.622(5)	1.000(13)	T2-01	1.717(6)	0.783(11)
-02	1.615(7)	1.019(16)	-02	1.718(5)	0.781(9)
-03	1.626(9)	0.989(23)	-03	1.727(5)	0.764(9)
-04	1.620(5)	1.005(13)	-04	1.747(7)	0.727(12)
Mean	1.621	Total 4.014	Mean	1.727	Total 3.056
		Expected** 4.0			Expected 3.0
Na1-01 x 3	2.894(5)	0.195(0)			
-02 x 3	2.417(5)	0.537(2)			
-06[a]	2.899(26)	0.065(3)			
-06[b]	2.369(26)	0.200(12)			
Mean for 8	2.650	Total 0.996			
4	2.405	Expected 1.0			
	trigonal bipyramid			octahedral	
Na2-01	2.462(7)	0.161(2)	Na2-01	2.462(7)	0.161(2)
-03	2.394(8)	0.189(3)	-03	2.394(8)	0.189(3)
-04	2.408(6)	0.182(2)	-04	2.408(6)	0.182(2)
-051[a]	2.636(30)	0.110(7)	-052[a]	2.659(70)	0.105(15)
-051[b]	2.589(67)	0.122(17)	-052[a]	2.670(35)	0.102(7)
-051[b]	2.646(34)	0.108(7)	-052[b]	2.523(33)	0.141(10)
Mean	2.523		Mean	2.519	
-03	2.879(7)	0.067(0)	-03	2.879(7)	0.067(0)
-04	2.913(11)	0.063(0)	-04	2.913(11)	0.063(0)
-07	2.966(6)	0.057(0)	-07	2.966(6)	0.057(0)
Mean	2.655	Total 1.058	Mean	2.653	Total 1.066
		Expected 1.0			Expected 1.0

\+ a = above; b = below
* universal curves
** expected from site population (see Table 7.1.2)

Table 7.1.5: Selected framework angles (°) for hydroxycancrinite

	Tetrahedral		
O1-T1-O2	107.6(3)	O1-T2-O2	106.3(2)
-O3	107.7(3)	-O3	109.7(3)
-O4	110.0(3)	-O4	107.5(4)
O2-T1-O3	112.4(3)	O2-T2-O3	113.9(3)
-O4	111.8(3)	-O4	113.4(4)
O3-T1-O4	107.4(4)	O3-T2-O4	105.8(2)
Mean	109.5	Mean	109.4

Bridging	
T1-O1-T2	148.5(4)
T1-O2-T2	149.2(3)
T1-O3-T2	135.9(4)
T1-O4-T2	135.9(3)
Mean	142.4

Fig. 7.1.7: Stereographic schematic of the framework of cancrinite viewed down the C-axis. The large channel is defined by the 'chains' of interconnected small cages parallel to the C-axis.

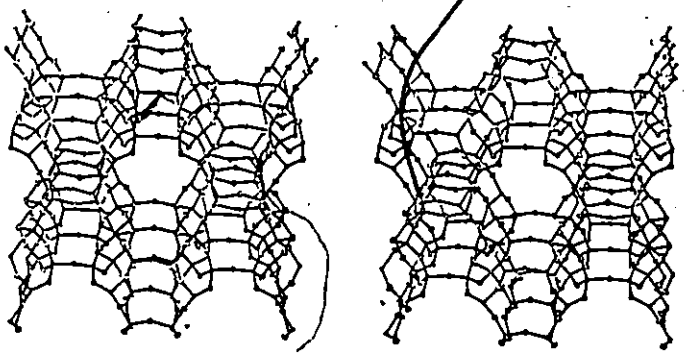

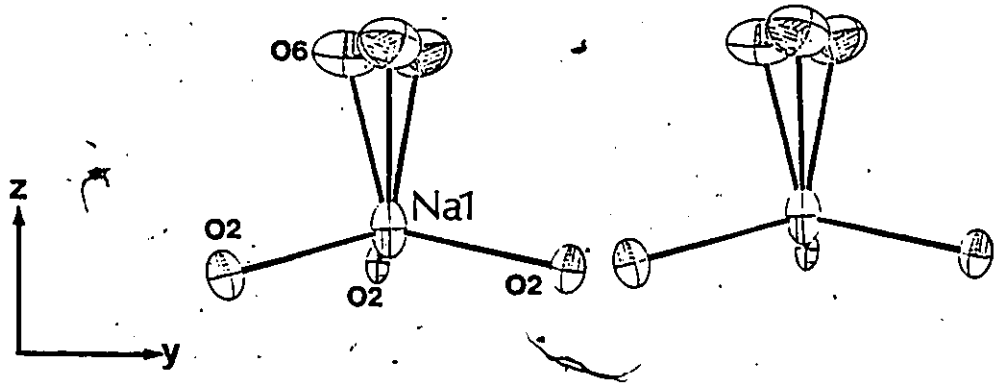

Fig. 7.1.8: Stereographic drawing in the vicinity of the Nal cation site showing the position of the framework and H_2O oxygens coordinating this site.

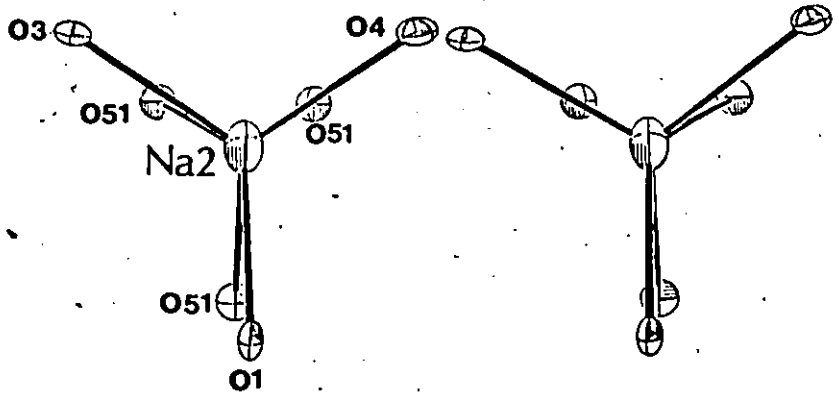

(a)

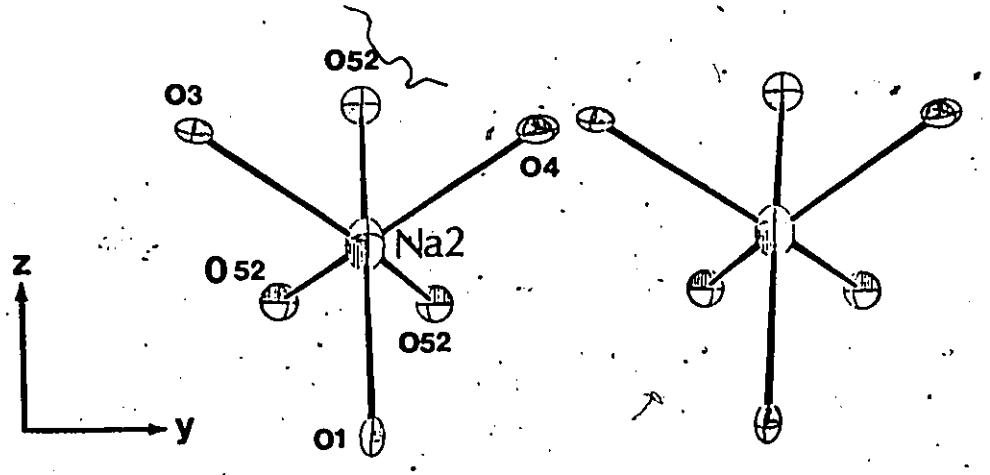

(b)

Fig. 7.1.9: Stereographic drawing in the vicinity of the Na2 cation site showing the position of framework and OH^- group oxygens coordinating this site for the two arrangements of the OH^- groups. (a) trigonal bipyramidal coordination and (b) octahedral coordination.

temperature factors than those in canerinite, but the difference is not substantial. However, the temperature factors for both the O6 and Na1 sites are smaller than those in cancrinite. The Na2 site in cancrinite has a smaller anisotropy compared to the Na1 site. The reverse is the case in hydroxycancrinite. The marked anisotropy of the Na2 site may be due to positional disorder since in hydroxycancrinite there are more vacant oxygen sites (O7, O51 and O52) than in cancrinite. However, the anisotropy of the Na2 site is not sufficiently extensive to warrant positionally disordering the atoms into more than one site. Finally, the sites (O51 and O52) on which the OH group is placed show a substantial electron density elongation parallel to the c-axis, which is similar to that for the CO_3 group in cancrinite.

Occupancy of the O7 site by water in any half of the cell excludes simultaneous occupancy of the O51 and O52 sites in that half of the cell due to the small interatomic distances. However, occupancy of one of the O51 sites in one half of the cell would allow occupancy of one O52 site in that half of the cell, therefore allowing four such sites to be occupied. Some complicated ordering of these sites must occur in order to explain the superstructures in hydroxycancrinite (Chapter 9).

The crystallochemical formula obtained from the refinement is

$$Na_8(Al_6Si_6O_{24}).(OH)_{2.04}\cdot 2.68H_2O.$$

This agrees remarkably with the total amount of OH and H_2O found by the chemical analysis (Table 7.1.1). On the other hand, the hydroxycancrinite of Pahor et al. (1982) has a composition of $Na_{7.44}(Al_6Si_{6.03}O_{24.06}).5.61H_2O$, from electron microprobe analysis, the water being determined by difference. The cell parameters are: a = 12.678(8), c = 5.179(6)Å and

$V = 720.9\text{Å}^3$. These parameters are larger than those found in the present study. However, they are consistent with the larger amount of (OH/H_2O) in Pahor et al. (1982) specimen. The R-factor obtained by them was 3.4% for 648 reflections collected from 2θ varying from 7° to 58° compared to 4.7% for 870 reflections collected from 2θ up to 65° in the present study.

The framework atom sites and the sodium cation sites in hydroxycancrinite are very similar to that found by Pahor et al. (1982). However, their occupancy factor for the water in the cage is 0.59 compared to 1.0 found presently as well as 1.0 found in cancrinite. In hydroxycancrinite the 07 oxygen is in the plane of three sodiums in the channel. However, Pahor et al. (1982) placed a similar oxygen at (0, 0, 0.9193) which would correspond to the position where hydrogen may be located in this study. Moreover, the 051 and 052 positions are different from that found by Pahor et al. (1982). Also, on these sites they have occupancy factor about twice the amount in the present study. Their crystallochemical formula is $Na_{7.84}(Al_6Si_6O_{24}).5.94(H_2O/OH)$ and they suggest an ideal formula, $Na_{7.5}(Al_6Si_6O_{24})(OH)_{1.5}\cdot 5H_2O$. However, the present study suggests an ideal formula, $Na_8(Al_6Si_6O_{24})(OH)_2\cdot 4H_2O$.

7.2 Vishnevite

7.2.1 Experimental:

Long exposure precession photographs of vishnevite from three different single crystals are shown in Figures 7.2.1, 7.2.2 and 7.2.3. They all show that the observed diffraction maxima are sharp and they also show symmetry which is consistent with the space group $P6_3$.

Although all of the crystals are from a very small specimen, the crystal used for Figure 7.2.1 shows no superstructure reflections. This crystal was used in the structure refinement. Figure 7.2.2 of the second crystal shows a very faint streaking between the 001 and 002 layers and this may be interpreted as satellite streaking. On the other hand, Figure 7.2.3 of the third crystal shows a well-defined superstructure giving a supercell twice the size of the subcell c-parameter. Unfortunately, this crystal was subsequently lost.

Cell dimensions determined by least-squares from 25 substructure reflections automatically aligned on a 4-circle diffractometer are presented in Table 7.2.1 together with other information pertaining to the material chosen, x-ray data collection and refinement.

7.2.2 Refinement:

The final positional parameters and temperature factors of cancrinite (Hassan, 1980) were used as the starting model. As is expected from the chemical composition and from previous refinements of cancrinites, the framework, contents of the cage and the cations (Na/K) in the channel were found to be identical to earlier refined structures. Consequently, further efforts were directed towards the channel to resolve the SO_4^{2-} anion group.

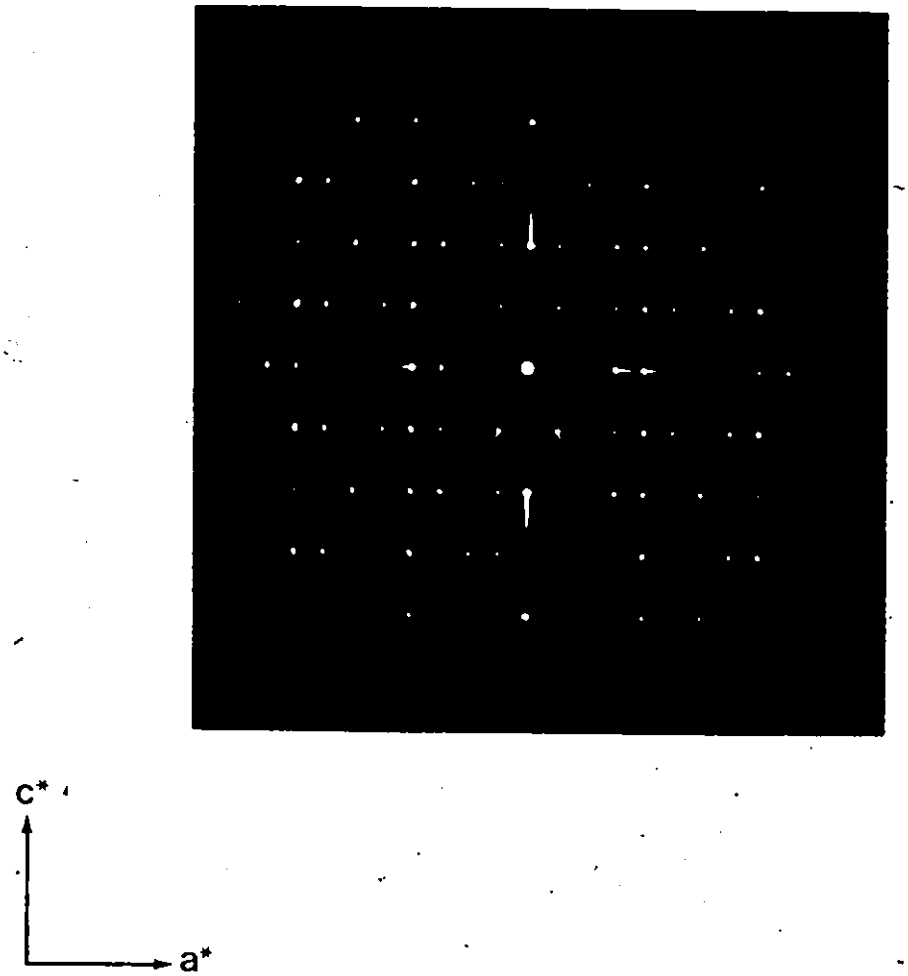

Fig. 7.2.1: X-ray diffraction photograph of the a*c* plane of the reciprocal lattice of vishnevite showing no satellite reflections (μ = 20°, MoK_{α}, Zr filter).

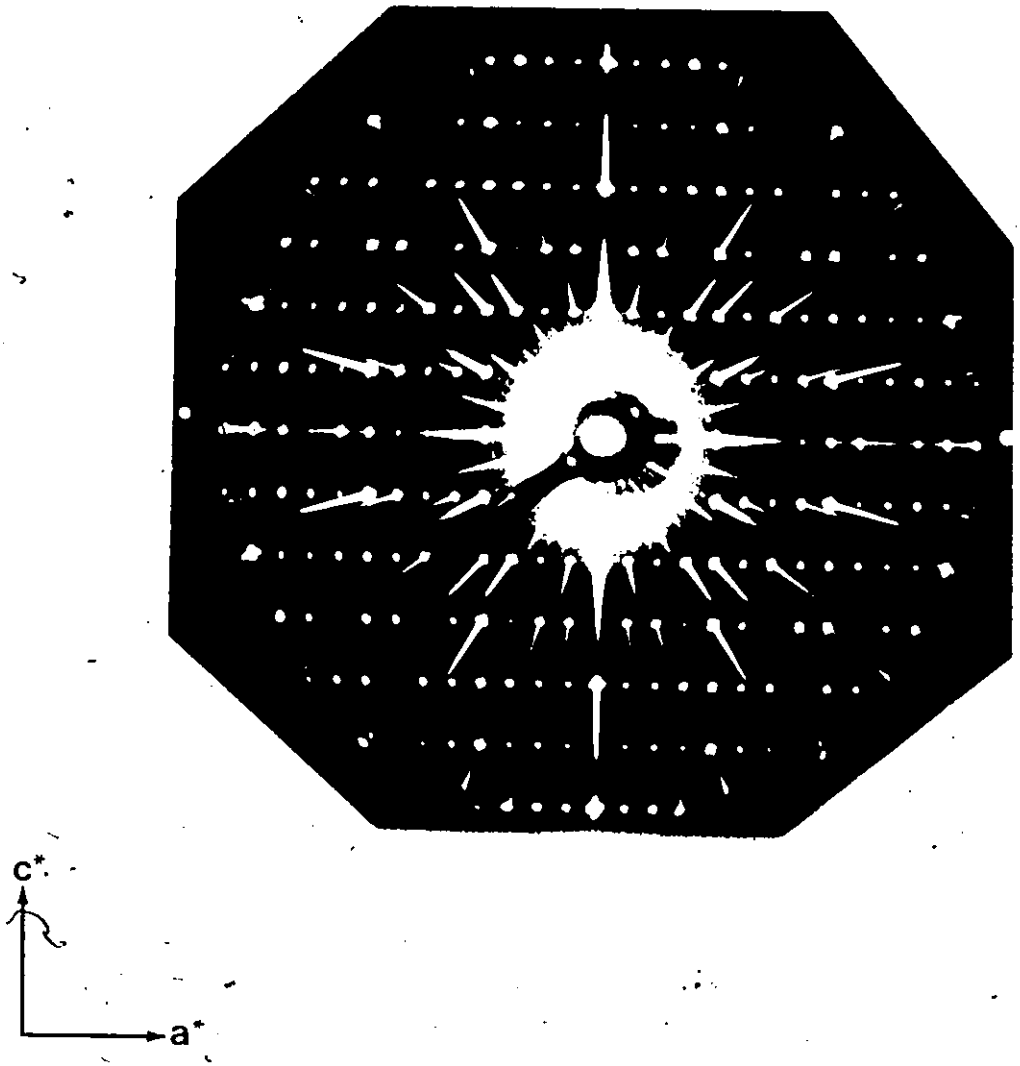

Fig. 7.2.2: X-ray diffraction photograph of the a^*c^* plane of the reciprocal lattice of vishnevite. Notice a faint streaking between the (001) and (002) planes. ($\mu = 25^o$; MoK_α, Zr filter).

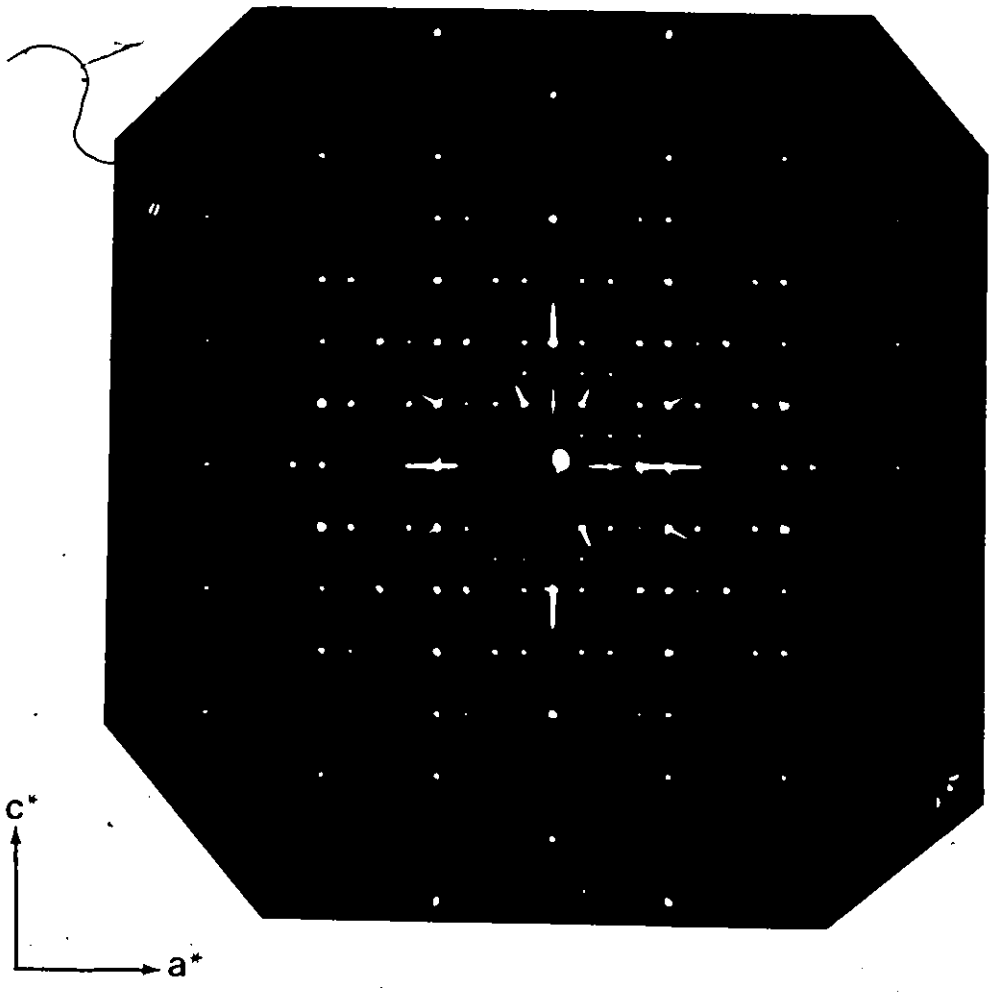

Fig. 7.2.3: X-ray diffraction photograph of the a^*c^* plane of the reciprocal lattice of vishnevite showing well-developed superstructure reflections in rows parallel to a^*. This gives a supercell twice that of the subcell c-parameter. ($\mu = 30^\circ$, MoK_α, Zr filter).

Table 7.2.1: Crystal data for vishnevite from Vishnevy Gory, Urals+

Chemical Analysis*		Cell Contents**		Miscellaneous	
SiO_2	37.24	Si	6.194	a	12.685(6)Å
Al_2O_3	29.64	Al	5.806	c	5.179(1)Å
Na_2O	20.08	Na	6.471	V	721.70 Å^3
K_2O	4.89	K	1.037	Space Group	$P6_3$
CaO	0.52	Ca	0.093	Z	1
SO_3	6.97	S	0.869	Density Calc.	2.37 g/cc
Cl	b.d.			μ	9.71 cm^{-1}
CO_3	n.d.			Crystal size:	sphere diameter of 0.30 mm
H_2O	n.d.			Radiation/Monochromator	Mo/C
wt %	99.35			Total no. of I	955
				No. of non-equiv. $\lvert F_o \rvert > 3\sigma$	873

Chemical formula from analysis:

$Na_{6.5}K_{1.0}Ca_{0.1}(Al_{5.8}Si_{6.2}O_{24})(SO_4)_{0.9}$

Ideal chemical formula from refinement:

$Na_8(Al_6Si_6O_{24})\ SO_4.2H_2O$

Final R(obs) = 3.7%

Final R_w(obs) = 4.6%

w = 1

+ specimen courtesy of the British Museum(no. 1974, 516)
* Microprobe analysis, F. C. Hawthorne, University of Manitoba.
** Calculated from chemical analysis based on Si + Al = 12

Large scale Fourier maps of electron density of the channel were prepared at various stages of the refinement. Without any anion groups in the channel, the R-factor was 6.1% and the difference Fourier map showed electron density all along the c-axis (Fig. 7.2.4a). Also density was seen in similar positions as the oxygens of the carbonate group in cancrinite (Fig. 7.2.4b). The latter electron density area was split in two sites (051 and 052). On the c-axis, the S cation site and the oxygen (07) anion site are shown in Figure 7.2.4a. Each of these site population was constrained firstly to the chemical analysis (Table 7.2.1) and the R-factor obtained was 4.2%. The isotropic temperature factors for the atoms on the c-axis (S and 07 sites) were quite large (0.130 and 0.128$\mathring{A}^2$ respectively). However, the 051 and 052 oxygen sites refined with reasonable temperature factors (0.039 and 0.055$\mathring{A}^2$ respectively).

The population of the sulphur cation site (S) was then refined to a value of 0.24(1) with reasonable temperature factors. Consequently, the population of the 07, 051 and 052 oxygen sites were adjusted to match the population of the S-site on the assumption that these oxygens belong to the SO_4 group. The R-factor obtained was 4.0% and the temperature factors were reasonable, except for the 051 oxygen site which was quite small. Although the difference Fourier map at this stage shows no electron density on the c-axis, residual density still remains on the 051 and 052 sites.

Population parameters for the 07, 051 and 052 were then refined individually by holding the remaining parts of the structure invariant. In each case, population of 0.24 was obtained. Consequently, the

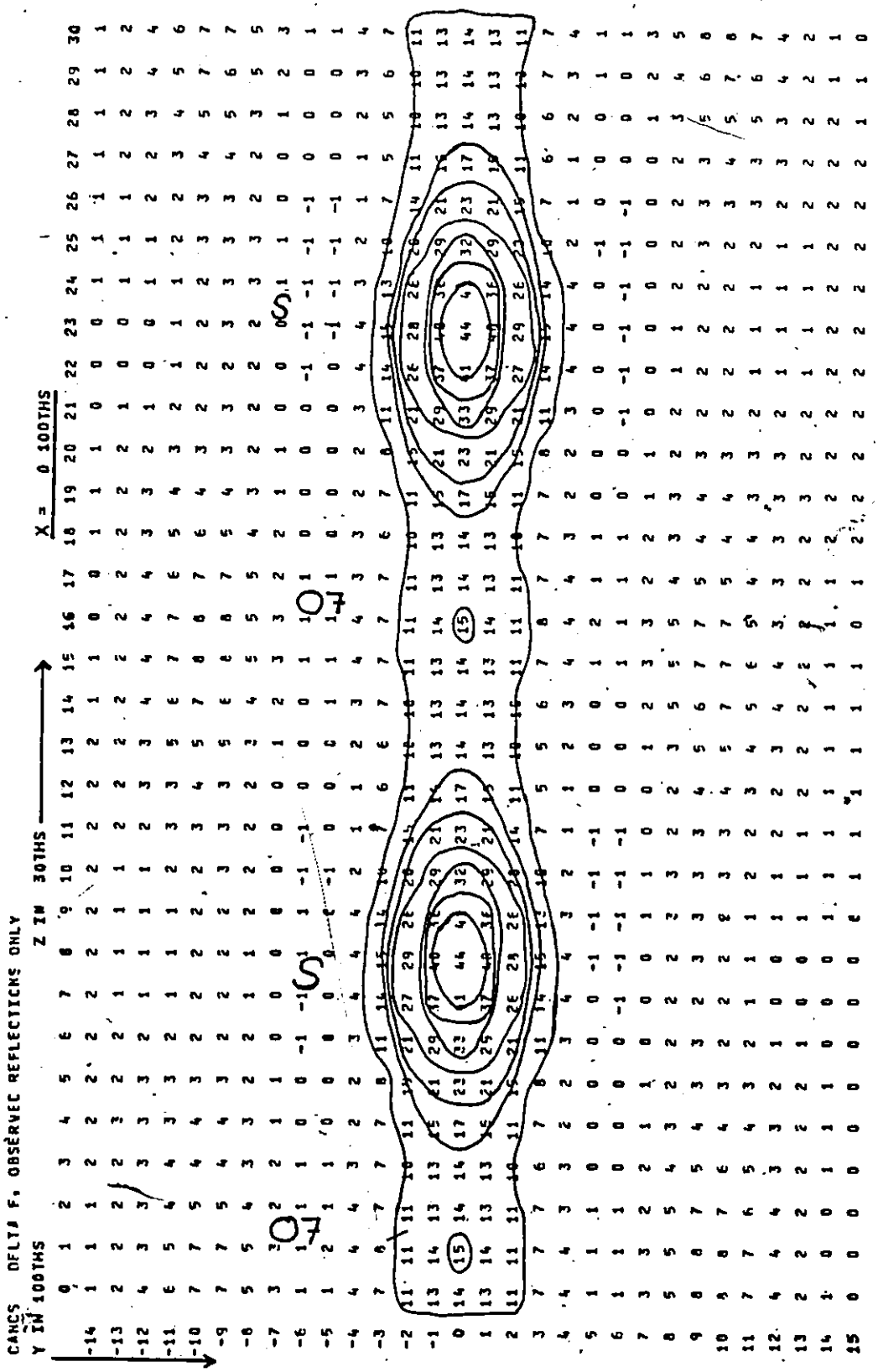

Fig. 7.2.4a: Difference Fourier synthesis through the 6_3 axis. This section shows the S cation site and the oxygen site O7.

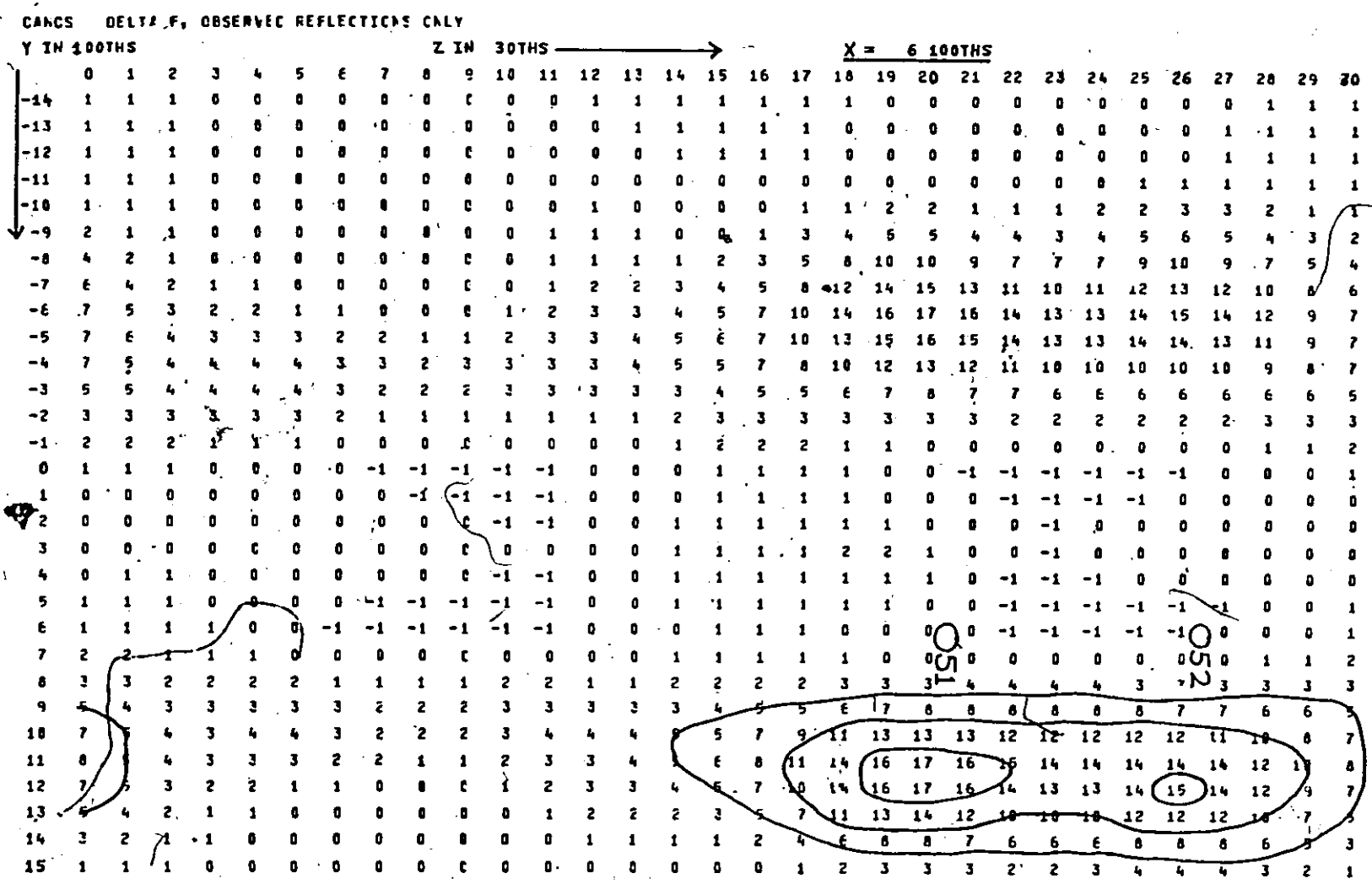

Fig. 7.2.4b: Difference Fourier map through the 051 and 052 sites, calculated with the oxygen on these sites removed from the structural model.

populations of all four sites (O51, O52, O7 and O5) were set at 0.24 and on varying all refineable parameters the structure converged with a conventional R-factor of 3.7%. The difference Fourier maps at this stage showed no residual electron density. The final forms of the electron density of the above sites are shown in Figure 7.2.5a and b. This was calculated using only the observed reflections.

The structural model at this stage has too many oxygens on the O51 and O52 sites if all of these oxygens belong to the SO_4 group. Alternatively, there is deficiency of sulphur and oxygen on the S and O7 sites respectively, according to the chemical analyses. It is possible that these sites are positionally disordered so that the 'split' peaks overlap and give rise to a spreading of the electron density. Thus the refinement may not account for all the electron density on the c-axis. The bond-lengths of the rigid SO_4 group suggest positional disordering of this group in order to obtain reasonable S-O bond distances comparable to those found in other materials. Moreover, at this stage of the refinement further details may be lost in the experimental errors.

The final positional parameters are shown in Table 7.2.2 and the anisotropic temperature factors are presented in Table 7.2.3. The observed and calculated structure factors are given in Appendix 1.

7.2.3 Discussion

The general features of the structure are similar to those of cancrinite and hydroxycancrinite. Important interatomic distances are shown in Table 7.2.4 and interframework angles are given in Table 7.2.5.

The average Si-O and Al-O bond lengths are 1.615Å and 1.732Å

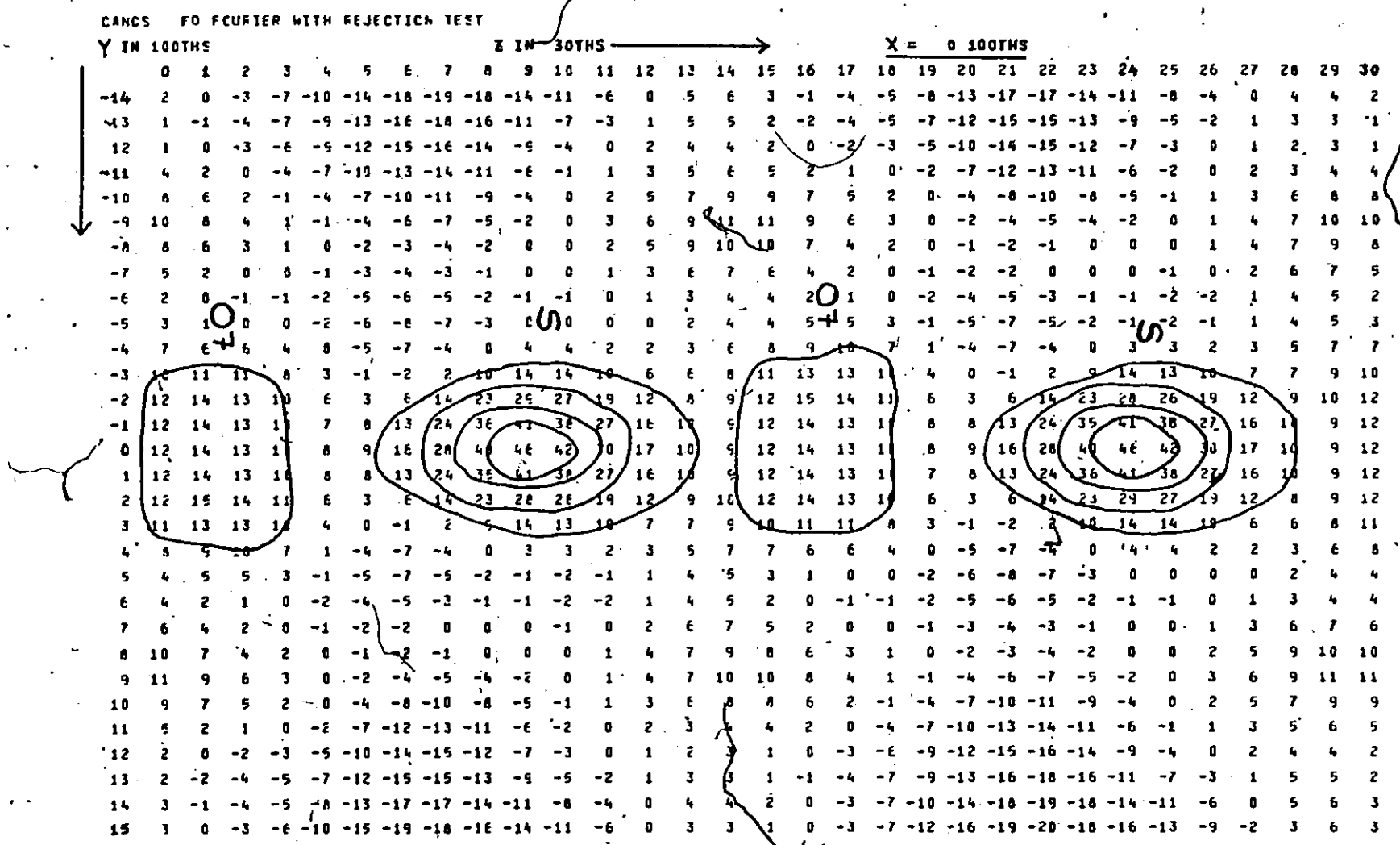

Fig. 7.2.5a: Fourier section showing the final form of the electron density of the O7 and S sites, calculated using only the observed reflections.

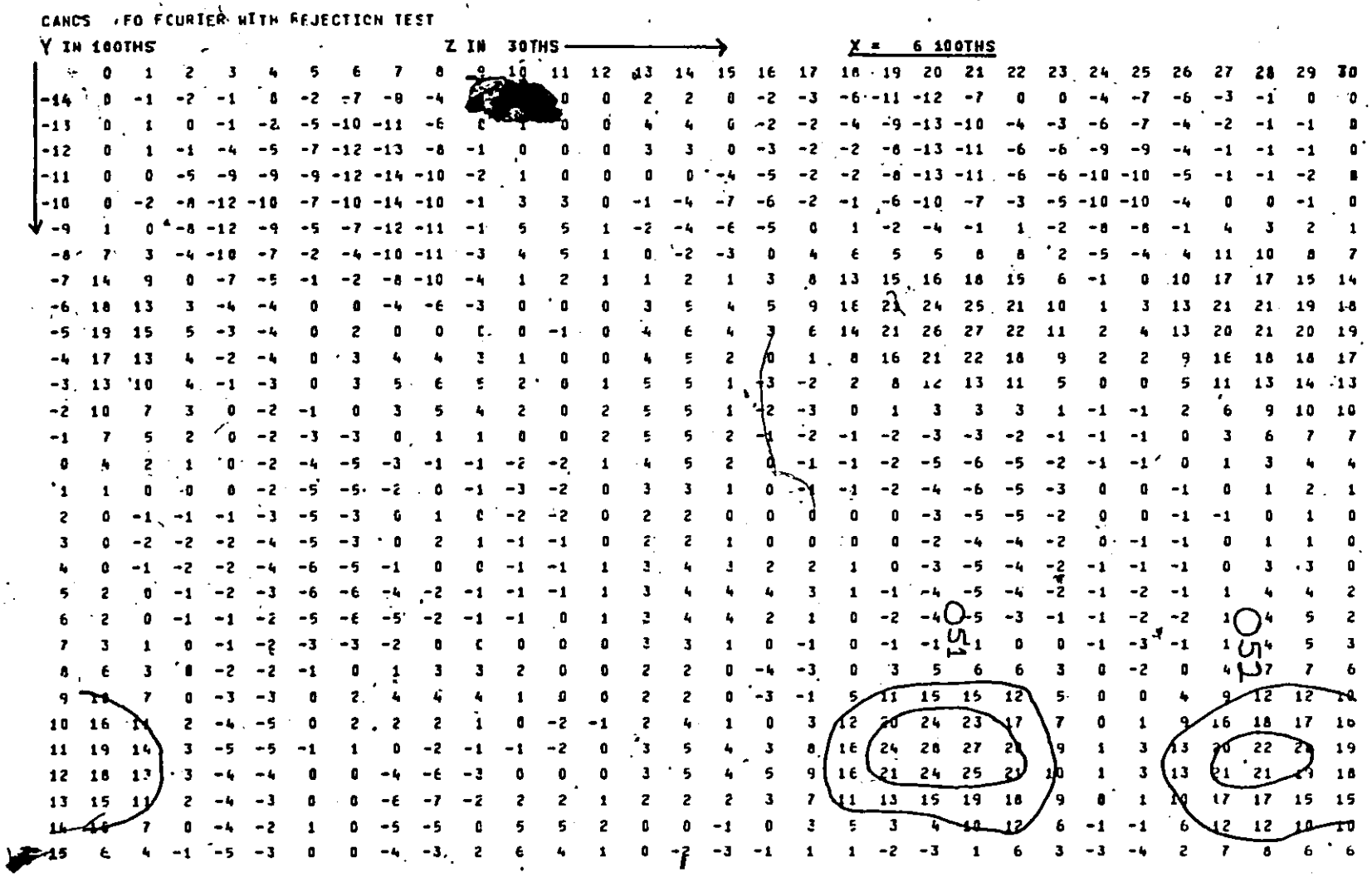

CANCS .FO FOURIER WITH REJECTION TEST

Y IN 100THS

Z IN 30THS →

X = 6 100THS

	0	1	2	3	4	5	6	7	8	9	10	11	12	13	14	15	16	17	18	19	20	21	22	23	24	25	26	27	28	29	30
-14	0	-1	-2	-1	0	-2	-7	-8	-4	[illegible]	0	0	2	2	0	-2	-3	-6	-11	-12	-7	0	0	-4	-7	-6	-3	-1	0	0
-13	0	1	0	-1	-2	-5	-10	-11	-6	[illegible]	0	0	4	4	0	-2	-2	-4	-9	-13	-10	-4	-3	-6	-7	-4	-2	-1	-1	0
-12	0	1	-1	-4	-5	-7	-12	-13	-8	-1	0	0	0	3	3	0	-3	-2	-2	-8	-13	-11	-6	-6	-9	-9	-4	-1	-1	-1	0
-11	0	0	-5	-9	-9	-9	-12	-14	-10	-2	1	0	0	0	0	-4	-5	-2	-2	-8	-13	-11	-6	-6	-10	-10	-5	-1	-1	-2	0
-10	0	-2	-8	-12	-10	-7	-10	-14	-10	-1	3	3	0	-1	-4	-7	-6	-2	-1	-6	-10	-7	-3	-5	-10	-10	-4	0	0	-1	0
-9	1	0	-8	-12	-9	-5	-7	-12	-11	-1	5	5	1	-2	-4	-6	-5	0	1	-2	-4	-1	1	-2	-8	-8	-1	4	3	2	1
-8	7	3	-4	-10	-7	-2	-4	-10	-11	-3	4	5	1	0	-2	-3	0	4	6	5	5	8	8	2	-5	-4	4	11	10	8	7
-7	14	9	0	-7	-5	-1	-2	-8	-10	-4	1	2	1	1	2	1	3	8	13	15	16	16	15	6	-1	0	10	17	17	15	14
-6	18	13	3	-4	-4	0	0	-4	-6	-3	0	0	0	3	5	4	5	9	16	21	24	25	21	10	1	3	13	21	21	19	18
-5	19	15	5	-3	-4	0	2	0	0	0	0	-1	0	4	6	4	3	6	14	21	26	27	22	11	2	4	13	20	21	20	19
-4	17	13	4	-2	-4	0	3	4	4	3	1	0	0	4	5	2	0	1	8	16	21	22	18	9	2	2	9	16	18	18	17
-3	13	10	4	-1	-3	0	3	5	6	5	2	0	1	5	5	1	-3	-2	2	8	12	13	11	5	0	0	5	11	13	14	13
-2	10	7	3	0	-2	-1	0	3	5	4	2	0	2	5	5	1	-2	-3	0	1	3	3	3	1	-1	-1	2	6	9	10	10
-1	7	5	2	0	-2	-3	-3	0	1	1	0	0	2	5	5	2	-1	-2	-1	-2	-3	-3	-2	-1	-1	-1	0	3	6	7	7
0	4	2	1	0	-2	-4	-5	-3	-1	-1	-2	-2	1	4	5	2	0	-1	-1	-2	-5	-6	-5	-2	-1	-1	0	1	3	4	4
1	1	0	0	0	-2	-5	-5	-2	0	-1	-3	-2	0	3	3	1	0	-1	-1	-2	-4	-6	-5	-3	0	0	-1	0	1	2	1
2	0	-1	-1	-1	-3	-5	-3	0	1	0	-2	-2	0	2	2	0	0	0	0	0	-3	-5	-5	-2	0	0	-1	-1	0	1	0
3	0	-2	-2	-2	-4	-5	-3	0	2	1	-1	-1	0	2	2	1	0	0	0	0	-2	-4	-4	-2	0	-1	-1	0	1	1	0
4	0	-1	-2	-2	-4	-6	-5	-1	0	0	-1	-1	1	3	4	3	2	2	1	0	-3	-5	-4	-2	-1	-1	-1	0	3	3	0
5	2	0	-1	-2	-3	-6	-6	-4	-2	-1	-1	-1	1	3	4	4	4	3	1	-1	-4	-5	-4	-2	-1	-2	-1	1	4	4	2
6	2	0	-1	-1	-2	-5	-6	-5	-2	-1	-1	0	1	3	4	4	2	1	0	-2	-4	-5	-3	-1	-1	-2	-2	1	4	5	2
7	3	1	0	-1	-2	-3	-3	-2	0	0	0	0	0	3	3	1	0	-1	0	-1	-1	1	0	0	-1	-3	-1	1	4	5	3
8	6	3	0	-2	-2	-1	0	1	3	3	2	0	0	2	2	0	-4	-3	0	3	5	6	6	3	0	-2	0	4	7	7	6
9	[illegible]	7	0	-3	-3	0	2	4	4	4	1	0	0	2	2	0	-3	-1	5	11	15	15	12	5	0	0	4	9	12	12	[illegible]
10	16	[illegible]	2	-4	-5	0	2	2	2	1	0	-2	-1	2	4	1	0	3	12	[illegible]	24	23	17	7	0	1	9	16	18	17	16
11	19	14	3	-5	-5	-1	1	0	-2	-1	-1	-2	0	3	5	4	3	8	16	24	28	27	[illegible]	9	1	3	13	[illegible]	22	[illegible]	19
12	18	13	3	-4	-4	0	0	-4	-6	-3	0	0	0	3	5	4	5	9	16	21	24	25	[illegible]	10	1	3	13	[illegible]	21	[illegible]	18
13	15	[illegible]	2	-4	-3	0	0	-6	-7	-2	2	2	1	2	2	2	3	7	[illegible]	13	15	19	18	9	0	1	[illegible]	17	17	15	15
14	[illegible]	7	0	-4	-2	1	0	-5	-5	0	5	5	2	0	0	-1	0	3	5	3	4	[illegible]	12	6	-1	-1	6	12	12	[illegible]	[illegible]
15	6	4	-1	-5	-3	0	0	-4	-3	2	6	4	1	0	-2	-3	-1	1	1	-2	-3	1	6	3	-3	-4	2	7	8	6	6

051

052

Fig. 7.2.5b: Fourier section showing the final form of the electron density of the 051 and 052 sites, calculated using only the observed reflections.

Table 7.2.2: Positional parameters, population parameters and isotropic temperature factors (x 10^4) in vishnevite

Framework atoms

atom	site	site content	x	y	z	$U_{(equiv)}$ A^2	
O1	c	O	.2017(3)	.4049(3)	.6698(8)	181	
O2	c	O	.1175(3)	.5527(3)	.7278(11)	225	
O3	c	O	.0406(3)	.3599(3)	.0393(7)	168	
O4	c	O	.3255(3)	.3522(3)	.0561(7)	193	
T1	c	Si	.0831(1)	.4124(1)	.7500	87	
T2	c	Al	.3380(1)	.4137(1)	.7506(5)	90	
Non-framework atoms*							
O51	c	0.24 O+.76□	.0615(18)	.1133(18)	.6725(39)	356	ch
O52	c	0.24 O+.76□	.0496(28)	.1090(26)	.9541(63)	637	ch
S	a	0.24 O+.76□	0	0	.2918(35)	489	ch
O7	a	0.24 O+.76□	0	0	.0737(83)	454	ch
O6	c	0.33 O	.6184(14)	.3043(35)	.6893(30)	564	cg
Na1	b	1.0 Na	2/3	1/3	.1272(12)	357	cg
Na2	c	0.75 Na + 0.17K +.08□	.13.9(3)	.2611(4)	.2885(6)	701	ch

* chemical symbol □ is vacancy
ch located in channel
cg located in cage

Table 7.2.3: Anisotropic temperature factors ($\times 10^4$) in vishnevite

Framework atoms

Atom	U_{11}	U_{22}	U_{38}	U_{12}	U_{13}	U_{23}
01	129(13)	247(15)	167(14)	123(12)	19(11)	27(13)
02	227(14)	133(12)	314(20)	106(11)	30(19)	13(18)
03	141(13)	259(16)	104(15)	85(12)	37(12)	43(13)
04	221(14)	265(16)	93(16)	171(13)	-1(12)	33(13)
T1	77(4)	104(4)	81(4)	48(3)	4(6)	11(6)
T2	89(4)	102(4)	81(4)	57(4)	4(7)	11(7)

Non-framework atoms

051	356(42)					
052	637(76)					
S	489(31)					
07	454(81)					
06	598(102)	818(219)	278(81)	-354(162)	51(61)	58(104)
Na1	253	253	566(31)	127(6)	0	0
Na2	472(15)	1326(29)	305(17)	678(19)	-70(13)	-133(18)

Table 7.2.4: Selected interatomic distances in vishnevite

Bond	Å	Bond	Å
T1-01	1.608(5)	T2-01	1.728(4)
-02	1.611(4)	-02	1.719(7)
-03	1.619(6)	-03	1.744(7)
-04	1.621(6)	-04	1.736(4)
Mean	1.615	Mean	1.732
Na1-01 x 3	2.884(4)	S-07	1.460(46)
-02 x 3	2.429(4)	-051 x 3	1.391(21)
-06[a]	2.960(16)	Mean	1.408
-06[b]	2.330(16)		
Mean for 8	2.654	S-07	1.130(46)
4	2.404	-052 x 3	1.465(32)
		Mean	1.381
Trigonal bipyramid		Octahedral	
Na2-01	2.529(5)	Na2-01	2.529(5)
-03	2.456(6)	-03	2.456(6)
-04	2.445(5)	-04	2.445(5)
-051[a]	2.568(21)	-052[a]	2.573(66)
-051[b]	2.616(46)	-052[a]	2.705(35)
-051[b]	2.510(24)	-052[b]	2.407(31)
Mean	2.521	Mean	2.519
-03	2.908(6)	-03	2.908(6)
-04	2.878(8)	-04	2.878(8)
Mean	2.614	Mean	2.613

Table 7.2.5: Selected framework angles in vishnevite

Tetrahedral			
O1-T1-O2	107.6(2)	O1-T2-O2	106.2(2)
-O3	110.1(3)	-O3	107.6(2)
-O4	108.1(4)	-O4	109.2(2)
O2-T1-O3	111.8(3)	O2-T2-O3	114.0(3)
-O4	111.9(3)	-O4	113.9(2)
O3-T1-O4	107.3(2)	O3-T2-O4	105.9(3)
Mean	109.5	Mean	109.5

Bridging	
T1-O1-T2	150.3(3)
T1-O2-T2	149.8(2)
T1-O3-T2	136.7(3)
T1-O4-T2	136.7(3)
Mean	143.4

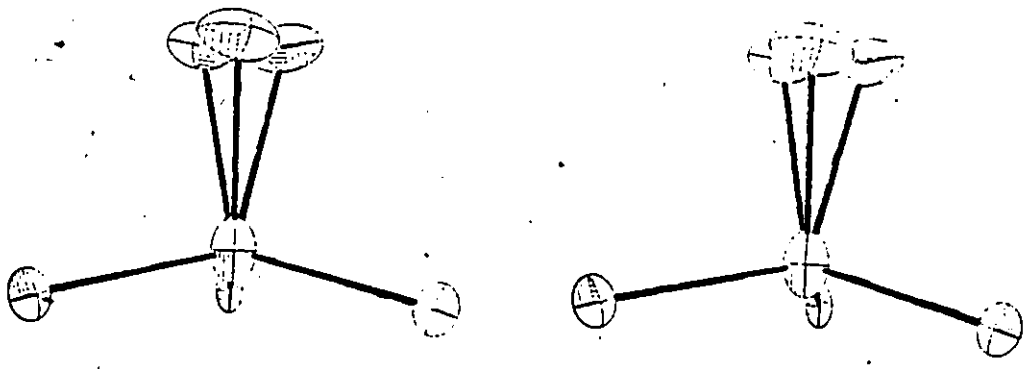

Fig. 7.2.6: Stereographic drawing in the vicinity of the Na1 cation site showing the position of the framework and H_2O oxygens coordinating this site.

respectively. These distances are similar to those in other cancrinites and they correspond to a fully ordered framework.

The coordination of the sodium cation site, Na1, is shown in Figure 7.2.6 and the two possible coordinations of the cation site Na2 are shown in Figure 7.2.7a and b. The bond lengths corresponding to the coordination of the Na1 site are similar to those in hydroxycancrinite and cancrinite. However, the bond lengths corresponding to the coordination of the Na2 site are larger than those in the previously refined structures. This is due to the presence of K on the Na2 site (Table 7.2.2). Therefore, the temperature factor of the Na2 site is larger than in the other cancrinites due in part, to positional disorder of K and Na and in part to vacancy of the SO_4 group.

From a chemical point of view, one may expect the S^{6+} to be as far away as possible from the cations on the Na2 site. However, the sulphur cation is in the triangular plane of the cations on the Na2 site while the O7 oxygen is remote from these cations. In hydroxycancrinite,

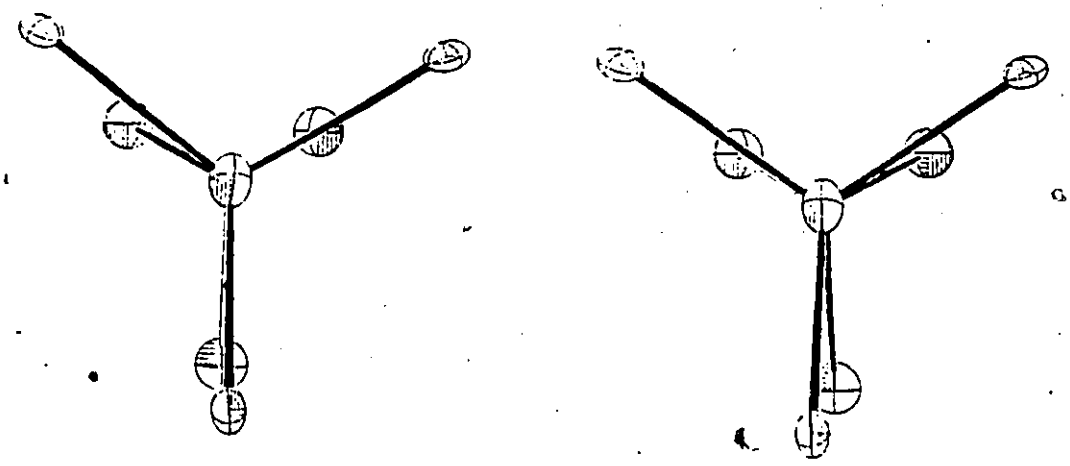

(a)

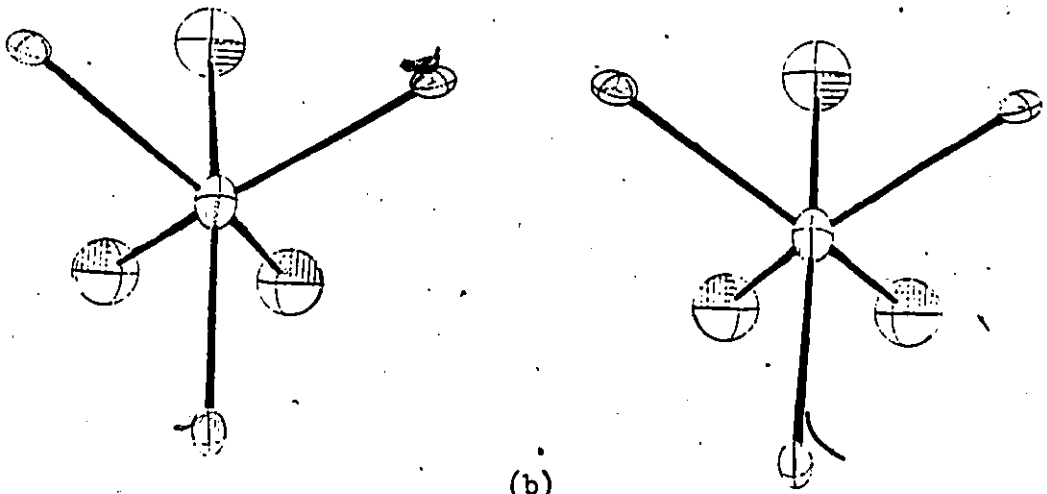

(b)

Fig. 7.2.7: Stereographic drawing in the vicinity of the Na2 cation site showing the position of framework and SO_4^{2-} group oxygens coordinating this site for the two arrangements of the SO_4 group. (a) trigonal bipyramidal coordination and (b) octahedral coordination.

the O7 oxygen is in similar position as the sulphur cation in vishnevite. Each sulphur is at a distance of 2.868(4)Å from three cations on the Na2 sites. However, this distance could increase since there is evidence of disorder on both the S and Na2 cation sites. Alternatively, the O7 and S sites may be interchanged. However, bond lengths and Fourier syntheses would reject this model.

Superstructures in vishnevite and their origin will be discussed in Chapter 9.

7.3 Davyne

7.3.1 Experimental:

Long exposed precession photographs of davyne from two single crystals of the same sample are shown in Figure 7.3.1 and Figure 7.3.2. Both crystals show that the observed diffraction maxima are sharp and they also show symmetry which is consistent with the space group $P6_3$. Neither crystal shows satellites. The crystal used for Figure 7.3.1 was used to collect the intensity data.

Cell dimensions determined by least-squares from twenty sub-structure reflections automatically aligned on a 4-circle diffractometer are presented in Table 7.3.1 together with other information pertaining to the material chosen, x-ray data collection and refinement.

7.3.2 Refinement:

The final positional parameters and isotropic temperature factors of vishnevite (sec. 7.2) were used as the starting model. According to the chemical analysis (Table 7.2.1) Ca and Cl were placed in the cage instead of Na and H_2O as were found in other cancrinites.

In the early stages of the refinement it was observed that the cation site Na(1) in the channel had an unusually large temperature factor. Since there is a high correlation between the population parameter and the temperature factor, the latter was set at about 3Å^2 and the former refined to a value of 0.55 for this Na(1) site. Difference Fourier map at this point revealed electron density in close proximity to the above position. K was placed on this position (K(1) site) and its population parameter refined in a similar way to give a value of 0.28. With this isotropic model the structure was refined.

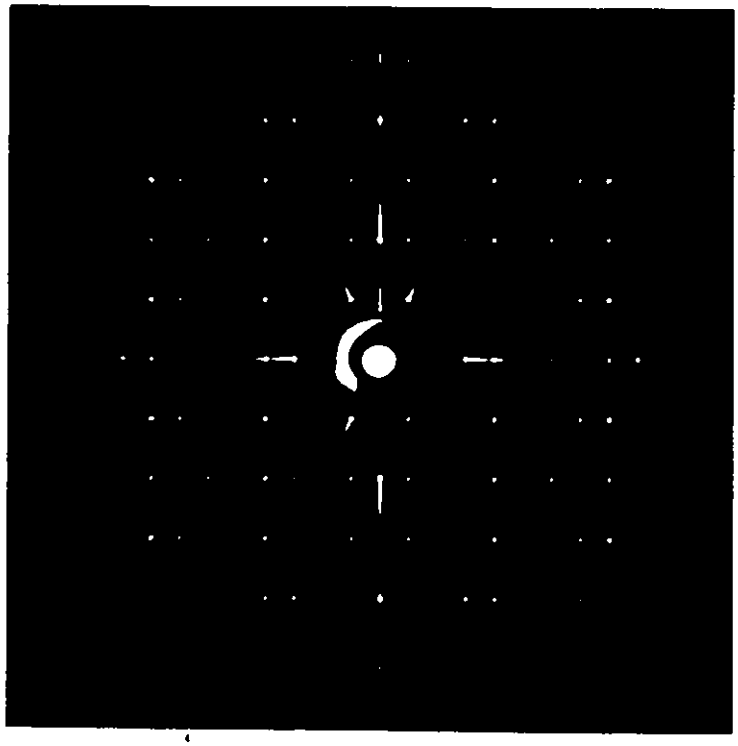

Fig. 7.3.1; X-ray diffraction photograph of the a*c* plane of the reciprocal lattice plane of davyne. ($\mu = 20^{o}$, MoK_{α}, Zr filter).

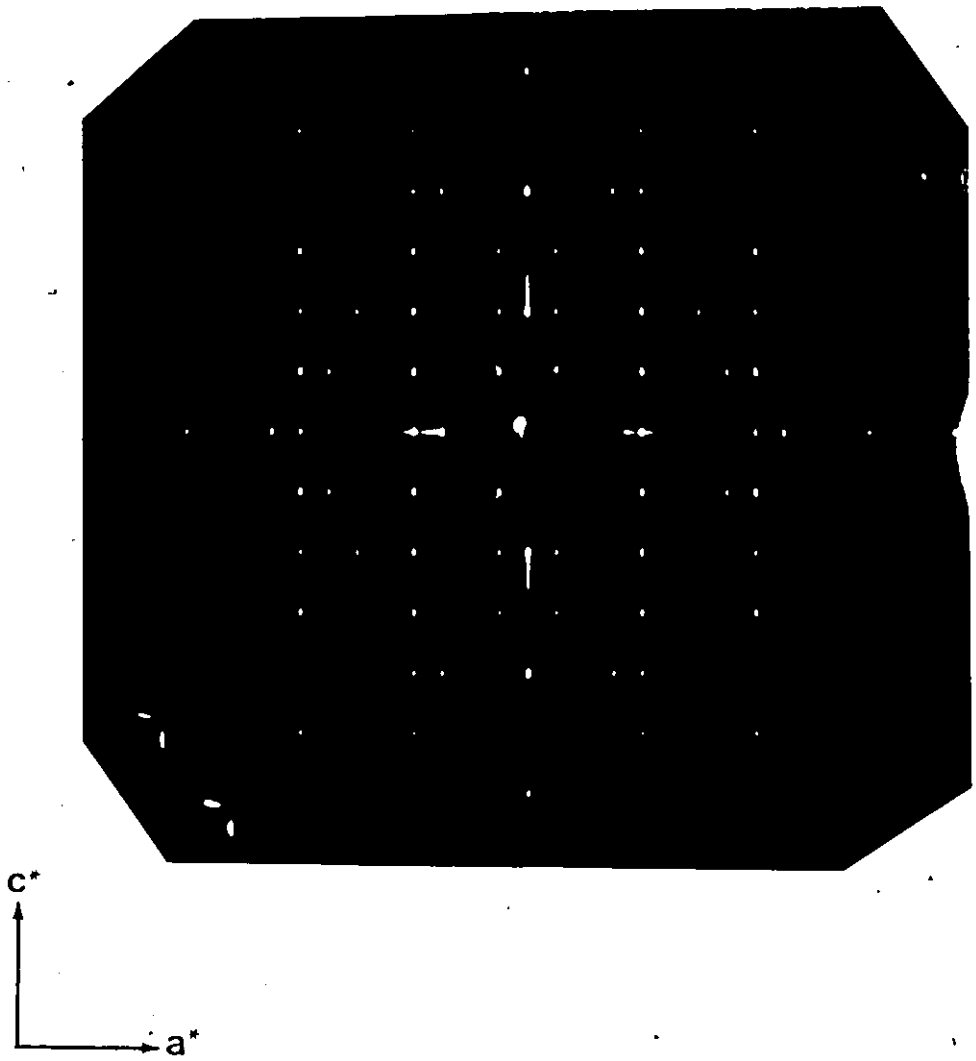

Fig. 7.3.2: X-ray diffraction photograph of the a^*c^* plane of the reciprocal lattice plane of davyne. (μ = 300, MoK_α, Zr filter).

Table 7.3.1: Crystal data for davyne from Mt. Vesuvius, Italy+

Chemical Analysis*		Cell Contents**
SiO_2	33.89	6.12
Al_2O_3	27.62	5.88
Na_2O	8.34	2.92
K_2O	5.09	1.17
CaO	12.48	2.41
SO_3	0.81	0.11
Cl	6.34	1.94
CO_3	n.d.	
H_2O	n.d.	
	94.56	
O=Cl	-1.43	
Total	93.13	

Chemical formula from analysis:

$Na_{2.9}K_{1.2}Ca_{2.4}(Al_{5.9}Si_{6.1}O_{24})Cl_{1.9}$

Ideal chemical formula from refinement:

$Na_6Ca_2(Al_6Si_6O_{24})Cl_2 \cdot (OH)_2$

Miscellaneous	
a (Å)	12.8535(9)
c (Å)	5.3574(5)
V (Å^3)	766.53
Space group	$P6_3$
Z	1
Density calc. (gcm^{-3})	2.15
Crystal size (mm)	0.14 x 0.12 x 0.10
Radiation/Monochromator	Mo/C
Total no. of I	1022
No. of non-equivalent $\|F_{obs}\| > 3\sigma$	688
Final $R_{(obs)}$	= 11.8%
Final $R_{w(obs)}$	= 12.8%
	w = 1

\+ Specimen courtesy of the British Museum (#Bm1907, 210)
* Microprobe analysis, F. C. Hawthorne, University of Manitoba
** Calculated from chemical analysis based on Si + Al = 12

Table 7.3.2: Positional parameters, population parameters and isotropic temperature factors ($\times 10^4$) in davyne

Framework atoms

atom	site	site content	x	y	z	$U_{(iso)}$ Å^2
O1	6c	O	.2122(10)	.4237(10)	.7211(30)	175(25)
O2	6c	O	.1116(11)	.5544(11)	.7475(42)	243(27)
O3	6c	O	.0102(11)	.3413(11)	.0103(29)	82(25)
O4	6c	O	.3282(17)	.3448(17)	.0261(40)	362(46)
T1	6c	Si	.0775(4)	.4135(4)	3/4	105(9)
T2	6c	Al	.3374(4)	.4126(4)	.7503(18)	102(9)

Non-framework atoms

Cl1	2b		Cl	2/3	1/3	.7172(72)	915(54) cg
Ca1	2b		Ca	2/3	1/3	.2181(14)	103(11) cg
Na1	6c	0.55	Na	.1537(15)	.3087(15)	.2601(48)	384(37) ch
K1	6c	0.28	K	.1175(19)	.2284(20)	.2685(57)	491(50) ch

ch located in channel
cg located in cage

However, during several stages of the refinement, the Al and Si positions had to be interchanged as was suggested by their average bond lengths to oxygen. The isotropic model converged to an R-factor of 11.8%. The final positional parameters and isotropic temperature factors are given in Table 7.3.2.

7.3.3 Discussion:

Although the temperature factors for Al and Si are equal, those of the O(3) and Ca(1) sites were unusually small while those of the O(4) and Cl were very large. An attempt was made to fix the temperature factors of all the atoms to values similar to that found in other cancrinites and Fourier maps were examined. However, nothing unusual was found. The parameters were then allowed to vary a few at a time and finally all were varied simultaneously and results similar to the original refinement were obtained. The difference Fourier section at this stage showed a little electron density close to the 6_3 axis in the plane of the cations; this may be H_2O. However, the refinement could not cope with the little electron density.

The errors for the parameters given in Table 7.3.2 are quite large, indicating that the model is not fully refined. Nevertheless, an attempt was made to refine an anisotropic model. The R-factor obtained was 9.1%. However, since this is no improvement and the errors were very large for the temperature factors, the anisotropic parameters are not reported.

Davyne shows many peculiarities when compared with the other refined cancrinite structures. Its cell parameters are much larger than those of the other cancrinites studied. However, its cell parameters are close to those of the new cancrinite-like minerals (Table 2.1).

Moreover, the positional parameters for davyne are significantly different from the positional parameters of other cancrinites. The difference is shown even in the second significant figure for the framework atoms. As a result, all the bond lengths are significantly different. If average Si-O and Al-O bond lengths of 1.612Å and 1.733Å correspond to 100% occupancy by Si and Al respectively, then in davyne (Table 7.3.3) the T(1) and T(2) sites contain (60% Si, 40% Al) and (57% Al, 43% Si) respectively. This indicates a disordered framework for davyne in contrast to the ordered framework of other cancrinites.

Furthermore, the average bridging angle in the davyne framework (Table 7.3.4) is about 8° larger than those in the other cancrinites. This is due to the large chlorine in the cage and as a result, larger cell parameters.

The most significant aspect of the structure refinement is that it shows that the Ca(1) and Cl(1) sites are fully occupied. The bond strength to Ca(1) (Table 7.3.3) from the O(1) and O(2) oxygens is about one valence unit. The remaining charge on Ca(1) is balanced by one chlorine above and one below, each contributing about half a valence unit. The bond strength sum about Na(1) is also consistent with the population parameter for this site. However, the bond strength sum about K(1) is about twice that expected from the site population refinement.

This structure of davyne undoubtedly raises the question of stacking faults. If the material contains stacking faults, it must be random in accordance with its lack of superstructure. Furthermore, it is surprising that the Al:Si ratio of 1:1 shown by the chemical analysis should give a disordered framework. The question of stacking faults in

Table 7.3.3: Selected interatomic distances and bond strength (valence units) in davyne

Bond	Å	Bond strength (v.u.)	Bond	Å	Bond strength (v.u.)
T1-O1	1.676(15)	0.87(3)	T2-O1	1.692(16)	0.83(3)
-O2	1.637(15)	0.96(4)	-O2	1.674(21)	0.87(5)
-O3	1.659(14)	0.91(3)	-O3	1.676(24)	0.87(5)
-O4	1.666(24)	0.89(6)	-O4	1.690(24)	0.84(5)
Mean	1.660	Total 3.63(8)	Mean	1.683	Total 3.42(9)
		Expected 4.0			Expected 3.0
Ca1-O1 x 3	2.705(11)	0.144(3) x 3			
-O2 x 3	2.743(13)	+0.133(3) x 3			
-Cl1[a]	2.674(39)	=0.831(8)			
-Cl1[b]	2.684(39)				
Mean	2.713				
Na1-O1	2.783(29)	0.081(4)			
-O3	2.478(29)	0.155(10)	K1-O3	2.814(35)	0.129(8)
-O3	2.646(28)	0.108(6)	-O3	2.811(27)	0.130(6)
-O4	2.404(31)	0.184(13)	-O4	2.685(30)	0.163(9)
-O4	2.727(46)	0.091(8)	-O4	2.955(50)	0.101(8)
Mean	2.608	Total 0.619(20)	Mean	2.816	Total 0.524(16)
		Expected 0.55			Expected 0.28

Table 7.3.4: Selected framework angles in davyne

	Tetrahedral		
O1-T1-O2	102.6(0.7)	O1-T2-O2	101.7(1.0)
O1-T1-O3	110.5(0.8)	O1-T2-O3	108.0(0.9)
O1-T1-O4	111.5(1.6)	O1-T2-O4	107.5(1.0)
O2-T1-O3	113.7(0.9)	O2-T2-O3	114.8(1.1)
O2-T1-O4	115.2(1.3)	O2-T2-O4	112.7(1.1)
O3-T1-O4	103.5(0.9)	O3-T2-O4	111.4(1.2)
Mean	109.5	Mean	109.4

Bridging	
T1-O1-T2	166.6(1.0)
T1-O2-T2	152.6(9)
T1-O3-T2	144.3(1.2)
T1-O4-T2	141.8(1.1)
Mean	151.3

this sample cannot be fully answered without further experimental work and in this regard, High Resolution Transmission Electron Microscopy may be fruitful. It should be noted that in hydroxycancrinite and cancrinite (proper) the Al and Si are arranged one way whereas in vishnevite the Al and Si positions are interchanged. Both of these arrangements are equally probable and depend only on chance. There is the possibility however of a stacking fault(s) which break the regular ABAB... alternation with a C type layer. This effectively reverses the order. Such materials will show apparent disorder of the framework with X-ray methods due to their averaging effect, the degree of disorder being directly proportional to the volume of each arrangement present. Superstructure will not be observed for random fault development.

CHAPTER 8

CRYSTAL CHEMISTRY OF THE SODALITE AND CANCRINITE GROUPS OF MINERALS

8.1 Introduction

Samples of sodalites and cancrinites have been analysed for the last hundred years. However, because these materials are extremely difficult to analyse, published analyses can be criticized from various points of view. With the exception of sodalite (proper) and cancrinite (proper) these materials occur in small quantities in which the chemical composition varies. Therefore, sample size and inhomogeneity are critical factors by which analytical methods used for analyses can be judged. Analytical methods based on 'large' sample size cannot be suitable due to the averaging procedure.

Today, the question of sample size does not arise as only small quantities of materials are available from museums. Therefore, the electron probe must be used for analyses. But this is not the ideal method of analysis for these zeolitic materials as they are very sensitive to the electron beam and, as a result, sodium is lost quite easily. Moreover, one cannot determine OH/H_2O and CO_2 by this method. These volatiles also may be lost in the electron beam.

Nevertheless, since the structures of several sodalites and cancrinites have been refined, it is useful to rationalize the general chemistry of these minerals in terms of their structures. This will indicate possible end-members and also show the extent of possible

solid solutions. Furthermore, criteria will be determined for judging the reliability of chemical analyses and identifying the essential chemical constituents.

This discussion on the overall chemical compositions of sodalites and cancrinites relied heavily on analyses taken from the literature since only a few selected samples were used in this study. Moreover, Hassan (1980) listed several cancrinite analyses from the literature and discussed their chemistry. Therefore only additional analyses on cancrinite will be listed and considered in the general discussion on cancrinites.

8.2 Framework Composition of Sodalite and Cancrinite:

The composition of the sodalite and cancrinite frameworks may be written as $(T_{12}O_{24})$. For these aluminosilicates, T = Al^{3+}, Si^{4+}. However, one may expect small amounts of substitution of Fe^{3+} for Al^{3+}.

According to the aluminum avoidance rule, a Si/Al ratio of 1:1 should correspond to complete ordering of Al and Si. Furthermore, if the departure from this ratio is small, a high degree of ordering should still exist. The question is whether available chemical analyses for these materials are sufficiently accurate to test the avoidance rule and what observed experimental deviation from a Si/Al ratio of 1:1 is acceptable for complete ordering. Taylor (1967) analyses of several samples of sodalite, nosean, hauyne and two lazurite specimens show that their Al/Si ratio is close to 1:1. Hogarth and Griffin (1976) analyses of lazurite specimens, however, show that Si exceeds Al by 0.1 to 0.6 atoms per cell. That is, the Si/Al ratio varies from 1:1 to at least 1.11:1. This departure of Al/Si ratio from 1:1 may well lie in the analytical technique and/or due to impurities.

The composition of the framework of sodalites and cancrinites is best justified from a structural point of view. Of the two possible space groups ($P\bar{4}3m$ and $P\bar{4}3n$) for sodalites, the space group $P\bar{4}3m$ would require the Al and Si to be completely disordered while the space group $P\bar{4}3n$ gives complete ordering of Al and Si. The structural refinements of sodalite in the latter space group as well as the refinements of the cancrinites conform to complete ordering of Al and Si. Therefore one criterion in judging the reliability of chemical analyses of these materials would be the extent of departure of the Al/Si ratio from 1:1. Moreover, all unit cell contents should be normalized to 12(Al + Si) rather than 24 Oxygens since the former is better characterized.

8.3 The Chemistry of Sodalite

Natural sodalites (proper) from plutonic and pegmatitic bodies closely approach the ideal formula of $Na_8(Al_6Si_6O_{24})Cl_2$. The studies by Taylor and others (Chapter 5) on synthetic sodalites show that complete solid solution exists between the K- and Na- end members. Therefore, potassium may be expected as an essential component in natural sodalite. However, its absence in natural sodalite may be a reflection of the environment. The volcanic specimen of sodalite analysed by Taylor (1967) shows a higher potassium content (0.2 atom/cell) than other analysed sodalites, indicating a wider variation in the solid solution for volcanic sodalites.

8.4 The Chemistry of Nosean-Hauyne Series

The end-member nosean, ideally $Na_8(Al_6Si_6O_{24})SO_4$, and the end-member hauyne, ideally $Na_6Ca_2(Al_6Si_6O_{24})(SO_4)_2$, have been synthesized by Taylor (1975). Moreover, Van Peteghem and Burley (1963) have shown that at 600°C and 1000 bars P_{H_2O} there is complete solid solution between these two end-members. In natural specimens, chlorine and S^{2-} are present only in small amounts. However, water varies from 0.40% to 4.60% and is generally higher in the noseans. Taylor (1967) believes that there is water present and this should be indicated by the structural formulae and that there is substitution of OH^- for SO_4. Water analysis is very difficult, and at the same time, one must distinguish between 'structural' water and 'zeolitic' water. On the basis of the structure of hydroxysodalite, if OH/H_2O is present as structural water then there should be no more than two OH/H_2O per cavity. The structural analysis of nosean suggest only one OH/H_2O per cavity. Present analyses do show this amount (Taylor, 1967). The oxygens of the SO_4 group were not well defined in nosean and hauyne. The disorder positions of the SO_4 group oxygens are expected to be on the 3-fold axes and should be well defined due to the rigidity of the SO_4 group. However, if OH/H_2O are present in similar positions as in hydroxysodalite, then this may be the cause for the ill-defined oxygens of the SO_4 group. Furthermore, the fact that nosean generally has a higher water content than hauyne is related to nosean having more vacancies in the interframework anion sites than hauyne.

In natural nosean-hauyne series both K and Ca are major constituents but Na is the most abundant of the interframework cations. On the unit cell basis ($Z = 1$) K ranges from 0.02 to 1.2 atoms, Ca from

0.2 to 2.0 atoms and Na from 4.5 to 7.2 atoms. From the above considerations the following formulae were proposed by Taylor (1967):

pure nosean: $Na_8(Al_6Si_6O_{24})SO_4 \cdot nH_2O$

nosean-hauyne series: $(Na_{5-8}K_{0-1}Ca_{0-2}\square_{0-1})(Al_6Si_6O_{24})(SO_4)_{1-2} \cdot nH_2O$.

These formulae however, are not quite reasonable in view of the structure analyses.

8.5 The Chemistry of Lazurite

Lazurite is a sulphur-bearing member of the sodalite group, closely related to hauyne. The chemistry of lazurite has recently been studied by Hogarth and Griffin (1976), but, unfortunately, its structure has not been refined as yet. This is due to the difficulty in obtaining a suitable single crystal. (Difficulty in obtaining pure lazurite samples, even for chemical analyses, has been mentioned repeatedly in the literature). Nevertheless, due to the similarity of lazurite to the sodalite group of minerals, it is worthwhile to speculate on its structure and discuss its chemistry.

Taylor (1967) studied two lazurite samples from Sary-Sang, Afghanistan but classified them as hauyne. A single crystal was not obtainable from one of his samples and his other sample showed superstructures. His data is consistent with the space group $P\bar{4}3n$. This was confirmed by a sample from the same locality, in this study.

Hogarth and Griffin (1976) observed isotropic (cubic) and also anisotropic and pleochroic (non-cubic) lazurites and noted various shades of blue in very small areas of several samples. From X-ray powder pattern, they determined that the cubic lazurite is consistent with the space group $P\bar{4}3m$. They also noted weak extra lines on Guinier photographs and were able to weaken them on heating. The 'extra lines' were strongest in the most anisotropic specimens and were ascribed to two

phases of lazurite, one cubic and the other of lower symmetry. These results indicate that Guinier photographs and X-ray powder patterns for sodalites can be misleading, in particular, as regards their superstructures and space group.

Hogarth and Griffin (1976) used the electron microprobe for the chemical analyses of lazurite. They resolved S and SO_3 on the basis of charge balance and assumed S^{2-} replacing O^{2-} in the framework. However, this is not a reasonable assumption. The variation of the SO_4, S^{2-} and Cl^- ions is shown in Figure 8.1. A lazurite field is defined, extending from about 50% S^{2-} - 50% SO_4 to 100% SO_4 and to 1% Cl^-. The deep blue lazurites are richest in S^{2-} and those richest in SO_4^{2-}, palest. Finally, Hogarth and Griffin (1976) proposed the following formula for lazurite:

$$(R', R'')_{7.5-8}(Si,Al)_{12}(O, S)_{24}(SO_4, Cl)_{1.3-2}\cdot nH_2O.$$

A more appropriate formula may be:

$$(Na, K, Ca)_{7.5-8}(Al_6Si_6O_{24})(SO_4, S, Cl)_{1.3-2}\cdot nH_2O$$

with a structure similar to nosean-hauyne.

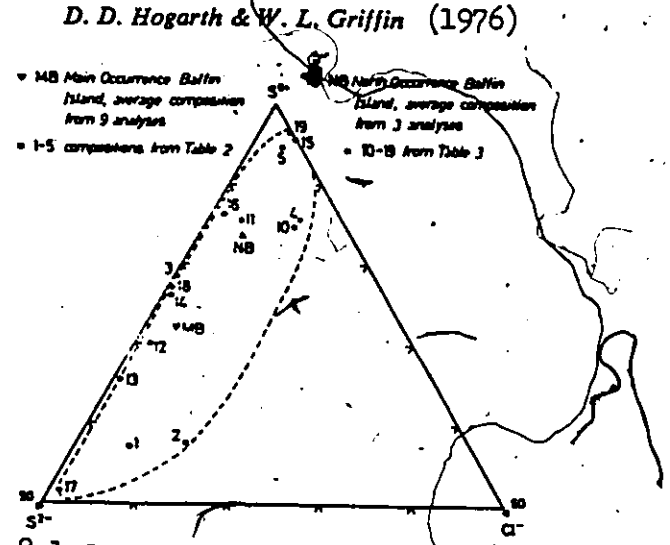

Fig. 8.1: Lazurite compositions plotted atomically with respect to S^{6+}, S^{2-} and Cl^-.

Hogarth and Griffin (1976) heated samples of lazurite to about 1000°C and noted that the extra lines had disappeared as had the weak diffractions diagnostic for the space group $P\bar{4}3m$, and the ignition product belong to the space group $P\bar{4}3n$. These results certainly need further investigation as both the chemistry and the structure of lazurite are inadequately defined.

8.6 The Chemistry of the Helvite Group

The variation of the interframework cations of the helvite group, $(Mn, Fe^{2+}, Zn)_8(Be_6Si_6O_{24})S_2$, is shown in Figure 8.2. This figure consists of seventy-five analyses of Dunn (1976) and fifty-seven analyses from the literature. From the plot of these analyses Dunn (1976) suggests that there is complete miscibility between the Fe and Mn members (danalite and helvite) and between the Fe and Zn members (danalite and genthelvite) but not between the Zn and Mn members (genthelvite and helvite). Essentially pure helvite and genthelvite occur naturally but the nearest approach to pure danalite is 86% Fe.

The structural analyses of the helvite-genthelvite series (sec. 4.2) indicate that: (1) complete miscibility is possible between all three end-members and (2) pure danalite is structurally stable. The rarity of intermediate Zn-Mn members in nature has been explained by Burt (1980) on the basis of the chalcophile-lithophile tendencies of the elements.

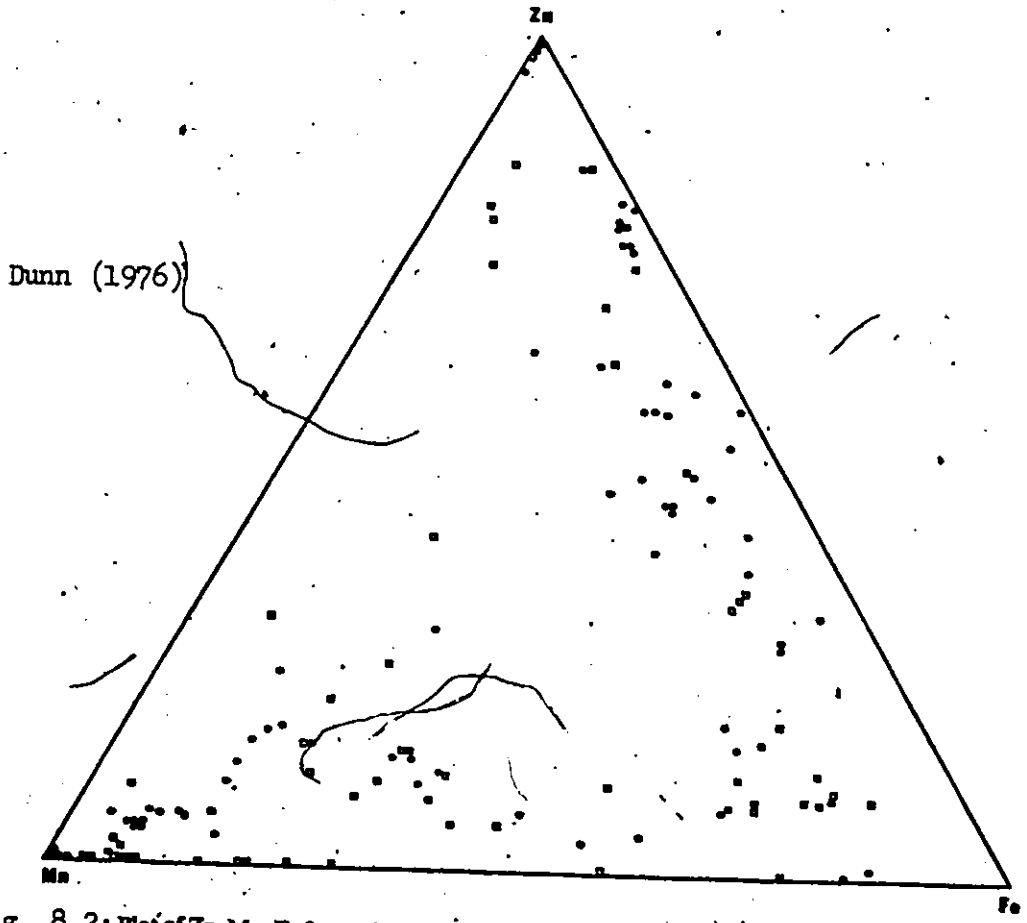

Fig. 8.2: Plot of Zn, Mn, Fe for analyses of the helvine group. □ from the literature; ● from this study.

8.7 The Chemistry of the Cancrinite Group of Minerals

The essential interframework cations in cancrinites are Na^+, Ca^{2+}, K^+ and the variation of these cations are shown in Figure 8.3. Each member appears to define rough compositional fields.

The variation of the interframework anions in cancrinites should be viewed in terms of H_2O-OH-SO_4-Cl-CO_3. However as OH^- is not common in natural minerals and as the amount of water is constant ($2H_2O$) in most cancrinites or absent in davyne/microsommite, the variation is shown in terms of SO_4-Cl-CO_3(Fig. 8.4). Again rough compositional fields are seen.

The essential unit of the cancrinite structure is the cage. The cage stabilizes the structure and it is always filled. Each cage prefers a water molecule and a sodium. However, if no water is present, the cage may be occupied by a monovalent anion and a divalent cation (eg. Ca^{2+} and Cl^- in davyne). Moreover, the contents of the cage has the most pronounced effect on the cell edges (Table 8.1). The largest cell parameter of davyne compared to the other cancrinites is clearly due to the cages containing chlorine rather than water.

The large channels are less important to the structure but they show many peculiarities. They contain the large anions (CO_3^{2-}, SO_4^{2-}) and the small hydroxyl ion (OH^-). From symmetry considerations, the maximum amount of SO_4^{2-} or CO_3^{2-} should be two, while that for OH^- should be six. Except for the OH ion, the large size of CO_3^{2-} and SO_4^{2-} restricts the amount of these ions to a value less than the maximum.

For the carbonate-rich cancrinite, the maximum amount of CO_3^{2-} appears to be 1.5 per cell from chemical analysis. However, the structural analysis (Hassan, 1980) shows no apparent reason why the

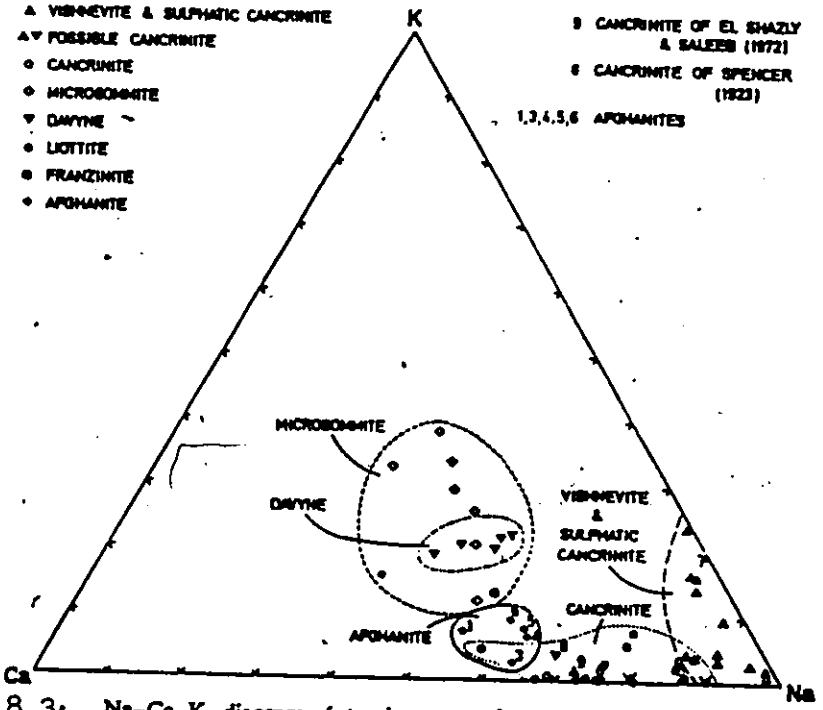

Fig. 8.3: Na–Ca–K diagram (atomic proportions) for minerals of the cancrinite group.

Hogarth (1979)

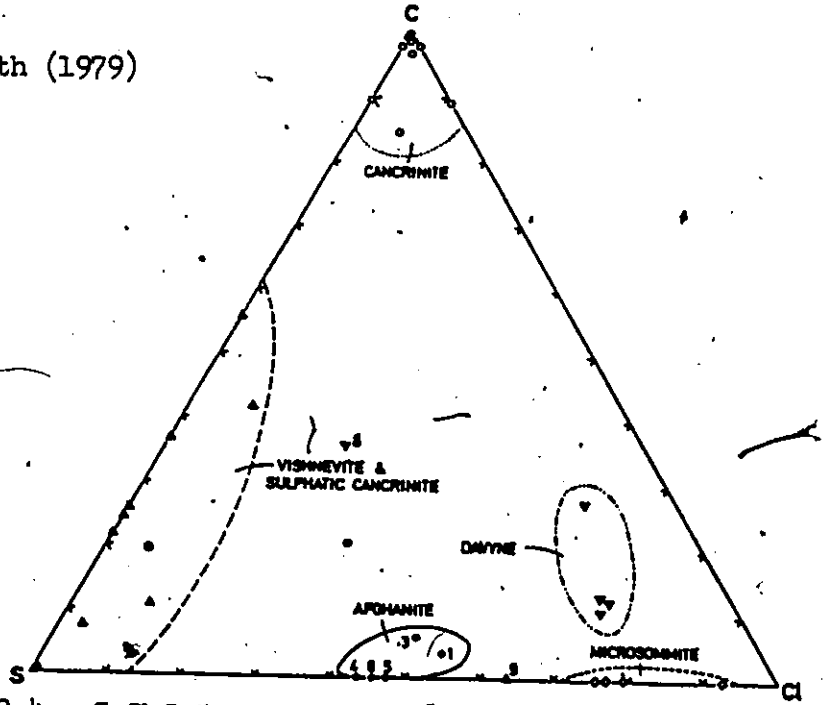

Fig. 8.4: S–Cl–C diagram (atomic proportions) for minerals of the cancrinite group. Symbols are the same as those in Figure 8.3.

maximum cannot be obtained. The structural analysis of vishnevite indicates that the maximum amount of SO_4^{2-} is one per cell due to the size of the SO_4^{2-} group. For hydroxycancrinite, structural analysis shows that the maximum amount of OH/H_2O in the channel is four per cell while davyne apparently contains no anion in the channel. Consequently, considerable anion vacancy is tolerable in the channel. The cations in the channel are Na^+, Ca^{2+} and K^+. Symmetry places all of these cations on the same site which may also be defective.

8.8 The Chemistry of New Cancrinite-like Minerals

Table 8.1 is a collection of all published analyses on newly discovered cancrinite-like minerals (liottite, afghanite, franzinite, giuseppetite, sacrofanite). The variations of the interframework ions in the cancrinite-like minerals have been shown on ternary diagrams and compared with cancrinites (Hogarth, 1979; Leoni et al., 1979; and Mazzi and Tadini, 1981). However, individual analysis (Table 8.1) should be scrutinized on the basis of a normalized cancrinite cell and viewed in terms of the cancrinite structure (Hassan, 1980).

Four main points deserve discussion: (1) the Si/Al ratio; (2) the K, Ca, Na content in the various minerals; (3) the SO_4^{2-} and CO_3^{2-} found in the large channels; (4) the Cl^- and OH^-/H_2O found in the small cages. Leoni et al. (1979) combined the last two points and concluded that no relationship can be evidenced between the interframework anionic groups and the nature of the cations.

(1) All the analyses show a Si/Al ratio of nearly one, which is a strong indication for ordered distribution of these cations.

(2) Most analyses show the sum (K + Na + Ca) to be close to eight,

Table 8.1: Chemical formulae and cell parameters of cancrinite-like minerals

	1	2	3	4	5	6	7	8	9	10	11	12	13
Si	6.11	6.30	6.11	6.13	6.06	6.03	6.20	6.28	6.26	6.08	6.22	5.96	6.26
Al	5.89	5.70	5.89	5.87	5.94	5.97	5.80	5.72	5.74	5.92	5.78	6.04	5.74
	12.00	12.00	12.00	12.00	12.00	12.00	12.00	12.00	12.00	12.00	12.00	12.00	12.00
Fe	0.05	0.02	0.01	n.d.	b.d.	n.d.	n.d.	b.d.	0.01	0.01	0.01	n.d.	0.05
Mg	n.d.	0.09	0.12	n.d.	b.d.	b.d.	0.01	b.d.	0.04	0.18	0.18	n.d.	n.d.
Na	3.10	4.33	4.39	4.87	4.98	4.53	5.03	4.83	4.31	5.26	4.16	5.00	6.25
K	1.37	1.33	1.23	0.68	0.63	0.21	0.55	0.75	1.04	1.19	1.80	1.82	1.39
Ca	2.59	2.72	2.06	3.52	2.37	2.48	2.45	2.45	3.50	2.07	2.18	0.94	1.83
	7.96	8.33 ?	7.68	9.07 ?	7.88	7.2	8.02	7.82	7.85	8.5 ?	8.14	7.76	9.47 ?
CO_3^{2-}	0.57	0.49	0.73	0.11	n.d.	0.30	n.d.	n.d.	0.41	0.49	0853	0.24	0.27
SO_4^{2-}	1.30	1.23	1.20	1.27	1.56	1.37	1.54	1.55	1.54	1.39	1.50	1.34	1.14
	1.88	1.72	1.93	1.38	1.56	1.56	1.54	1.55	1.95	1.88	2.03	1.58	1.41
Cl^-	0.87	0.80	1.35	1.55	1.4	1.45	1.19	1.29	0.12	0.37	0.04	0.29	0.20
H_2O	0.61	0.49	1.84	0.46	n.d.	1.32	n.d.	n.d.	0.86	1.12	0.79	n.d.	3.21
OH^-	1.19	1.38	0	n.d.	n.d.	0	n.d.	n.d.	0.70	0.96	0.64	n.d.	n.d.
	2.67 ?	2.67 ?	3.08 ?	2.01	1.4	2.77 ?	1.19	1.99	1.68	2.44	1.97	n.d.	3.41 ?
O^{2-}	24.00	24.00	23.48	24.74	23.88	23.58	24.21	24.09	24.00	24.00	24.00		
a (Å)	12.842(2)	12.843(2)	12.796(2)	12.77(3)	—	12.74	—	—	12.824(9)	12.841(5)	12.904(5)	12.854(1)	12.865(4)
c (Å)	5.364(5)	5.366(5)	5.340(2)	5.39(4)	—	5.32	—	—	5.316(2)	5.32(3)	5.29(2)	5.28(3)	5.30(1)
V_c (Å^3)	766.0	767.0	757.2	754.1	—	747.8	—	—	764.2	762.1	763.1	755.0	759.7

1) Liottite, Pitigliano (Merlino & Orlandi, 1977a); Afghanites: 2) Pitigliano (Leoni et al. 1979), 3) Sacrofano (Leoni et al. 1979), 4) Sar-e-Sang (Bariand et al. 1968), 5) Sar-e-Sang (Hogart, 1979), 6) Tultuisk (Ivanov and Sapozhnikov, 1975), 7) Lyadshuar-Darinsk (Hogart, 1979), 8) Edwards (Hogart, 1979); Franzinite: 9) Pitigliano (Merlino and Orlandi, 1977b), 10) Sacrofano (Leoni et al. 1979), 11) Ariccia (Leoni et al. 1979); 12) Giuseppettite, Sacrofano (Mazzi & Tadini, 1981); 13) Sacrofanite, Sacrofano (Burragato et al. 1980).

indicating that all the cation sites are filled. Those analyses that show excess over eight are considered to be in error (anal. # 2, 4, 10, 13). (3) The analyses show the sum ($SO_4 + CO_3$) to be always less than two. The maximum amount reported for CO_3^{2-} is 0.57 and the average value of SO_4^{2-} for all the analyses is 1.38. This amount of SO_4 is quite high for the cancrinite structure since the refinement of vishnevite shows the maximum amount is one SO_4 group per cell. The high amount of SO_4 may be taken as an indication for a different framework than cancrinite or perhaps the form of the sulphur is SO_3^{2-} rather than SO_4^{2-} or even S^{2-}. (4) The role of H_2O/OH^- cannot be fully assessed from the analyses since it has not been determined in some and in others it is highly variable. Therefore the sum ($Cl^- + H_2O/OH^-$) is variable, however, it is expected to be two in keeping with the cancrinite structure and those analyses showing greater values are questionable (anal. # 3, 13 in particular and # 1, 2, 6).

CHAPTER 9

SUPERSTRUCTURES IN CANCRINITE AND SODALITE GROUPS OF MINERALS

9.1 Introduction

Superstructures are seen on single crystal diffraction photographs as satellites or superstructure reflections. They are sometimes referred to as non-Bragg reflections and occur in addition to the main reflection corresponding to the fundamental structure or substructure. The intensity of the superstructure reflections seen on X-ray diffraction photographs are, in general, much weaker than those of the substructure. However, on electron diffraction photographs they are much more apparent (see Hassan, 1980) and can approach the intensity of the substructure reflections. This is due to the enhancement of the diffraction effect with electrons.

Superstructure reflections are further classified as commensurate or incommensurate. Commensurate superstructure reflections divide the interval between the main reflections into simple integral parts, indicating that the unit cell corresponding to the superstructure is a simple multiple of the subcell, otherwise, the superstructure reflections are classified as incommensurate. In general, only few lower order superstructure reflections are observable and, on heating, these reflections may move continuously in reciprocal space, according to temperature and/or composition, with no practical change in either intensity or position of

the main reflections. Therefore, these types of superstructure reflections cannot give rise to a simple multiple of the subcell and are classified strictly as incommensurate by Sadanaga et al. (1978). Although a material may exhibit this type of behaviour with temperature (and composition) it is possible that for certain temperature ranges, the superstructure may 'lock' into place and give rise to an integral multiple of the subcell.

9.2 Superstructure Characteristics in Cancrinites and Sodalites

Superstructure reflections have strong intensities and are common in carbonate-rich cancrinites (see Chen, 1970). However, sulphatic cancrinites may or may not show superstructures. Some of the single crystals which were obtained from the small vishnevite for this study, show superstructure corresponding to twice that of the substructure, but the crystal used in the refinement (sec. 7.2) shows no superstructure reflections. Furthermore, the davyne crystals studied (sec. 7.5) also showed no superstructure reflections.

Generally, the superstructures in cancrinite are similar in that they are one-dimensional in nature and affect the c-axis repeat. The repeats, based on the superstructure, approximate integral number of substructure repeats and can increase the unit cell to as much as sixteen times that of the substructure (Brown and Cesbron, 1973). Hassan (1980) listed eleven cancrinites which were obtained from various localities and have superstructures that approximate various integral numbers of subcells.

The high temperature work of Foit et al. (1973) on CO_3^{2-} rich cancrinite showed that on heating, the superstructure intensity decreased

with time whereas that of the substructure remained constant. With prolonged heating (Chen, 1970) the position of the superstructure shifted towards the origin in reciprocal space. Thus the superstructure spacings vary with temperature. Therefore, according to Sadanaga et al. (1978) the superstructures in cancrinite should be classified as incommensurate. Moreover, although unheated carbonate-rich cancrinites show well-defined superstructure reflections these spots streak normal to the c^*-axis on heating. Also, hydroxycancrinite shows streaking parallel to the c^*-axis (Fig. 7.1) even at room temperature.

Only the sulphatic sodalites, nosean and lazurite, showed superstructures in this study. The hauyne investigated showed no superstructure but superstructures for hauyne were reported by Taylor (1968), Saalfeld (1961) and Sadanaga et al. (1978). The superstructure in these minerals are three-dimensional in nature.

Saalfeld (1961) considered the superstructure of the nosean sample he studied to be commensurate, having a cell edge six times that of the subcell. However, Ito and Sadanaga (1966) interpreted the same superstructure in terms of multiple twinning of an orthorhombic cell. Taylor (1968) noted that potassium-poor specimens of hauyne having cell edge less than 9.09Å do not show superstructures and, on the basis of measured superstructure spacings of nine different specimens, concluded that superstructures are incommensurate for the sulphatic sodalites.

9.3 Origin of Superstructures in Cancrinites and Sodalites

The rationalization of the superstructure in cancrinites and sodalites is based on two models, both of which are theoretically reasonable:

1. Substitutional and/or positional ordering of interframework cations and anions (see Foit et al., 1973).
2. Periodic variation in the framework stacking sequence giving polytypes transitional between those of cancrinite (ABAB...) and sodalite (ABCABC...) (see Rinaldi and Wenk, 1979). Based on experimental observations, the first model appears to be the most appropriate, in particular, for those materials that have been investigated in this study. The weak intensity of the superstructure and the ease in decreasing its intensity and position with moderate temperature is unlikely to involve the reorganization of the framework. Model 2 has been suggested for those cases where the intensity of the superstructure approaches that of the substructure (Merlini and Orlandi, 1977a).

Afghanite is an example of a cancrinite of this type and has been assigned a tentative stacking sequence of ABABACAC by Merlino and Mellini (1976), however, although the electron diffraction pattern (Rinaldi and Wenk, 1979) shows a reasonably intense superstructure the X-ray diffraction pattern (Bariand, 1968) shows the extra reflections to be very much weaker than those of the substructure. Rinaldi and Wenk (1979) observed lattice fringes with the T.E.M. for both Afghanite and Franzinite and following the proposals of Merlino and Mellini (1976) and Merlino and Orlandi (1977a, b) interpreted these in terms of differing stacking sequences. Cancrinites which have been associated with model 2 are in general $SO_4^=$ rich and $CO_3^=$ poor. As yet there have been no

succesful structure refinements of the proposed polytypes, with current R-factors varying from 16 to 30% (Rinaldi and Wenk, 1979; Bariand et al., 1968; Barrer et al., 1970; Mazzi et al., 1981).

Foit et al. (1973) also noted that the superstructure reflections were still observable after the heating experiments although greatly reduced in intensity. It is possible that such residual intensity could perhaps be assigned to a type 2 model. More recently prolonged heating at 400°C of Sacrofanite (Burragato et al., 1980) had no effect at all on the superstructure and would suggest that in this case it was due in total to a type 2 origin, this material is $SO_4^=$ rich with only minor CO_2 and H_2O and therefore differs from the $CO_3^=$ rich cancrinites which readily lose CO_2 and H_2O on heating. In order to determine the role of stacking variations in the cancrinites under study a CO_3^{2-} rich cancrinite was imaged using high resolution transmission electron microscopy (HRTEM) so that any periodic variation in the stacking sequence could be incorporated into the structural model.

The HRTEM images revealed that the stacking sequence of the CO_3^{2-} rich cancrinites was of the ABAB... type with neither systematic deviations nor even random stacking faults (Hassan, 1980). Therefore in this case, a model 2 contribution to the superstructure intensity could be eliminated completely for the CO_3^{2-} rich cancrinite.

The structure of the carbonate-rich cancrinite (Hassan, 1980) showed that the Al/Si framework was positionally well-defined and also the contents of the small cages showed nothing unusual that could contribute to the superstructure reflections. The cause of these reflections was in the large channels which show 'split' carbonate group positions. According to the space group $P6_3$ the chemical formula shows

that there is a deficiency in each Na(2) cation site (consisting of Na and Ca) of 0.08 ions and a deficiency of double that in the CO_3^{2-} group position. It is the ordering of these ions in a supercell of approximately 41Å (8 x C) that is responsible for the superstructure reflections. A possible arrangement for Na^+, Ca^{2+}, CO_3^{2-} and vacancy over the available atom sites which are positionally defined by the $P6_3$ symmetry according to the chemical analysis has been established through computer simulation of the 001 superstructure intensities and semi-quantitative comparison with the observed pattern (Grundy and Hassan, 1982).

The chemical formula for hydroxycancrinite is given below and should be compared with the carbonate-rich cancrinite discussed above.

$$Na_8(Al_6Si_6O_{24})(OH)_2.2H_2O$$

$$(Na_6Ca_{1.6})(Al_6Si_6O_{24})(CO_3)_{1.6}.2H_2O.$$

Structural refinements show that the framework and small cages for both materials are identical. Furthermore, the cation site in the large channel for hydroxycancrinite is completely filled and positionally well-defined and therefore can be eliminated from contributing to the very weak superstructure reflections observed (Fig. 7.1) for hydroxycancrinite.

Consequently, the single component that is giving rise to the weak superstructures in hydroxycancrinite is the hydroxyl ions. These ions are located in similar positions as the oxygen atoms in the CO_3 group in the carbonate-rich cancrinite. The superstructures are expected to be weak since there is considerable deficiency on the OH sites. A possible ordering pattern based on OH and vacancy may be able to simulate the superstructures, as was done for the carbonate-rich cancrinite.

The vishnevite sample used in the structure refinement showed no superstructure since the SO_4^{2-} group in the channel was completely disordered. However, if the ions in the channel were ordered, then superstructure would arise as was found in other crystals from the same small specimen. The framework and cage content are also identical to the carbonate-rich cancrinite and therefore do not contribute to superstructure.

The davyne crystal used in the structure refinement also showed no superstructure. The cage contained Ca^{2+} and Cl^- in contrast to the other cancrinites which contained Na^+ and H_2O. Furthermore, the Al-O and Si-O bond lengths are different from those found in the other cancrinites.

These bond lengths suggest that the framework is disordered. The Al and Si atoms are arranged one way in hydroxycancrinite and cancrinite but in vishnevite they are interchanged. Since there are two possible Al and Si arrangements, if a crystal were to contain both type of arrangements, X-ray would see it as a disorder framework even though large sections would be ordered. In such a situation, the boundary between the various sections could be stacking faults which are arranged randomly. Random stacking faults cannot give rise to superstructures. However, if the stacking faults were ordered then superstructures that are commensurate would develop since the sizes of the TO_4 tetrahedra are nearly equal.

For cancrinites we can now conclude that if the framework atoms are ordered, then they do not contribute to the incommensurate superstructure reflections which are caused by ordering of the interframework atoms. The same is true for sodalites. However, the slight positional disorder of the framework atoms in the sulphatic sodalites also add to the intensities of the incommensurate superstructure reflections.

CHAPTER 10

GENERAL DISCUSSION AND CONCLUSIONS

This work uses X-ray diffraction to characterize the structures of all the members of the cancrinite and the sodalite group of minerals.

The three-dimensional frameworks of these minerals have an ordered distribution of TO_4 tetrahedra (T = Al, Si, Be). In cancrinites, the T1 and T2 sites could be occupied by either Si or Al atoms. The two possible arrangements are equally probable and depend only on chance. There is the possibility, however, of a stacking fault(s) which breaks the regular ABAB... sequence with a C type layer. This effectively reverses the order. This situation was found in davyne which shows apparent disorder of the framework due to the averaging effect of the X-ray method, the degree of disorder being directly proportional to the volume of each arrangement present.

Cancrinite has large continuous framework channels and also cages which are smaller than those of sodalite. All the channels and all the cages are identical according to the space group $P6_3$. However, they can be chemically different since they can contain different cations and anions. The oxygens of the cancrinite cage have a total residual charge of -1v.u. which must be satisfied by the cage cations and anions. The various combinations of cations and anions having an overall charge of +1v.u. are limited by spatial requirements. The cages of natural cancrinites contain either $(NaH_2O)^+$ or $(CaCl)^+$. The channels of cancrinites also contain various cations and anions. The synthetic cancrinite studied by Klaska and Jarchow (1977) had channels with OH^-,

H_2O and channels with SO_4^{2-} in the ratio of 1:2 and these channels are distributed in a fully ordered pattern. The various cations and anions found in natural cancrinites together with their ideal end-member compositions which were deduced from their structures are listed on p. 199. The cages in cancrinite are always filled and they hold the structure together. The anion group in the cancrinite channel occupies split positions. The relative position of the 'basal' oxygen of the SO_4^{2-} group in vishnevite and the oxygens of OH/H_2O in hydroxycancrinite are very similar to the oxygens of the CO_3^{2-} group positions in cancrinite. This emphasizes the control exerted by the framework on the channel cation positions which in turn regulate the positions of the anion groups.

Sodalite has a network of large framework cages or cavities. In each cell there are two cavities which are identical according to the space group $P\bar{4}3n$. However, the two cavities could be chemically distinct since they can contain different cations and anions and also the proportion of each different cavity can vary. In each sodalite cavity the twelve framework oxygen atoms have a total residual charge of -3v.u. which must be satisfied by the interframework ions. Various combinations of cations and anions having an overall charge of +3v.u. can satisfy this requirement, but the combinations are restricted by spatial requirements. The various combinations of interframework ions that were found in the cavities of natural sodalites are listed on p. 199 and the ideal end-member compositions that were deduced from their structures are also given. The synthetic sodalites (see Chapter 5) show that other types of sodalite cavities also exist. For example, cavities containing $(Li_4Cl)^{3+}$;

MINERALS	CONTENTS OF		END-MEMBER COMPOSITION
	Cage		
Sodalite	$(Na_4Cl)^{3+}$		$Na_8(Al_6Si_6O_{24})Cl_2$
Hydroxysodalite	$(Na_4OH\ H_2O)^{3+}$		$Na_8(Al_6Si_6O_{24})(OH)_2.2H_2O$
Hauyne	$(Na_3CaSO_4)^{3+}$ 75%; $(K_2CaOH)^{3+}$ 25%		$Na_6Ca_2(Al_6Si_6O_{24})(SO_4)_2$
Nosean	$(Na_4SO_4)^{2+}$ 50%; $(Na_4H_2O)^{4+}$ 50%		$Na_8(Al_6Si_6O_{24})SO_4.H_2O$
Tugtupite	$(Na_4Cl)^{3+}$		$Na_8(Al_2Be_2Si_8O_{24})Cl_2$
Helvite	$(Mn_4S)^{6+}$		$Mn_8(Be_6Si_6O_{24})S_2$
Danalite	$(Fe_4S)^{6+}$		$Fe_8(Be_6Si_6O_{24})S_2$
Genthelvite	$(Zn_4S)^{6+}$		$Zn_8(Be_6Si_6O_{24})S_2$
	Cage	Channel	
Cancrinite	$(NaH_2O)^{+}$	CO_3, Na, Ca	$Na_6Ca_2(Al_6Si_6O_{24})(CO_3)_2.2H_2O$
Hydroxycancrinite	$(NaH_2O)^{+}$	OH, H_2O, Na	$Na_8(Al_6Si_6O_{24})(OH)_2.4H_2O$
Vishnevite	$(NaH_2O)^{+}$	SO_4, Na, K	$Na_8(Al_6Si_6O_{24})SO_4.2H_2O$
Davyne	$(CaCl)^{+}$	?H_2O, Na, K	$Na_6Ca_2(Al_6Si_6O_{24})Cl_2.(OH)_2$

Table 10.1: End-member composition and contents of cages and/or channels for sodalite and cancrinite groups of minerals

MINERALS	CONTENTS OF Cage		END-MEMBER COMPOSITION
Sodalite	$(Na_4Cl)^{3+}$		$Na_8(Al_6Si_6O_{24})Cl_2$
Hydroxysodalite	$(Na_4OH\ H_2O)^{3+}$		$Na_8(Al_6Si_6O_{24})(OH)_2.2H_2O$
Hauyne	$(Na_3CaSO_4)^{3+}$ 75%; $(K_2CaOH)^{3+}$ 25%		$Na_6Ca_2(Al_6Si_6O_{24})(SO_4)_2$
Nosean	$(Na_4SO_4)^{2+}$ 50%; $(Na_4lH_2O)^{4+}$ 50%		$Na_8(Al_6Si_6O_{24})SO_4.H_2O$
Tugtupite	$(Na_4Cl)^{3+}$		$Na_8(Al_2Be_2Si_8O_{24})Cl_2$
Helvite	$(Mn_4S)^{6+}$		$Mn_8(Be_6Si_6O_{24})S_2$
Danalite	$(Fe_4S)^{6+}$		$Fe_8(Be_6Si_6O_{24})S_2$
Genthelvite	$(Zn_4S)^{6+}$		$Zn_8(Be_6Si_6O_{24})S_2$
	Cage	Channel	
Cancrinite	$(NaH_2O)^{+}$	CO_3, Na, Ca	$Na_6Ca_2(Al_6Si_6O_{24})(CO_3)_2.2H_2O$
Hydroxycancrinite	$(NaH_2O)^{+}$	OH, H_2O, Na	$Na_8(Al_6Si_6O_{24})(OH)_2.4H_2O$
Vishnevite	$(NaH_2O)^{+}$	SO_4, Na, K	$Na_8(Al_6Si_6O_{24})SO_4.2H_2O$
Davyne	$(CaCl)^{+}$	$?H_2O$, Na, K	$Na_6Ca_2(Al_6Si_6O_{24})Cl_2.(OH)_2$

$(K_4Cl)^{3+}$; $(Na_4Br)^{3+}$ and $(Na_4I)^{3+}$ occur in the corresponding end-member sodalites and the sodalite model (Chapter 5) also indicates that $(C_4F)^{3+}$ (C = Li, Na, K, Rb) cavities are also possible. The model also shows how the framework distorts to accommodate different ions.

Natural lazurite contains SO_4^{2-} and S^{2-}. If these are the only types of anions present then the amount of Ca^{2+} should equal to $SO_4^{2-}+S^{2-}$ and the lazurite end-member should be $Na_6Ca_2(Al_6Si_6O_{24})S_2$. Analyses of natural lazurite (Hogarth & Griffin, 1976) show that the amount of Ca is two or less and also Cl and OH/H_2O may be present. A variety of cavities are therefore possible in natural lazurite.

Sodalite containing varying proportions of different types of cations have been synthesized, for example, compositions between $Na_8(Al_6Si_6O_{24})Cl_2$ (a = 8.882) to $K_8(Al_6Si_6O_{24})Cl_2$ (a = 9.253) have been synthesized by Henderson and Taylor (1978). The difference in size between the $(Na_4Cl)^{3+}$ and $(K_4Cl)^{3+}$ cavities is reflected in the difference in the cell edges of 0.37Å. This difference incidentally, is identical to the difference in radii between K^+(r = 1.37Å) and Na^+(r = 0.99Å). The solid solution between the two end-members may contain cavities of the type $(Na_4Cl)^{3+}$, $(K_4Cl)^{3+}$, $(Na_2K_2Cl)^{3+}$ etc. and the different sizes of cavities can link together. The different sizes of cavities may cause the framework to split as was found in nosean which contains cavities of the type $(Na_4SO_4)^{2+}$ and $(Na_4H_2O)^{4+}$ in the ratio of 1:1. However, only if the different sized cavities are ordered would the split oxygen positions be resolvable. Synthetic nosean and hauyne have cell dimensions of 9.071 and 9.084 (Taylor, 1975) and synthetic hydroxysodalite, which have cavities of the type $(Na_4OH.H_2O)$, has a cell dimension of 8.890Å. The size of $(Na_4SO_4)^{2+}$ can be approximated by the cell edge of hauyne while

that of $(Na_4H_2O)^{4+}$ may be approximated by the cell edge of hydroxysodalite, although this is expected to be smaller. Therefore difference in cavity size greater than 0.194Å may therefore result in a split framework. As a rule, we can safely assume that if the difference in cell edges is greater than 0.2Å as a result of different cavities, then the framework would be split but it is geometrically possible to link together the different cavities. If the difference in the size of cavities is significantly greater than 0.37Å (difference between $(Na_4Cl)^+$ and $(K_4Cl)^+$), then it may be geometrically impossible to link the different cavities together. Based on these criteria, cavities which can link together geometrically could be selected and could be mixed in varying proportions to indicate solid solution.

The difference in cell edges between sodalite (proper) and hauyne is 0.202Å. Therefore, a complete solid-solution is geometrically possible between hauyne and sodalite and this would consist of $(Na_3CaSO_4)^{3+}$ and $(Na_4Cl)^{3+}$ cavities. Similarly, in a geometrical sense, solid solution is possible between sodalite and nosean and between nosean and hauyne. However, in these solid-solutions, the nosean cavities: $(Na_4SO_4)^{2+}$ and $(Na_4H_2O)^{4+}$ would cluster due to charge requirements but the clusters could be distributed randomly. Therefore, the possible solid solutions can be viewed as sodalite or hauyne containing nosean inclusions, but it should be noted that the framework is continuous.

Whether a solid-solution does or does not exist would have to be answered experimentally. Solid solution among the sodalites has never been demonstrated by analysis of natural minerals coupled with X-ray or optical techniques. The experimental work of Van Peteghem and Burley (1963)

shows that complete solid solution exists between nosean-hauyne but only limited solid-solution occurs between sodalite-nosean and sodalite-hauyne at 600°C and 15,000 p.s.i. in the presence of excess water. Experimental work may have failed to demonstrate complete solid-solution involving sodalite since hydroxysodalite type cavity $(Na_4OH.H_2O)^{3+}$ may have been involved. This cavity is larger than the $(Na_4Cl)^{3+}$ cavity and, therefore links up more easily with a large cage containing a SO_4 group.

The structure refinement of members of the helvite-genthelvite series indicates that complete miscibility should occur between the Mn, Fe and Zn end-members.

Moreover, the structure refinement of members in the cancrinite group shows that the solid-solution between cancrinite and vishnevite should be complete and may be visualized as mixtures of CO_3-type channels and SO_4-type channels. Solutions should also exist among all the cancrinite members since different channels and/or different parts of the same channel may contain different ions.

Stacking faults could occur in sodalite and cancrinite if the regular ABCABC... or ABAB... sequence is interrupted. If the stacking faults are random, they cannot give rise to superstructure. The superstructure observed in cancrinites and sodalites is due to the ordering of the interframework ions.

The new cancrinite-like minerals are thought to have different frameworks which are closely related to the frameworks of cancrinite and sodalite. Examination of the stacking sequence (Table 2.1) shows that both liottite and afghanite have a significant part of the cancrinite

stacking sequence while franzinite has a significant part of the sodalite sequence. These cancrinite-like phases are therefore expected to consist of some cancrinite cages and channels as well as some sodalite cages. In terms of the chemistry of the cancrinite-like phases, the ABAB and ABCABC stacking sequence of cancrinite and sodalite respectively may be considered as end-members since they restrict the number of interframework ions. The chemical analyses of the cancrinite-like phases (Table 8.1) should therefore be viewed in terms of the cancrinite cell. The analyses show an average value of 1.38 SO_4^{2-} and varying amounts of CO_3^{2-} per cell. This amount of SO_4 is too much for the cancrinite structure and random introduction of a C-type layer into the ABAB sequence would not form a complete sodalite cage. The C-type layer causes the cancrinite channel to be closed off by a six-membered ring and this type of channel is unlikely to accommodate the amount of SO_4 in excess of one. We probably need complete sodalite cages within a cancrinite-like host to accommodate more than one SO_4 group and the varying amounts of CO_3^{2-}, since the sodalite cage cannot accommodate this anion group.

Solid solution among the natural sodalites involves strain in the framework and may exist only at high temperature. However, in natural environment we can examine whether the (P, T) condition or the chemical composition is more important for the formation of cancrinite and sodalite. Sodalite (proper) does not contain Ca^{2+}, therefore if this cation is available davyne may be formed instead of sodalite proper. If P_{SO_2} is very high and Ca^{2+} is available, hauyne may be formed instead of vishnevite or nosean. If P_{CO_2} is high and Ca^{2+} is available then

cancrinite would be formed instead of a sodalite species which does not seem to accommodate CO_3^{2-}. This clearly shows that the chemical composition is important in deciding what species would be formed although the experimental studies (Anderson and Burley, 1982) on the hydroxyvarieties show that sodalite may be formed as in all cases in the high temperature phase.

Finally, future work in this area is needed to characterize the stacking sequences of the cancrinite-like phases. High resolution transmission electron microscopy may be useful in this regard. Furthermore, the sodalite and cancrinite cages are common in many zeolites and since these cages are well characterized, the results from this study could be applied in future work to examine the complex structures of zeolites.

REFERENCES

ANDERSON, P. and BURLEY, B. J. (1981): The System Nepheline-NaOH-H_2O. Tsch. Min. und Pett. Mitt. (in press).

BARIAND, P., CESBRON, F. & GIRAUD, R. (1968): Une nouvelle espece minerale: l'afghanite de Sar-e-Sang, Badakhshan, Afghanistan. Bull. Soc. fr. Mineral. Crystallogr. 91, 34-42.

BARRER, R. M., COLE, J. F., and VILLIGER, H. (1970): Chemistry of soil minerals. Part VII. Synthesis, properties, and crystal structures of salt-filled cancrinites. J. Chem. Soc., 9, 1523-31.

_____, and VAUGHAN, D. E. W. (1971): Trapping of inert gases in sodalite and cancrinite crystals. J. Phys. Chem. Solids. 32, 731-743.

BARTH, T. F. W. (1926): Die Kristallographische Beziehung Zwischen Helvin und Sodalit. Norsk Geol Tidssk., 9, 40-42.

_____ (1927): Die Pegmatitgange im Seilandgebiete. Vidensk. Akad. Skr., I. Mat.-Nat. Kl., Oslo, No. 8.

_____ (1932a): The Structure of the minerals of the sodalite group. Z. Krist. 83, 405-415.

_____ (1932b): The chemical composition of noselite and hauyne. Amer. Min., 17, 466-471.

BEUS, A. A. (1966): Geochemistry of beryllium and genetic types of beryllium deposits (in transl.). Freeman, San Francisco.

BROWN, G. E., GIBBS, G. V., and RIBBE, P. H. (1969): The nature and variation of the Si-O and Al-O bonds in framework silicates. Amer. Min. 54, 1044-61.

BROWN, I. D. (1976): On the Geometry of O-H...O Hydrogen Bonds. Acta Cryst. A32, 24-31.

_____, and SHANNON, R. D. (1973): Empirical Bond Strength-Bond Length curves for Oxides. Acta. Cryst. A29, 266-82.

BROWN, W. L. and CESBRON, F. (1973): Sur le surstructures des cancrinites. C. R. Acad. Sci. Paris, 276, Series D, 1-4.

BUKIN, V. I. and MAKAROV, Ye. S. (1967): Crystal Strucutre of Hydroxy-sodalite according to Neutron diffraction Analysis. Geochem. International, 4, 19-28; translated from Geokhimiya, No. 1, pp. 31-40, 1967.

BURRAGATO, F., PARODI, G. C. & ZANAZZI, P. F. (1980): Sacrofanite -- A new mineral of the Cancrinite Group. N. Jb. Miner. Abh. 140, 102-110.

BURT, D. M. (1974): Concepts of acidity and basicity in petrology -- the exchange operator approach. Geol. Soc. Am. Abstracts with Programs, 6, 674-676.

_____ (1977): Chalcophile-lithophile tendencies in the helvite group: genthelvite stability in the system ZnO-BeO-Al_2O_3-SiO_2-SO_{-1}-F_2O_{-1} (abstr.). Am. Geophys. Union Trans., 58, 1242.

_____ (1980): The stability of danalite, $Fe_3Be_3(SiO_4)_3S$ Am. Mineral., 65, 355-360.

CHEN, S. M. (1970): A chemical thermogravimetric and X-ray study of cancrinite. M.Sc. Thesis, McMaster University.

CROMER, D. T. and MANN, J. B. (1968): X-ray scattering factors computed from numerical Hartree-Fock wave functions. Acta. Cryst. A24, 321-324.

CRUICKSHANK, D. W. J. (1961): The role of 3d-orbitals in π-bonds between (a) silicon, phosphorous, sulphur or chlorine and (b) oxygen or nitrogen. Journ, Chem. Soc., 5486-504 (V32).

DANØ, M. (1966): The crystal structure of Tugtupite -- a new mineral, $Na_8Al_2Be_2Si_8O_{24}(Cl, S)_2$. Acta. Cryst. 20, 812-816.

DEER, W. A., HOWIE, R. A. & ZUSSMAN, J. (1963): Rock-forming minerals. 4. Framework silicates. Longmans, London.

DEMPSEY, M. J. & TAYLOR, D. (1980): Distance least squares modelling of the cubic sodalite structure and of the thermal expansion of $Na_8(Al_6Si_6O_{24})I_2$ Phys. Chem. Minerals. 6, 197-208.

DUNN, P. J. (1976): Genthelvite and the helvine group. Min. Mag. 40, 627-36.

FOIT, Jr. F. F., PEACOR, D. R. and HEINRICH, E. W. (1973): Cancrinite with a new superstructure from Bancroft, Ontario. Can. Min. II, 940-951.

GALITSKII, V. Yu., SHCHERBAKOV, V. N. and GABUDA, S. P. (1973): PMR determination of the location of the water molecules and hydroxyl groups in hydroxysodalite. Sov. Phys. Crystallogr. 17, 691-695.

_____, _____ and _____ (1974): Position of the hydroxyl groups in the structure of hydroxysodalite. Sov. Phys. Crystallogr. 18, 620-622.

GIBBS, G. V., HAMIL, M. M., LOUISNATHAN, S. J., BARTELL, L. S. and YOW, H. (1972): Correlations between Si-O bond length, Si-O-Si angle and bond overlap populations calculated using extended Huckel molecular orbital theory. Am. Mineral. 57, 1578-1613.

GLASS, J. J., JAHNS, R. H. and STEVENS, R. E. (1944): Helvite and danalite from New Mexico and the Helvite group. Amer. Min., 29, 163-191.

GOSSNER, R. and MUSSGNUG, F. (1930): Uber Davyn und seine Beziehungen zu Hauyn und Cancrinit, Z. Krist., 73, 52-60 (Min. Abst., 4, 279).

GOTTFRIED, K. (1927): Die Raumgruppe des Helvins: Zeits. Kryst., 65, 425.

GRUNDY, H. D. & HASSAN, I. (1982): The crystal structure of a carbonate-rich cancrinite. Can. Min. 20, 239-251.

HASSAN, I. (1980): The submicroscopic and average structures of cancrinite. M.Sc. Thesis, McMaster University.

HASSAN, I. and GRUNDY, H. D. (1982): The structure of basic sodalite. Acta. Cryst. (accepted).

HENDERSON, C. M.B. and TAYLOR, D. (1977): Infrared spectra of anhydrous members of the sodalite family. Spectrochem. Acta. 33A, 283-290.

_____ and _____ (1978): The Thermal Expansion of synthetic Aluminosilicate-Sodalites, $M_8(Al_6Si_6O_{24})X_2$. Phys. Chem. Minerals 2, 337-347.

_____ and _____ (1979): Infrared spectra of aluminogermanate- and aluminate sodalites and a re-examination of the relationship between T-O bond length, T-O-T angle and the position of the main i.r. absorption band for compounds with framework structures. Spectrochimiça Acta. 35A, 929-935.

HOGARTH, D. D. (1979): Afghanite: New Occurrences and Chemical Composition. Can. Mineral, 17, 47-52.

_____ and GRIFFIN, W. L. (1976): New data on Lazurite. Lithos 9, 39-54.

HOLLOWAY, Jr., W. M., GIORDANO, T. J. and PEACOR, D. R. (72): Refinement of the crystal structure of Helvite, $Mn_4(BeSiO_4)_3S$. Acta. Cryst. B28, 114-117.

ITO, T. and SADANAGA, R. (1966): On the polysynthetic structure of hauyne (abstract only). Int. Union. Cryst. Seventy int. Congr. and Symp. on crystal growth. Moscow.

IVANOV, V. G., & SAPOZHNIKOV, A. N. (1975): The first find of afghanite in the U.S.S.R., Zap. Uses. Mineral. Obshchest, 104, 328-331.

JARCHOW, O. (1965): Atomanordnung und Strukturverfeinerung von Cancrinit. Zeit Kristallogr. Bd. 122, S. 407-422.

KLASKA, R. & JARCHOW, O. (1977): Synehetischer Sulfat-Hydrocancrinit von Mikrosommit-Typ. Naturwissenschaften, 64, 93.

LEONI, L., MELLINI, M., MERLINO, S. and ORLANDI, P. (1979): Cancrinite-like minerals: new data and crystal chemical considerations. Rendiconti S.I.M.P. 35, (2), 713-719.

LOEWENSTEIN, W. (1954): The distribution of aluminum in the tetrahedra of silicates and aluminates. Amer. Mineral. 39, 92-96.

LOHN, J. and SCHULZ, H. (1968): Strukturverfeinerung am gestorten Hauyn, $(Na_5K_1Ca_2)Al_6Si_6O_{24}(SO_4)_{1.5}$. N. Jb. Miner. Abh. 109, 201-210.

LONS, Von J. and SCHULZ, H. (1967): Strukturverfeinerung von Sodalite, $Na_8Al_6Si_6O_{24}Cl_2$. Acta. Cryst. 23, 434-436.

MACHATSCHKI, F. (1933): Zur Hauynformel. Centr. Mineral., Geol. A, 145-150.

_____ (1934): Kristallstruktur von hauyne und nosean. Centr. Mineral., Geol. A, 136-144.

MARAKUSHEV, A. A. and BEZMEN, N. I. (1969): Chemical affinity of metals for oxygen and sulfur. Geol. Rudnykh Mestorozhdeniy, 11, 8-23. (transl. Int. Geol. Rev., 13, 1781-1794 (1974)).

MAZZI, F. and TADINI, C. (1981): Giuseppettite, a new mineral from Sacrofano (Italy), related to the cancrinite group. N. Jb. Miner. MH. 3, 103-110.

MEGAW, H. D. (1973): Crystal Structures: a working approach. Philadelphia; W. B. Saunders Co.

MEIER, W. M. and OLSON, D. H. (1971): Zeolite frameworks Adv. Chemistry Ser. 100, 155-170.

MEL'NIKOV, O. K., LATVIN, B. M. and FEDOSOVA, S. P. (1968): Production of helvite-group compounds (in Russian). In A. M. Lobachev, Ed. Gidrotermal'nyi Sintez Kristallov, pp. 167-174. Nauka Press, Moscow.

MERLINO, S. and MELLINI, M. (1976): Crystal structures of cancrinite-like minerals. Zeolite '76. An International Conference on the Occurrence, Properties, and Utilization of Natural Zeolites. Program and Abstracts. Tucson, Arizona. P. 47.

_____ and ORLANDI, P. (1977a): Liottite, a new mineral in the cancrinite-davyne group. Am. Mineral., 62, 321-326.

_____ and _____ (1977b): Franzinite, a new mineral phase from Pitigliano (Italy). Neves Jahrb. Mineral. Monatsh. pp. 163-167.

NITHOLLON, P. (1955): Structure Cristalline de la Cancrinite. Publications Scientifiques et Techniques du Ministere de lair France, N. T. 53, 48.

NYMAN, H. and HYDE, B. G. (1981): The Related Structures of α-Mn, Sodalite, Sb_2Tl_7, etc. Acta. Cryst. A37, 11-17.

PAHOR, N. B., CALLIGARIS, M., Nardin, G. and RANDACCIO, L. (1982): Structure of a Basic Cancrinite. Acta. Cryst. (1982). B38, 893-895.

PAULING, L. (1930a): The structure of Sodalite and Helvite. Z. Kristallogr. 74, 213-225.

PAULING, L. (1930b): The structure of some sodium and calcium aluminosilicates. Proc. Nat. Acad. Sci., 16, 453-459.

RINALDI, R. and WENK, H.-R. (1979): Stacking Variations in Cancrinite Minerals. Acta. Cryst. A35, 825-828.

SAALFELD, H. (1959): Untersuchungen uber die Nosean-Struktur. Neues Jahrb. Min. Monatsh. 34-46.

_____ (1961): Strukturbesonderheiten des Hauyngitters. Z. Krist. 115, 132-140.

SADANAGA, R., TAKEUCHI, Y. & MORIMOTO, N. (1978): Complex Structures of Minerals. Recent Prog. Nat. Sci. Jpn., 3, 141-206.

SCHULZ, H. (1970): Struktur-und Uberstrukturuntersuchungen an Nosean-Einkristallen. Z. Kristallogr. 131, 114-138.

_____ and SAALFELD, H. (1965): Zur Kristallstruktur des Nóseans, $Na_8(SO_4(Al_6Si_6O_{24}))$. Tsch. Min. petr. Mitt. 10, 225-232.

SHANNON, R. D. (1976): Revised effective ionic radii and systematic studies of interatomic distances in halides and chalcogenides. Acta. Cryst. A32, 751-767.

SIEBER, W. and MEIER, W. M. (1974): Formation and Properties of Losod, a new sodium zeolite. Helvetica Chimica Acta. 57, 1533-1549.

SMITH, J. V. (1976): Origin and Structures of zeolites: In Rabo, J. A. Ed., Zeolite Chemistry and Catalysis. ACS Monograph 171. Am. Chem. Soc., Washington, D.C., 3-79.

SØRENSEN, H., DANØ, M. and PETERSEN, O. V. (1971): On the mineralogy and Paragenesis of tugtupite $Na_8Al_2Be_2Si_8O_{24}(Cl,S)_2$. Medd. om Grønland, 181 (no. 13), 38pp.

STEWART, J. M. (1976): XRAY 76 Crystallographic System. Comp. Sc. Tech. Rep. TR-446, University of Maryland, Maryland.

STEWART, R. F., DAVIDSON, E. R. and SIMPSON, W. T. (1965): Coherent X-ray scattering for the hydrogen atom in the hydrogen molecule. J. Chem. Phys., 42, 3175-3187.

STRUNZ, H. (1957): Mineralogische Tabellen. Leipzig, Akad. verlag.

TAYLOR, D. (1967): The Sodalite group of minerals. Contr. Mineral and Petrol 16, 172-188.

_____ (1968): The thermal expansion of the sodalite group of minerals. Mineral. Mag. 36, 761-769.

_____ (1972): The thermal expansion behaviour of the framework silicates. Mineral. Mag. 38, 593-604.

_____ (1975): Cell Parameter Correlations in the Aluminosilicate-sodalites. Contrib. Mineral. Petrol. 51, 39-47.

_____ and HENDERSON, C. M. B. (1978): A Computer Model for the Cubic Sodalite Structure. Phys. Chem. Minerals 2, 325-336.

VAN PETEGHEM, J. and BURLEY, B. J. (1962): Studies on the sodalite group of minerals. Trans. Roy. Soc. Canada, LVI, Ser. III, Sect. III, 37-53.

_____ and _____ (1963): Studies on solid solution between sodalite, nosean and hauyne. Can. Mineral. 7, 808-813.

WINTER, J. K., OKAMURA, F. P. and GHOSE, S. (1979): A high-temperature structural study of high albite, monalbite and the analbite monalbite phase transition. Am. Mineral. 64, 409-423.

YOUNG, R. A. (1962): Mechanism of phase transition in quartz. Defence Documentation Center, Washington, Report No. AD276235.

APPENDIX 1

OBSERVED AND CALCULATED STRUCTURE FACTORS

In the list of structure factors, the columns are l index, F_o, F_c and phase in millicycles. The unobserved reflections are indicated by *.

SODALITE

1,0,L

0	44	0	0

1,1,L

0	470	475	500
1	24*	0	0

2,0,L

0	412	410	0

2,1,L

0	101	99	0
1	1054	1036	915

2,2,L

0	36*	26	500
1	18*	0	0
2	1147	1127	918

3,0,L

0	28*	0	0

3,1,L

0	404	412	500
1	26*	0	0

3,2,L

0	35*	23	500
1	531	535	948
2	22*	0	0

3,3,L

0	1001	982	0
1	26*	0	0
2	418	404	904
3	8*	0	0

4,0,L

0	389	422	0

4,1,L

0	24*	24	500
1	828	812	209

4,2,L

0	434	445	0
1	0*	27	217
2	438	425	785

4,3,L

0	29*	23	0
1	306	292	923
2	78	77	223
3	452	438	942

4,4,L

0	1252	1269	0
1	0*	0	0
2	756	751	883
3	0*	0	0
4	1024	1013	76

5,0,L

0	0*	0	0

5,1,L

0	104	109	0
1	19*	0	0

5,2,L

0	39	41	0
1	316	315	976
2	0*	0	0

5,3,L

0	486	495	500
1	53	50	93
2	650	653	3
3	0*	0	0

5,4,L

0	31*	26	0
1	430	434	152
2	47*	48	930
3	88	94	203
4	0*	0	0

5,5,L

0	58	57	0
1	0*	0	0
2	437	444	154
3	0*	0	0
4	195	189	881
5	19*	0	0

6,0,L

0	956	969	0

6,1,L

0	53	55	500
1	251	257	54

6,2,L

0	246	251	500
1	33*	37	189
2	620	623	42

6,3,L

0	12*	21	0
1	470	473	79
2	10*	10	897
3	629	638	33

6,4,L

0	300	301	0
1	54*	53	930
2	198	199	46
3	41*	45	61
4	251	246	19

6,5,L

0	69	74	0
1	479	480	5
2	0*	13	102
3	151	150	855
4	52*	55	764
5	395	395	951

6,6,L

0	22*	19	0
1	8*	0	0
2	586	589	37
3	0*	0	0
4	186	182	792
5	8*	0	0
6	434	425	952

7,0,L

0	18*	0	0

7,1,L

0	73	71	500
1	0*	0	0

7,2,L

0	0*	19	500
1	531	540	910
2	27*	0	0

7,3,L

0	513	527	500
1	34*	32	823
2	284	281	5
3	0*	0	0

7,4,L

0	16*	1	0
1	289	286	792
2	53	55	131
3	59	59	912
4	0*	0	0

7,5,L

0	103*	112	500
1	45*	53	132
2	314	313	88
3	49*	51	796
4	200	201	137
5	23*	0	0

7,6,L

0	21*	18	500
1	202	200	968
2	43*	45	220
3	230	231	26
4	21*	8	160
5	262	263	2
6	9*	0	0

7,7,L

0	234	239	0
1	25*	0	0
2	304	304	925
3	0*	0	0
4	312	308	913
5	16*	0	0
6	244	249	970
7	0*	0	0

8,0,L

0	537	550	0

8,1,L

0	48	47	0
1	374	386	77

8,2,L

0	541	552	0
1	21*	26	174
2	252	258	937

8,3,L

0	33*	27	500
1	139	139	894
2	66*	67	100
3	371	374	36

8,4,L

0	791	800	0
1	33*	27	112
2	233	230	110
3	32*	24	789
4	534	534	947

8,5,L

0	23*	20	0
1	121	122	982
2	24*	19	74
3	49*	41	807
4	0*	15	844
5	228	233	986

8,6,L

0	36*	18	0
1	5*	17	987
2	49*	44	973
3	19*	24	91
4	357	353	971
5	39*	38	836
6	273	271	50

8,7,L

0	8*	4	0
1	207	206	77
2	16*	15	90
3	65	66	21
4	0*	20	184
5	86	86	874
6	70	70	953
7	97	98	92

8,8,L

0	519	521	0
1	30*	0	0
2	182	184	21
3	29*	0	0
4	527	519	25
5	13*	0	0
6	164	155	28
7	9*	0	0

9,0,L

0	64	0	0

9,1,L

0	91	94	500
1	22*	0	0

9,2,L

0	49	47	500
1	310	313	78
2	0*	0	0

9,3,L

0	18*	10	500
1	50*	48	55
2	224	225	948
3	18*	0	0

9,4,L

0	38*	41	500
1	177	178	4
2	14*	14	416
3	122	116	427
4	13*	0	0

9,5,L

0	226	231	500
1	21*	14	831
2	381	385	890
3	26*	32	41
4	43*	45	948
5	13*	0	0

9,6,L

0	0*	0	0
1	265	262	61
2	13*	7	961
3	255	247	47
4	30*	33	871
5	104	102	5
6	24*	0	0

9,7,L

0	59	54	500
1	53	49	45
2	172	165	25
3	22*	29	789
4	140	139	56
5	41*	35	930
6	209	203	38
7	0*	0	0

9,8,L

0	63	64	0
1	31*	24	205
2	27*	25	59
3	215	214	37
4	40	39	924
5	99	99	186

9,9,L

0	42*	42	500
1	0*	0	0
2	165	154	73
3	0*	0	0
4	85	88	845

10,0,L

0	27*	30	500

10,1,L

0	32*	47	0
1	335	344	31

10,2,L

0	147	158	500
1	31*	38	183
2	392	394	968

10,3,L

0	0*	13	0
1	220	226	937
2	36*	30	807
3	115	115	948

10,4,L

0	359	367	0
1	0*	24	248
2	71	71	130
3	0*	19	980
4	178	181	83

10,5,L

0	0*	6	0
1	197	194	970
2	14*	20	1
3	199	195	45
4	46*	54	800
5	207	197	33

10,6,L

0	112	112	500
1	25*	22	989
2	412	412	967
3	0*	13	886
4	131	130	125
5	34*	31	870
6	252	249	30

10,7,L

0	14*	21	0
1	184	178	77
2	0*	31	201
3	315	314	988
4	35*	29	986
5	149	147	960

10,8,L

0	144	140	0
1	42*	37	16
2	105	99	940
3	24*	26	100
4	112	111	999

10,9,L

0	34*	11	0

11,0,L

0	0*	0	0

11,1,L

0	28*	23	0
1	11*	0	0

11,2,L

0	7*	2	0
1	137	141	107
2	36*	0	0

11,3,L

0	147	147	500
1	38*	28	855
2	323	322	30
3	32*	0	0

11,4,L

0	0*	5	0
1	204	208	84
2	28*	37	887
3	64	67	125
4	8*	0	0

11,5,L

0	21*	14	500
1	19*	32	199
2	141	142	972
3	53*	47	239
4	98	95	864
5	19*	0	0

11,6,L

0	54	56	500
1	292	290	961
2	47	47	219
3	66*	66	829
4	26*	13	140

11,7,L

0	150	153	500
1	21*	16	976
2	114	112	48
3	0*	11	905

12,0,L

0	490	493	0

12,1,L

0	51	49	500
1	100	96	145

12,2,L

0	123	128	0
1	19*	26	944
2	243	243	218

12,3,L

0	0*	20	0
1	124	123	925
2	19*	11	158
3	46*	45	842

12,4,L

0	391	394	0
1	27*	30	77
2	182	175	38
3	31*	28	187
4	368	362	994

12,5,L

0	0*	16	0
1	143	139	821
2	19*	18	691
3	109	114	17

12,6,L

0	196	193	0
1	31*	27	75

13,0,L

0	0*	0	0

13,1,L

0	120	118	500
1	26*	0	0

13,2,L

0	20*	1	500
1	196	192	994
2	11*	0	0

13,3,L

0	82	80	500
1	0*	28	52

HELVITE (M30349)

1,0,L

0	40*	0	0

1,1,L

0	0*	29	500
1	0*	0	0

2,0,L

0	326	309	500

2,1,L

0	325	339	0
1	1320	1270	818

2,2,L

0	364	368	0
1	38*	0	0
2	794	702	950

3,0,L

0	0*	0	0

3,1,L

0	609	620	500
1	19*	0	0

3,2,L

0	273	285	500
1	642	626	951
2	19*	0	0

3,3,L

0	1533	1535	0
1	0*	0	0
2	289	298	158
3	0*	0	0

4,0,L

0	625	598	500

4,1,L

0	20*	3	500
1	1200	1213	230

4,2,L

0	575	590	0
1	252	258	998
2	831	818	772

4,3,L

0	26*	0	0
1	147	155	169
2	237	242	999
3	574	557	959

4,4,L

0	1283	1314	0
1	0*	0	0
2	895	874	803
3	22*	0	0
4	861	808	193

5,0,L

0	0*	0	0

5,1,L

0	474	493	0
1	0*	0	0

5,2,L

0	223	237	500
1	506	489	218
2	2*	0	8

5,3,L

0	767	781	500
1	0*	2	43
2	703	702	5
3	0*	0	0

5,4,L

0	11*	3	500
1	796	795	194
2	216	208	3
3	325	313	957
4	0*	0	0

5,5,L

0	220	230	0
1	0*	0	0
2	165	172	881
3	0*	0	0
4	507	495	771
5	0*	0	0

6,0,L

0	1311	1325	0

6,1,L

0	288	220	0
1	279	297	14

6,2,L

0	453	460	500
1	0*	3	506
2	416	406	208

6,3,L

0	202	210	0
1	208	199	186
2	0*	3	762
3	946	945	24

6,4,L

0	57*	36	500
1	194	196	3
2	98	92	36
3	183	178	3
4	315	310	991

6,5,L

0	181	185	0
1	588	581	20
2	0*	1	215
3	301	304	500
4	157	155	996
5	440	437	938

6,6,L

0	546	543	0
1	0*	0	0
2	576	569	983
3	0*	0	0
4	201	180	914
5	0*	0	0
6	207	193	3

7,0,L

0	21*	0	0

7,1,L

0	177	181	0
1	33*	0	0

7,2,L

0	187	194	500
1	545	571	828
2	0*	0	0

7,3,L

0	554	569	500
1	12*	2	217
2	360	357	41
3	29*	0	0

7,4,L

0	0*	1	0
1	533	530	773
2	167	167	3
3	257	256	956
4	0*	0	0

7,5,L

0	174	169	0
1	37*	1	177
2	404	384	201
3	0*	3	182
4	416	399	203
5	0*	0	0

7,6,L

0	146	147	500
1	249	248	910
2	24*	5	201
3	58*	70	935
4	139	136	995
5	377	371	43
6	0*	0	0

7,7,L

0	374	375	0
1	0*	0	0
2	448	450	812
3	27*	0	0
4	497	502	836
5	0*	0	0
6	230	215	954
7	20*	0	0

8,0,L

0	145	156	0

8,1,L

0	31*	0	0
1	650	661	178

8,2,L

0	545	563	0
1	168	172	1
2	364	362	170

8,3,L

0	25*	4	500
1	339	335	945
2	164	158	3
3	514	514	35

8,4,L

0	565	577	0
1	0*	4	915
2	469	458	222
3	0*	2	172
4	569	576	861

8,5,L

0	0*	7	500
1	414	412	770
2	143	140	998
3	161	167	83
4	0*	3	886
5	320	326	148

8,6,L

0	251	255	500
1	136	132	998
2	224	231	981
3	136	129	996
4	410	404	991
5	119	117	3
6	394	396	26

8,7,L

0	0*	0	0
1	317	309	186
2	127	121	990
3	102	98	83
4	10*	3	73
5	226	218	767
6	101*	94	14

8,8,L

0	533	527	0
1	25*	0	0
2	300	304	792
3	35*	0	0
4	445	409	139
5	15*	0	0

9,0,L

0	0*	0	0

9,1,L

0	309	309	500
1	9*	0	0

9,2,L

0	149	150	500
1	420	434	91
2	0*	0	0

9,3,L

0	547	589	0
1	0*	3	928
2	103	108	31
3	20*	0	0

9,4,L

0	0*	4	0
1	96*	103	921
2	140	131	999
3	251	247	949
4	37*	0	0

9,5,L

0	345	354	500
1	0*	1	53
2	490	484	882
3	0*	3	885
4	137	135	76
5	0*	0	0

9,6,L

0	116	113	500
1	36*	46	25
2	0*	1	982
3	621	619	9
4	114	112	3
5	160	156	896
6	18*	0	0

9,7,L

0	194	183	500
1	0*	1	832
2	264	262	74
3	0*	2	0
4	135	131	826
5	20*	4	809

9,8,L

0	22*	6	500
1	138	131	84
2	99	97	2
3	295	298	38

10,0,L

0	85	85	980

10,1,L

0	133	135	0
1	429	423	132

10,2,L

0	26*	20	0
1	0*	3	213
2	422	432	839

10,3,L

0	125	127	0
1	195	199	886
2	3*	5	100
3	104*	117	890
4	302	295	0
1	121	119	998
2	301	306	247
3	120*	114	998
4	368	354	209

10,5,L

0	109	107	0
1	258	266	787
2	0*	5	877
3	324	313	51
4	109	108	4
5	284	270	167

10,6,L

0	84	70	500
1	0*	4	890
2	175	180	913
3	0*	2	172
4	121	129	207

10,7,L

0	92*	97	0
1	420	409	182
2	26*	0	247

11,0,L

0	0*	0	0

11,1,L

0	122	124	0
1	0*	0	0

11,2,L

0	115	112	500
1	283	283	229
2	0*	0	0

11,3,L

0	195	195	500
1	0*	2	145
2	361	360	10
3	0*	0	0

11,4,L

0	32*	1	0
1	307	298	215
2	97	100	997
3	40*	19	922
4	0*	0	0

11,5,L

0	157	164	0
1	12*	3	910
2	202	214	790
3	58*	5	86

11,6,L

0	97*	69	500

12,0,L

0	764	757	0

12,1,L

0	0*	4	500
1	169	161	954

12,2,L

0	107	112	500
1	94	96	1
2	254	254	831

12,3,L

0	0*	1	0
1	287	288	953
2	95	93	996

HELVITE (M36390)

1,0,L

8	18°	0	0

1,1,L

0	53°	24	0
1	9°	0	0

2,0,L

8	344	326	500

2,1,L

0	343	342	0
1	1250	1324	811

2,2,L

8	354	365	0
1	11°	0	0
2	787	685	963

3,0,L

8	22°	0	0

3,1,L

0	710	671	500
1	0°	0	0

3,2,L

8	289	289	500
1	645	659	943
2	18°	0	0

3,3,L

8	1504	1563	0
1	0°	0	0
2	349	387	153
3	0°	0	0

4,0,L

0	813	734	500

4,1,L

0	16°	2	500
1	1225	1203	236

4,2,L

0	624	622	0
1	262	261	998
2	889	861	775

4,3,L

0	16°	2	0
1	232	194	147
2	241	245	997
3	666	622	963

4,4,L

0	1485	1439	0
1	14°	0	0
2	982	861	798
3	8°	0	0
4	756	762	209

5,0,L

0	0°	0	0

5,1,L

0	472	485	0
1	0°	0	0

5,2,L

0	239	241	500
1	579	583	221
2	0°	0	0

5,3,L

0	762	772	500

1	21°	1	169
2	701	682	14
3	11°	0	0

5,4,L

0	15°	1	500
1	829	832	192
2	221	216	1
3	316	320	946
4	0°	0	0

5,5,L

0	187	172	0
1	0°	0	0
2	302	267	840
3	19°	0	0
4	572	547	765
5	0°	0	0

6,0,L

0	1381	1379	0

6,1,L

0	223	224	0
1	340	333	37

6,2,L

0	498	480	500
1	22°	3	234
2	391	411	200

6,3,L

0	216	216	0
1	163	193	221
2	18°	2	208
3	1005	989	24

6,4,L

0	108	93	500
1	204	204	1
2	104	106	971
3	194	192	1
4	372	356	5

6,5,L

0	192	195	0
1	578	571	7
2	4°	1	796
3	312	297	55
4	170	165	0
5	409	393	951

6,6,L

0	585	586	0
1	0°	0	0
2	689	688	972
3	17°	0	0
4	235	239	933
5	6°	0	0
6	194	211	969

7,0,L

0	0°	0	0

7,1,L

0	227	213	0
1	21°	0	0

7,2,L

0	202	203	500
1	589	555	824
2	13°	0	0

7,3,L

0	654	646	500
1	14°	1	969
2	390	384	37
3	0°	0	0

7,4,L

0	11°	0	0
1	538	523	787
2	178	179	3
3	295	290	967
4	0°	0	0

7,5,L

0	170	170	0
1	0°	2	106
2	387	397	304
3	17°	2	932
4	410	411	191
5	0°	0	0

7,6,L

0	157	159	500
1	264	266	928
2	21°	1	750
3	63	41	776
4	144	145	997
5	394	382	34
6	0°	0	0

7,7,L

0	412	416	0
1	0°	0	0
2	461	451	884
3	0°	0	0
4	553	524	853
5	6°	0	0
6	255	246	983
7	13°	0	0

8,0,L

0	259	259	0

8,1,L

0	19°	4	0
1	708	711	183

8,2,L

0	537	530	0
1	181	180	1
2	432	436	183

8,3,L

0	23°	2	500
1	314	322	927
2	170	170	3
3	498	490	40

8,4,L

0	534	526	0
1	0°	2	965
2	492	498	222
3	9°	2	500
4	665	627	869

8,5,L

0	0°	2	500
1	475	483	762
2	151	151	999
3	175	151	136
4	3°	2	968
5	394	407	164

8,6,L

0	226	225	500
1	141	143	999
2	138	191	12
3	137	137	997
4	395	382	977
5	128	127	1000
6	399	390	29

8,7,L

0	15°	1	0
1	310	322	182
2	128	130	994
3	92	79	94
4	6°	0	914

5	233	238	766
6	113	110	6

8,8,L

0	556	550	0
1	0°	0	0
2	373	373	786
3	0°	0	0
4	418	441	153
5	0°	0	0

9,0,L

0	21°	0	0

9,1,L

0	361	371	500
1	4°	0	0

9,2,L

0	163	163	500
1	420	414	71
2	0°	0	0

9,3,L

0	623	629	0
1	18°	2	208
2	123	110	35
3	0°	0	0

9,4,L

0	8°	0	0
1	115	119	0
2	146	143	999
3	304	328	956
4	10°	8	0

9,5,L

0	351	342	500
1	7°	1	775
2	437	448	891
3	14°	2	213
4	107	93	19
5	26°	0	0

9,6,L

0	128	127	500
1	73	88	4
2	20°	0	847
3	655	662	8
4	125	123	1000
5	132	146	883
6	15°	0	0

9,7,L

0	251	265	500
1	19°	3	162
2	274	271	51
3	0°	2	870
4	124	130	876
5	15°	2	17?

9,8,L

0	12°	1	500
1	99	94	949
2	106	110	2
3	289	282	49

10,0,L

0	151	143	500

10,1,L

0	147	146	0
1	389	403	134

10,2,L

0	57°	41	0
1	14°	4	791
2	493	492	641

10,3,L

0	136	137	0
1	203	213	898
2	4°	3	758
3	107	92	802

10,4,L

0	340	345	0
1	123	129	0
2	302	303	229
3	126	124	999
4	330	336	212

10,5,L

0	119	121	0
1	268	266	771
2	0°	2	196
3	336	334	44
4	116	117	998
5	263	294	168

10,6,L

0	130	144	500
1	17°	2	238
2	174	161	962
3	19°	2	154
4	94	102	245

10,7,L

0	187	189	0
1	387	404	188
2	0°	2	141

11,0,L

0	0°	0	0

11,1,L

0	87	81	0
1	23°	0	0

11,2,L

0	126	124	500
1	305	317	226
2	8°	0	0

11,3,L

0	162	166	500
1	0°	2	977
2	346	342	12
3	34°	0	0

11,4,L

0	0°	0	0
1	318	323	216
2	115	114	997
3	40°	32	99
4	0°	0	0

11,5,L

0	132	124	0
1	0°	2	50
2	266	264	792
3	10°	3	956

12,0,L

0	768	771	0

12,1,L

0	18°	3	500
1	167	171	20

12,2,L

0	119	124	500
1	104	108	0
2	186	188	837

12,3,L

0	4°	4	0
1	315	333	947

DANALITE (M37261)

1,0,L

0	28	0	0

1,1,L

0	44	54	0
1	22*	0	0

2,0,L

0	406	415	500

2,1,L

0	359	343	0
1	1371	1404	886

2,2,L

0	411	409	0
1	16*	0	0
2	689	694	977

3,0,L

0	0*	0	0

3,1,L

0	733	726	500
1	8*	0	0

3,2,L

0	304	292	500
1	685	693	950
2	22*	0	0

3,3,L

0	1634	1684	0
1	25*	0	0
2	374	344	126
3	0*	0	0

4,0,L

0	830	779	500

4,1,L

0	0*	1	500
1	1275	1298	237

4,2,L

0	679	663	0
1	276	264	999
2	969	938	776

4,3,L

0	13*	1	0
1	223	201	134
2	255	247	997
3	650	693	966

4,4,L

0	1439	1464	0
1	0*	0	0
2	963	943	793
3	16*	0	0
4	814	842	211

5,0,L

0	15*	0	0

5,1,L

0	557	535	0
1	0*	0	0

5,2,L

0	255	244	500
1	623	644	227
2	13*	0	0

5,3,L

0	862	855	500

1	0*	1	114
2	744	727	10
3	22*	0	0

5,4,L

0	0*	0	500
1	898	906	194
2	228	220	1000
3	355	359	957
4	0*	0	0

5,5,L

0	215	203	0
1	0*	0	0
2	317	298	829
3	0*	0	0
4	588	599	768
5	0*	0	0

6,0,L

0	1524	1500	0

6,1,L

0	237	227	0
1	372	354	26

6,2,L

0	548	537	500
1	0*	2	181
2	424	442	219

6,3,L

0	227	219	0
1	159	178	249
2	17*	1	175
3	1090	1089	22

6,4,L

0	125	117	500
1	214	208	0
2	126	120	1
3	195	194	2
4	383	371	3

6,5,L

0	202	208	0
1	620	619	13
2	0*	1	805
3	349	346	45
4	168	172	1
5	440	437	945

6,6,L

0	654	669	0
1	20*	0	0
2	656	664	968
3	6*	0	0
4	241	245	947
5	0*	0	0
6	252	272	971

7,0,L

0	0*	0	0

7,1,L

0	232	221	0
1	0*	0	0

7,2,L

0	213	206	500
1	692	617	817
2	30*	0	0

7,3,L

0	672	665	500
1	0*	1	851
2	423	417	38
3	0*	0	0

7,4,L

0	23*	0	0
1	599	588	740
2	187	186	3
3	293	289	966
4	21*	0	0

7,5,L

0	216	212	0
1	14*	2	127
2	434	442	211
3	13*	2	850
4	456	466	196
5	8*	0	0

7,6,L

0	168	167	500
1	284	283	927
2	19*	1	148
3	68	49	772
4	146	150	998
5	420	426	37
6	10*	0	0

7,7,L

0	415	409	0
1	0*	0	0
2	525	517	882
3	0*	0	0
4	583	561	848
5	16*	0	0
6	247	246	984
7	33*	0	0

8,0,L

0	289	213	0

8,1,L

0	10*	3	0
1	764	769	186

8,2,L

0	587	571	0
1	187	185	2
2	466	472	184

8,3,L

0	28*	1	500
1	351	356	938
2	179	176	4
3	563	550	36

8,4,L

0	596	576	0
1	0*	1	75
2	536	547	227
3	0*	2	960
4	700	678	863

8,5,L

0	17*	1	0
1	517	521	764
2	159	158	500
3	184	163	111
4	15*	1	44
5	410	422	168

8,6,L

0	272	269	500
1	152	150	999
2	233	224	993
3	142	142	997
4	418	424	985
5	128	133	998
6	437	439	24

8,7,L

0	0*	1	0
1	359	366	185
2	130	136	996
3	121	117	79
4	0*	0	205

5	265	269	770
6	111	116	3

8,8,L

0	588	599	0
1	0*	0	0
2	404	395	787
3	17*	0	0
4	448	464	158
5	39*	0	0

9,0,L

0	0*	0	0

9,1,L

0	408	408	500
1	0*	0	0

9,2,L

0	170	169	500
1	464	459	75
2	20*	0	0

9,3,L

0	716	716	0
1	22*	2	99
2	147	145	18
3	0*	0	0

9,4,L

0	0*	1	500
1	139	136	986
2	150	150	0
3	337	341	963
4	0*	0	0

9,5,L

0	391	381	500
1	11*	1	886
2	495	495	890
3	7*	2	90
4	123	120	44
5	19*	0	0

9,6,L

0	132	134	500
1	104	99	40
2	13*	0	0
3	725	739	8
4	126	129	998
5	166	178	885
6	9*	0	0

9,7,L

0	294	282	500
1	7*	3	106
2	299	303	56
3	3*	2	858
4	140	138	878
5	0*	2	74

9,8,L

0	0*	1	0
1	115	114	992
2	121	116	1000
3	323	317	43

10,0,L

0	145	135	500

10,1,L

0	150	153	0
1	445	460	141

10,2,L

0	64	54	0
1	3*	2	797
2	554	547	836

10,3,L

0	141	143	0
1	217	219	899
2	14*	2	860
3	117	98	822

10,4,L

0	349	347	0
1	134	135	1
2	361	355	237
3	130	131	1000
4	382	389	204

10,5,L

0	126	128	0
1	319	310	766
2	0*	2	119
3	376	379	43
4	123	123	997
5	303	325	176

10,6,L

0	136	137	500
1	26*	2	114
2	174	158	989
3	22*	1	208
4	93	104	225

10,7,L

0	113	115	0
1	443	462	184
2	0*	1	870

11,0,L

0	14*	0	0

11,1,L

0	121	111	0
1	31*	0	0

11,2,L

0	132	132	500
1	329	342	228
2	15*	0	0

11,3,L

0	212	208	500
1	0*	1	850
2	380	380	5
3	5*	0	0

11,4,L

0	0*	0	0
1	360	362	217
2	116	121	997
3	35*	10	760
4	0*	0	0

11,5,L

0	150	144	0
1	13*	2	146
2	286	274	996
3	0*	3	832

12,0,L

0	855	858	0

12,1,L

0	0*	1	500
1	193	190	10

12,2,L

0	146	144	500
1	109	115	998
2	225	224	840

12,3,L

0	0*	3	0
1	349	356	952

DANALITE (M34769)

1,0,L

0	19*	0	0

1,1,L

0	38*	61	0
1	14*	0	0

2,0,L

0	397	406	500

2,1,L

0	357	343	0
1	1351	1403	805

2,2,L

0	404	402	0
1	28*	0	0
2	691	687	977

3,0,L

0	0*	0	0

3,1,L

0	729	724	500
1	0*	0	0

3,2,L

0	303	292	500
1	697	697	947
2	0*	0	0

3,3,L

0	1582	1665	0
1	5*	0	0
2	369	338	130
3	0*	0	0

4,0,L

0	848	805	500

4,1,L

0	1*	2	500
1	1293	1280	238

4,2,L

0	688	672	0
1	273	264	999
2	988	932	776

4,3,L

0	0*	1	0
1	239	219	131
2	299	247	997
3	685	660	967

4,4,L

0	1457	1401	0
1	0*	0	0
2	971	926	792
3	27*	0	0
4	797	817	214

5,0,L

1	0*	0	0

5,1,L

0	546	531	0
1	27*	0	0

5,2,L

0	254	243	500
1	640	661	226
2	0*	0	0

5,3,L

0	842	840	500
1	12*	2	116
2	736	717	13
3	19*	0	0

5,4,L

0	17*	0	0
1	905	905	193
2	230	220	1000
3	366	363	954
4	0*	0	0

5,5,L

0	190	187	0
1	0*	0	0
2	352	325	828
3	0*	0	0
4	620	607	766
5	28*	0	0

6,0,L

0	1484	1495	0

6,1,L

0	215	227	0
1	376	362	31

6,2,L

0	543	531	500
1	0*	2	778
2	418	439	213

6,3,L

0	227	219	0
1	154	175	249
2	0*	1	847
3	1086	1084	22

6,4,L

0	134	128	500
1	211	209	0
2	134	137	990
3	199	195	2
4	410	386	7

6,5,L

0	205	200	0
1	629	615	10
2	25*	1	148
3	346	334	45
4	177	172	1
5	431	423	948

6,6,L

0	678	672	0
1	0*	0	0
2	652	660	965
3	0*	0	0
4	256	253	952
5	0*	0	0
6	257	278	966

7,0,L

0	13*	0	0

7,1,L

0	241	232	0
1	12*	0	0

7,2,L

0	209	206	500
1	639	601	817
2	0*	0	0

7,3,L

0	681	677	500
1	0*	1	854
2	433	424	36
3	13*	0	0

7,4,L

0	0*	0	0
1	576	573	783
2	190	185	3
3	305	299	969
4	0*	0	0

7,5,L

0	233	218	0
1	0*	2	127
2	423	437	210
3	7*	2	851
4	457	461	194
5	23*	0	0

7,6,L

0	167	167	500
1	293	289	933
2	0*	1	814
3	78	52	244
4	148	150	948
5	433	430	35
6	0*	0	0

7,7,L

0	419	417	0
1	23*	0	0
2	517	506	802
3	27*	0	0
4	575	551	843
5	0*	0	0
6	264	253	990
7	30*	0	0

8,0,L

0	255	244	0

8,1,L

0	15*	1	0
1	777	775	188

8,2,L

0	567	557	0
1	187	185	2
2	479	485	190

8,3,L

0	5*	3	500
1	345	350	933
2	174	177	4
3	538	528	38

8,4,L

0	581	563	0
1	0*	2	28
2	539	552	225
3	0*	1	897
4	722	684	865

8,5,L

0	0*	1	500
1	531	538	781
2	161	158	500
3	183	160	124
4	0*	0	915
5	436	440	175

8,6,L

0	250	248	500
1	151	151	999
2	220	214	1000
3	143	143	997
4	418	419	982
5	132	133	998
6	423	421	24

8,7,L

0	32*	0	0
1	357	361	187
2	133	136	996
3	121	115	77
4	0*	1	913
5	265	270	766
6	115	119	3

8,8,L

0	581	594	0
1	0*	0	0
2	422	414	789
3	17*	0	0
4	456	472	160
5	38*	0	0

9,0,L

0	39*	0	0

9,1,L

0	407	416	500
1	0*	0	0

9,2,L

0	173	168	500
1	457	454	69
2	0*	0	0

9,3,L

0	722	726	0
1	0*	2	102
2	141	142	16
3	3*	0	0

9,4,L

0	19*	1	500
1	151	149	2
2	144	149	0
3	346	353	965
4	0*	0	0

9,5,L

0	374	369	580
1	0*	1	881
2	473	480	893
3	19*	2	93
4	118	117	26
5	14*	0	0

9,6,L

0	133	134	500
1	109	104	45
2	0*	0	500
3	737	747	7
4	129	128	998
5	155	173	878
6	0*	0	0

9,7,L

0	294	297	500
1	0*	3	107
2	305	308	50
3	3*	2	856
4	152	144	898
5	0*	2	73

9,8,L

0	33*	3	0
1	109	112	971
2	114	116	1000
3	307	300	46

10,0,L

0	144	141	500

10,1,L

0	155	154	0
1	417	452	140

10,2,L

0	75*	68	0
1	12*	3	167
2	549	549	836

10,3,L

0	143	144	0
1	216	222	904
2	5*	2	186
3	111	97	814

10,4,L

0	356	354	0
1	135	136	1
2	343	349	235
3	131	132	1000
4	366	379	204

10,5,L

0	128	128	0
1	310	309	765
2	0*	1	789
3	382	386	40
4	120	124	997
5	306	328	176

10,6,L

0	150	147	500
1	0*	1	229
2	150	148	970
3	0*	1	877
4	90*	93	242

10,7,L

0	122	116	0
1	427	455	183
2	12*	1	117

11,0,L

0	0*	0	0

11,1,L

0	108	100	0
1	0*	0	0

11,2,L

0	124	131	500
1	332	346	224
2	0*	0	0

11,3,L

0	185	186	500
1	0*	2	854
2	366	370	5
3	0*	0	0

11,4,L

0	0*	0	0
1	359	361	221
2	116	120	997
3	0*	13	168
4	15*	0	0

11,5,L

0	136	135	0
1	18*	2	143
2	297	283	799
3	0*	3	833

12,0,L

0	846	861	0

12,1,L

0	0*	4	500
1	199	198	28

12,2,L

0	137	140	500
1	110	117	998
2	205	202	850

12,3,L

0	21*	1	0
1	339	358	951

GENTHELVITE (M37267)

1,0,L

8	32	0	0

1,1,L

0	129	141	0
1	0*	0	0

2,0,L

8	499	503	500

2,1,L

0	355	340	0
1	1440	1549	795

2,2,L

0	458	448	0
1	20*	0	0
2	672	698	13

3,0,L

8	29*	0	0

3,1,L

0	841	845	500
1	22*	0	0

3,2,L

0	380	291	500
1	779	772	967
2	0*	0	0

3,3,L

0	1847	1863	0
1	17*	0	0
2	461	421	101
3	27*	0	0

4,0,L

0	1042	1081	500

4,1,L

8	25*	1	500
1	1442	1387	245

4,2,L

0	763	751	0
1	271	264	999
2	1078	1087	777

4,3,L

8	0*	1	0
1	302	284	101
2	259	248	999
3	798	779	973

4,4,L

0	1652	1631	0
1	12*	0	0
2	1056	1026	781
3	23*	0	0
4	878	888	233

5,0,L

8	29*	0	0

5,1,L

0	603	583	0
1	0*	0	0

5,2,L

0	257	246	500
1	810	855	234
2	8*	0	0

5,3,L

0	912	916	500
1	11*	0	883
2	768	749	17
3	21*	0	0

5,4,L

0	0*	2	500
1	1027	1040	196
2	229	210	1
3	421	420	957
4	26*	8	0

5,5,L

0	198	192	0
1	17*	0	0
2	540	588	799
3	13*	0	0
4	751	741	762
5	0*	0	0

6,0,L

0	1711	1711	0

6,1,L

0	235	230	0
1	461	447	37

6,2,L

0	636	630	500
1	16*	2	219
2	417	446	231

6,3,L

0	227	220	0
1	167	207	844
2	11*	2	188
3	1297	1290	19

6,4,L

0	243	247	500
1	213	207	1
2	203	205	975
3	201	194	1
4	479	463	13

6,5,L

0	201	197	0
1	663	659	2
2	12*	1	860
3	404	387	39
4	175	174	999
5	439	430	961

6,6,L

0	855	858	0
1	17*	0	0
2	748	750	958
3	38*	0	0
4	347	344	969
5	30*	0	0
6	414	434	960

7,0,L

0	0*	0	0

7,1,L

0	308	302	0
1	18*	0	0

7,2,L

0	211	208	500
1	713	682	801
2	0*	0	0

7,3,L

0	767	775	500
1	11*	1	118
2	495	492	32
3	0*	0	0

7,4,L

0	18*	0	0
1	654	661	786
2	185	185	1
3	355	358	978
4	21*	0	0

7,5,L

0	276	277	0
1	0*	0	500
2	510	531	221
3	0*	1	88
4	540	546	196
5	19*	0	0

7,6,L

0	166	165	500
1	337	345	951
2	11*	2	760
3	136	112	99
4	160	154	998
5	483	475	28
6	13*	0	0

7,7,L

0	460	464	0
1	20*	0	0
2	608	582	790
3	0*	0	0
4	634	605	838
5	0*	0	0
6	296	307	9
7	24*	0	0

8,0,L

0	261	257	0

8,1,L

0	0*	3	0
1	895	900	196

8,2,L

0	581	575	0
1	188	186	0
2	809	630	205

8,3,L

0	0*	1	500
1	369	379	933
2	177	175	1
3	560	562	37

8,4,L

0	573	553	0
1	31*	1	912
2	630	661	229
3	28*	2	36
4	807	775	860

8,5,L

0	23*	2	500
1	644	667	757
2	159	158	999
3	199	174	130
4	24*	2	952
5	553	556	192

8,6,L

0	259	270	500
1	148	150	999
2	237	231	16
3	148	146	998
4	443	447	978
5	126	134	1
6	433	435	22

8,7,L

0	12*	1	0
1	424	429	194
2	141	139	997
3	156	144	63
4	25*	0	750
5	337	335	763
6	115	116	4

8,8,L

0	648	645	0
1	29*	0	0
2	524	513	784
3	0*	0	0
4	501	519	180

9,0,L

0	22*	0	0

9,1,L

0	512	516	500
1	9*	0	0

9,2,L

0	164	169	500
1	497	484	49
2	0*	0	0

9,3,L

0	894	898	0
1	0*	1	851
2	212	204	11
3	8*	0	0

9,4,L

0	19*	1	0
1	226	223	27
2	144	151	998
3	433	443	973
4	11*	0	0

9,5,L

0	399	388	500
1	6*	0	148
2	457	473	989
3	0*	1	839
4	144	133	983
5	0*	0	0

9,6,L

0	134	136	500
1	180	172	31
2	15*	0	923
3	881	880	6
4	127	130	2
5	180	186	885

9,7,L

0	374	381	500
1	12*	1	784
2	350	348	34
3	15*	1	916
4	185	186	946

9,8,L

0	0*	3	500
1	121	127	927
2	115	118	3

10,0,L

0	224	222	500

10,1,L

0	153	151	0
1	463	498	158

10,2,L

0	127	126	0
1	0*	3	846
2	672	664	826

10,3,L

0	141	144	0
1	254	265	926
2	30*	3	769
3	134	102	195

10,4,L

0	396	403	0
1	139	138	999
2	416	414	269
3	127	132	999
4	483	418	213

10,5,L

0	130	130	0
1	389	373	753
2	35*	2	189
3	432	440	33
4	116	123	1
5	372	390	185

10,6,L

0	225	225	500
1	0*	2	771
2	96	100	51
3	0*	2	119
4	64	84	836

10,7,L

0	114	118	0
1	473	498	198

11,0,L

0	32*	0	0

11,1,L

0	115	114	0
1	0*	0	0

11,2,L

0	131	132	500
1	480	419	226
2	0*	0	0

11,3,L

0	204	194	500
1	0*	1	96
2	373	382	0
3	0*	0	0

11,4,L

0	0*	0	0
1	423	424	227
2	116	123	998
3	36*	13	855

11,5,L

0	142	138	0
1	0*	1	920
2	377	355	795

12,0,L

0	927	933	0

12,1,L

0	0*	1	500
1	256	251	56

12,2,L

0	169	169	500
1	106	116	1
2	181	180	897

GENTHELVITE (M32727)

1,0,L

0	36*	0	0

1,1,L

0	140	146	0
1	23*	0	0

2,0,L

0	497	492	500

2,1,L

0	344	340	0
1	1480	1548	794

2,2,L

0	456	452	0
1	42*	0	0
2	792	693	15

3,0,L

0	53*	0	0

3,1,L

0	872	847	500
1	30*	0	0

3,2,L

0	294	288	500
1	814	775	947
2	0*	0	0

3,3,L

0	1778	1838	0
1	5*	0	0
2	406	418	102
3	0*	0	0

4,0,L

0	1060	1019	500

4,1,L

0	0*	2	500
1	1398	1367	246

4,2,L

0	770	756	0
1	275	261	999
2	1117	1089	778

4,3,L

0	28*	2	0
1	294	297	98
2	255	244	999
3	822	783	974

4,4,L

0	1596	1633	0
1	25*	0	0
2	1003	996	781
3	56*	0	0
4	868	858	235

5,0,L

0	30*	0	0

5,1,L

0	586	583	0
1	43*	0	0

5,2,L

0	244	242	500
1	903	870	234
2	0*	0	0

5,3,L

0	896	889	500
1	42*	0	795
2	756	737	18
3	0*	0	0

5,4,L

0	30*	2	500
1	1045	1040	196
2	230	215	2
3	437	421	956
4	33*	0	0

5,5,L

0	182	184	0
1	0*	0	3
2	526	542	798
3	40*	0	0
4	762	752	760
5	0*	0	0

6,0,L

0	1646	1687	0

6,1,L

0	227	226	0
1	460	460	37

6,2,L

0	623	637	500
1	39*	2	212
2	457	435	234

6,3,L

0	214	215	3
1	252	208	853
2	0*	3	192
3	1282	1281	20

6,4,L

0	264	260	500
1	205	202	1
2	221	222	973
3	193	188	1
4	480	467	12

6,5,L

0	189	192	0
1	654	653	1
2	46*	1	850
3	383	377	35
4	159	167	999
5	426	415	961

6,6,L

0	454	871	0
1	43*	0	0
2	765	743	958
3	0*	0	0
4	367	364	976
5	35*	0	0
6	482	458	967

7,0,L

0	39*	0	0

7,1,L

0	319	315	0
1	0*	0	3

7,2,L

0	203	203	500
1	641	669	799
2	35*	0	0

7,3,L

0	763	761	500

1	46*	1	43
2	499	490	31
3	54*	0	0

7,4,L

0	29*	0	0
1	648	640	788
2	191	179	2
3	372	362	978
4	0*	0	0

7,5,L

0	290	274	0
1	27*	0	58
2	559	537	224
3	56*	1	48
4	558	530	198
5	0*	0	0

7,6,L

0	160	158	500
1	359	348	953
2	34*	2	770
3	115	120	106
4	154	147	998
5	468	472	25
6	18*	0	0

7,7,L

0	454	450	0
1	0*	0	0
2	536	560	790
3	24*	0	0
4	562	584	836
5	0*	0	0
6	304	287	11
7	0*	0	0

8,0,L

0	275	270	0

8,1,L

0	47*	5	0
1	882	899	196

8,2,L

0	552	559	0
1	176	180	1
2	641	641	211

8,3,L

0	0*	1	500
1	380	362	932
2	164	169	1
3	521	529	37

8,4,L

0	541	542	0
1	34*	1	929
2	674	658	257
3	0*	2	26
4	722	752	859

8,5,L

0	0*	2	500
1	675	679	753
2	155	151	998
3	161	165	136
4	0*	3	361
5	577	580	196

8,6,L

0	244	250	500
1	129	143	999
2	229	222	16
3	132	138	998
4	442	430	480
5	124	127	1
6	396	394	19

9,7,L

0	0*	2	0
1	425	420	198
2	137	132	996
3	136	137	65
4	0*	0	750
5	145	135	763
6	109*	108	5

9,8,L

0	616	607	0
1	47*	0	0
2	499	516	786
3	0*	0	0
4	542	515	177

9,0,L

0	60*	0	0

9,1,L

0	509	515	500
1	71*	0	0

9,2,L

0	159	163	500
1	466	480	43
2	37*	0	0

9,3,L

0	895	901	0
1	0*	1	816
2	209	214	4
3	50*	0	0

9,4,L

0	0*	1	0
1	235	242	33
2	142	144	998
3	457	444	975
4	22*	0	0

9,5,L

0	373	381	500
1	42*	1	169
2	459	446	915
3	0*	1	620
4	159	146	967
5	0*	0	0

9,6,L

0	122	128	500
1	167	191	35
2	0*	0	0
3	871	889	5
4	113*	123	2
5	205	193	881

9,7,L

0	392	369	500
1	0*	1	750
2	347	347	24
3	27*	1	917
4	194	188	953

9,8,L

0	0*	4	500
1	156	124	909
2	109*	110	3

10,9,L

0	236	228	500

11,1,L

0	145	144	0
1	52?	491	161

10,2,L

0	149	136	0
1	9*	4	843
2	627	658	825

10,3,L

0	125*	137	0
1	279	272	931
2	0*	3	784
3	44*	109	201

10,4,L

0	401	388	0
1	132	130	999
2	410	414	226
3	136	124	999
4	439	413	218

10,5,L

0	109*	122	0
1	386	386	755
2	69*	2	174
3	435	435	29
4	104	116	1
5	421	408	191

10,6,L

0	241	239	500
1	0*	2	250
2	103	75	61
3	31*	3	125

10,7,L

0	103*	110	0
1	503	493	190

11,0,L

0	0*	0	0

11,1,L

0	104*	112	0
1	29*	0	0

11,2,L

0	122	125	500
1	428	419	226
2	0*	0	0

11,3,L

0	184	181	500
1	0*	1	76
2	366	365	0
3	75*	0	0

11,4,L

0	0*	0	0
1	404	406	231
2	113	116	994
3	31*	16	989

11,5,L

0	137	142	0
1	0*	1	966
2	333	367	794

12,0,L

0	499	514	0

12,1,L

0	0*	2	500
1	257	257	63

12,2,L

0	178	164	500
1	97*	106	2

HYDROXYSODALITE

1,0,L

0	48	0	0

1,1,L

0	527	557	500
1	244	0	0

2,0,L

0	298	275	0

2,1,L

0	101	103	0
1	844	861	907

2,2,L

0	249	257	500
1	0°	0	0
2	1325	1321	922

3,0,L

0	24°	0	0

3,1,L

0	658	648	500
1	0°	0	0

3,2,L

0	22°	17	500
1	298	383	933
2	7°	0	0

3,3,L

0	817	787	0
1	29°	0	0
2	201	195	895
3	0°	0	0

4,0,L

0	158	160	0

4,1,L

0	23°	44	500
1	884	786	757

4,2,L

0	229	236	0
1	26°	23	776
2	542	546	838

4,3,L

0	19°	12	0
1	491	471	931
2	75	79	207
3	687	618	949

4,4,L

0	1110	1109	0
1	0°	0	0
2	585	597	868
3	18°	0	0
4	860	885	84

5,0,L

0	14°	0	0

5,1,L

0	152	142	500
1	0°	0	0

5,2,L

0	46°	61	0
1	154	150	979
2	28°	0	0

5,3,L

0	688	683	500
1	56	54	988
2	474	472	18
3	0°	0	0

5,4,L

0	12°	51	0
1	484	489	118
2	42	40	929
3	172	182	83
4	0°	0	0

5,5,L

0	77°	78	500
1	30°	0	0
2	386	395	180
3	0°	0	0
4	261	276	937
5	23°	0	0

6,0,L

0	798	788	0

6,1,L

0	49°	40	500
1	164	145	165

6,2,L

0	377	383	500
1	36°	39	769
2	773	764	24

6,3,L

0	29°	31	0
1	359	358	99
2	31°	35	977
3	513	523	39

6,4,L

0	181	185	0
1	51°	58	914
2	293	304	44
3	44	52	40
4	154	151	56

6,5,L

0	67	68	0
1	369	366	998
2	0°	37	25
3	121	119	781
4	56°	62	239
5	281	283	929

6,6,L

0	79	62	500
1	27°	0	0
2	627	649	30
3	33°	0	0
4	195	203	678
5	0°	0	0
6	494	497	965

7,0,L

0	0°	0	0

7,1,L

0	211	204	500
1	0°	0	0

7,2,L

0	22°	2	500
1	432	429	891
2	18°	0	0

7,3,L

0	638	645	500
1	30°	38	863
2	200	197	990
3	11°	0	0

7,4,L

0	23°	16	0
1	296	295	840
2	58	48	166
3	51°	47	48
4	0°	0	0

7,5,L

0	179	174	500
1	55	47	136
2	234	231	113
3	50°	49	785
4	259	263	97
5	0°	0	0

7,6,L

0	32°	7	0
1	130	123	993
2	40°	55	761
3	135	126	35
4	0°	11	61
5	196	197	979
6	0°	0	0

7,7,L

0	147	149	0
1	0°	0	0
2	225	223	916
3	35°	0	0
4	323	339	940
5	14°	0	0
6	186	196	974
7	37°	0	0

8,0,L

0	473	473	0

8,1,L

0	47°	16	0
1	462	463	62

8,2,L

0	417	417	0
1	22°	32	104
2	319	318	951

8,3,L

0	24°	59	500
1	84	87	754
2	56°	73	62
3	419	409	31

8,4,L

0	729	716	0
1	13°	58	58
2	174	173	148
3	27°	41	136
4	462	464	937

8,5,L

0	28°	3	500
1	186	183	991
2	28°	16	999
3	119	122	947
4	18°	35	935
5	261	264	918

8,6,L

0	32°	17	500
1	28°	32	991
2	51°	51	994
3	23°	8	88
4	279	279	960
5	39°	34	852
6	292	290	47

8,7,L

0	0°	22	500
1	258	264	57
2	32°	22	28
3	125	120	18
4	0°	24	802
5	133	132	934
6	69	70	928
7	128	123	68

8,8,L

0	429	428	0
1	7°	0	0
2	142	140	43
3	0°	0	0
4	451	452	28
5	45°	0	0
6	96	99	34
7	19°	0	0

9,0,L

0	0°	0	0

9,1,L

0	179	180	500
1	19°	0	0

9,2,L

0	39°	16	500
1	213	212	83
2	31°	0	0

9,3,L

0	92	89	500
1	46	51	60
2	177	171	935
3	23°	0	0

9,4,L

0	39°	35	500
1	244	242	980
2	27°	26	139
3	154	154	897
4	16°	0	0

9,5,L

0	269	272	500
1	0°	23	245
2	301	302	878
3	38°	32	80
4	106	106	998
5	0°	0	0

9,6,L

0	0°	22	0
1	211	207	69
2	34°	4	908
3	182	179	71
4	26°	27	771
5	70°	67	8
6	25°	0	0

9,7,L

0	124	125	500
1	29°	38	4
2	106	107	12
3	0°	20	229
4	180	177	15
5	20°	36	880
6	149	153	38
7	0°	0	0

9,8,L

0	53°	92	0
1	55°	58	951
2	34°	20	132
3	240	239	30
4	36°	32	859
5	127	121	123
6	42°	31	89

9,9,L

0	76	96	500
1	0°	0	0
2	120	125	91
3	0°	0	0
4	92°	103	987

10,0,L

0	136	140	500

10,1,L

0	46°	50	0
1	264	258	31

10,2,L

0	213	203	500
1	41°	71	79
2	466	462	977

10,3,L

0	0°	27	0
1	166	169	934
2	47°	49	112
3	42°	42	845

10,4,L

0	303	303	0
1	0°	29	130
2	113	114	49
3	26°	35	971
4	114	109	96

10,5,L

0	25°	21	0
1	135	135	966
2	33°	19	88
3	155	156	48
4	55°	53	795
5	134	137	46

10,6,L

0	187	187	500
1	47°	4	841
2	454	444	976
3	22°	33	929
4	144	144	71
5	39°	55	896
6	292	294	23

10,7,L

0	16°	28	0
1	129	128	80
2	42°	57	111
3	261	261	996
4	35°	23	5
5	105	102	964

10,8,L

0	106	112	0
1	34°	56	25
2	141	147	992
3	0°	34	79
4	63°	68	0

10,9,L

0	0°	11	0

11,0,L

0	1°	0	0

11,1,L

0	62°	57	500
1	0°	0	0

11,2,L

0	0°	44	0
1	98	100	151
2	24°	0	0

11,3,L

0	185	178	500
1	19°	32	909
2	250	245	36
3	0°	0	0

11,4,L

0	0°	14	0
1	255	250	71
2	25°	20	766
3	101	108	73
4	21°	0	0

11,5,L

0	81°	86	500
1	19°	29	209
2	104	111	980
3	43°	45	225
4	127	127	900
5	38°	0	0

11,6,L

0	55°	35	500
1	239	233	956
2	44°	47	164
3	45°	50	796
4	8°	14	884

11,7,L

0	169	172	500
1	0°	27	36
2	60°	76	83
3	19°	21	864

12,0,L

0	431	424	0

12,1,L

0	35°	106	500
1	129	131	58

12,2,L

0	82	88	0
1	43°	39	994
2	244	232	178

12,3,L

0	0°	37	500
1	149	155	952
2	0°	8	983
3	94	86	937

12,4,L

0	360	353	0
1	20°	16	915
2	138	131	23
3	15°	32	848
4	315	318	8

12,5,L

0	19°	29	500
1	145	147	875
2	24°	28	999
3	137	139	13

12,6,L

0	146	148	0
1	28°	50	53

13,0,L

0	0°	0	0

13,1,L

0	146	144	500
1	22°	0	0

13,2,L

0	34°	28	0
1	152	143	1
2	16°	0	0

13,3,L

0	139	150	500
1	0°	25	79

TUGTUPITE

TUGTUPITE (continued)

8,8,L

6	196	198	100
8	402	398	11
10	176	167	927

8,1,L

1	229	236	998
3	412	421	910
5	115	114	53
7	147	149	167
9	112	100	957

8,-1,L

1	383	389	696
3	382	373	20
5	120	113	949
7	157	162	984
9	166	164	1

8,2,L

0	66	52	0
2	150	154	198
4	323	327	51
6	59	47	926
8	253	251	82
10	82	82	150

8,-2,L

0	661	654	0
2	231	231	152
4	60	57	14
6	164	160	19
8	150	145	967
10	105	107	645

8,3,L

1	74	65	66
3	390	401	440
5	220	223	889
7	252	255	56
9	268	254	1

8,-3,L

1	125	130	54
3	136	131	878
5	77	77	191
7	183	182	764
9	148	139	829

8,4,L

0	819	834	0
2	136	138	115
4	388	391	963
6	505	506	956
8	334	339	25

8,-4,L

0	447	437	0
2	367	369	934
4	510	510	47
6	230	233	992
8	483	468	982

8,5,L

1	108	104	918
3	109	113	102
5	202	198	247
7	119	124	863
9	81	81	766

8,-5,L

1	271	276	895
3	144	137	200
5	247	250	97
7	206	202	25
9	140	139	912

8,6,L

0	166	175	0
2	161	161	57
4	206	208	999
6	84	89	43
8	161	158	78

8,-6,L

0	22*	12	500
2	141	141	245
4	276	273	5
6	233	237	833
8	78	65	138

8,7,L

1	420	421	997
3	124	126	237
5	251	244	954
7	191	188	26

8,-7,L

1	113	111	212
3	143	144	190
5	56	56	864
7	45*	53	985

8,8,L

0	373	376	0
2	264	261	69
4	382	383	984
6	160	151	56

9,0,L

1	202	203	217
3	89	88	140
5	92	86	49
7	56*	53	101
9	38*	29	788

9,1,L

0	123	122	500
2	106	113	109
4	347	353	537
6	115	116	191
8	41*	38	72

9,-1,L

0	161	163	0
2	163	167	945
4	55	57	818
6	342	334	968
8	32*	28	39

9,2,L

1	196	197	46
3	281	284	983
5	287	286	834
7	180	175	35
9	184	172	947

9,-2,L

1	303	305	953
3	291	295	61
5	405	401	40
7	136	135	145
9	201	198	898

9,3,L

0	210	217	0
2	288	295	23
4	130	137	839
6	298	303	37
8	61	61	966

9,-3,L

0	243	235	500
2	70	68	771
4	213	213	140
6	106	98	212
8	258	252	965

9,4,L

1	116	122	10
3	171	175	777
5	0*	9	978
7	195	188	924

9,-4,L

1	151	155	170
3	115	117	40
5	110	114	884
7	103	100	160

9,5,L

0	201	208	500
2	226	225	801
4	54	55	847
6	66	68	800
8	128	130	23

9,-5,L

0	59	55	500
2	284	286	86
4	68	72	978
6	104	106	913
8	71	68	69

9,6,L

1	181	182	883
3	135	140	130
5	88	96	18
7	126	122	970

9,-6,L

1	392	398	949
3	218	225	960
5	234	229	952
7	276	270	999

9,7,L

0	161	157	0
2	324	321	19
4	131	134	15
6	223	229	27

9,-7,L

0	128	124	500
2	176	183	915
4	233	234	1
6	59	55	992

9,8,L

1	10*	33	821
3	247	247	35
5	194	195	148

9,-8,L

1	91	83	867
3	87	89	157
5	87	93	54

9,9,L

0	124	127	500
2	146	137	131

10,0,L

0	119	122	500
2	142	141	98
4	257	256	81
6	158	155	133
8	82	83	889

10,1,L

1	412	422	10
3	337	344	949
5	344	346	3
7	269	264	977

10,-1,L

1	314	316	1
3	36*	33	171
5	122	122	179
7	169	155	933

10,2,L

0	195	208	500
2	261	261	956
4	42*	45	833
6	365	364	958
8	226	221	13

10,-2,L

0	108	109	500
2	350	351	997
4	166	167	66
6	227	221	12
8	65	70	50

10,3,L

1	176	178	198
3	88	85	817
5	90	85	57
7	210	213	74

10,-3,L

1	405	404	85
3	213	208	958
5	288	286	10
7	374	365	23

10,4,L

0	97	104	0
2	104	106	234
4	52	52	913
6	114	119	54

10,-4,L

0	160	157	0
2	83	78	907
4	177	170	928
6	152	144	950

10,5,L

1	398	394	23
3	304	301	36
5	252	256	46
7	294	285	963

10,-5,L

1	71	70	942
3	203	202	992
5	99	97	697
7	58*	45	821

10,6,L

0	50*	59	500
2	344	344	40
4	153	146	974
6	161	144	52

10,-6,L

0	122	133	500
2	261	267	51
4	112	113	854
6	213	213	995

10,7,L

1	140	134	143
3	87	85	975

10,-7,L

1	288	290	30
3	246	238	988

10,8,L

0	62	60	0
2	59	67	946

10,-8,L

0	210	213	0
2	135	124	961

11,0,L

1	125	131	227
3	70	75	837
5	71	71	858
7	144	140	988

11,1,L

0	114	108	0
2	79	77	60
4	225	221	0
6	177	173	989

11,-1,L

0	45*	23	500
2	330	323	947
4	129	131	76
6	242	239	40

11,2,L

1	151	147	994
3	67	60	239
5	189	182	971
7	164	153	15

11,-2,L

1	34*	15	104
3	300	295	0
5	177	170	791
7	9*	42	862

11,3,L

0	164	159	0
2	365	371	61
4	102	103	899
6	172	167	998

11,-3,L

0	53	41	500
2	161	165	98
4	56	54	57
6	96	92	194

11,4,L

1	163	166	85
3	116	119	7
5	87	90	13

11,-4,L

1	166	166	932
3	252	240	949
5	157	150	200

11,5,L

0	302	295	500
2	94	95	241
4	101	98	67

11,-5,L

0	299	292	0
2	307	304	954
4	118	112	51

11,6,L

1	248	249	924
3	160	151	976

11,-6,L

1	157	157	874
3	93	90	817

11,7,L

0	91	93	0

11,-7,L

0	160	158	500

12,0,L

0	347	340	0
2	198	205	92
4	323	318	925

12,1,L

1	132	128	237
3	43*	44	85
5	54	64	65

12,-1,L

1	227	217	941
3	124	122	87
5	256	249	8

12,2,L

0	251	261	0
2	147	145	770
4	152	159	48

12,-2,L

0	137	132	0
2	110	110	186
4	164	156	102

12,3,L

1	260	265	41
3	187	178	30

12,-3,L

1	153	147	803
3	167	160	248

12,4,L

0	342	342	0
2	205	199	945

12,-4,L

0	382	374	0
2	106	103	27

12,5,L

1	126	126	199

12,-5,L

1	155	154	8

13,0,L

1	0*	22	0

13,1,L

0	259	258	500

1,0,L

0	27*	0	2

1,1,L

+ 0	278	458	1
1	0*	0	14

2,0,L

+ 0	310	279	2

2,1,L

0	93	85	1
1	942	939	14

2,2,L

0	141*	36	2
1	10*	0	8
2	1155	1197	4

3,0,L

0	0*	0	18

3,1,L

0	471	470	5
1	0*	0	19

3,2,L

0	26*	25	4
1	270	284	5
2	13*	0	5

3,3,L

0	302	886	3
1	11*	0	5
2	295	327	6
3	0*	0	16

4,0,L

0	798	812	10

4,1,L

0	38	33	3
1	182	186	7

4,2,L

0	122	74	2
1	0*	15	14
2	144	113	2

4,3,L

0	18*	0	7
1	411	404	7
2	24*	24	4
3	358	339	4

4,4,L

0	971	934	1
1	0*	0	14
2	321	343	1
3	0*	0	14
4	915	911	1

5,0,L

0	20*	0	6

5,1,L

0	255	246	1
1	9*	0	14

5,2,L

0	32*	29	6
1	248	250	6
2	12*	0	6

5,3,L

0	309	297	1
1	50	39	1
2	400	389	1
3	14*	0	10

5,4,L

0	47	47	2
1	154	140	2
2	11*	9*	2
3	267	267	2
4	12*	0	6

5,5,L

0	15*	3	7
1	0*	0	14
2	143	146	1
3	7*	0	5
4	123	118	2
5	24*	0	7

6,0,L

0	625	619	5

6,1,L

0	27*	12	5
1	131	123	2

6,2,L

0	90	103	2
1	20*	6	8
2	764	759	4

6,3,L

0	13*	19	11
1	254*	244	5
2	12*	27	5
3	487	492	7

6,4,L

0	59	66	6
1	0*	37	4
2	153	167	3
3	15*	36	6
4	84*	93	12

6,5,L

0	22*	21	10
1	196	198	2
2	11*	25	10
3	141	168	5
4	27*	29	5
5	145	145	6

6,6,L

0	94	100	3
1	49*	0	14
2	0*	496	8
3	0*	0	15
4	87	103	2
5	0*	0	15
6	266	266	3

7,0,L

0	1*	0	21

7,1,L

0	262	268	2
1	20*	0	9

7,2,L

0	26*	13	5
1	347	336	4
2	8*	0	8

7,3,L

0	298	307	5
1	13*	0	7
2	57	65	4
3	8*	0	13

7,4,L

0	0*	7	22
1	85	59	7
2	24*	11	3
3	107	122	3
4	0*	0	15

7,5,L

0	263	266	2
1	21*	24	4
2	17*	219	4
3	17*	14	8
4	136	123	4
5	0*	0	22

7,6,L

0	10*	2	13
1	86	120	3
2	14*	7	13
3	61*	75	5
4	11*	0	12
5	84*	83	5
6	0*	0	24

7,7,L

0	19*	12	7
1	0*	0	22
2	11*	120	5
3	11*	0	15
4	80	82	5
5	0*	0	22
6	65	77	5
7	0*	0	23

8,0,L

0	566	548	11

8,1,L

0	26*	2	8
1	229	227	3

8,2,L

0	21*	185	1
1	0*	24	22
2	136	146	3

8,3,L

0	14*	31	11
1	108	100	1
2	40*	44	7
3	173	162	2

8,4,L

0	475	468	7
1	0*	24	18
2	53	62	4
3	28*	31	5
4	348	359	5

8,5,L

0	18*	10	6
1	141	143	4
2	9*	18	11
3	64	74	3
4	10*	17	16
5	131	126	5

8,6,L

0	27*	42	5
1	0*	14	27
2	28*	0	7
3	0*	14	21
4	58	63	9
5	0*	13	23
6	61*	43	10

8,7,L

0	0*	5	14
1	12*	16	3
2	6*	5	14
3	103	112	4
4	11*	7	13
5	62	59	5
6	19*	12	10
7	96	93	5

8,8,L

0	294	287	5
1	7*	0	19
2	64	34	3
3	15*	0	15
4	225	247	2
5	10*	0	11
6	45	28	4
7	19*	0	10

9,0,L

0	0*	0	23

9,1,L

0	106	104	2
1	9*	0	15

9,2,L

0	24*	12	5
1	89	115	1
2	8*	0	14

9,3,L

0	65	62	5
1	26*	20	12
2	146	149	4
3	0*	0	25

9,4,L

0	29*	16	8
1	151	169	4
2	12*	7	12
3	109	116	2
4	0*	0	22

9,5,L

0	87	75	3
1	11*	0	15
2	0*	0	24
3	0*	0	20
4	72	72	3
5	0*	0	18

9,6,L

0	0*	3	15
1	113	115	8
2	0*	3	15
3	129	128	4
4	0*	2	17
5	32	59	7
6	17*	0	17

9,7,L

0	112	103	5
1	19*	11	12
2	71	73	6
3	7*	0	17
4	93	102	4
5	0*	0	24
6	53	55	5
7	21*	0	8

9,8,L

0	0*	22	22
1	50	56	5
2	0*	11	23
3	73	66	3
4	0*	7	17
5	42*	59	10
6	0*	10	17

9,9,L

0	10*	9	16
1	25*	0	6
2	47	37	5
3	21*	0	10
4	42*	31	8
5	0*	0	14

10,0,L

0	59	65	2

10,1,L

0	14*	29	7
1	175	164	2

10,2,L

0	141	125	2
1	27*	33	8
2	293	287	4

10,3,L

0	16*	22	13
1	73	103	3
2	15*	25	14
3	12*	29	8

10,4,L

0	97	89	3
1	21*	20	4
2	35	37	5
3	13*	21	4
4	75	63	3

10,5,L

0	0*	13	15
1	105	113	4
2	14*	15	9
3	37*	41	8
4	16*	12	15
5	81	87	3

10,6,L

0	91	89	6
1	14*	6	19
2	259	259	4
3	0*	12	20
4	41*	40	8
5	0*	9	17
6	164	187	8

10,7,L

0	21*	13	13
1	85	90	3
2	11*	19	11
3	33	19	11
4	21*	13	11
5	46	56	6
6	0*	5	29

10,8,L

0	21*	9	10
1	11*	24	6
2	13*	20	10
3	13*	9	18
4	15*	25	10
5	14*	16	17

10,9,L

0	21*	6	8
1	37*	34	10
2	19*	15	11

11,0,L

0	13*	0	7

11,1,L

0	65	55	3
1	0*	0	20

11,2,L

0	14*	17	3
1	0*	50	6
2	0*	0	28

11,3,L

0	73	66	6
1	13*	11	10
2	97	91	1
3	0*	0	19

11,4,L

0	14*	11	12
1	121	118	2
2	19*	5	9
3	56	50	5
4	14*	0	16

11,5,L

0	55	59	7
1	21*	5	11
2	72	63	2
3	7*	10	22
4	68	61	5
5	0*	0	19

11,6,L

0	12*	8	10
1	81	83	4
2	0*	14	27
3	22*	42	11
4	21*	6	14
5	57	55	4

11,7,L

0	37*	43	3
1	0*	3	24
2	17*	23	10
3	0*	2	22
4	45	46	6

11,8,L

0	0*	11	21
1	33	39	5
2	8*	3	15

12,0,L

0	223	210	5

12,1,L

0	39	41	6
1	97	110	5

12,2,L

0	57	51	6
1	19*	22	12
2	72	62	5

12,3,L

0	8*	22	10
1	62	69	2
2	0*	10	19
3	56	63	5

12,4,L

0	198	196	1
1	16*	15	12
2	34*	30	14
3	0*	7	16
4	152	141	2

12,5,L

0	13*	18	11
1	67	59	6
2	23*	31	7
3	10*	14	21

12,6,L

0	47	34	1
1	16*	23	13
2	30*	11	8
3	5*	16	17

13,0,L

0	0*	0	18

13,1,L

0	71	49	2
1	14*	0	20

13,2,L

0	0*	8	19
1	64	63	6
2	12*	0	13

13,3,L

0	99	98	3
1	3*	4	16
2	36	32	5
3	0*	0	26

13,4,L

0	17*	6	10
1	10*	46	6
2	21*	3	14

+ these reflections were omitted from the final model. (See text)

HAUYNE (153K)

1,0,L	1 47* 0 3	7,0,-	3,4,L
0 61* 0 2	7,2,L	3 [illegible] 0 18	0 731 724 14
1,1,L	0 3[illegible] 36 4	7,1,-	1 33* 17 8
+0 237 368 2	1 31[illegible] 308 5	2 50* 0 8	2 71 70 8
1 30* 0 6	2 50* 0 8	0 356 358 6	3 44* 45 8
2,0,L	3,3,L	1 30* 0 5	4 585 587 3
+0 264 77 4	0 38[illegible] 385 7	7,2,L	3,5,L
2,1,L	1 [illegible]70 79 10	0 74[illegible] 66 3	0 32* 37 6
0 110 110 4	2 486 479 10	1 488 475 6	1 244 237 2
1 1091 1084 22	3 30* 0 9	2 26* 0 12	2 34* 24 8
2,2,L	3,4,L	7,3,L	3 107 111 6
0 219 199 3	0 76 69 5	0 460 467 9	4 21* 10 16
1 35* 0 7	1 225 202 5	1 44 41 6	5 321 333 5
2 1390 1415 5	2 [illegible]6 38 5	2 75 83 2	4,6,L
2,3,L	3 391 392 5	3 41* 0 8	0 45 62 7
0 27* 25 10	4 29* 0 13	7,4,-	1 15* 26 23
1 17* 0 12	3,5,L	1 29* 10 10	2 63 87 6
2 33[illegible] 305 2	0 27* 25 10	2 240 228 2	3 7* 3 16
3 26* 0 6	1 17* 0 12	3 42 44 3	4 141 140 6
3,0,L	2 33[illegible] 305 2	4 16[illegible] 174 3	5 23* 15 12
0 31* 0 5	3 26* 0 6	5 0* 0 22	6 133 122 5
3,1,L	4 214 215 2	7,5,L	4,7,L
0 541 572 10	5 62* 0 5	0 416 395 5	0 25* 37 12
1 38* 0 3	3,6,L	1 49 39 4	1 244 245 3
3,2,L	0 749 737 25	2 361 351 6	2 27* 16 16
0 63 31 4	3,7,L	3 34* 58 9	3 144 205 2
1 306 324 5	0 52 34 5	4 259 251 4	4 34* 23 7
2 25* 0 5	1 144 146 2	5 10* 0 17	5 153 152 5
3,3,L	3,8,L	7,6,L	4,8,L
0 1098 1059 24	0 144 101 4	0 30* 0 9	0 593 599 3
1 23* 0 10	1 47 49 6	1 164 170 2	1 1* 0 23
2 373 407 7	2 1059 1043 8	2 53 67 5	2 135 143 4
3 0* 0 21	3,9,L	3 74 69 6	3 31* 0 22
4,0,L	0 39* 18 7	4 11* 16 22	5,0,L
0 917 933 27	1 37[illegible] 411 6	5 169 145 7	0 1* 0 10
4,1,L	2 3[illegible] 7 9	6 0* 0 23	5,1,L
0 69 35 5	3 664 689 16	7,7,-	0 191 193 4
1 649 682 8	4,0,L	0 49 6 6	1 21* 0 21
4,2,L	0 16* 3 9	1 26* 0 10	5,2,L
0 195 194 4	1 51* 52 10	2 203 213 4	0 51 58 8
1 27* 12 4	2 202 191 4	3 27* 0 12	1 123 132 5
2 310 291 4	3 60 49 4	4 175 182 5	2 23* 0 13
4,3,L	4 57 44 9	5 23* 0 7	5,3,L
0 44 24 3	4,1,L	6 156 175 3	0 102 81 9
1 473 449 3	0 45 38 7	7,8,L	1 33* 43 9
2 64 72 7	1 283 278 6	0 804 791 12	2 241 238 6
3 501 496 3	2 47* 22 8	8,1,-	3 21* 0 10
4,4,L	3 211 209 8	0 64 81 2	5,4,L
0 1220 1199 5	4 72 84 5	1 346 359 7	0 81 86 4
1 0* 0 22	5 225 222 5	8,2,L	1 264 262 4
2 491 487 7	4,6,L	0 257 244 4	2 31* 41 13
3 28* 0 11	0 175 183 2	1 24* 17 9	3 245 240 4
4 1291 1305 7	1 47* 0 4	2 277 273 4	4 25* 0 8
5,0,L	2 779 784 4	8,3,-	5,5,L
0 71* 0 3	3 24* 0 14	0 29* 2 9	0 143 162 3
5,1,L	4 262 263 14	1 229 229 4	1 46* 34 11
0 339 323 6	5 11* 0 18	2 68 74 6	2 31* 108 7
	6 488 490 5	3 284 275 2	3 33* 10 8
			4 35 163 6
			5 12* 0 22
			5,6,L
			0 30* 27 7
			1 230 226 5
			2 27* 14 18
			3 269 263 4
			4 25* 18 18
			9,7,L
			0 267 252 2
			1 34 39 5
			2 182 154 2
			3 31* 32 14
			10,0,L
			0 163 136 5
			10,1,L
			0 38* 15 10
			1 281 278 10
			10,2,L
			0 224 216 3
			1 27* 19 15
			2 535 543 7
			10,3,L
			0 32* 27 17
			1 166 166 5
			2 37* 33 11
			3 52 52 5
			10,4,L
			0 174 171 5
			1 32* 17 8
			2 83 87 8
			3 11* 29 23
			4 145 163 4
			10,5,L
			0 36* 9 13
			1 230 228 2
			2 55 32 8
			3 84 86 8
			10,6,L
			0 235 247 4
			1 29* 34 10
			2 533 542 11
			11,0,L
			0 0* 0 33
			11,1,L
			0 122 118 5
			1 27* 0 14
			11,2,L
			0 17* 15 11
			1 92 96 5
			2 27* 0 13
			11,3,L
			0 144 147 3
			1 43 43 5
			2 188 194 5
			3 17* 0 18
			11,4,L
			0 31* 32 13
			1 256 253 2

+ these reflections were omitted from the final model. (See text)

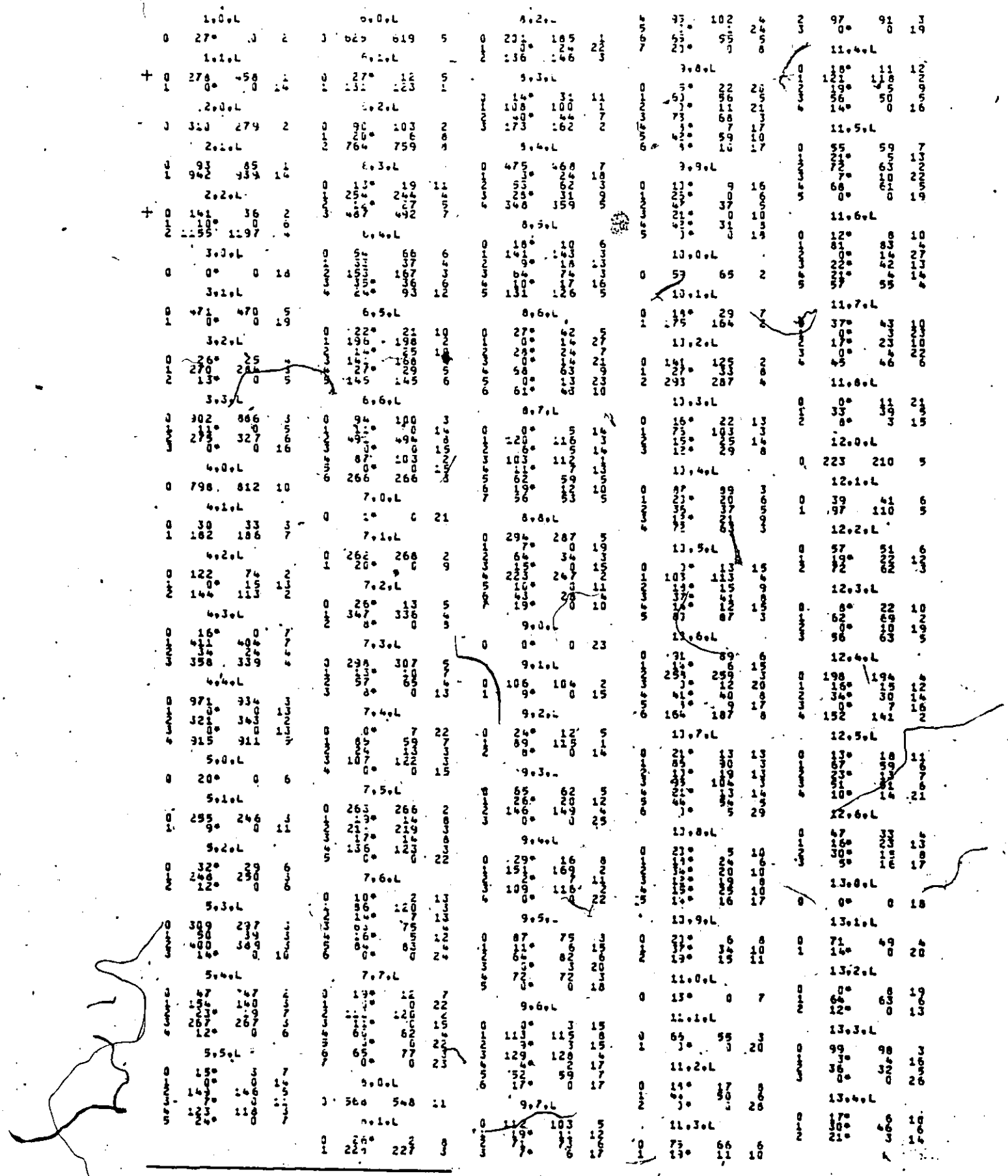

+ these reflections were omitted from the final model. (See text)

HYDROXYCANCRINITE

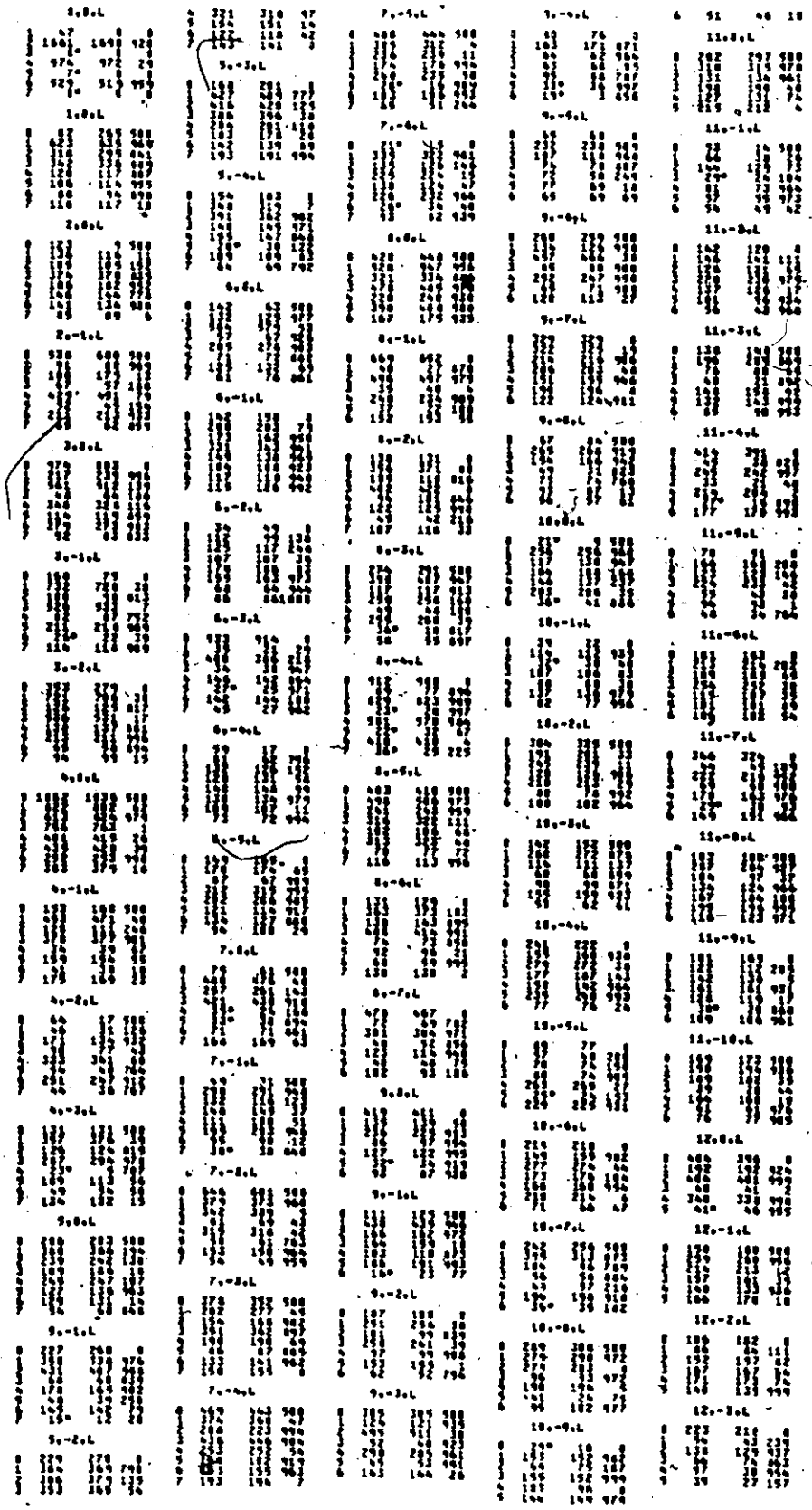

HYDROXYCANCRINITE (continued)

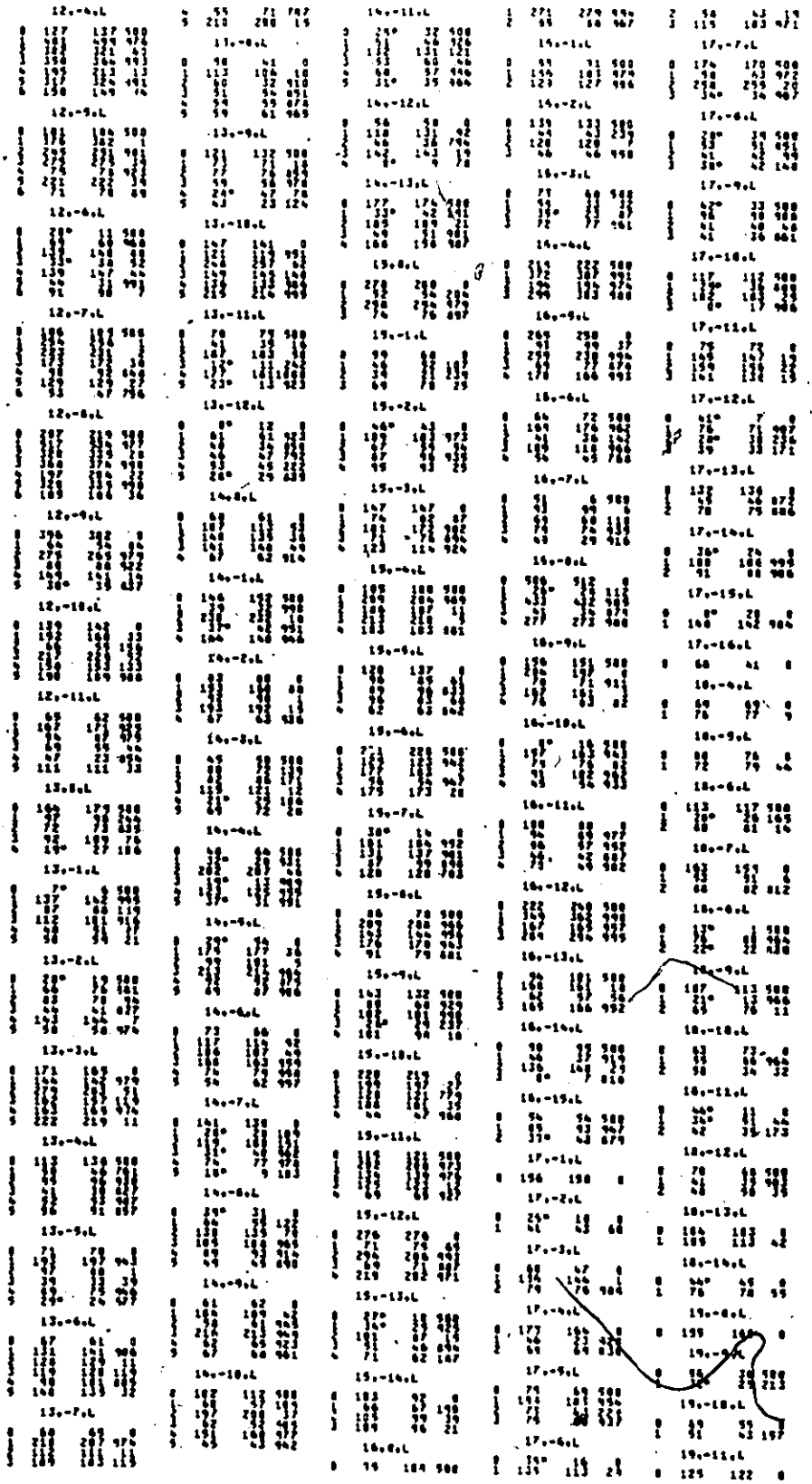

VISHNEVITE (continued)

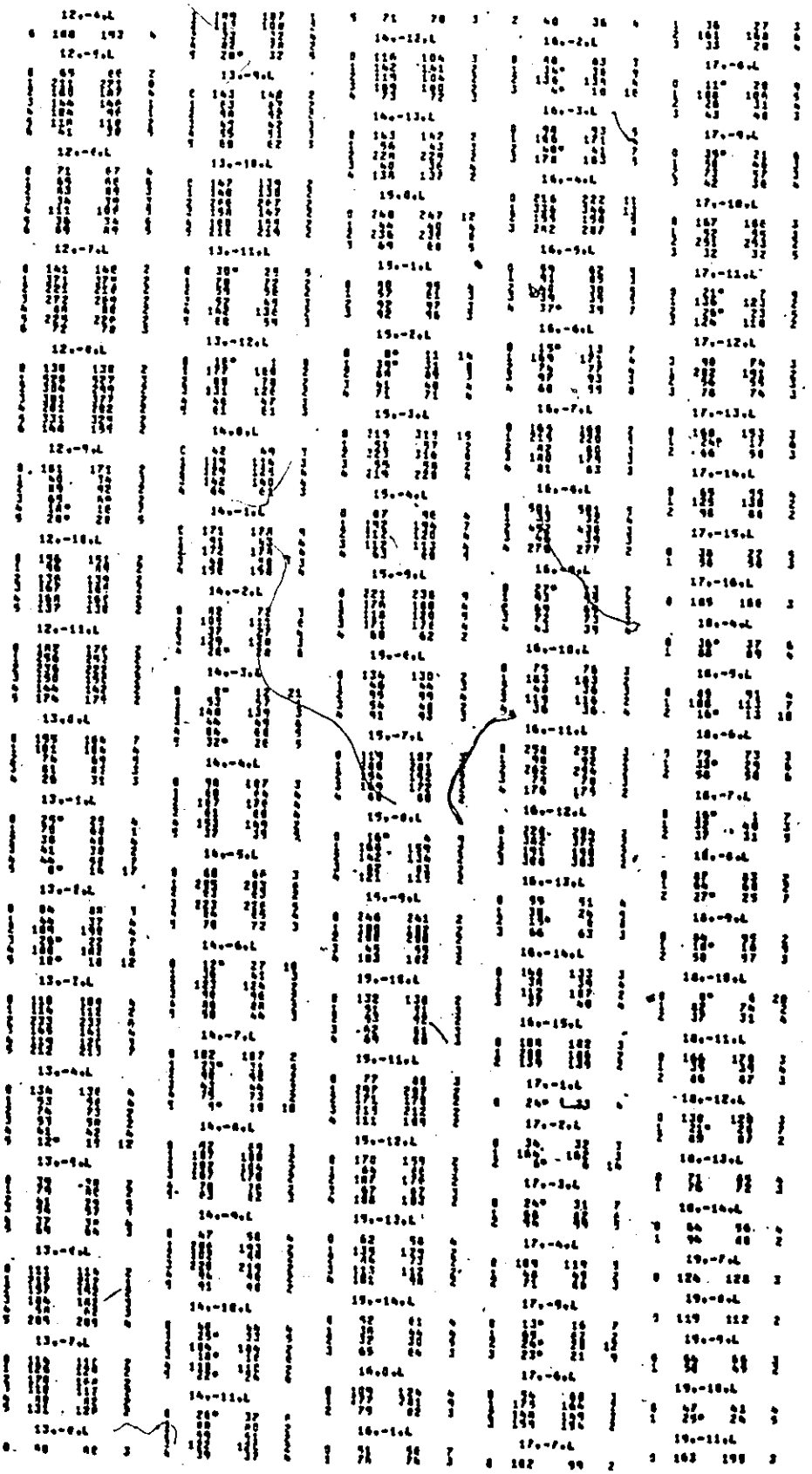

DAVYNE (continued)

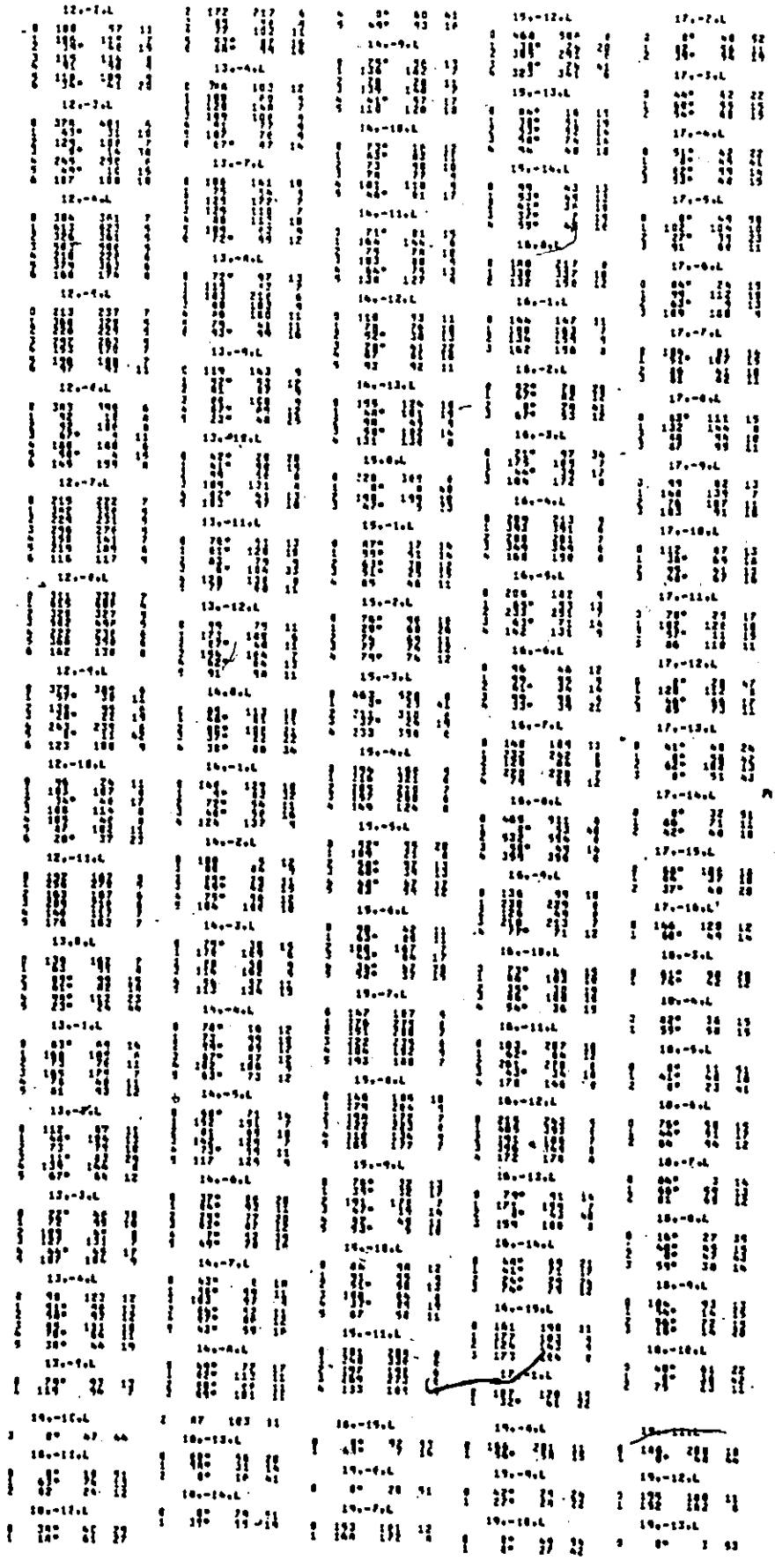

HAUY DELTA F, OBSERVED REFLECTIONS ONLY

Y IN 100THS ↓ X IN 100THS →

Z = 74 100THS

	50	52	54	56	58	60	62	64	66	68	70	72	74	76	78	80
50	13	11	5	0	-1	-1	0	0	-2	-3	-4	-3	-2	-1	-1	0
52	11	9	5	1	0	-1	0	-1	-2	-3	-4	-3	-1	-1	-1	0
54	6	5	4	2	0	0	0	0	-1	-2	-2	0	0	0	0	-1
56	1	2	3	3	1	0	0	1	1	0	0	1	1	1	0	0
58	0	0	2	2	1	0	1	2	3	2	2	1	0	0	0	0
60	0	0	1	1	1	0	0	1	3	3	3	1	0	-1	-2	-1
62	0	0	1	2	2	0	0	0	1	3	3	2	0	-1	-2	-1
64	0	0	0	2	3	2	0	0	0	1	1	0	-1	-1	0	0
66	-1	-1	0	2	4	3	1	0	-1	-3	-4	-4	-4	-4	-2	0
68	-3	-3	-2	0	3	3	3	1	-3	-6	-6	-1	0	-4	-8	-5
70	-3	-4	-2	0	2	3	4	1	-4	-6	3	20	27	13	-6	-13
72	-3	-3	0	1	1	1	2	0	-3	-1	17	24	30	22	3	-11
74	-2	-1	0	1	0	0	0	-1	-4	0	27	32	37	32	17	0
76	-2	-1	0	1	0	-1	-2	-1	-4	-4	27	32	32	23	4	6
78	-3	-2	0	0	0	-1	-2	0	-3	-6	-2	7	13	8	2	1
80	-3	-2	-1	1	1	0	-1	0	0	-6	-14	-11	0	6	2	-7

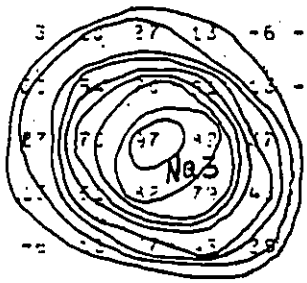

Fig. 6.2.5: Difference Fourier synthesis calculated with the Na(3) cation site removed from the structural model (R = 0.154).

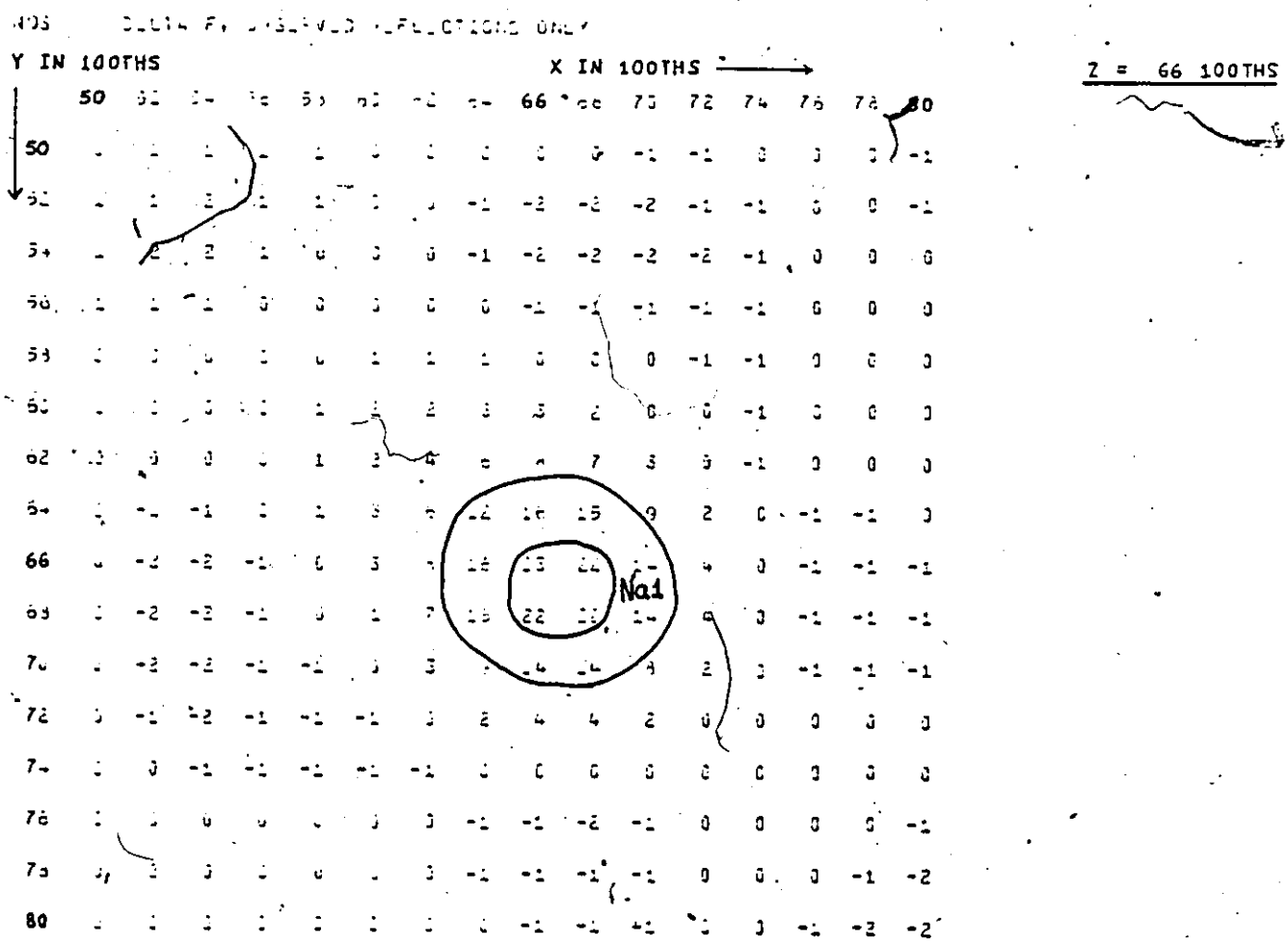

Fig. 6.3.4: Difference Fourier synthesis calculated with Na(1) site removed from the structural model (R = 0.087).

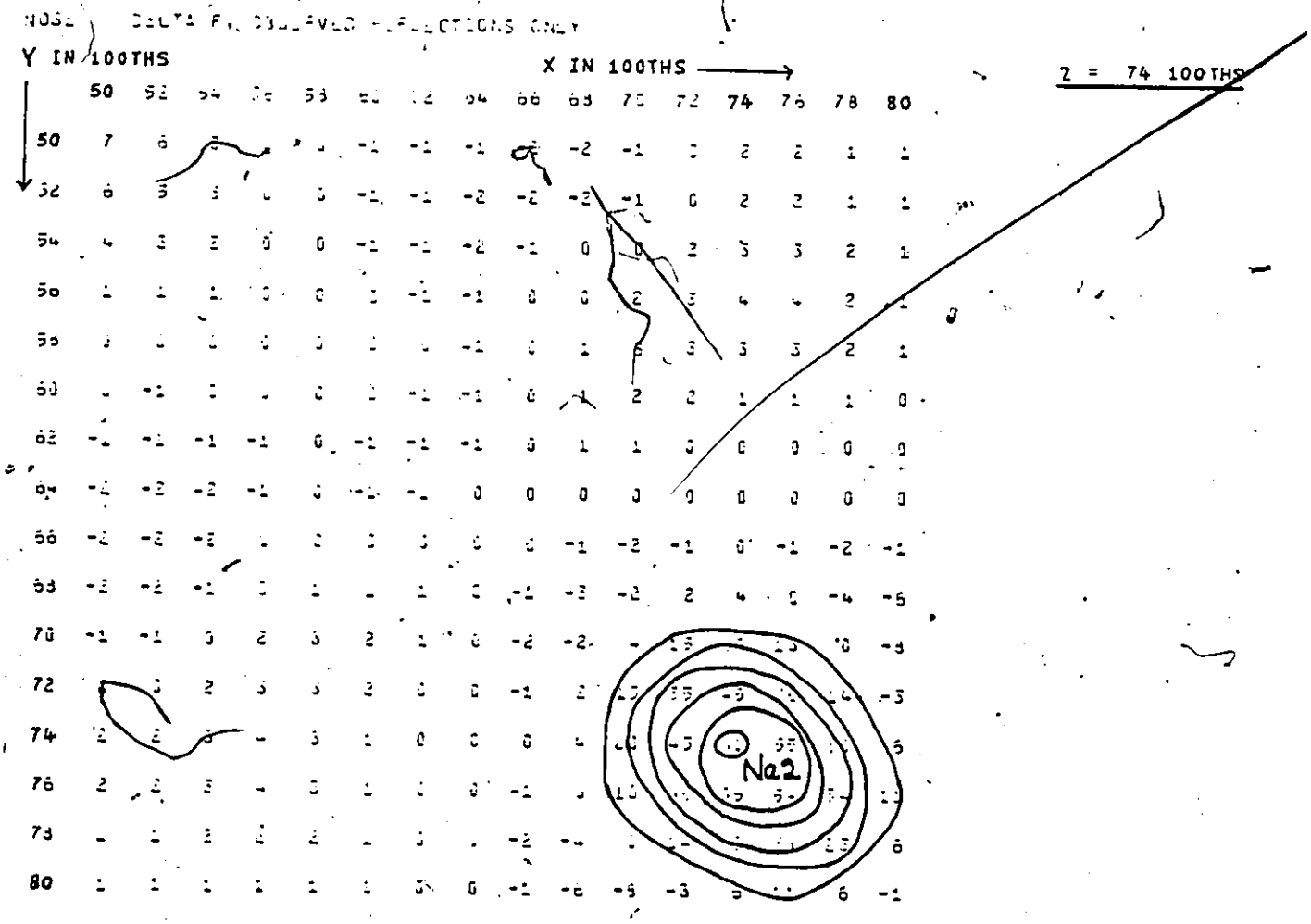

Fig. 6.3.5: Difference Fourier synthesis calculated with Na(2) site removed from the structural model (R = 0.153).

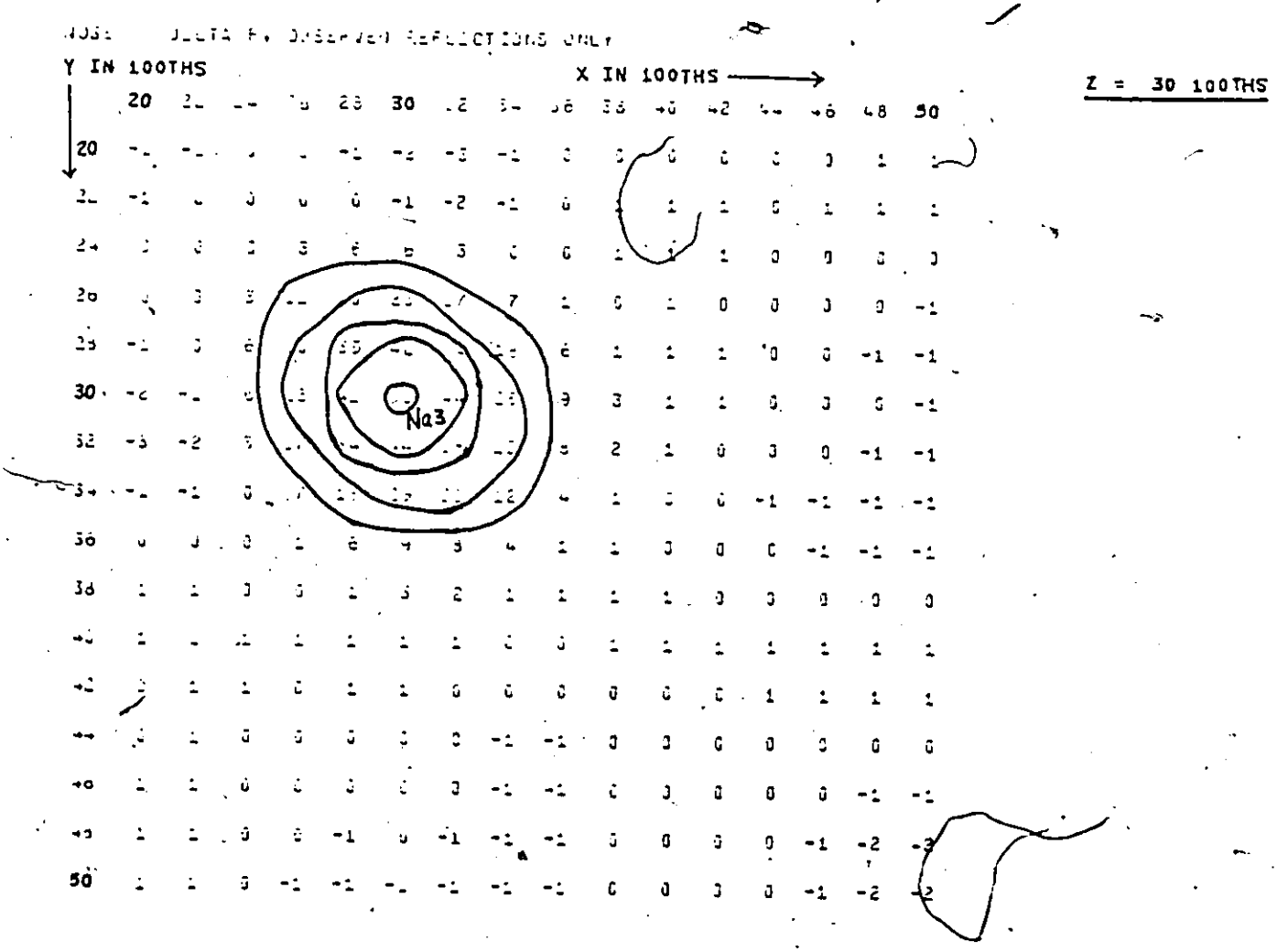

Fig. 6.3.6: Difference Fourier synthesis calculated with Na(3) site removed from the structural model (R = 0.151).